

Green Chemistry

Cutting-edge research for a greener sustainable future

www.rsc.org/greenchem

Volume 8 | Number 4 | April 2006 | Pages 313–400



Downloaded on 07 November 2016
Published on 30 March 2006. http://pubs.rsc.org | doi:10.1039/B605562K

ISSN 1463-9262

RSC Publishing

Scott *et al.*
Oxidative coupling revisited

Hirashita *et al.*
Hydrothermal reaction of
hydroxybenzyl alcohols

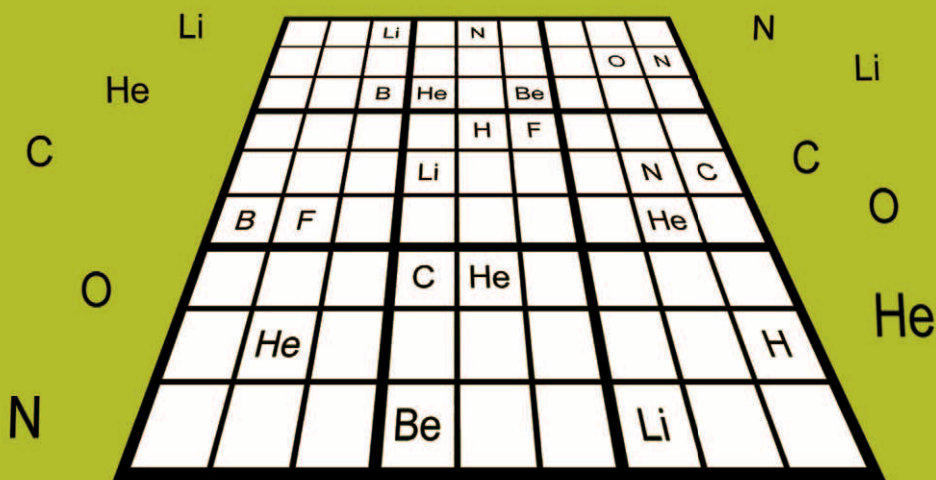
Kumar *et al.*
Catalytic oxidation of alcohols in water

Poliakoff *et al.*
Hydrogenation reactions in high
temperature water



1463-9262(2006)8:4;1-A

Numerical Alchemy ?

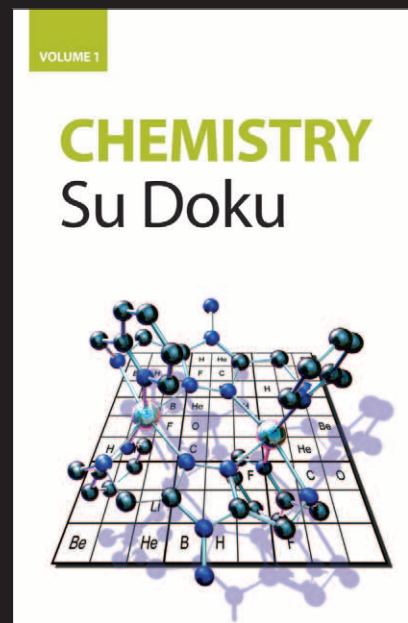


Chemistry Su Doku

- Specially developed to incorporate chemical symbols instead of numbers
- The perfect gift for a chemist
- Go online buy your copy today!

Try our other puzzle book
Chemistry Crosswords Vol.1

Softcover | 0 85404 693 3 | 2005 | 116 pages | £7.95



RSC Publishing

www.rsc.org/puzzle

Green Chemistry

Cutting-edge research for a greener sustainable future

www.rsc.org/greenchem

RSC Publishing is a not-for-profit publisher and a division of the Royal Society of Chemistry. Any surplus made is used to support charitable activities aimed at advancing the chemical sciences. Full details are available from www.rsc.org

IN THIS ISSUE

ISSN 1463-9262 CODEN GRCHFJ 8(4) 313-400 (2006)



Cover

The cover illustrates the use of the same continuous reactor for either hydrogenation or oxidation in high pressure high temperature water, merely by changing the precursor for the reacting gas. In the background are the Tis Abay (Blue Nile Falls), Ethiopia. Image reproduced by permission of Martyn Poliakoff from *Green Chem.*, 2006, **8**(4), 359.

CHEMICAL TECHNOLOGY

T13

Chemical Technology highlights the latest applications and technological aspects of research across the chemical sciences.

Chemical Technology

April 2006/Volume 3/Issue 4

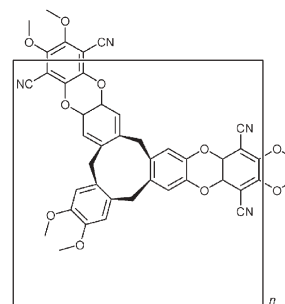
www.rsc.org/chemicaltechnology

HIGHLIGHT

322

Highlights

Markus Hölscher reviews some of the recent literature in green chemistry.



EDITORIAL STAFF

Editor

Sarah Ruthven

News writer

Markus Hölscher

Publishing assistant

Emma Hacking

Team leader, serials production

Stephen Wilkes

Administration coordinator

Sonya Spring

Editorial secretaries

Lynne Braybrook, Jill Segev, Julie Thompson

Publisher

Adrian Kybett

Green Chemistry (print: ISSN 1463-9262; electronic: ISSN 1463-9270) is published 12 times a year by the Royal Society of Chemistry, Thomas Graham House, Science Park, Milton Road, Cambridge, UK CB4 0WF.

All orders, with cheques made payable to the Royal Society of Chemistry, should be sent to RSC Distribution Services, c/o Portland Customer Services, Commerce Way, Colchester, Essex, UK CO2 8HP. Tel +44 (0) 1206 226050; E-mail sales@rscdistribution.org

2006 Annual (print + electronic) subscription price: £859; US\$1571. 2006 Annual (electronic) subscription price: £773; US\$1414. Customers in Canada will be subject to a surcharge to cover GST. Customers in the EU subscribing to the electronic version only will be charged VAT.

If you take an institutional subscription to any RSC journal you are entitled to free, site-wide web access to that journal. You can arrange access via Internet Protocol (IP) address at www.rsc.org/ip. Customers should make payments by cheque in sterling payable on a UK clearing bank or in US dollars payable on a US clearing bank. Periodicals postage paid at Rahway, NJ, USA and at additional mailing offices. Airfreight and mailing in the USA by Mercury Airfreight International Ltd., 365 Blair Road, Avenel, NJ 07001, USA.

US Postmaster: send address changes to Green Chemistry, c/o Mercury Airfreight International Ltd., 365 Blair Road, Avenel, NJ 07001. All despatches outside the UK by Consolidated Airfreight.

PRINTED IN THE UK

Advertisement sales: Tel +44 (0) 1223 432246; Fax +44 (0) 1223 426017; E-mail advertising@rsc.org

Green Chemistry

Cutting-edge research for a greener sustainable future

www.rsc.org/greenchem

Green Chemistry focuses on cutting-edge research that attempts to reduce the environmental impact of the chemical enterprise by developing a technology base that is inherently non-toxic to living things and the environment.

EDITORIAL BOARD

Chair

Professor Colin Raston,
Department of Chemistry
University of Western Australia
Perth, Australia
E-mail clration@chem.uwa.edu.au

Dr Janet Scott, Centre for Green
Chemistry, Monash University,
Australia

Professor Buxing Han, Chinese
Academy of Sciences
E-mail hanbx@iccas.ac.cn

Dr A Michael Warhurst,
University of Massachusetts,
USA
E-mail michael-warhurst@uml.edu

Associate editors

Professor C. J. Li, McGill
University, Canada
E-mail cj.li@mcgill.ca

Scientific editor

Professor Walter Leitner,
RWTH-Aachen, Germany
E-mail leitner@itmc.rwth-aachen.de

Professor Tom Welton,
Imperial College, UK
E-mail t.welton@ic.ac.uk

Professor Kyoko Nozaki
Kyoto University, Japan
E-mail nozaki@chembio.tu-tokyo.ac.jp

Professor Roshan Jachuck,
Clarkson University, USA
E-mail rjachuck@clarkson.edu

Members

Professor Joan Brennecke,
University of Notre Dame, USA
Professor Steve Howdle, University
of Nottingham, UK

Dr Paul Anastas, Green Chemistry
Institute, USA
E-mail p_anastas@acs.org

INTERNATIONAL ADVISORY EDITORIAL BOARD

James Clark, York, UK
Avelino Corma, Universidad
Politécnica de Valencia, Spain
Mark Harmer, DuPont Central
R&D, USA
Herbert Hugel, Lanxess Fine
Chemicals, Germany
Makato Misono, Kogakuin
University, Japan
Robin D. Rogers, Centre for Green
Manufacturing, USA

Kenneth Seddon, Queen's
University, Belfast, UK
Roger Sheldon, Delft University of
Technology, The Netherlands
Gary Sheldrake, Queen's
University, Belfast, UK
Pietro Tundo, Università ca
Foscari di Venezia, Italy
Tracy Williamson, Environmental
Protection Agency, USA

INFORMATION FOR AUTHORS

Full details of how to submit material for publication in Green Chemistry are given in the Instructions for Authors (available from <http://www.rsc.org/authors>). Submissions should be sent via ReSource: <http://www.rsc.org/resource>.

Authors may reproduce/republish portions of their published contribution without seeking permission from the RSC, provided that any such republication is accompanied by an acknowledgement in the form: (Original citation) – Reproduced by permission of the Royal Society of Chemistry.

© The Royal Society of Chemistry 2006. Apart from fair dealing for the purposes of research or private study for non-commercial purposes, or criticism or review, as permitted under the Copyright, Designs and Patents Act 1988 and the Copyright and Related Rights Regulations 2003, this publication may only be reproduced, stored or transmitted, in any form or by any means, with the prior permission in writing of the Publishers or in the case of reprographic reproduction in accordance with the terms of

licences issued by the Copyright Licensing Agency in the UK. US copyright law is applicable to users in the USA.

The Royal Society of Chemistry takes reasonable care in the preparation of this publication but does not accept liability for the consequences of any errors or omissions.

Ⓢ The paper used in this publication meets the requirements of ANSI/NISO Z39.48-1992 (Permanence of Paper).

Royal Society of Chemistry: Registered Charity No. 207890

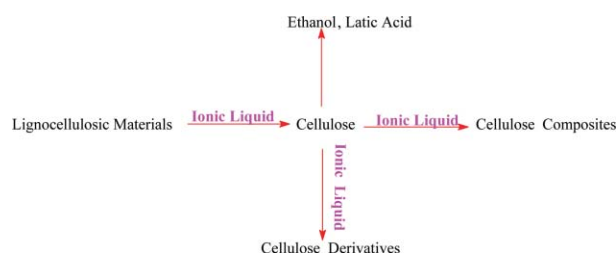
CRITICAL REVIEW

325

Dissolution of cellulose with ionic liquids and its application: a mini-review

Shengdong Zhu,* Yuanxin Wu, Qiming Chen, Ziniu Yu, Cunwen Wang, Shiwei Jin, Yigang Ding and Gang Wu

Dissolution of cellulose with ionic liquids allows the complete use of cellulose resources. This mini-review presents recent progress and applications.



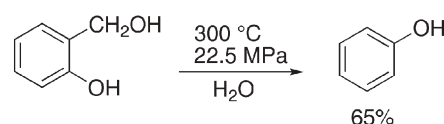
COMMUNICATIONS

328

Reaction of hydroxybenzyl alcohols under hydrothermal conditions

Tsunehisa Hirashita,* Shuki Araki, Takao Tsuda, Shinya Kitagawa, Takayuki Umeyama, Mutsumi Aoki and Koichi Nakamura

Under hydrothermal conditions, salicylic alcohol and *p*-hydroxybenzyl alcohol were transformed into phenol in high or moderate yields, whereas *m*-hydroxybenzyl alcohol and benzyl alcohol proved to be stable and remained almost intact.

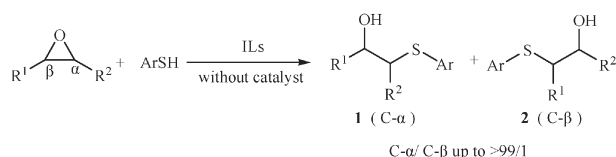


330

Highly regioselective ring-opening of epoxides with thiophenols in ionic liquids without the use of any catalyst

Jiuxi Chen, Huayue Wu, Can Jin, Xingxian Zhang, Yuanyuan Xie and Weike Su*

Clean thiolysis reaction of various epoxides in ionic liquids (ILs) without the use of any catalyst generates β -hydroxy sulfides in excellent yields (83–98%) with high regioselectivity and chemoselectivity under mild reaction conditions.



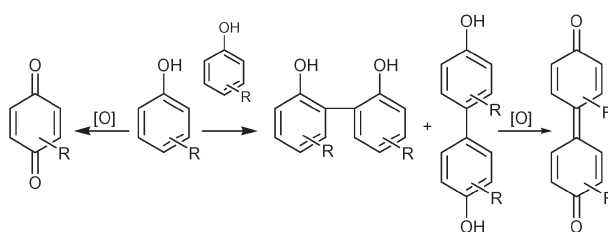
PAPERS

333

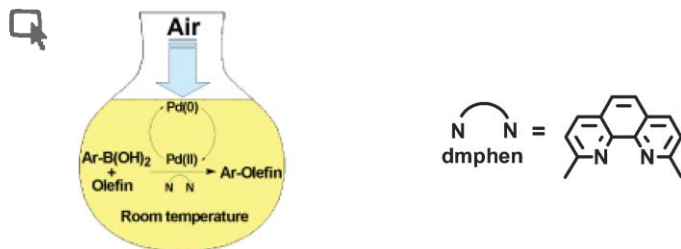
Oxidative coupling revisited: solvent-free, heterogeneous and in water

Philip J. Wallis, Katrina J. Booth, Antonio F. Patti and Janet L. Scott*

FeCl_3 in water is a universally applicable set of conditions for coupling, removing the need for organic solvents. Solvent-free conditions are efficient where a liquid phase is generated above critical and often mild temperatures.



338

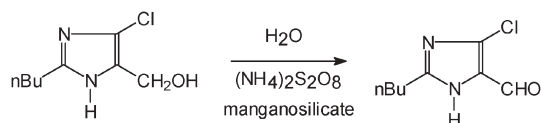


Open-air oxidative Heck reactions at room temperature

Per-Anders Enquist, Jonas Lindh, Peter Nilsson and Mats Larhed*

Palladium(II)-catalyzed Heck arylation of both electron-poor and electron-rich olefins with arylboronic acids as arylpalladium precursors were conducted under air. The bidentate 2,9-dimethyl-1,10-phenanthroline (dmphen) ligand was found not only to control the regioselectivity but also both to produce an efficient catalytic system at low reaction temperatures and to enable direct palladium(II) regeneration with air as the sole reoxidant.

344

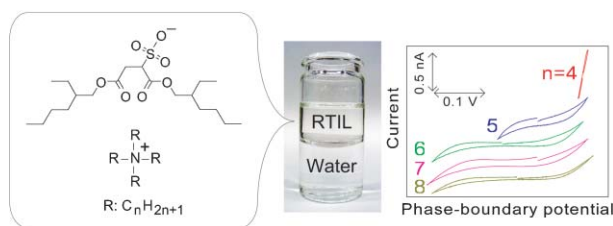


The green catalytic oxidation of alcohols in water by using highly efficient manganosilicate molecular sieves

Haresh G. Manyar, Ganesh S. Chaurse and Ashok Kumar*

A facile methodology to synthesise uniform cubic manganosilicate molecular sieves and their use as recyclable catalysts in the benign oxidation protocol for difficult-to-oxidize heterocyclic and aliphatic alcohols.

349

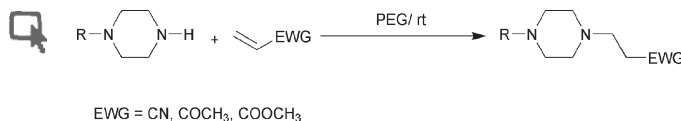


Fluorine-free and hydrophobic room-temperature ionic liquids, tetraalkylammonium bis(2-ethylhexyl)sulfosuccinates, and their ionic liquid–water two-phase properties

Naoya Nishi, Takahiro Kawakami, Fumiko Shigematsu, Masahiro Yamamoto and Takashi Kakiuchi*

Fluorine-free and hydrophobic room-temperature ionic liquids (RTILs), tetraalkylammonium bis(2-ethylhexyl)sulfosuccinates, have been prepared. The mutual solubility of the RTIL–water two-phase systems is correlated with the electrochemical polarizability of the RTIL|W interface.

356



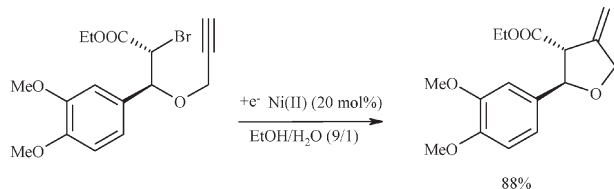
Polyethylene glycol as a non-ionic liquid solvent for Michael addition reaction of amines to conjugated alkenes

Rupesh Kumar, Preeti Chaudhary, Surendra Nimesh and Ramesh Chandra*

Polyethylene glycol (PEG) is an inexpensive, non-toxic, environmentally friendly reaction medium for the conjugate addition of amines to conjugated alkenes in excellent yields under mild reaction condition.

PAPERS

380

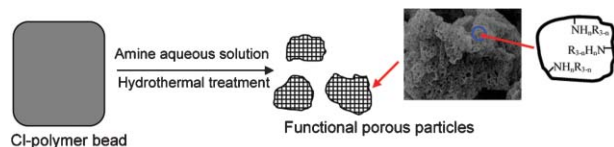


Reductive cyclisation of propargyloxy and allyloxy α -bromoester derivatives using environmentally friendly electrochemical methodologies

E. Duñach, A. P. Esteves, M. J. Medeiros* and S. Olivero

Ni-catalysed radical-type cyclisation in EtOH and EtOH–H₂O mixtures.

386

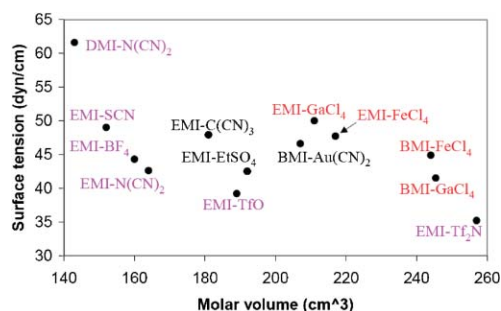


Fabrication of porous polymer particles with high anion exchange capacity by amination reaction in aqueous medium

Jin Liu, Jianfeng Yao, Huanting Wang* and Kwong-Yu Chan*

Porous polymer particles with high ion exchange capacity were created by hydrothermal amination of chlorinated aliphatic polymers. The approach developed here is effective and environmentally friendly for functionalizing chlorinated polymers.

390



Surface tension measurements of highly conducting ionic liquids

W. Martino, J. Fernandez de la Mora, Y. Yoshida, G. Saito and J. Wilkes

Surface tensions are measured for a diversity of imidazolium-based ionic liquids and sample consumption is minimized ($\sim 0.1 \text{ cm}^3$) by using the capillary rise method.

ADDITIONS AND CORRECTIONS

398

W. Martino, J. Fernandez de la Mora, Y. Yoshida, G. Saito and J. Wilkes

Surface tension measurements of highly conducting ionic liquids

AUTHOR INDEX

- Aoki, Mutsumi, 328
 Araki, Shuki, 328
 Booth, Katrina J., 333
 Chan, Kwong-Yu, 386
 Chandra, Ramesh, 356
 Chaudhary, Preeti, 356
 Chaure, Ganesh S., 344
 Chen, Jiuxi, 330
 Chen, Qiming, 325
 de la Mora, J. Fernandez, 390
 Ding, Yigang, 325
 Duñach, E., 380
 Enquist, Per-Anders, 338
 Esteves, A. P., 380
 Ferreira, Frederico Castelo, 373
 Fraga-Dubreuil, Joan, 359
 Garcia-Serna, Juan, 359
 Garcia-Verdugo, Eduardo, 359
 Hamley, Paul A., 359
- Hirashita, Tsunehisa, 328
 Hyde, Jason R., 359
 Jin, Can, 330
 Jin, Shiwei, 325
 Kakiuchi, Takashi, 349
 Kawakami, Takahiro, 349
 Kitagawa, Shinya, 328
 Krishna Mohan, K. V. V., 368
 Kulkarni, S. J., 368
 Kumar, Ashok, 344
 Kumar, Rupesh, 356
 Larhed, Mats, 338
 Lindh, Jonas, 338
 Liu, Jin, 386
 Liu, Zhimin, 359
 Livingston, Andrew Guy, 373
 Manyar, Haresh G., 344
 Martino, W., 390
 Medeiros, M. J., 380
- Nakamura, Koichi, 328
 Narender, N., 368
 Nilsson, Peter, 338
 Nimesh, Surendra, 356
 Nishi, Naoya, 349
 Olivero, S., 380
 Patti, Antonio F., 333
 Pink, Christopher John, 373
 Poliakov, Martyn, 359
 Ramirez, Eliana, 359
 Saito, G., 390
 Scott, Janet L., 333
 Shigematsu, Fumiko, 349
 Su, Weike, 330
 Sun, Wei, 365
 Sun, Xiaoyu, 365
 Tsuda, Takao, 328
 Umeyama, Takayuki, 328
 Wallis, Philip J., 333
- Wang, Cunwen, 325
 Wang, Huanting, 386
 Wilkes, J., 390
 Wong, Hau-to, 373
 Wu, Gang, 325
 Wu, Huayue, 330
 Wu, Jie, 365
 Wu, Yuanxin, 325
 Xia, Hong-Guang, 365
 Xie, Yuanyuan, 330
 Yamamoto, Masahiro, 349
 Yao, Jianfeng, 386
 Yoshida, Y., 390
 Yu, Ziniu, 325
 Zhang, Xingxian, 330
 Zhu, Shengdong, 325

FREE E-MAIL ALERTS AND RSS FEEDS

Contents lists in advance of publication are available on the web *via* www.rsc.org/greenchem - or take advantage of our free e-mail alerting service (www.rsc.org/ej_alert) to receive notification each time a new list becomes available.

RSS Try our RSS feeds for up-to-the-minute news of the latest research. By setting up RSS feeds, preferably using feed reader software, you can be alerted to the latest Advance Articles published on the RSC web site. Visit www.rsc.org/publishing/technology/rss.asp for details.

ADVANCE ARTICLES AND ELECTRONIC JOURNAL

Free site-wide access to Advance Articles and the electronic form of this journal is provided with a full-rate institutional subscription. See www.rsc.org/ejs for more information.

* Indicates the author for correspondence: see article for details.


 Electronic supplementary information (ESI) is available *via* the online article (see <http://www.rsc.org/esi> for general information about ESI).

Image reproduced by permission of Tom Schweich, *J. Environ. Monit.* 2005, 1



JEM

Journal of Environmental Monitoring

Comprehensive, high quality coverage of multidisciplinary, international research relating to the measurement, pathways, impact and management of contaminants in all environments.

- Dedicated to the analytical measurement of environmental pollution
- Assessing exposure and associated health risks.
- Fast times to publication
- Impact factor: 1.366
- High visibility - cited in MEDLINE

RSC Publishing

www.rsc.org/jem

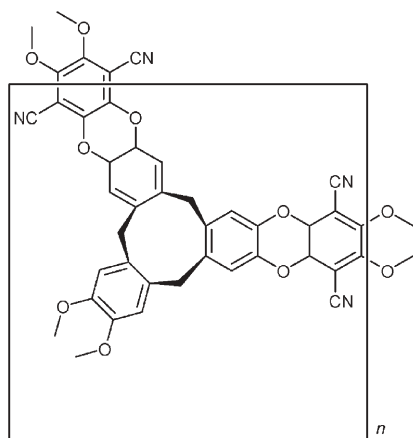
Highlights

DOI: 10.1039/b603071h

Markus Hölscher reviews some of the recent literature in green chemistry

Polymers as hydrogen storage materials—large capacities by intrinsic microporosity

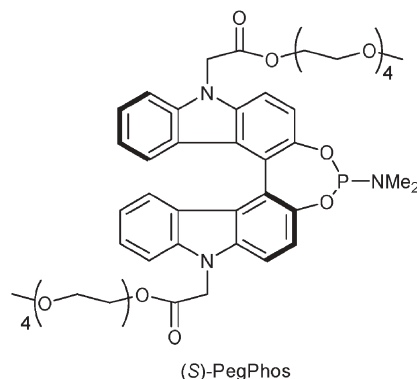
The combustion of hydrogen as a non-polluting fuel in cars would be a much greener energy basis, than the hydrocarbon fuels that are used presently. The importance of hydrogen technology has been recognized politically: The US department of energy has set an ambitious target in which a practical hydrogen storage system should be available by 2010 that holds 6.0% of H₂ by mass. One step on the road to this desirable goal is the exploration of alternative hydrogen storage materials. Microporous materials such as zeolites and metal organic frameworks (MOFs) have been under investigation for quite a while, however so far even the highest storage quantities obtained are too low to be considered in practical applications. Due to their structural flexibility polymers have not yet been extensively explored for hydrogen storage, but this might change in the future. McKeown and coworkers investigated the possibility of creating polymers with intrinsic microporosity (PIMs) by polymerizing monomers of which one contains either a spiro-center or a rigid nonplanar unit.¹ The resulting polymers, one of them shown below, contain micropores in the size range of around 0.6 nm, as was shown by N₂ adsorption experiments.



The surface area amounts to *ca.* 800 m² g⁻¹ and by careful examination of the H₂ storage capacity the authors found an encouraging capacity of 1.4 to 1.7% H₂ by mass. The different materials tested adsorbed most of the H₂ at pressures lower than 1 bar, with saturation being achieved at less than 10 bar. The capacity obtained compares well with other material types. However, to be useful in practical applications PIMs with surface areas of >2000 m² g⁻¹ must be developed.

Enantioselective hydrogenations in water with monodentate phosphoramidite rhodium complexes

Catalytic asymmetric hydrogenations in environmentally friendly solvents such as water are highly desirable due to the expected economical and ecological benefits. However, these types of reactions have not been extensively investigated as both catalysts and substrates often don't dissolve in water. One of the approaches to circumvent these problems is the modification of the ligand in such a way that it becomes water soluble, while the addition of appropriate surfactants in small amounts helps dissolve the substrates. Minnaard and coworkers recently developed the (*S*)-PegPhos ligand, which carries tetraethylene glycol units as side chains to enable sufficient solubility in polar solvents.²

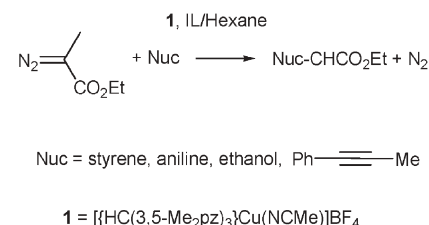


Structurally the ligand design relies on the (*S*)-MonoPhos ligand, which proved highly efficient in enantioselective hydrogenations of a variety of substrates, *e.g.* *N*-acyl dehydroamino acids. The novel ligand showed promising results in rhodium catalyzed hydrogenations of *N*-acyl dehydroalanine. The ligand yields *ee*'s of *ca.* 90% with TOFs of 1200 in methanol and methanol/water, while in pure water the high *ee* is retained to a large extent (82%) at the expense of rate (TOF = 55). The addition of 10% sodium dodecylsulfate to water increased the TOF to 600, while the *ee* value again reached the high value of 89%. The parent MonoPhos ligand performed much poorer in all control experiments.

Recyclable copper catalysts for carbene transfer in biphasic IL/organic phase reactions

The usage of diazo compounds for the introduction of carbene units into a wide variety of organic molecules has been developed into an established technique in organic chemistry. Many processes of this kind operate under homogeneous catalytic conditions, however, only a few systems allow for the separation of the catalyst. As biphasic catalysis with ionic liquids (ILs) has attracted increasing interest in the past years Nicasio *et al.* have set out to explore the catalytic performance and separation behaviour of copper scorpionate catalysts in reactions of ethyl diazoacetate (EDA) with various substrates, *e.g.* styrene, 1-phenyl-1-propyne, aniline and ethanol.³

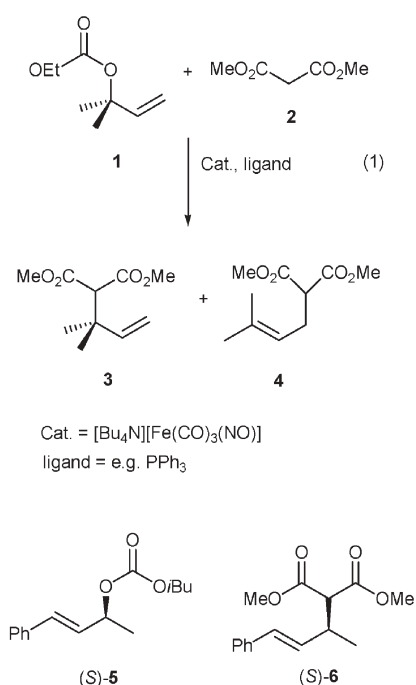
The idea was to use cationic copper complex **1** as the catalyst dissolved in IL



[bmim][PF₆], while the substrate was dissolved in hexane forming the second phase. EDA was added over prolonged periods of time to the reaction mixture and after the reaction ended the IL was washed with hexane. The combined organic extracts were analyzed for the reaction products and showed yields in the 95 to 98% range for styrene, aniline and ethanol. Also the reaction of 1-phenyl-1-propyne to the corresponding cyclopropene proved to be very efficient. Yields up to 77% were achieved and the authors report this reaction to be accomplished successfully for the first time in this biphasic reaction medium. Test experiments indicated that the organic phase does not show any catalytic activity, proving the complete retention of the catalyst in the IL. Recycling experiments showed the catalyst phase to be active in 5 consecutive runs with no loss of activity with conversions for different reactions remaining fairly stable in the 95 to 98% region.

Highly regioselective allylic alkylations *via* salt-free iron catalysis

Allylic alkylations are among the most successful catalytic reactions for carbon–carbon bond formation. While many different catalysts were developed for this type of reaction—with palladium catalysts being the dominant metal in the field—industrial considerations always include cost/efficiency evaluations, which often hinders otherwise well performing catalysts to be used in practical applications. Considerably cheaper catalyst alternatives are desirable, which was one of the reasons why Plietker from the University of Dortmund employed iron based catalysts for allylic alkylations.⁴ The author searched for a method to introduce the novel C–C bond at the carbon atom of the olefinic substrate which carries the leaving group. Though developed some years earlier by Roustan as well as Xu and Zhou, [Bu₄N][Fe(CO)₃(NO)]—containing a formally anionic iron complex—is a useful catalyst for the reaction. Plietker succeeded in introducing appropriate ligands to replace the toxic CO environment which was used in the initial experiments to render an active catalyst.

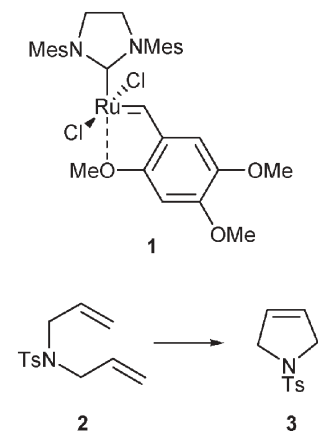


Moreover he found the solvent to be of crucial influence for high conversion and good regioselectivity. Most important is the fact that deprotonation of the pronucleophile is not necessary, when the leaving group is a carbonate—generating a salt free catalytic process which is useful for a wide variety of substrates. Ratios of possible regioisomers could be as high as 98 : 2 with maximum conversion for the reaction shown in eqn (1) of up to 95%. As initial evidence for the postulated σ -allyl mechanism in favor of a π -allyl mechanism the reaction of enantiomerically pure carbonate 5 to yield product 6 which could be accomplished with high enantioselectivity indicating the σ -allyl mechanism to be operative.

Simply reusable homogeneous metathesis catalyst

Modern Grubbs and Hoveyda–Grubbs metathesis catalysts though being very efficient are often contained in the product material to fairly large extents, reaching ruthenium levels of >2000 ppm. This is a drawback with regard to the required product specifications and also from an economical viewpoint as the catalysts are not cheap. Consequently powerful though simple separation methods are desirable. One approach

has recently been pursued by Grell *et al.* from the Polish Academy of Sciences, who introduced the metathesis catalyst **1**, which shows comparable activities to related Hoveyda complexes.



Interestingly the authors discovered that in the ring closing metathesis (RCM) of *N,N*-diallyl-*p*-toluenesulfonamide **2** to yield *N*-*p*-tosyl-2,5-dihydro-1*H*-pyrrole the crude product contained only 83 ppm of Ru according to ICP-MS analyses.⁵ This is a much lower value than obtained before with comparable catalysts and workup techniques. Advantage was taken of the high affinity of **1** to silica gel, which allowed for a very efficient separation of catalyst and product mixture. By simply loading the reaction mixture onto a short silica gel column elution with dichloromethane yielded the desired product while the catalyst remained on the silica gel. Elution of the catalyst was possible subsequently by switching to ethyl acetate. In nine consecutive runs the yield of the reaction product dropped linearly from 96 to 73%. Though not entirely green the discovery might be suitable to complement laboratory techniques for the fast and facile generation of small quantities of metathesis products for biological screening.

McGill University establishes green chemistry chair position

Apart from the interesting scientific results concerned with green chemistry issues during the past few years, more politically oriented decisions support the general need for sustainable chemical development and production. This has been emphasized by the creation of

different scientific or governmental based institutions at various locations around the world. However, chemistry chair positions at universities that are officially devoted to green chemistry, have not been reported to a large extent. Canadian McGill University now plans to establish a green chemistry chair, starting september 1, 2006. Candidates are requested to have a strong background in green chemistry, with the focus

of the position lying on green synthesis. The development of an appropriate teaching and research program is expected. Interested researchers can obtain more information on <http://www.chemistry.mcgill.ca>.

References

- 1 N. B. McKeown, B. Ghanem, K. J. Msayib, P. M. Budd, C. E. Tattershall, K. Mahmood, S. Tan, D. Book, H. W. Langmi and A. Walton, *Angew. Chem.*, 2006, **118**, 1–5.
- 2 R. Hoen, S. Leleu, P. N. M. Botman, V. A. M. Appelman, B. L. Feringa, H. Hiemstra, A. J. Minnaard and J. H. van Maarseveen, *Org. Biomol. Chem.*, 2006, **4**, 613–615.
- 3 P. Rodríguez, A. Caballero, M. M. Díaz-Requejo, M. Carmen Nicasio and P. J. Pérez, *Org. Lett.*, 2006, **8**, 557–560.
- 4 B. Plietker, *Angew. Chem.*, 2006, **118**, 1497–1501.
- 5 A. Michrowska, Ł. Gułajski and K. Grela, *Chem. Commun.*, 2006, 841–843.

Chemical Biology

An exciting news supplement providing a snapshot of the latest developments in chemical biology



Free online and in print issues of selected RSC journals!*

Research Highlights – newsworthy articles and significant scientific advances

Essential Elements – latest developments from RSC publications

Free links to the full research paper from every online article during month of publication

*A separately issued print subscription is also available

RSC Publishing

www.rsc.org/chemicalbiology

30110533

Dissolution of cellulose with ionic liquids and its application: a mini-review

Shengdong Zhu,*^a Yuanxin Wu,^a Qiming Chen,^a Ziniu Yu,^b Cunwen Wang,^a Shiwei Jin,^a Yigang Ding^a and Gang Wu^c

Received 30th January 2006, Accepted 22nd February 2006

First published as an Advance Article on the web 13th March 2006

DOI: 10.1039/b601395c

Dissolution of cellulose with ionic liquids allows the comprehensive utilization of cellulose by combining two major green chemistry principles: using environmentally preferable solvents and bio-renewable feed-stocks. In this paper, the dissolution of cellulose with ionic liquids and its application were reviewed. Cellulose can be dissolved, without derivation, in some hydrophilic ionic liquids, such as 1-butyl-3-methylimidazolium chloride (BMIMCl) and 1-allyl-3-methylimidazolium chloride (AMIMCl). Microwave heating significantly accelerates the dissolution process. Cellulose can be easily regenerated from its ionic liquid solutions by addition of water, ethanol or acetone. After its regeneration, the ionic liquids can be recovered and reused. Fractionation of lignocellulosic materials and preparation of cellulose derivatives and composites are two of its typical applications. Although some basic studies, such as economical syntheses of ionic liquids and studies of ionic liquid toxicology, are still much needed, commercialization of these processes has made great progress in recent years.

1. Introduction

Cellulose is the most abundant renewable resource in the world. The cellulose-containing materials and their derivatives have been widely used in our society. Apart from the use of unmodified cellulose-containing materials, such as wood and cotton, the cellulose can be extracted from its primitive resources (for example, lignocellulosic materials) and then be processed into its derivatives *via* chemical, enzymatic or microbiological methods.^{1–3} The preparation of cellulose

derivatives and their applications have been described in many literatures.^{1,3–6} However, the full potential of cellulose has not yet been exploited for four main reasons: the historical shift to petroleum-based polymers from the 1940s onward, the lack of an environmental-friendly method to extract cellulose from its primitive resources, the difficulty in modifying cellulose properties, and the limited number of common solvents that readily dissolve cellulose.⁷ Traditional cellulose dissolution processes, including the cuprammonium and xanthate processes, are often cumbersome or expensive and require the use of unusual solvents, typically with high ionic strength and use relatively harsh conditions.^{4,7–10} Moreover, these processes sometimes cause serious environmental problems because these solvents cannot be recovered and reused.⁹ In recent years, the “green” comprehensive utilization of cellulose resources has drawn much attention from the governments and researches.^{7,8,10–13} Traditional cellulose extraction and dissolution processes are facing challenges because of the energy and environmental problems.^{8,10,13–15} Therefore, to make full use of cellulose resources, it is necessary to develop “green” cellulose extraction methods and suitable cellulose dissolution approaches.

Ionic liquids are a group of new organic salts that exist as liquids at a relatively low temperature (<100 °C). They have many attractive properties, such as chemical and thermal stability, non-flammability and immeasurably low vapor pressure. In contrast to traditional volatile organic compounds, they are called “green” solvents and have been widely used.^{16,17} Some studies have shown that cellulose can be dissolved in some hydrophilic ionic liquids, for example, 1-butyl-3-methylimidazolium chloride (BMIMCl) and 1-allyl-3-methylimidazolium chloride (AMIMCl).^{7,9} This has been providing a new platform for the “green” comprehensive utilization of cellulose resources. In this paper, the

^aSchool of Chemical Engineering and Pharmacy, Wuhan Institute of Chemical Technology, Hubei Key Laboratory of Novel Chemical Reactor and Green Chemical Technology, Wuhan 430073, P. R. China

^bCollege of Life Science and Technology, Huazhong Agricultural University, Wuhan 430070, P. R. China

^cCollege of Life Science and Technology, Wuhan University, Wuhan 430070, P. R. China



Dr Shengdong Zhu was born in 1968, and studied the comprehensive utilization of cellulose resources and green chemistry at Wuhan Institute of Chemical Technology. He obtained his Master's degree in Chemical Engineering at Shanghai Research Institute of Chemical Industry in 1992, and he gained his PhD degree in Microbiology Engineering at Huazhong Agricultural University in 2005. Since 2000, he has been conducting research on “fuel ethanol production from lignocellulosic materials”.

dissolution of cellulose with ionic liquids and its application were reviewed.

2. Dissolution of cellulose with ionic liquids

As early as 1934, Graenacher discovered that molten *N*-ethylpyridinium chloride, in the presence of nitrogen-containing bases, could be used to dissolve cellulose.¹⁸ This might be the first example of cellulose dissolution using ionic liquids. However, this was thought of little practical value because the concept of ionic liquids had not been put forward at the time. Until recently, the value of dissolution of cellulose with ionic liquids is re-evaluated based on the understanding of ionic liquids. Rogers and his group have carried out comprehensive studies on cellulose dissolution in ionic liquids and its regeneration.^{7,8,19} Because of his great contribution, Rogers has become a winner of the 2005 US Presidential Green Chemistry Challenge Awards. Zhang and his coworkers have also conducted extensive research in this field.^{9,10} Cellulose, whether it is refined or natural, can be dissolved, without derivation, in some hydrophilic ionic liquids such as BMIMCl and AMIMCl.^{8,9} Cellulose solubility and the solution properties can be controlled by selection of the ionic liquid constitutes. Microwave heating can significantly accelerate its dissolution. Solutions containing up to 25 wt% cellulose can be prepared in BMIMCl under microwave heating. The high chloride concentration and activity in BMIMCl, which is assumed highly effective in breaking the extensive hydrogen-bonding network present in cellulose, plays an important role in its dissolution. The presence of water in BMIMCl greatly decreases the solubility of cellulose through competitively hydrogen-bonding its microfibrils.^{7,8} Cellulose is disordered in its BMIMCl solution and this cellulose solvation process was confirmed at the atomic level by high-resolution ¹³C NMR studies.²⁰ When high concentrations of cellulose (>10 wt%) are dissolved in BMIMCl, the liquid crystalline solutions of cellulose, which are optically anisotropic between crossed polarizing filters and displays birefringence, are formed.^{7,8} Cellulose in its BMIMCl solution can be easily precipitated by addition of water, ethanol or acetone. The regenerated cellulose has almost the same degree of polymerization and polydispersity as the initial one, but its morphology is significantly changed and its microfibrils are fused into a relatively homogeneous macrostructure. By changing regeneration processes, the regenerated cellulose can be in a range of structural forms, such as powder, tube, beard, fiber and film. The regeneration processes also have an impact on the regenerated cellulose microstructure. The degree of crystallinity of the cellulose can be manipulated during its regeneration and the cellulose with micro-crystallinity varying from amorphous to crystalline can be obtained under different regeneration conditions. The store time of the cellulose–ionic-liquid solution also affects the regenerated cellulose microstructure. The amorphous cellulose can be obtained after the cellulose–ionic-liquid solution is stored for a few weeks.⁷ The ionic liquids can be recovered and reused after cellulose regeneration. Various methods, such as evaporation, ionic exchange, pervaporation, reverse osmosis and salting out are used to recover the ionic liquid.¹⁹

3. Application

3.3. Fraction of lignocellulosic materials

Lignocellulosic materials have been proposed as large renewable resources for chemicals and sugars to reduce society's dependence on nonrenewable petroleum-based feedstocks.^{21,22} And fraction of lignocellulosic materials has become one of most headache problems in “green” comprehensive utilization of lignocellulosic materials because of the presence of the complex structure of lignin and hemicellulose with cellulose.^{23,24} Based on the fact that cellulose can be dissolved in ionic liquids and it can be easily regenerated from the ionic liquids, Myllymaki and Aksela have found a facile method of fraction of lignocellulosic materials although their objective is delignification from lignocellulosic materials for pulping process.²⁵ Lignocellulosic materials, such as wood and straw, are directly dissolved in BMIMCl under microwave irradiation and/or pressure. Then cellulose is precipitated from the BMIMCl solution by the addition of water, and other organic compounds, such as lignin and extractives, still remain in the solution. In our laboratory, a similar approach is also used to extract cellulose from lignocellulosic materials. Our preliminary results have shown that conversion this extracted cellulose into ethanol has a much higher yield than other refined cellulose, such as from lignocellulosic materials pretreated by steam explosion or chemical pretreatment. Besides the extraction of cellulose from lignocellulosic materials, this method also can be used to extract some natural products. Liu and his group have used this method to extract the essential oil from pine needles.²⁶ It has a much higher essential oil yield than such traditional methods as steam distillation and solvent extraction. However, this essential oil has a different composition from that obtained by steam distillation.

3.2. Preparation of cellulose derivatives

Homogeneous derivation of cellulose has been one focus of cellulose research for a long time, although heterogeneous methods are the actually applied ones in the production of most commercial cellulose derivatives.^{4–6} The advantages of the homogeneous reaction include: creating more options to induce novel functional groups, opening new avenues for the design of products, and opening up the opportunity to control the total degree of substitution.¹⁰ Traditional homogeneous cellulose derivations require the use of unusual solvents, typically with high ionic strength and are used relatively harsh conditions.^{4,7,9} Moreover, these processes sometimes cause serious environmental problems because the solvents cannot be recovered and reused.⁹ Ionic liquids as the “green” reaction media for homogeneous cellulose derivations have drawn much attention in recent years.^{10,27,28} Zhang and his coworkers reported that the homogeneous acetylation of cellulose could be carried out in AMIMCl without any catalysts and cellulose acetates with a wide range of degree of substitution could be obtained.²⁹ Handa and his group found the efficient O-acetylation of cellulose could be accomplished using a zinc based ionic liquid.²⁸ Heinze and Barthel successfully carried out such reactions as acylation and carbonylation of cellulose

in BMIMCl without any catalysts under mild conditions, low excess of reagent and a short reaction time.²⁷ In all these reports, the reaction media (ionic liquids) could be easily recycled and reused.^{10,27,28}

3.3. Preparation of cellulose composites

Preparation of cellulose composites using ionic liquids has broadened the conventional cellulose application scope. It can reduce society's dependence on nonrenewable petroleum-based synthetic polymers. Rogers and his coworkers have prepared various cellulose blended or composite materials.^{29,30} The incorporated functional additives can be either dissolved (e.g., dyes, complexants, other polymers) or dispersed (e.g., nanoparticles, clays, enzymes) in the ionic liquids before or after dissolution of the cellulose. With this simple, non-covalent approach, Rogers and his group can readily prepare encapsulated cellulose composites of tunable architecture, functionality, and rheology. Zhang and his coworkers have prepared wool keratin/cellulose composite materials such as fiber and membrane using BMIMCl as a solvent.³¹ In our laboratory, we have prepared the anti-UV cellulose blending by adding UV filter into the cellulose-BMIMCl solution. In order to prevent the pesticide powder (*Bacillus thuringiensis* crystal protein) degrading in use, we coated this blending on the pesticide powder. The coated pesticide powder was much more stable in use than the uncoated one, whose half-life period extended from 4 to 7 days.

4. Future prospects

The dissolution of cellulose using ionic liquids has been providing a new platform for "green" cellulose utilization. It also provides the possibilities of comprehensive utilization of lignocellulosic materials by fractionation of the lignocellulosic materials with "green" means. This might bring the breakthrough in production of such basic chemical feed-stocks as ethanol and lactic acid from lignocellulosic materials and reduce society's dependence on nonrenewable petroleum-based feed-stocks. A new avenue is opened for solving the environmental and energy problems to maintain social sustainable development. Besides the comprehensive "green" utilization of lignocellulosic materials, it also provides the possibilities of preparation of various advanced materials, including cellulose derivatives and cellulose composites, in place of the synthetic polymers, which biodegrade slowly. In fact, some of the above-mentioned cellulose derivatives and cellulose composites have great potential in industrial applications. For example, the wool keratin/cellulose composite could be used in the textile industry to produce fibers. Although lots of basic studies, such as economical syntheses of ionic liquids and studies of the ionic liquid toxicology, are much needed, commercialization of these processes has made great progress in recent years. In China, the Institute of Process Engineering, Chinese Academy of Sciences and Wuliangyi Corporation have jointly launched a program to produce an anti-bacterial fiber using the wool keratin/cellulose composite technology. BASF has also just taken out a licence on the technology developed by Rogers for industrial production of some advanced materials. It is quite

clear that commercialization of these processes will take place in the near future and we will benefit a lot from these technologies.

Acknowledgements

This work was supported by the Natural Science Foundation of Hubei Province, the Hubei Provincial Department of Education and the National Natural Science Foundation of China.

References

- 1 *Kirk-Othmer Encyclopedia of Chemical Technology*, Wiley, New York, 4th edn, 1993, vol. 5, 476 pp.
- 2 S. D. Zhu, PhD thesis, Huazhong Agricultural University, 2005.
- 3 D. C. Johnson, in *Cellulose Chemistry and its Application*, ed. T. P. Nevell and S. H. Zeronian, E. Horwood, Chichester, 1985, 181 pp.
- 4 T. Heinze and T. Liebert, *Prog. Polym. Sci.*, 2001, **26**, 1689–1762.
- 5 K. J. Edgar, C. M. Buchanan, J. S. Debenham, P. A. Rundquist, B. D. Seiler, C. Michael, M. C. Shelton and D. Tindall, *Prog. Polym. Sci.*, 2001, **26**, 1605–1688.
- 6 S. Fischer, K. Thümmel, K. Pfeiffer, T. Liebert and T. Heinze, *Cellulose*, 2002, **9**, 293–300.
- 7 R. P. Swatloski, R. D. Rogers and J. D. Holbrey, WO Pat., 03/029329, 2003.
- 8 R. P. Swatloski, S. K. Spear, D. John, J. D. Holbrey and R. D. Rogers, *J. Am. Chem. Soc.*, 2002, **124**, 4974–4975.
- 9 H. Zhang, J. Wu, J. Zhang and J. S. He, *Macromolecules*, 2005, **38**, 8272–8277.
- 10 J. Wu, J. Zhang, H. Zhang, J. S. He, Q. Ren and M. L. Guo, *Biomacromolecules*, 2004, **5**, 266–268.
- 11 S. Zhu, Y. Wu, Z. Yu, J. Liao and Y. Zhang, *Process Biochem.*, 2005, **40**, 3082–3086.
- 12 S. Zhu, Y. Wu, Z. Yu, X. Zhang, H. Li and M. Gao, *Chem. Eng. Commun.*, 2005, **192**, 1559–1566.
- 13 R. Reddy and Y. Q. Yang, *Green Chem.*, 2005, **7**, 190–195.
- 14 S. Zhu, Y. Wu, Z. Yu, X. Zhang, C. Wang, F. Yu, S. Jin, Y. Zhao, S. Tu and Y. Xue, *Biosystems Eng.*, 2005, **92**, 229–235.
- 15 S. Zhu, Y. Wu, Z. Yu, X. Zhang, Y. Zhao, S. Tu and Y. Xue, *Chem. Eng. Commun.*, 2006, **193**, 639–648.
- 16 K. R. Seddon, *J. Chem. Technol. Biotechnol.*, 1997, **68**, 351–356.
- 17 *Green Solvents: Synthesis and Application of Ionic Liquids*, ed. R. X. Li, China Chemical Industry Press, Beijing, 2005, pp. 298–300.
- 18 C. Graenacher, US Pat, 1943176, 1934.
- 19 K. E. Gutowski, G. A. Broker, H. D. Willauer, J. G. Huddleston, R. P. Swatloski, J. D. Holbrey and R. D. Rogers, *J. Am. Chem. Soc.*, 2003, **125**, 6632–6633.
- 20 J. S. Moulthrop, R. P. Swatloski, G. Moyna and R. D. Rogers, *Chem. Commun.*, 2005, 1557–1559.
- 21 S. Zhu, Y. Wu, Z. Yu, C. Wang, F. Yu, S. Jin, Y. Ding, R. Chi, J. Liao and Y. Zhang, *Biosystems Eng.*, 2006, **93**, 279–283.
- 22 S. Zhu, Y. Wu, Z. Yu, X. Zhang, C. Wang, F. Yu and S. Jin, *Process Biochem.*, 2006, **41**, 869–873.
- 23 S. Zhu, Y. Wu, Z. Yu, X. Zhang, H. Li and M. Gao, *Bioresour. Technol.*, DOI: 10.1016/j.biortech.2005.08.008.
- 24 Y. Sun and J. Cheng, *Bioresour. Technol.*, 2002, **83**, 1–11.
- 25 V. Myllymaki and R. Aksela, WO Pat, 2005/017001, 2005.
- 26 X. G. Liu, X. R. Ju, X. D. Mao and Z. Zhang, *Chem. Ind. Forest. Prod.*, 2005, **25**, 3, 111–114.
- 27 S. Barthel and T. Heinze, *Green Chem.*, 2006, **8**, 301–306.
- 28 A. P. Abbott, T. J. Bell, S. Handa and B. Stoddart, *Green Chem.*, 2005, **7**, 10, 705–707.
- 29 M. B. Turner, S. K. Spear, J. D. Holbrey and R. D. Rogers, *Biomacromolecules*, 2004, **5**, 1379–1384.
- 30 M. B. Turner, S. K. Spear, J. D. Holbrey, D. T. Daly and R. D. Rogers, *Biomacromolecules*, 2005, **6**, 2497–2502.
- 31 H. B. Xie, S. H. Li and S. B. Zhang, *Green Chem.*, 2005, **7**, 8, 606–608.

Reaction of hydroxybenzyl alcohols under hydrothermal conditions

Tsunehisa Hirashita,^{*a} Shuki Araki,^a Takao Tsuda,^{ab} Shinya Kitagawa,^a Takayuki Umeyama,^a Mutsumi Aoki^c and Koichi Nakamura^{cd}

Received 20th January 2006, Accepted 8th February 2006

First published as an Advance Article on the web 15th February 2006

DOI: 10.1039/b600920d

Under hydrothermal conditions, salicylic alcohol and *p*-hydroxybenzyl alcohol were transformed into phenol in high or moderate yields, whereas *m*-hydroxybenzyl alcohol and benzyl alcohol proved to be stable and remained almost intact.

Organic reactions in water have attracted considerable attention as a way of improving environmentally benign chemical processes, which obviate the need for harmful organic solvents.¹ One of the major obstacles is the poor solubility of organic compounds in ambient water. The properties of water can be tuned to overcome this difficulty by performing the reaction under hydrothermal conditions.² The dielectric constant of water decreases with increasing temperature close to the critical point, which makes it easier to solvate hydrophobic organic compounds in water. In addition, the ionic product of water increases with increasing temperature up to 10^{-11} in the range of 200–300 °C. Hence, the reaction under hydrothermal conditions provides a broad range of possibilities for chemical transformations that are not realized in ambient water.

Recently some researchers have focused their attention on woody biomass due to the growing concern of new energy and chemical resources.³ After cellulose, lignin is the second most abundant polymer on earth.⁴ In order to utilize lignin for any purpose, we must depolymerize lignin and convert it into low molecular weight compounds in an environmentally friendly way. The hydrothermal reaction seems to be a desirable procedure for this and reactions of lignin and related compounds have been documented.⁵ Hydroxybenzyl alcohols can be regarded as some of the model compounds of lignin. However, less attention has been paid to their reactions under hydrothermal conditions. The reactions of hydroxybenzyl alcohols in *organic* solvents at elevated temperature have been reported, where the benzylic cation is considered to be a reactive intermediate and benzyl ethers were mainly formed when alcohols were employed as a solvent.⁶

Here we describe the reaction behaviour of a series of hydroxybenzyl alcohols (Fig. 1), in which the location of the phenolic hydroxy and hydroxymethyl groups proved to be

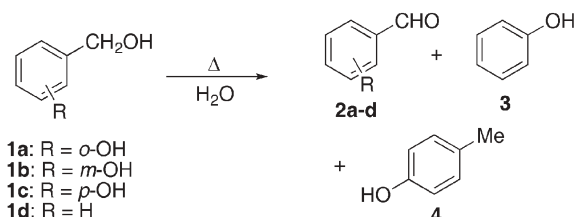


Fig. 1 Reaction of benzyl alcohols under hydrothermal conditions.

important for the level of conversion into phenol under hydrothermal conditions.

The present experiment was conducted with a laboratory made apparatus based on a commercially available HPLC system and a GC oven as shown in Fig. 2.⁷ The sample was dissolved in water containing a small amount of methanol (1%) and the aqueous solution (80 mM) was pumped to the reaction pressure and heated in the oven. The reaction period was regulated by the flow rate of pump A; pump B controlled the pressure by supplying distilled water.⁸ The length of the reactor line was 5 m (0.8 mm id) and the flow rate was adjusted to 0.2 mL min⁻¹ for all experiments. After cooling to room temperature, the products were immediately analyzed by LC and GC-MS. This system permits us to perform a rapid analysis under changing conditions; approximately only 20 min are required to complete a single experiment.

The hydrothermal reaction of salicylic alcohol (**1a**) did not proceed at 200 °C and 22.5 MPa and the starting alcohol was completely recovered (entry 1, Table 1). However, by elevating the temperature up to 300 °C, salicylic aldehyde (**2a**) and phenol (**3**) were obtained in 20% and 65% yields, respectively (entry 2). Under supercritical conditions, **1a** completely disappeared and **2a** and **3** were also obtained (entry 3). *m*-Hydroxybenzyl alcohol (**1b**) was more stable than **1a** under the hydrothermal conditions and the oxidation proceeded at 300 °C to give a small amount of *m*-hydroxybenzaldehyde (**2b**) (entry 4). Phenol (**3**) was not observed from **1b** under supercritical conditions (entry 5). The reaction of *p*-hydroxybenzyl alcohol (**1c**) at 300 °C afforded **3** together with trace amounts of *p*-hydroxybenzaldehyde (**2c**) and *p*-cresol (**4**) (entry 6). It should be noted that the formation of cresol from hydroxybenzyl alcohols was only observed in the case of **1c**. Benzyl alcohol (**1d**) was stable compared with hydroxybenzyl alcohols and small amounts of benzaldehyde (**2d**) were found at 300 °C and 390 °C, with the recovery of unreacted **1d** (entries 8 and 9).

At the high temperature (390 °C), low total yields were obtained (entries 3, 5, and 7). We found unidentified resinous materials between the cooling loop and the sample collecting loop, indicating some side reactions took place to cause the erosion of the mass balance.

^aDepartment of Materials Science and Engineering, Graduate School of Engineering, Nagoya Institute of Technology, Gokiso, Showa, Nagoya 466-8555, Japan. E-mail: hirasita@nitech.ac.jp; Fax: +81 52-735-5206; Tel: +81 52-735-5206

^bPico-Device Co., Ltd., Incubation Center, Nagoya Institute of Technology, Gokiso, Showa, Nagoya 466-8555, Japan

^cDepartment of Computer Science and Engineering, Graduate School of Engineering, Nagoya Institute of Technology, Gokiso, Showa, Nagoya 466-8555, Japan

^dKaela R&D Co., Inc., Incubation Center, Nagoya Institute of Technology, Gokiso, Showa, Nagoya 466-8555, Japan

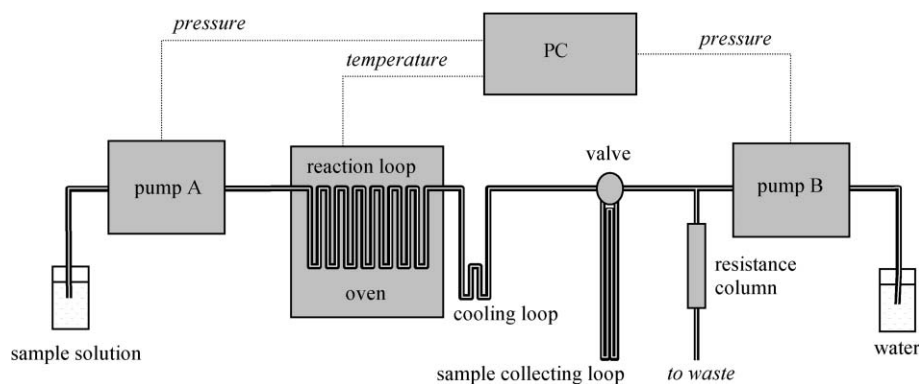
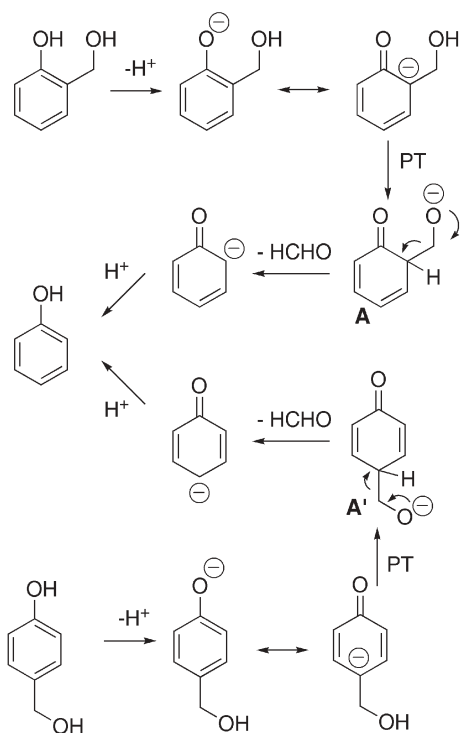


Fig. 2 Apparatus for hydrothermal reactions.

Table 1 Results of hydrothermal treatment of a series of benzyl alcohols

Entry	1	$T/^\circ\text{C}$	P/MPa	Yield and recovery (%)			
				2	3	4	1
1	1a	200	22.5	<1	<1	0	>99
2	1a	300	22.5	20	65	0	17
3	1a	390	23.5	7	63	0	0
4	1b	300	22.5	2	0	0	98
5	1b	390	23.5	39	0	0	32
6	1c	300	22.5	<1	34	3	56
7	1c	390	23.5	1	21	24	11
8	1d	300	22.5	<1	0	0	86
9	1d	390	23.5	8	0	0	85

A most plausible mechanism to form phenol is depicted in Scheme 1. The formation of phenol may be attributed to a facile dissociation of the phenolic proton under the hydrothermal conditions. The resulting phenoxide liberates formaldehyde *via*



Scheme 1 Plausible reaction pathway to form phenol.

proton transfer leading to phenol. The distinctive reaction behaviour observed in 1a and 1c reveals the crucial contribution of the intermediates A and A' which can be easily transformed into phenol by release of formaldehyde. The highest conversion was achieved with the reaction of 1a in which the *o*-hydroxymethyl group is considered to promote a dissociation of the phenolic hydroxy proton under the hydrothermal conditions.⁹

The present results provide informative examples for depolymerization of lignin and related compounds under hydrothermal conditions. Further studies for transformation of organic compounds using this system are currently in progress.

Acknowledgements

This work was supported by the special research foundation program of Nagoya Institute of Technology, and the joint research foundation with Toenec Co., Ltd.

References

- (a) *Organic Reactions in Aqueous Media*, ed. C. J. Li and T. H. Chan, Wiley, New York 1997; (b) *Organic Synthesis in Water*, ed P. A. Grieco, Blackie Academic & Professional, London 1998; (c) C.-J. Li, *Chem. Rev.*, 1993, **93**, 2023; (d) U. M. Lindström, *Chem. Rev.*, 2002, **102**, 1751.
- (a) *High Pressure Chemistry: Synthetic, Mechanistic, and Supercritical Applications*, ed R. van Eldik and F.-G. Klärner, Wiley-VCH, Weinheim, 2002; (b) P. E. Savage, *Chem. Rev.*, 1999, **99**, 603; (c) N. Akiya and P. E. Savage, *Chem. Rev.*, 2002, **102**, 2725.
- T. Nussbaumer, *Energy Fuels*, 2003, **17**, 1510.
- (a) *Lignins: Occurrence, Formation, Structure, and Reactions*, ed. K. V. Sarkanen and C. H. Ludwig, Wiley-Interscience, New York, 1971; (b) *Lignin: Historical, Biological, and Materials Perspectives, American Chemical Society Symposium Series 742*, ed. W. G. Glasser, R. A. Northey and T. P. Schultz, American Chemical Society, Washington, DC, 2000.
- (a) G. L. Huppert, B. C. Wu, S. H. Townsend, M. T. Klein and S. C. Paspek, *Ind. Eng. Chem. Res.*, 1989, **28**, 161; (b) J. R. Lawson and M. T. Klein, *Ind. Eng. Chem. Fundam.*, 1985, **24**, 203; (c) C. J. Martino and P. E. Savage, *Ind. Eng. Chem. Res.*, 1999, **38**, 1784; (d) T. Yoshida, Y. Oshima and Y. Matsumura, *Biomass Bioenergy*, 2004, **26**, 71; (e) M. Osada, T. Sato, M. Watanabe, T. Adschiri and K. Arai, *Energy Fuels*, 2004, **18**, 327; (f) G. González and D. Montañé, *AIChE J.*, 2005, **51**, 971.
- E. Dorrestijn, M. Kranenburg, M. V. Ciriano and P. Mulder, *J. Org. Chem.*, 1999, **64**, 3012.
- T. Tsuda, S. Kitagawa, T. Umeyama, S. Araki, T. Hirashita, M. Aoki and K. Nakamura, *Anal. Sci.*, 2006, **22**, in press.
- Y. Miyake, N. Yamasaki, S. Kitagawa and T. Tsuda, *Proceedings of the International Symposium on Hydrothermal Reactions*, Changchun, China, 7th edn, 2003, p. 161.
- H.-G. Korth, M. I. de Heer and P. Mulder, *J. Phys. Chem. A*, 2002, **106**, 8779.

Highly regioselective ring-opening of epoxides with thiophenols in ionic liquids without the use of any catalyst†

Jiuxi Chen,^a Huayue Wu,^a Can Jin,^b Xingxian Zhang,^b Yuanyuan Xie^b and Weike Su^{*ab}

Received 16th January 2006, Accepted 2nd March 2006

First published as an Advance Article on the web 10th March 2006

DOI: 10.1039/b600620e

Clean thiolysis reaction of various epoxides in ionic liquids (ILs) without the use of any catalyst generates β -hydroxy sulfides in excellent yields (83–98%) with high regioselectivity and chemoselectivity under mild reaction conditions.

The highly strained three membered ring in epoxide molecules makes them susceptible to reaction with various nucleophiles. Ring-opening of epoxides is an atom economical reaction. Moreover, highly regioselective products could be obtained under the given reaction conditions.¹ Due to these advantages, epoxides are widely used as starting materials and intermediates in organic synthesis.²

β -Hydroxy sulfides are important compounds, which have become increasingly important in medicinal chemistry and organic synthesis for the preparation of building blocks and target molecules.³ One of the most practically and widely used routes for the synthesis of these compounds is the direct thiolysis of epoxides with thiols in different organic solvents in the presence of Lewis acids.⁴ Recently, a new methodology for the ring opening of epoxides with thiophenols was reported in water⁵ or under solvent-free conditions (SFC).⁶ However, there are some limitations with these methodologies such as use of an excess of thiols and environmentally unfriendly catalyst or relatively long reaction periods.

Ionic liquids have received recognition as green media in organic synthesis due to the ease of tuning physical–chemical properties.⁷ Therefore, ionic liquids have found wide use in various chemical reactions^{7a,b} and biotransformations.⁸ To the best of our knowledge, there are no examples on the use of ionic liquids for the conversion of epoxides to β -hydroxy sulfides.

Herein, we report that ionic liquids could be used as efficient reaction media in the ring-opening reaction of epoxides with thiophenols.

Initially, we investigated the thiolysis of 1,2-epoxy-3-phenoxypropane by using stoichiometric amounts of 4-thiocresol at 50 °C under different reaction media, and the results are illustrated in Table 1.

Surprisingly, we found that this reaction could be performed in 1-ethyl-3-methylimidazolium tetrafluoroborate ([Emim]BF₄), 1-butyl-3-methylimidazolium tetrafluoroborate ([Bmim]BF₄),

1-butylpyridinium tetrafluoroborate ([Bpy]BF₄), 1-butyl-3-methylimidazolium chloride ([Bmim]Cl), 1-butylpyridinium bromide ([Bpy]Br) for 10 min without the use of any catalyst in excellent yields (Table 1, entries 2, 4, 6). The reaction of 1,2-epoxy-3-phenoxypropane with 4-thiocresol in organic solvent (CH₃CN, CH₃NO₂, CH₂Cl₂) or under solvent-free conditions gave lower conversions even when the reaction was prolonged to 60 min (Table 1, entries 9–12). Compared to common organic solvents, the unique feature of the ionic liquids used was based on their well-organized hydrogen-bonded polymeric supramolecule structure, which helped to introduce other molecules to form inclusion compounds.⁹ Unexpectedly, their hexafluorophosphate analogue (Table 1, entries 1, 3, 5) showed unsatisfactory yield compared to other ionic liquids (Table 1, entries 2, 4, 6, 7, 8) in this thiolysis reaction. In addition, [Emim]BF₄ has the lowest viscosity and is easy to operate. Therefore, [Emim]BF₄ was chosen as the reaction media as the research was extended to other epoxides and other thiophenols without the use of any catalyst.

Table 2 illustrates the results of the thiolysis of variously substituted 1,2-epoxides in [Emim]BF₄ at 50 °C. In our experiment,¹⁰ the nucleophilic attack of thiophenols occurred almost exclusively on the less substituted α -carbon of all the epoxides with the exception of styrene oxide, in which the attack of the nucleophile is driven predominantly, as expected, at the benzylic β -carbon by electronic effects (Table 2, entries 9, 10). Moreover, when AlCl₃ was used as Lewis acid catalyst, the β -regioselective

Table 1 Thiolysis of 1,2-epoxy-3-phenoxypropane by 4-thiocresol under different reaction conditions at 50 °C^a

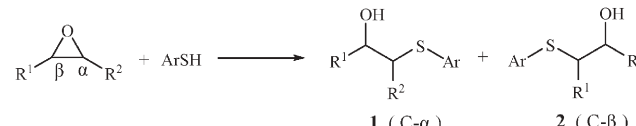
Entry	Reaction medium	Time/min	Yield (%) ^b
1	[Emim]PF ₆	60	65
2	[Emim]BF ₄	10	95
3	[Bmim]PF ₆	60	61
4	[Bmim]BF ₄	10	94
5	[BPy]PF ₆	60	60
6	[BPy]BF ₄	10	95
7	[Bmim]Cl	10	87
8	[Bpy]Br	10	85
9	CH ₃ CN	60	43 ^c
10	CH ₃ NO ₂	60	42 (49)
11	CH ₂ Cl ₂	60	48 (53)
12	SFC	60	47 (50)

^a For a typical experimental procedure, see ref. 10. ^b Isolated total yield (isolated total yield if the reaction was carried out at 50 °C for 24 h). ^c Reflux temperature.

^a College of Chemistry and Materials Science, Wenzhou University, Wenzhou, 325027, P. R. China. E-mail: suweike@zjut.edu.cn; Fax: +86 571 88320752

^b College of Pharmaceutical Sciences, Zhejiang University of Technology, Zhejiang Key Laboratory of Pharmaceutical Engineering, Hangzhou, 310014, P. R. China

† Electronic supplementary information (ESI) available: Experimental details and characterisation data. See DOI: 10.1039/b600620e

Table 2 Ring-opening reaction in [Emim]BF₄^a


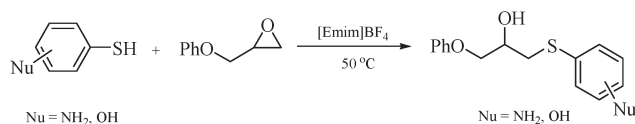
Entry	Epoxide		Thiophenols	Product	Yield (%) ^b	Regioselectivity (α/β) ^c
	R ¹	R ²				
1	PhOCH ₂	H	C ₆ H ₅ SH	1a	97	98/2
2	PhOCH ₂	H	<i>p</i> -(CH ₃)C ₆ H ₄ SH	1b	95	>99/1
3	PhOCH ₂	H	<i>p</i> -(F)C ₆ H ₄ SH	1c	93	>99/1
4	PhOCH ₂	H	2,3-(Cl) ₂ -C ₆ H ₃ SH	1d	94	97/3
5	PhOCH ₂	H	<i>p</i> -(Br)C ₆ H ₄ SH	1e	93	>99/1
6	PhOCH ₂	H	2-(NH ₂)-4-(Cl)C ₆ H ₃ SH	1f	92	98/2
7	PhOCH ₂	H	<i>o</i> -(CH ₃ O)C ₆ H ₄ SH	1g	98	>99/1
8	PhOCH ₂	H	<i>m</i> -(OH)C ₆ H ₄ SH	1h	91	>99/1
9	Ph	H	C ₆ H ₅ SH	2i, 1i	90 (93) ^d	28/72 (7/93)
10	Ph	H	<i>m</i> -(OH)C ₆ H ₄ SH	2j, 1j	88 (94) ^d	35/65 (6/94)
11	-(CH ₂) ₄ -	H	2-(NH ₂)-4-(Cl)C ₆ H ₃ SH	1k	93	—
12	-(CH ₂) ₄ -	H	<i>p</i> -(F)C ₆ H ₄ SH	1l	90	—
13	-(CH ₂) ₆ -	H	C ₆ H ₅ SH	1m	87	—
14	CH ₃	H	<i>p</i> -(F)C ₆ H ₄ SH	1n	84 (91) ^e	>99/1
15	CH ₃	H	<i>p</i> -(Br)C ₆ H ₄ SH	1o	83 (94) ^e	>99/1
16	CH ₃	H	2,4-(CH ₃) ₂ C ₆ H ₃ SH	1p	84 (92) ^e	98/2
17	CH ₂ Cl	H	<i>p</i> -(F)C ₆ H ₄ SH	1q	93 (93) ^f	98/2
18	CH ₂ Cl	H	<i>m</i> -(OH)C ₆ H ₄ SH	1r	94 (94) ^f	>99/1
19	CH ₂ Cl	H	2,3-(Cl) ₂ -C ₆ H ₃ SH	1s	94 (92) ^f	97/3
20	CH ₃ (CH ₂) ₅	H	<i>o</i> -(F)C ₆ H ₄ SH	1t	90	94/6

^a Reaction conditions: epoxide (2 mmol), thiophenols (2 mmol), and [Emim]BF₄ (1 mL), 50 °C, 10 min. ^b Isolated total yield. ^c Ratios of the two regioisomers were determined by 400 MHz ¹H NMR. ^d The reaction was run in [Emim]BF₄ in the presence of 1 equiv. of AlCl₃ at 50 °C. ^e The reaction was run at room temperature for 4 h. ^f The reaction was run at 50 °C for 5 min.

products (**2i**, **2j**) were obviously increased and the yield were also increased greatly (Table 2, entries 9, 10).

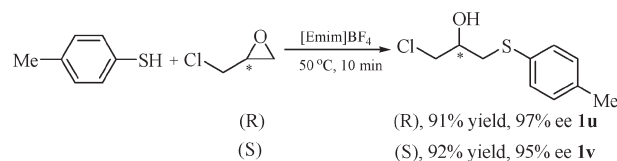
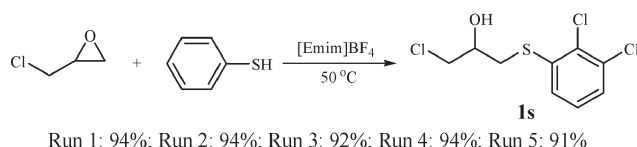
The procedure worked well with thiophenols bearing a variety of substituents (see Table 2). Not only less hindered thiophenols but also sterically more hindered thiophenols led to the product in excellent yields. When less nucleophilic thiophenols (entries 3, 12, 14, 17, 20) were used, the reaction could also work efficiently compared to electron rich thiophenols (entries 7, 8, 10, 18) under the same conditions. On the other hand, this reaction gave high chemoselective product with thiophenols bearing different nucleophilic groups (entries 6, 8, 10, 11, 18; Scheme 1). The reaction was completed with nucleophilic attack of the thiohydroxy, and the hydroxy or amino group remained untouched.

To extend the scope of the ring-opening reaction, the thiolysis of (*R*)-epichlorohydrin^{11a} or (*S*)-epichlorohydrin^{11b} was also studied in [Emim]BF₄. The reaction was found to be highly regioselective and stereospecific, which demonstrated original chirality in the epoxides was remained. The corresponding products (**1u**, **1v**) were obtained in excellent yield and high ee value (Scheme 2). Enantiopure β -hydroxy sulfides are widely used as chiral building blocks for the synthesis of a variety of chiral organic compounds.¹²

**Scheme 1** Chemoselective thiolysis of epoxides.

Next, we investigated the recycling of the ionic liquid in subsequent thiolysis, for example, thiolysis of epichlorohydrin with 2,3-dichlorothiophenol (Scheme 3). The ionic liquid ([Emim]BF₄) was reused for five runs without any appreciable loss of activity.

In summary, we report that [Emim]BF₄, [Bmim]BF₄, [Bpy]BF₄, [Bmim]Cl, and [Bpy]Br are convenient and efficient reaction media for the ring-opening reaction of epoxides with thiophenols. The title reactions proceeded smoothly in ionic liquid without the use of any catalyst. This method generates β -hydroxy sulfides in excellent yields with high regioselectivity and chemoselectivity. Obviously, the advantages of this method include using recyclable ionic liquid as reaction media, high regioselectivity and chemoselectivity, high yields, fast reaction, simple operations and it is

**Scheme 2** Thiolysis of chiral epoxides.**Scheme 3** Reusing of ionic liquid in subsequent thiolysis reactions.

environmentally benign. Further applications of ionic liquids in green synthesis are ongoing in our group.

Acknowledgements

We are grateful to the National Basic Research Program (No. 2003CB114402), National Natural Science Foundation of China (No. 20276072 and 20476098) and Natural Science Foundation of Zhejiang Province (No. 2002095) and Wenzhou University for financial support.

Notes and references

- J. Cossy, V. Bellosta, C. Hamoir and J. R. Desmurs, *Tetrahedron Lett.*, 2002, **43**, 7083; J. S. Yadav, B. V. S. Reddy, A. K. Basak and A. V. Narsaiah, *Tetrahedron Lett.*, 2003, **44**, 1047; J. S. Yadav, B. V. S. Reddy, B. Jyothirmai and M. S. R. Murty, *Tetrahedron Lett.*, 2005, **46**, 6559.
- A. S. Rao, S. K. Paknikar and J. G. Kirtane, *Tetrahedron*, 1983, **39**, 2323; J. Gorzyski Smith, *Synthesis*, 1984, 629; R. M. Hanson, *Chem. Rev.*, 1991, **91**, 437; C. Bonini and G. Righi, *Synthesis*, 1994, 225; D. M. Hodgson, A. R. Gibbs and G. P. Lee, *Tetrahedron*, 1996, **52**, 14361; M. H. Bolli and S. V. Ley, *J. Chem. Soc., Perkin Trans. 1*, 1998, 2243; A. K. Ghosh and Y. Wang, *J. Org. Chem.*, 1999, **64**, 2789.
- E. J. Corey, D. A. Clark, G. Goto, A. Marfat, C. Mioskowski, B. Samuelsson and S. Hammarström, *J. Am. Chem. Soc.*, 1980, **102**, 1436; A. Conchillo, F. Camps and A. Messeguer, *J. Org. Chem.*, 1990, **55**, 1728; J. R. Luly, N. Yi, J. Soderquist, H. Stein, J. Cohen, T. J. Perun and J. J. Plattner, *J. Med. Chem.*, 1987, **30**, 1609; R. McCague, T. C. Nugent and S. M. Roberts, *J. Chem. Soc., Perkin Trans. 1*, 1997, 3501.
- H. Yamashita, *Bull. Chem. Soc. Jpn.*, 1988, **61**, 1213; T. Iida, N. Yamamoto, H. Sasai and M. Shibasaki, *J. Am. Chem. Soc.*, 1997, **119**, 4783; S. Fukuzawa, H. Kato, M. Ohtaguchi, Y. Hayashi and H. Yamazaki, *J. Chem. Soc., Perkin Trans. 1*, 1997, 3059; M. H. Wu and E. N. Jacobsen, *J. Org. Chem.*, 1998, **63**, 5252; J. Wu, X.-L. Hou, L.-X. Dai, L.-J. Xia and M.-H. Tang, *Tetrahedron: Asymmetry*, 1998, **9**, 3431; J. S. Yadav, B. V. S. Reddy and G. Baisha, *Chem. Lett.*, 2002, 906; S. Chanrasekar, C. R. Reddy, B. N. Babu and G. Chandrashekar, *Tetrahedron Lett.*, 2002, **43**, 3801; D. Albanese, D. Landini and M. Penso, *Synthesis*, 1994, 34; P. N. Guivisdalsky and R. Bittman, *J. Am. Chem. Soc.*, 1989, **111**, 3077; J. Choi and N. M. Yoon, *Synthesis*, 1995, 373; M. R. Younes, M. M. Chaabouni and A. Baklouti, *Tetrahedron Lett.*, 2001, **42**, 3167; Z.-M. Li, Z.-H. Zhou, K.-Y. Li, L.-X. Wang, Q.-L. Zhou and C.-C. Tang, *Tetrahedron Lett.*, 2002, **43**, 7609; V. Polshettiwar and M. P. Kaushik, *Catal. Commun.*, 2004, **5**, 515; M. Bandini, M. Fagioli, A. Melloni and A. Umani-Ronchi, *Adv. Synth. Catal.*, 2004, **346**, 573; M. M. Mojtahedi, M. H. Ghasemi, M. S. Abaee and M. Bolourtchian, *ARKIVOC*, 2005, 68; J. Wu and H.-G. Xia, *Green Chem.*, 2005, **7**, 708.
- D. Amantini, F. Fringuelli, F. Pizzo, S. Tortoioli and L. Vaccaro, *Synlett*, 2003, **15**, 2292; F. Fringuelli, F. Pizzo, S. Tortoioli and L. Vaccaro, *J. Org. Chem.*, 2003, **68**, 8248; F. Fringuelli, F. Pizzo, S. Tortoioli and L. Vaccaro, *Adv. Synth. Catal.*, 2002, **344**, 379 and references therein; F. Fringuelli, F. Pizzo, S. Tortoioli and L. Vaccaro, *Org. Lett.*, 2005, **7**, 4411; V. Pironti and S. Colonna, *Green Chem.*, 2005, **7**, 43; R.-H. Fan and X.-L. Hou, *J. Org. Chem.*, 2003, **68**, 726.
- F. Fringuelli, F. Pizzo and L. Vaccaro, *J. Org. Chem.*, 2004, **69**, 8780; F. Fringuelli, F. Pizzo, S. Tortoioli and L. Vaccaro, *Tetrahedron Lett.*, 2003, **44**, 6785.
- (a) T. Welton, *Chem. Rev.*, 1999, **99**, 2071; (b) P. Wasserscheid and W. Keim, *Angew. Chem., Int. Ed.*, 2000, **39**, 3772; (c) J. Dupont, R. F. de Souza and P. A. Z. Suarez, *Chem. Rev.*, 2002, **102**, 3667.
- G. R. Castro and T. Knubovets, *Crit. Rev. Biotechnol.*, 2003, **23**, 195; S. J. Nara, S. S. Mohile, J. R. Harjani, P. U. Naik and M. M. Salunkhe, *J. Mol. Catal. B: Enzym.*, 2004, **28**, 39.
- J. Dupont, *J. Braz. Chem. Soc.*, 2004, **15**, 341.
- Representative procedure: To a mixture of 1,2-epoxy-3-phenoxypropane (300.4 mg, 2 mmol) and 4-thiocresol (248 mg, 2 mmol), [Emim]BF₄ (1 mL) was added. The mixture was stirred at 50 °C for 10 min. After completion of the reaction, as indicated by TLC, the reaction mixture was extracted with diethyl ether (3 × 10 mL). The combined ether extracts were concentrated *in vacuo* and the crude product **1b** was obtained. The corresponding purified form was obtained by flash column chromatography. Selected data for compounds **1e**: *R*_f = 0.4 (petroleum ether/EtOAc = 6 : 1); ¹H NMR (400 MHz, CDCl₃): δ (ppm) = 7.33 (d, *J* = 8.0 Hz, 2 H), 7.27–7.20 (m, 4 H), 6.95 (t, *J* = 7.2 Hz, 1 H), 6.84 (d, *J* = 8.0 Hz, 2 H), 4.08–3.98 (m, 3 H), 3.19 (dd, *J* = 13.6, 5.6 Hz, 1 H), 3.12 (br s, 1 H, OH), 3.09 (dd, *J* = 13.6, 6.8 Hz, 1 H). ¹³C NMR (100 MHz, CDCl₃): δ (ppm) = 158.0, 134.4, 131.9, 130.9, 129.4, 121.1, 120.2, 114.3, 69.7, 68.4, 37.2. IR (neat): 3418, 3061, 2925, 1599, 1496, 1474, 1243, 1091, 1007, 810, 754, 691 cm⁻¹. *m/z* (EI) 340 ([M + 2]⁺, 88), 340 (M⁺, 100), 247 (33), 245 (36), 229 (23), 227 (18), 33 (36). Found: C, 53.19; H, 4.50. Anal. calcd for C₁₅H₁₅BrO₂S: C, 53.11; H, 4.46. **1n**: *R*_f = 0.4 (petroleum ether/EtOAc = 6 : 1); ¹H NMR (400 MHz, CDCl₃): δ (ppm) = 7.41–7.38 (m, 2 H), 7.00 (t, *J* = 8.4 Hz, 2 H), 3.85–3.77 (m, 1 H), 3.04 (dd, *J* = 13.6, 3.6 Hz, 1 H), 2.81 (dd, *J* = 13.6, 8.4 Hz, 1 H), 2.67 (br s, 1 H, OH), 1.25 (d, *J* = 6.4 Hz, 3 H). ¹³C NMR (100 MHz, CDCl₃): δ (ppm) = 162.0 (d, *1J*_{CF} = 245.7 Hz), 133.0 (d, *3J*_{CF} = 8.3 Hz), 130.0, 116.1 (d, *2J*_{CF} = 21.2 Hz), 65.4, 44.7, 21.8. IR (neat): 3404, 2971, 2926, 1590, 1491, 1456, 1228, 1157, 1090, 824, 629 cm⁻¹. *m/z* (EI) 186 (M⁺, 100), 169 (77), 141 (13). Found: C, 58.12; H, 5.86. Anal. calcd for C₉H₁₁FOS: C, 58.04; H, 5.95. **1s**: *R*_f = 0.4 (petroleum ether/EtOAc = 6 : 1); ¹H NMR (400 MHz, CDCl₃): δ (ppm) = 7.32–7.35 (m, 2 H), 7.21–7.10 (m, 1 H), 4.04–3.98 (m, 1 H), 3.72 (d, *J* = 4.8 Hz, 2 H), 3.22 (dd, *J* = 14.0, 5.6 Hz, 1 H), 3.12 (dd, *J* = 14.0, 6.8 Hz, 1 H), 2.83 (br s, 1 H, OH). ¹³C NMR (100 MHz, CDCl₃): δ (ppm) = 137.0, 133.7, 131.7, 127.9, 127.5, 126.6, 69.3, 48.0, 36.8. IR (neat): 3388, 2955, 2923, 1565, 1435, 1399, 1043, 767, 697 cm⁻¹. *m/z* (EI) 276 ([M + 6]⁺, 5), 274 ([M + 4]⁺, 33), 272 ([M + 2]⁺, 94), 270 (M⁺, 100), 255 (42), 253 (48), 193 (46), 191 (74), 142 (31). Found: C, 39.86; H, 3.26. Anal. calcd for C₉H₉C₁₃OS: C, 39.80; H, 3.34.
- The reagents were purchased from Shanghai KeLy Bio-Pharmaceutical Co., Ltd., (a) the optical purity is 99%; (b) the optical purity is 98%.
- B. T. Cho and D. J. Kim, *Tetrahedron*, 2003, **59**, 2457; S. France, H. Wack, A. E. Taggi, A. M. Hafez, T. R. Wagerle, M. H. Shah, C. L. Dusich and T. Lectka, *J. Am. Chem. Soc.*, 2004, **126**, 4245; M. Wielechowska and J. Plenkiewicz, *Tetrahedron: Asymmetry*, 2005, **16**, 1199.

Oxidative coupling revisited: solvent-free, heterogeneous and in water†

Philip J. Wallis,^a Katrina J. Booth,^a Antonio F. Patti^{ab} and Janet L. Scott^{*a}

Received 21st December 2005, Accepted 22nd February 2006

First published as an Advance Article on the web 13th March 2006

DOI: 10.1039/b518132a

Fe(III) treated K-10 montmorillonite and FeCl₃ (both hydrated and anhydrous) are compared as catalysts for oxidative coupling of phenol substrates under a range of conditions. While the commonly reported coupling of 2-naphthol proceeds under a range of conditions, other substrates are far less readily coupled. Counterintuitively, biphasic reactions of poorly water soluble substrates in contact with aqueous solutions of FeCl₃ are the most universally applicable conditions while many homogeneous reaction mixtures yield little or no coupling product. Fe(III) treated K-10 proved to be a poor catalyst for oxidative coupling of most substrates. Comparison of coupling conditions provides a framework for optimisation of green methodologies using oxidative coupling catalysts.

Introduction

The formation of C–C linked biaryl dimers is an important synthetic tool, and is involved in the biosynthesis of natural products containing biaryl linkages.¹ Additionally, oxidative coupling is believed to be an important process in the formation of humic materials in soils *via* enzymatic and abiotic routes.² Understanding such synthetic processes on a molecular scale is the basis of ongoing study within our group. The knowledge obtained from soil chemistry studies and from the wider soil literature, aids understanding of the inorganic/abiotic processes which promote C–C bond formation, from a synthetic point of view.³

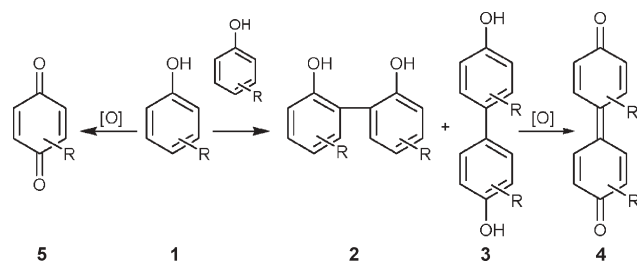
The oxidative dimerisation of phenols is a long-established reaction, which can be promoted stoichiometrically by FeCl₃·6H₂O,^{4,5} and catalytically by Cu(II)-amine complexes⁶ as well as supported transition metals.⁷ The coupling mechanism is believed to involve either one two-electron or two one-electron oxidations to form an aryl-aryl coupled dimer through the *ortho* **2** and/or *para* positions **3** (Scheme 1).^{5,8} Protonation

of the phenol, as determined by pH, can also influence the coupling mechanism, and overall two protons and two electrons are lost during coupling.⁹ In some cases, competing and/or subsequent oxidation to form quinones occurs, either from the coupled product **4** or the original substrate **5**.

Modified clay minerals are commonly used as heterogeneous catalysts in organic synthesis¹⁰ and oxidative coupling of phenols has been effected using clay-supported transition metals,^{7,11,12} as naturally derived, environmentally benign and re-useable heterogeneous catalysts. Treating clays with transition metal ions, such as Cu(II) or Fe(III) salts, causes ion-exchange and surface adsorption of these hydrated cations, increasing the Lewis acidity and redox activity of the clay. K-10 montmorillonite is a commercially available clay that is acid-treated to increase surface area, and to effect protonation of the remaining negatively charged exchange sites. While K-10 is not a particularly pure or structurally intact clay, it is easily obtained and modified for use in organic synthesis, hence its ongoing popularity.

Remarkably, when we sought to compare the activity of the potentially green catalysts, Fe(III) treated clays, with various other methods described in the literature, it appeared that many of the greener methods described were so highly substrate specific, that procedures to effect oxidative coupling were not universally applicable and also exhibited some surprising phase dependence.

In this paper a range of coupling conditions, utilising either FeCl₃ (both in the hexahydrate and anhydrous forms), or Fe(III) treated clays as oxidants/catalysts in solvents (toluene, acetonitrile, water) or solvent-free, were compared in the oxidative coupling of a varied group of substrates.



Scheme 1 Coupling of substituted phenols to form *o-o'* **2** or *p-p'* **3** dimers.

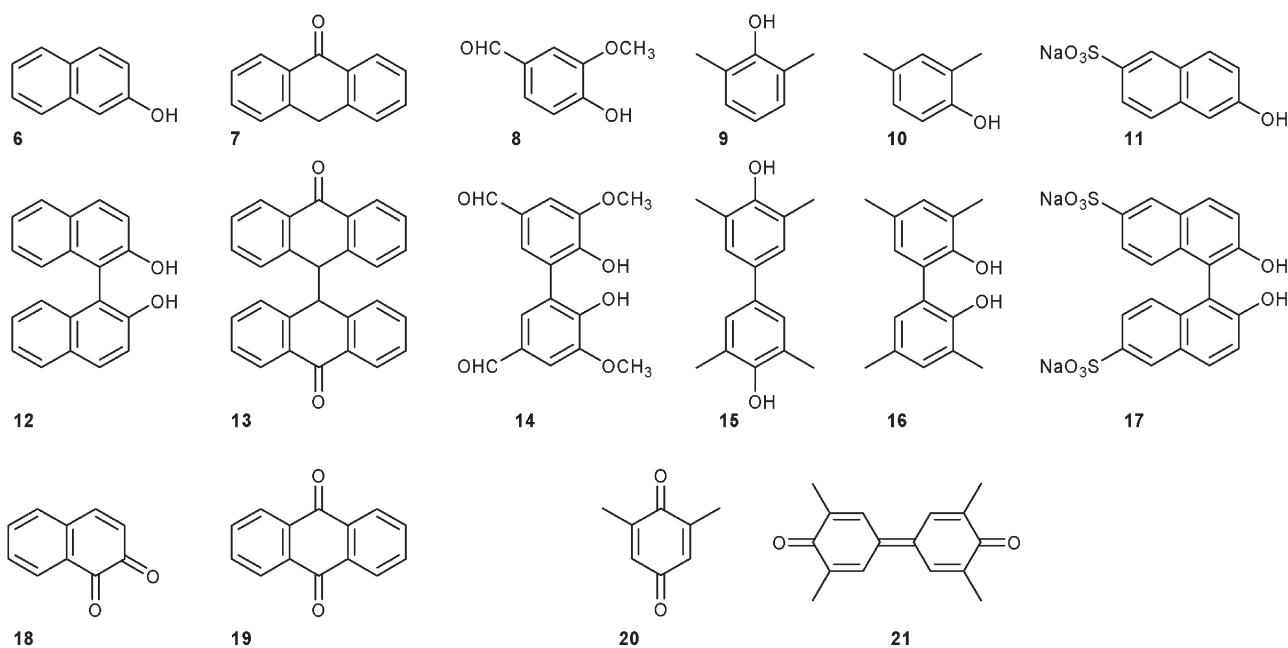
^aCentre for Green Chemistry, Monash University, Melbourne, Australia. E-mail: Janet.Scott@sci.monash.edu.au; Fax: +61 03 99054597; Tel: +61 03 99054600

^bSchool of Applied Sciences and Engineering, Monash University, Churchill, Australia. E-mail: Antonio.Patti@sci.monash.edu.au; Fax: +61 03 99054597; Tel: +61 03 99051620

† Electronic supplementary information (ESI) available: additional experimental data. See DOI: 10.1039/b518132a

Results and discussion

Substrates for oxidative coupling are depicted in Scheme 2. 2-Naphthol **6**, as the most often referred to substrate in reports of new or more effective oxidative coupling reactions, was tested alongside anthrone **7**, vanillin **8**, 2,6-dimethylphenol **9**, 2,4-dimethylphenol **10** and sodium 6-hydroxynaphthalene-2-sulfonate **11** to yield variously, C–C biaryl coupled products



Scheme 2 Substrates and products. Substrates **6**, **7**, **8**, **10** and **11** yield coupled products **12**, **13**, **14**, **16** and **17** while **9** provides the further oxidised diphenoquinone **21** along with **15**. Oxidation of substrates **6**, **7** and **9** to yield **18**, **19** and **20** competes with biaryl coupling.

12–17 or diphenoquinone **21**. Anthrone is reported to undergo keto-enol tautomerism to 9-anthrol in the presence of transition metals, including FeCl_3 .¹³ Some competitive substrate oxidation without coupling to yield naphthoquinone **18**, anthraquinone **19** or benzoquinone **20** occurred under some conditions tested.

Catalysts Fe(III) treated K-10 montmorillonite and $\text{FeCl}_3 \cdot 6\text{H}_2\text{O}$ (or dehydrated) were employed under a range of conditions similar to those previously described: Fe(III) treated clays,⁷ in biphasic systems with aqueous FeCl_3 ,^{4,14} so-called ‘solid-state’,⁵ and using acetonitrile as solvent, as well as a two-phase toluene/molten $\text{FeCl}_3 \cdot 6\text{H}_2\text{O}$ system.

Results are summarised in Table 1 and additionally depicted as maximum recoverable yields of coupled product in Fig. 1. This graphically illustrates the huge differences in efficacy of the various conditions. Many reports of greener conditions

describe only the coupling of 2-naphthol or substituted 2-naphthol, yet, coupling of 2-naphthol **6** to yield BINOL **12** is readily achieved under a range of conditions including: with $\text{FeCl}_3 \cdot 6\text{H}_2\text{O}$ in toluene, neat, or in water and, to a reasonable extent, by reaction in toluene (replacing the chlorobenzene reported by Kantam *et al.*⁷) with the catalyst Fe(III) treated K-10. Thus, this reaction is readily achieved under conditions that may prove useless for other substrates and is not a good probe for comparison of green oxidative coupling protocols.

Remarkably, in spite of the poor aqueous solubility exhibited by most of these substrates, reaction at 50 °C in aqueous FeCl_3 solution provided significant conversion to coupled products for most substrates, except anthrone. These reactions were biphasic (except for **11**) and Ding *et al.* suggest that reaction occurs at the crystalline substrate surface, *via* an interaction between solid and liquid phases.^{4,15} This does not

Table 1 Mass recovery and product distribution in oxidative coupling reactions, compound number in parentheses

Catalyst: Fe^{3+} -K10																
(A) Toluene, 111 °C, 6 h				(B) Water, 100 °C, 6 h				(C) Neat, 50 °C, 24 h				(D) Neat, 160 °C, 24 h				
Rec ^a	Sm ^b	Cp ^c	Ox ^d	Rec	Sm	Cp	Ox	Rec	Sm	Cp	Ox	Rec	Sm	Cp	Ox	
6	79	33	67(12)		88	96	4(12)		96	93	7(12)		100	82	18(12)	
7	94	21	78(13)	1(19)	91	65	32(13)	3(19)	90	82	4(13)	14(19)	82	58	2(13)	40(19)
8	96	100	0(14)		90	100	0(14)		100	100	0(14)		70	72	28(20)	
9	86	100	0(15,21)	0(20)	24	0	29(15,21)	71(20)	99	100	0(15,21)	0(20)	13	10	90(15,21)	0(20)
10	81	85	15(16)		17	36	64(16)		100	100	0(16)		10	98	2(16)	
11	100	100	0(17)		97	100	0(17)		97	100	0(17)		100	100	0(17)	
Catalyst: $\text{FeCl}_3 \cdot 6\text{H}_2\text{O}$																
(E) Water, 50 °C, 4 h				(F) Acetonitrile, 82 °C, 4 h				(G) Neat, 50 °C, 4 h				(H) Toluene, 50 °C, 4 h				
Rec ^a	Sm ^b	Cp ^c	Ox ^d	Rec	Sm	Cp	Ox	Rec	Sm	Cp	Ox	Rec	Sm	Cp	Ox	
6	99	0	100(12)		99	80	18(12)	2(18)	99	0	100(12)		86	0	100(12)	
7	87	88	3(13)	9(19)	78	27	64(13)	9(19)	80	7	30(13)	63(19)	82	0	89(13)	11(19)
8	68	43	57(14)		65	97	3(14)		99	100	0(14)		95	100	0(14)	
9	89	12	87(15,21)	1(20)	85	57	16(15,21)	27(20)	88	100	0(15,21)	0(20)	25	55	15(15,21)	30(20)
10	75	25	75(16)		100	100	0(16)		92	31	69(16)		63	92	8(16)	
11	97	0	100(17)		58	100	0(17)		99	100	0(17)		99	100	0(17)	

^a Mass recovery (%) ^b Starting material (%) ^c Coupled products (%) ^d Oxidised products (%)

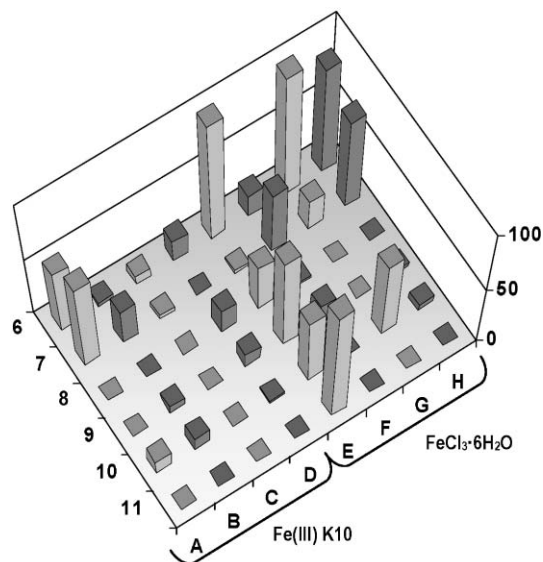


Fig. 1 Quantities of coupled products, represented as (mass recovery/100 × % Cp), recovered under various reaction conditions. **Fe³⁺-K10**: A = toluene reflux, 6 h; B = water reflux, 6 h; C = solvent-free 50 °C, 24 h; D = solvent-free 160 °C, 24 h. **FeCl₃·6H₂O**: E = water, 50 °C, 4h; F = CH₃CN reflux, 4 h; G = solvent-free, 50 °C, 4 h; H = toluene 50 °C, 4 h.

appear to be supported by the lack of reactivity of anthrone, the least water soluble material, and instead it is postulated that it is indeed dissolved substrate which reacts (as previously suggested¹⁶) possibly *via* a phenoxide radical mechanism due to the low pH of FeCl₃ solutions (measured to be 2.5). Coupled products, which (bar 17) exhibited poor aqueous solubility, largely separated from the aqueous solution, facilitating easy recovery, along with other benefits associated with reactions 'on water'.¹⁷

It was expected that reaction in acetonitrile (F), which yielded a homogeneous solution, would proceed rapidly, however, reasonable conversion was only obtained with anthrone 7. Attempts to effect coupling in other solvents including diethyl ether and ethyl acetate (both yielding homogeneous reaction mixtures) were also unsuccessful. When dissolved in toluene (H), anthrone readily reacted, yielding coupled product 13 almost as efficiently as 2-naphthol. FeCl₃·6H₂O is insoluble in toluene and forms a separate molten lower phase at 50 °C. Nonetheless, some reactions proceeded rapidly and such conditions provided for easy product recovery by simple filtration of the Fe salt residue and evaporation of the toluene solution post reaction. Given that, above 37 °C, FeCl₃·6H₂O is a liquid comprised of Fe(H₂O)₄Cl₂⁺ and FeCl₄⁻, with excess water molecules,¹⁸ this might be described as a biphasic reaction with an ionic liquid catalyst.

Previous reports of direct solvent-free reaction of 2-naphthol 6 with FeCl₃·6H₂O,⁵ coupled with the observation that this hydrated salt may form low melting mixtures with certain substrates,¹⁹ led to the examination of solvent-free reaction mixtures (G). Grinding of solid FeCl₃·6H₂O with substrates 6-11 and gentle heating (50 °C) resulted in reaction mixtures that differed significantly in physical appearance (Fig. 2): 6 yields the yellow reaction mixture noted previously¹⁹ as does 7;

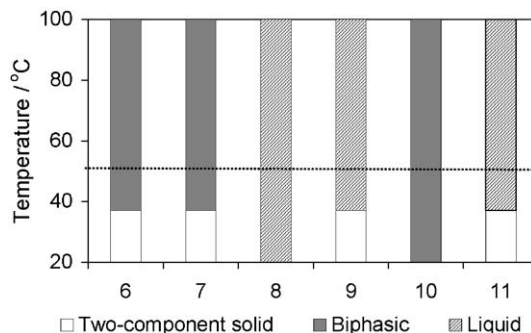


Fig. 2 Observed phase-changes with changes in *T* for solvent-free reaction mixtures (G) for substrates 6-11.

vanillin 8, forms a black liquid upon contact with the Fe salt; the mixture with 9 liquefies completely above the melting point of FeCl₃·6H₂O; 10, a liquid at room temperature (at 37 °C the entire mixture melts and immediately solid Fe residues begin to separate), yields a mixture of solid and liquid across the entire temperature range and 11 remains a mixture of two solids up to 37 °C.

Only the reaction mixtures that were designated as biphasic at the chosen reaction temperature in Fig. 2 yielded significant quantities of coupled products. A powder-XRD trace obtained immediately for the reaction mixture of 6 and FeCl₃·6H₂O on heating to 50 °C, indicated a dramatic loss of overall crystallinity. (A similar order of reactivity was demonstrated using anhydrous FeCl₃ (m.p. 304 °C) at 21 °C in a glove box challenging the suggestion that this was due to separation of products from the hydrated ionic liquid or concentrated aqueous solution of Fe(H₂O)₄Cl₂⁺ and FeCl₄⁻.)

A final observation: in the presence of FeCl₃, substrates 9 and 10 were usually recovered as dark red oils, indicating the possible formation of charge-transfer complexes. However, these are unlikely to play a mechanistic role due to their appearance in both reactive and unreactive systems.

Conclusion

Biphasic oxidative coupling of poorly water soluble substrates in contact with aqueous solutions of FeCl₃ were the most universally applicable conditions, while many homogeneous reaction mixtures yielded little or no coupling product. Fe(III) treated K-10 proved to be a poor catalyst for oxidative coupling of most substrates. The more successful conditions for Fe(III)-promoted coupling were observed when reactions were biphasic, indicating that homogeneous conditions may not always be the best choice for similar synthetic processes.

Experimental

2-Naphthol, anthrone, 2,6-dimethylphenol, 2,4-dimethylphenol, sodium 6-hydroxynaphthalene-2-sulfonate, K-10 montmorillonite clay, and anhydrous FeCl₃, were purchased from Sigma-Aldrich chemical company, vanillin from Ajax Chemicals Ltd and FeCl₃·6H₂O from BDH. All reagents and organic solvents were used as purchased from the supplier without any further purification.

^1H nuclear magnetic resonance (NMR) and ^{13}C NMR spectra were recorded on 200 MHz, 300 MHz or 400 MHz Bruker spectrometers in CDCl_3 , DMSO-d_6 or D_2O with tetramethylsilane (TMS) as an internal standard ($\delta = 0$ ppm), except in the case of D_2O (H_2O $\delta = 4.79$ ppm). Gas chromatography (GC) was performed on an Agilent 6850 Series II Network GC System, equipped with an FID detector and an HP-1 column (30 m \times 0.32 mm ID). Helium was used as a carrier gas at a flow-rate of 2.0 ml min^{-1} , and a temperature program of 100–300 $^\circ\text{C}$ at 10 $^\circ\text{C}$ min^{-1} was employed. Conversions were deduced from comparison of integrated areas of well-resolved signals in ^1H NMR spectra ($\pm 1\%$ error was determined for this method), or from resolved signals in GC analysis (compared to mixtures of standards made up to known concentrations). In addition, GC-MS analysis was used to confirm identity of the components of product mixtures. GC-MS was performed on a ThermoQuest TRACE DSQ GC-MS using an SGE BP5 column (30 m \times 0.22 mm ID) and an Electron Impact (EI) detector with an ionisation energy of 70 eV. Helium was used as a carrier gas at a flow-rate of 0.8 ml min^{-1} , and a temperature program of 50 $^\circ\text{C}$ for 2 min, 20 $^\circ\text{C}$ min^{-1} to 250 $^\circ\text{C}$ held for 16 min was employed. Atomic absorption spectroscopy (AAS) was carried out using a Perkin Elmer atomic absorption spectrometer Model 3110. Inductively coupled plasma optical emission spectroscopy (ICP-OES) was carried out using a Varian VistaPro ICP-OES with simultaneous CCD and axial view torch detectors. Melting points were recorded on a Gallenkamp variable heat melting point apparatus at a heating rate of 1 $^\circ\text{C}$ min^{-1} .

Preparation of Fe(III)-treated K-10 montmorillonite

Commercially available acid treated K-10 montmorillonite was washed with cold, dilute hydrochloric acid to remove exchangeable cations. The clay was then stirred in an aqueous FeCl_3 solution containing five times the metal ion concentration, compared with the approximated cation exchange capacity of the clay (~ 100 mequiv per 100 g). The clay was washed thoroughly with deionised water until chloride ions could no longer be detected in the washings. After drying (105 $^\circ\text{C}$) and milling, the clay thus obtained was independently analysed by AAS and ICP-OES to determine the Fe content of the clay. Fe content determination by AAS involved acid-washing of a small amount of Fe(III)-treated K-10 and its precursor (~ 300 mg) in 0.1 M HCl twice, and analysing the combined washings bracketed by Fe standards. Fe content determination by ICP-OES involved digestion of Fe(III)-treated K-10 and its precursor (~ 1 g) in *aqua regia* followed by multi-elemental analysis bracketed by mixed-standards. The exchangeable Fe content of the clay was determined to be 0.0098 g Fe per 1.000 g of clay by AAS and 0.0083 g Fe per 1.000 g of clay by ICP-OES (average 0.0090 g Fe per 1.000 g of clay). Assuming saturation with Fe(III), the CEC of the clay was calculated to be ~ 50 mequiv per 100 g.

Example procedure for clay-catalysed reactions in toluene (A)

Fe(III)-treated K10 montmorillonite (0.2368 g, 0.0380 mmol Fe) was added to a solution of anthrone **7** (0.2002 g,

1.0310 mmol) in toluene (30 ml) at reflux (111 $^\circ\text{C}$) for 6 h. After cooling, solids were removed by filtration, the organic solution was dried (MgSO_4), filtered and the solvent removed *in vacuo* to give a yellow solid (0.1883 g, 94% mass recovery). ^1H NMR (CDCl_3 , TMS, 300 MHz) revealed 21% anthrone **7**, 78% bianthranyl **13** and 1% anthraquinone **19**.

Example procedure for clay-catalysed reactions in water (B)

Anthrone **7** (0.1980 g, 1.0190 mmol) was added to a suspension of Fe(III)-treated K-10 montmorillonite (0.2345 g, 0.0380 mmol Fe) in water (30 ml) and stirred at reflux (100 $^\circ\text{C}$) for 6 h. The mixture was filtered, extracted with dichloromethane, dried (MgSO_4), filtered and the solvent removed *in vacuo* to give a yellow solid (0.1807 g, 91% mass recovery). ^1H NMR (CDCl_3 , TMS, 300 MHz) revealed 65% anthrone **7**, 32% bianthranyl **13**, and 3% anthraquinone **19**.

Example procedure for solvent-free reactions with clays (C,D)

2-Naphthol **6** (0.2008 g, 1.3930 mmol) and Fe(III)-treated K-10 montmorillonite (0.3231 g, 0.0520 mmol Fe) were ground together, placed in a sealed Pyrex test-tube in an aluminium dry block heater and kept at 50 $^\circ\text{C}$ (160 $^\circ\text{C}$ for high-temp experiments (D)) for 24 hours. The organic component was extracted with dichloromethane, filtered to remove clay, dried (MgSO_4), filtered and the solvent removed *in vacuo* to give a white solid (0.1931 g, 96% mass recovery). ^1H NMR (CDCl_3 , TMS, 300 MHz) revealed 93% 2-naphthol **6** and 7% 1,1'-binaphthalene-2,2'-diol **12**.

Example procedure for reactions with Fe salt in water (E)

2,6-Dimethylphenol **9** (0.2024 g, 1.6570 mmol) was added to a solution of $\text{FeCl}_3 \cdot 6\text{H}_2\text{O}$ (1.7695 g, 6.5470 mmol) in distilled water (30 ml) and slurried at 50 $^\circ\text{C}$ for 4 h. The solid organic phase was filtered off after cooling, and the remaining mixture was extracted with dichloromethane, dried (MgSO_4), filtered, combined and the solvent removed *in vacuo* to give a red solid (0.1801 g, 89% mass recovery). ^1H NMR (CDCl_3 , TMS, 300 MHz) revealed 12% 2,6-dimethylphenol **9**, 68% 3,3',5,5'-tetramethyldiphenylquinone **21**, 19% 3,3',5,5'-tetramethyl-1,1'-biphenyl-4,4'-diol **15**, and 1% 2,6-dimethylbenzoquinone **20**.

Example procedure for reactions with Fe salt in acetonitrile (F)

2-Naphthol **6** (0.2010 g, 1.3940 mmol) was added to a solution of $\text{FeCl}_3 \cdot 6\text{H}_2\text{O}$ (0.7531 g, 2.7860 mmol) in acetonitrile (30 ml) and stirred at reflux (82 $^\circ\text{C}$) for 4 h. The reaction was quenched with 1 M HCl (10 ml), partitioned with an aliquot of dichloromethane, dried (MgSO_4), filtered and the solvent removed *in vacuo* to give a white solid (0.1995 g, 99% mass recovery). ^1H NMR (CDCl_3 , TMS, 400 MHz) revealed 80% 2-naphthol **6**, 18% 1,1'-binaphthalene-2,2'-diol **12**, and 2% 1,4-naphthoquinone **18**.

Example procedure for neat reactions with Fe salts (G)

2,4-Dimethylphenol **10** (0.2000 g, 1.6370 mmol) and $\text{FeCl}_3 \cdot 6\text{H}_2\text{O}$ (0.8825 g, 3.2650 mmol) were placed in a sealed

test-tube, mixed together and kept at 50 °C for 4 h. The reaction was quenched with 1 M HCl (10 ml), washed with an aliquot of distilled water and the organic component extracted with dichloromethane. The solution was dried (MgSO₄), filtered and the solvent removed *in vacuo* to give a red solid (0.1835 g, 92% mass recovery). ¹H NMR (CDCl₃, TMS, 200 MHz) revealed 31% 2,4-dimethylphenol **10** and 69% 3,3',5,5'-tetramethyl-1,1'-biphenyl-2,2'-diol **16**.

Example procedure for reactions with Fe salt in toluene (H)

FeCl₃·6H₂O (0.7484 g, 2.7690 mmol) was added to a solution of 2-naphthol **6** (0.1999 g, 1.3870 mmol) in toluene (30 ml) and slurried at 50 °C for 4 h. The mixture was filtered and the solvent removed *in vacuo* to give a white solid (0.1770 g, 86% mass recovery). ¹H NMR (CDCl₃, TMS, 200 MHz) revealed 0% 2-naphthol **6** and 100% 1,1'-binaphthalene-2,2'-diol **12**.

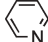
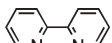
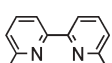
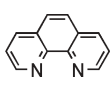
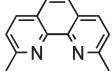
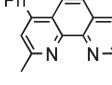
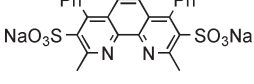

Acknowledgements

The authors acknowledge the financial support of the Australian Research Council Special Research Centre for Green Chemistry and P.W. gratefully acknowledges support in the form of an Australian Postgraduate Award. We thank Dr Will Gates for expert advice pertaining to the structure and chemistry of clay minerals.

References

- 1 P. P. Reddy, C. Y. Chu, D. R. Hwang, S. K. Wang and B. J. Uang, *Coord. Chem. Rev.*, 2003, **237**, 257.
- 2 S. Pal, J. M. Bollag and P. M. Huang, *Soil Biol. Biochem.*, 1994, **26**, 813.
- 3 J. M. Bollag, J. Dec and P. M. Huang, *Adv. Agron.*, 1998, **63**, 237.
- 4 K. Ding, Y. Wang, L. Zhang and Y. Wu, *Tetrahedron*, 1996, **52**, 1005.
- 5 F. Toda, K. Tanaka and S. Iwata, *J. Org. Chem.*, 1989, **54**, 3007.
- 6 J. Brussee, J. L. G. Groenendijk, J. M. te Koppele and A. C. A. Jansen, *Tetrahedron*, 1985, **41**, 3313.
- 7 M. L. Kantam, B. Kavita and F. Figueras, *Catal. Lett.*, 1998, **51**, 113.
- 8 S. Kobayashi and H. Higashimura, *Prog. Polym. Sci.*, 2003, **28**, 1015.
- 9 G. Lessene and K. S. Feldman, in *Modern Arene Chemistry*, Wiley-VCH, 2002.
- 10 M. Balogh and P. Laszlo, in *Organic Chemistry Using Clays*, Springer-Verlag, 1993.
- 11 M. L. Kantam and P. L. Santhi, *Synth. Commun.*, 1996, **26**, 3075.
- 12 T. S. Li, H. Y. Duan, B. Z. Li, B. B. Tewari and S. H. Li, *J. Chem. Soc., Perkin Trans. 1*, 1999, 291.
- 13 T. Fujii, N. Tanaka, K. Kodaira, Y. Kawai, H. Yamashita and M. Anpo, *J. Photochem. Photobiol., A*, 1999, **125**, 85.
- 14 R. G. R. Bacon and A. R. Izzat, *J. Chem. Soc. C*, 1966, 791.
- 15 H. Dianin, *Ber. Dtsch. Chem. Ges.*, 1873, **6**, 1252.
- 16 Š. Vyskočil, M. Smrčina, M. Lorenc, V. Hanuš, M. Poláček and P. Kočovský, *Chem. Commun.*, 1998, 585.
- 17 S. Narayan, J. Muldoon, M. G. Finn, V. V. Fokin, H. C. Kolb and K. B. Sharpless, *Angew. Chem.*, 2005, **117**, 3339.
- 18 K. Murata and D. E. Irish, *Spectrochim. Acta, Part A*, 1988, **44**, 739.
- 19 G. Rothenberg, A. P. Downie, C. L. Raston and J. L. Scott, *J. Am. Chem. Soc.*, 2001, **123**, 8701.

Table 1 Impact of different ligands on oxidative arylation of *n*-butyl acrylate (**2a**) with *p*-tolylboronic acid (**1c**) under air at 80 °C^a

Entry	Ligand	Reaction time/h	Yield of 4c ^b (%)
1	3a 	144	0
2	3b 	12	73
3	3c 	15	75 ^c
4	3d 	48	39
5	3e 	1 72	94 35 ^d
6	3f 	8	87
7	3g 	12 48	77 26 ^e
8	3h 	24	81

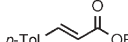
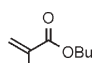
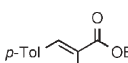
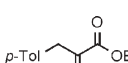
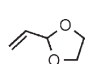
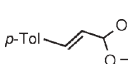

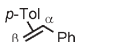
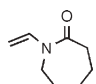
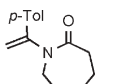
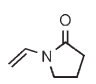
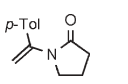
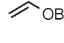

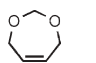
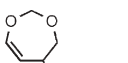
^a Reaction conditions: Open vessel charged with *p*-tolylboronic acid (2.0 mmol), *n*-butyl acrylate (1.0 mmol), *N*-methylmorpholine (2.0 mmol), Pd(OAc)₂ (0.02 mmol), ligand (0.048 mmol **3a** or 0.024 mmol **3b–h**) and acetonitrile (3 mL). Rapid stirring. ^b Isolated yield. ^c Performed at rt. ^d Water–acetonitrile 95 : 5. ^e Water as solvent.

butyl vinyl ether (**2g**), the yield was almost identical regardless of reaction temperature, although reaction times varied considerably. As expected with a bidentate ligand and a reaction pathway proceeding *via* charged intermediates,¹⁴ the insertions were electronically controlled and occurred with high regioselectivity,¹⁸ delivering predominantly terminal (**4c**, **5–7**) or branched (**8–10**) products.^{3,21} The high reactivity of electron-poor **2a** was somewhat surprising under the cationic conditions applied, producing an excellent yield (93%) after 24 h at rt (entry 1, Table 2). Disubstituted olefins such as **2b** and prochiral **2h**, reacted more sluggishly than the mono-substituted analogues and did not afford more than modest yields, despite increased reaction temperatures.

The reaction with **2a** was next examined with respect to the choice of transmetalation precursor (Table 3). Clearly, the arylation was most productive with electron-rich arylboronic acids (entry 1, Table 2 and entries 1–4, 6 and 7, Table 3), in complete agreement with previous examples performed under oxygen gas and in accordance with recent DFT calculations.¹⁴ However, most electron-poor arylboronic acids provided useful yields, and in fact, *p*-acetylphenylboronic acid underwent an efficient oxidative Heck coupling reaction for the first time.¹⁴

Rewardingly, high chemoselectivity was obtained with bromo-substituted substrates **1f,g** in entries 8 and 9 affording

Table 2 Oxidative arylation of different olefins with *p*-tolylboronic acid (**1c**) at ambient and elevated temperatures^a

Entry	Olefin	Temp/°C	Reaction time/h	Product	Yield ^b (%)
1	2a	rt 80	24 1	4c 	93 94
2	2b 	80	96	5a 	35 ^c
				5b 	
3	2c 	rt	96	6 	63
4	2d 	rt 80	24 96	7 	85 ^d 75 ^d
5	2e 	rt 80	144 24	8 	57 67
6	2f 	rt 60	48 6	9 	71 68
7	2g 	rt 60	24 24	10 	35 ^c 91 ^c
8	2h 	rt 80	18 6	11 	35 45

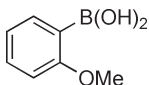
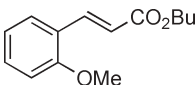
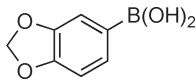
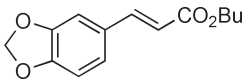
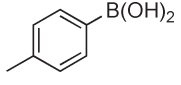
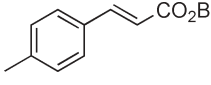
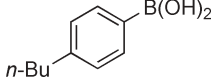
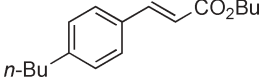
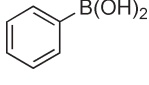
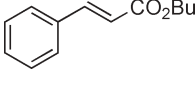
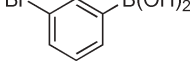
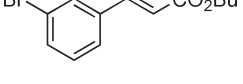
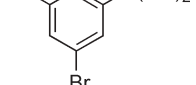
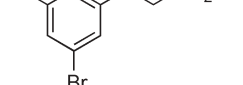
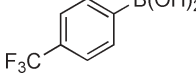
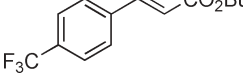
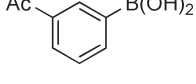
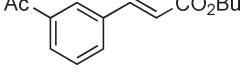
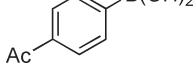
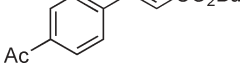
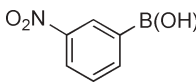
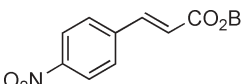
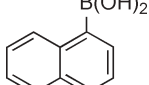
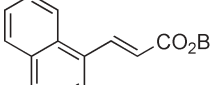
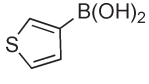
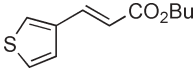
^a Reaction conditions: Open vessel charged with *p*-tolylboronic acid (2.0 mmol), olefin (1.0 mmol), *N*-methylmorpholine (2.0 mmol), Pd(OAc)₂ (0.02 mmol), dmphen (0.024 mmol) and acetonitrile (3 mL). Rapid stirring. ^b Isolated yield >95% pure by GC-MS. ^c **5a** : **5b** = 40 : 60, determined by NMR. ^d α/β 15 : 85, determined by GC-MS. ^e Isolated as the corresponding *p*-tolyl methyl ketone, after acidic *in situ* hydrolysis (glacial HOAc).

cinnamic esters **4f,g** without a competing Pd(0)-catalyzed Heck process. The opposite chemoselectivity under Pd(0)-conditions was not possible due to competing Suzuki couplings. Of particular mechanistic interest were the highly successful arylations starting with zero-valent Pd₂(dba)₃ (entries 3 and 4, Table 3) and the complete inhibition of the catalysis by switching from air to a nitrogen atmosphere (entry 5, Table 3), demonstrating the efficient and essential oxidative role of molecular oxygen. Employing heteroaromatic boronic acid **1m** generated product **4m** in workable yield.

Intrigued by the high reactivity of electron-deficient olefins under dmphen-controlled cationic conditions, a series of competitive experiments were performed under air at room temperature using electron-poor olefin **2a** and electron-rich olefin **2f**. The high regioselectivity remained intact for both olefins but the results in Table 4 demonstrate that **2a** reacts faster than **2f**, reaching a maximum **4c/8** product ratio after 20 h. This is in sharp contrast to the cationic situation with aryl triflates as substrates and Pd(0) as catalyst, where electron-rich olefins react faster than their electron-poor counterparts.^{17,21}

To investigate the robustness of the system, a reaction was performed with 50 mmol olefin **2i** in an open vessel at

Table 3 Oxidative arylation of *n*-butyl acrylate (**2a**) with a set of arylboronic acids^a

Entry	Arylboronic acid	Temp/°C	Reaction time/h	Product	Yield ^b (%)
1	1a 	80	72	4a 	82
2	1b 	rt	48	4b 	81
3	1c 	rt	24	4c 	94 ^c
4	1c	80	1	4c	95 ^c
5	1c	80	24	4c	0 ^d
6	1d 	80	24	4d 	96
7	1e 	rt	24	4e 	81
8	1f 	rt	48	4f 	63
9	1g 	80	24	4g 	87
10	1h 	80	96	4h 	68
11	1i 	80	18	4i 	67
12	1j 	rt	120	4j 	61
13	1j	80	24	4j	64
14	1k 	80	48	4k 	70
15	1l 	80	18	4l 	64
16	1m 	80	96	4m 	50

^a Reaction conditions: Open vessel charged with boronic acid (2.0 mmol), *n*-butyl acrylate (1.0 mmol), *N*-methylmorpholine (2.0 mmol), Pd(OAc)₂ (0.02 mmol), dmphen (0.024 mmol) and acetonitrile (3 mL). Rapid stirring. ^b Isolated yield >95% pure by GC-MS. ^c 0.02 mmol Pd₂(dba)₃ instead of Pd(OAc)₂. ^d Closed vessel with nitrogen atmosphere.

rt (Scheme 2). The isolated yield of 83% **4n** (7.30 g) demonstrated the good scalability of the reaction and indicated that the methodology may also be applicable for large scale processing.

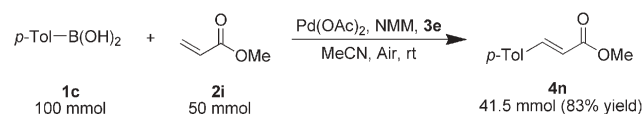
Conclusions

In summary, we have demonstrated a robust protocol where aryl- and heteroarylboronic acids serve as powerful arylating

Table 4 Competitive experiment between *n*-butyl acrylate (**2a**) and *N*-vinylpyrrolidinone (**2f**) using **1c** as the arylating agent at room temperature^a

Entry	Time/h	Yield ^b 4c (%)	Yield ^b 8 (%)	Ratio ^c
1	1	8	5	1.6
2	2	13	8	1.8
3	4	24	9	2.8
4	8	63	23	2.7
5	20	80	30	2.8
6	30	92	33	2.7
7	48	99	41	2.5

^a Reaction conditions: Open vessel charged with *p*-tolylboronic acid (1.5 mmol), *N*-vinyl-2-pyrrolidinone (0.5 mmol), *n*-butyl acrylate (0.5 mmol), *N*-methylmorpholine (2.0 mmol), Pd(OAc)₂ (0.02 mmol), dmphen (0.024 mmol) in acetonitrile (3 mL) and rapid stirring at room temperature. ^b NMR yield. ^c Product ratio of **4c**/**8**.



Scheme 2

agents at ambient temperature using the stable and inexpensive phenanthroline-class ligand **3e**. Different olefins were smoothly converted to the corresponding arylated analogues in high yields by conducting Pd(II)-catalyzed oxidative Heck reactions under air, instead of using Cu(II) salts²² or pure O₂ gas as the reoxidant. The reaction was smoothly scaled up from 1 mmol to 50 mmol. Thus, this is a rare example of a general protocol enabling different Heck couplings to be conducted at room temperature.

The improvement of the oxidative Heck reaction that we have achieved has an environmental impact by reducing waste, additives, risks, cost and energy consumption. Added together, these factors cover a big part of what makes the concept of “green chemistry” so important today.

Experimental

General

All starting materials and reagents were commercially available and used as received. Products **4a**,²² **4b**,²² **4c**,²³ **4f**,²⁴ **4g**,¹⁸ **4h**,²⁵ **4j**,²² **4k**,²⁵ **4l**,²⁵ **4m**,²⁵ **4n**,²⁶ **7**,²⁷ and **9**¹⁴ have been previously reported and characterized. Compounds **5a**,^b²⁸ and **11**²⁹ have also been previously reported but without proper spectral characterization. Structures **4d**, **4i**, **6** and **8** are to the best of our knowledge new compounds. Compounds **4e** and hydrolyzed **6** (3-(4-methylphenyl)-2-propenal), **8** (*p*-methylacetophenone) and **10** (*p*-methylacetophenone) are commercially available. All known products gave satisfactory analytical and spectroscopic data corresponding to the reported literature values. Analytical TLC was performed using Merck glass-backed 0.2 mm silica gel 60 F-254 plates. Visualization was done with UV light. NMR spectra were obtained on a Varian Mercury + spectrometer at 400 MHz for ¹H, at 100 MHz for ¹³C NMR, both at 25 °C. Chemical shifts for ¹H and ¹³C were referenced to CHCl₃ and CDCl₃, respectively. Low-resolution mass spectra were recorded on a

GC-MS instrument equipped with a CP-Sil 8 CB capillary column (30 m × 0.25 mm, 0.25 μm) operating at an ionization energy of 70 eV. The oven temperature was 40–300 °C.

General procedure for oxidative Heck reactions using Pd(OAc)₂ (Tables 1–3)

All reagents were weighed in air and the reactions were conducted in an open vessel. A 100 mL round-bottomed flask, fitted with a glass tube as cooler, or a glass vial, was charged with arylboronic acid **1** (2.0 mmol), olefin **2** (1.0 mmol), *N*-methylmorpholine (0.22 mL, 2.0 mmol) and acetonitrile (2 mL). The reaction mixture was stirred until all the reagents were thoroughly dissolved. Pd(OAc)₂ (4.5 mg, 0.02 mmol) and the bidentate ligand (0.024 mmol) dissolved in 1 mL acetonitrile were then added to the reaction mixture. The mixture was vigorously stirred at the specified temperature, until full conversion of the starting material was obtained. The reaction mixture was filtered and the flask washed with warm dichloromethane. The crude product was thereafter purified on silica gel using isohexane or a mixture of isohexane and ethyl acetate to give the pure product **4**–**11**.

General procedure for oxidative Heck reactions using Pd₂(dba)₃ (Table 3)

The same protocol as above but using Pd₂(dba)₃ (18.3 mg, 0.020 mmol) instead of Pd(OAc)₂.

Procedure for large-scale experiment (Scheme 2)

A 500 mL round-bottomed flask, fitted with a glass tube as cooler was charged with *p*-tolylboronic acid (100 mmol), methyl acrylate (50 mmol), *N*-methylmorpholine (11 mL, 100 mmol) and acetonitrile (150 mL). The reaction mixture was stirred until all the reagents were thoroughly dissolved. Pd(OAc)₂ (225 mg, 1 mmol) and ligand **3e** (250 mg, 1.2 mmol) dissolved in 50 mL acetonitrile were then added to the reaction mixture. The mixture was vigorously stirred at ambient temperature for 48 h. The solvent was removed *in vacuo* and the residue was dissolved in 200 mL dichloromethane and subsequently washed with sodium hydrogen carbonate (aq., sat.). After concentration of the crude mixture, purification on silica gel (isohexane–ethyl acetate, 20 : 1) delivered the pure product, methyl-3-(*p*-tolyl)acrylate (**4n**).

Procedure for competitive experiment (Table 4)

All reagents were weighed in air and the reactions were conducted in an open vessel. A 100 mL round-bottomed flask, fitted with a glass tube as cooler, was charged with *p*-tolylboronic acid (204 mg, 1.5 mmol), *N*-vinyl-2-pyrrolidinone (56 mg, 0.5 mmol), butyl acrylate (64 mg, 0.5 mmol), *N*-methylmorpholine (0.22 mL, 2.0 mmol) and acetonitrile (2 mL). The reaction mixture was stirred until all the reagents were dissolved. Pd(OAc)₂ (2.25 mg, 0.02 mmol) and dmphen (2.6 mg, 0.024 mmol) dissolved in 1 mL acetonitrile were then added to the reaction mixture. This procedure was repeated six times and the mixtures were vigorously stirred at room temperature for the appropriate time (1, 2, 4, 8, 20, 30 or 48 h). The reactions were quenched by gentle evaporation of

the solvent with N₂ gas, and benzaldehyde (0.5 mmol) was added as internal standard for determination of NMR yield.

NMR spectral data for compounds 5a,b and 11

***n*-Butyl (*E*)-2-methyl-3-(*p*-tolyl)acrylate (5a).** ¹H NMR (400 MHz, CDCl₃): δ 0.97 (t, *J* = 7.4 Hz, 3H), 1.40–1.50 (m, 2H), 1.67–1.74 (m, 2H), 2.12 (d, *J* = 1.5 Hz, 3H), 2.37 (s, 3H), 4.21 (t, *J* = 6.6 Hz, 2H), 7.19–7.21 (XX' part of an AA'XX' system, 2H), 7.30–7.32 (AA' part of an AA'XX' system, 2H), 7.65 (br s, 1H). ¹³C NMR (100 MHz, CDCl₃): δ 13.9, 14.2, 19.4, 21.5, 31.0, 64.9, 127.9, 129.2, 129.9, 133.3, 138.5, 138.8, 169.1.

***n*-Butyl 2-(4-methylbenzyl)acrylate (5b).** ¹H NMR (400 MHz, CDCl₃): δ 0.91 (t, *J* = 7.3 Hz, 3H), 1.30–1.40 (m, 2H), 1.58–1.65 (m, 2H), 2.32 (s, 3H), 3.59 (br s, 2H), 4.12 (t, *J* = 6.6 Hz, 2H), 5.44 (dt, *J* = 1.5 Hz, 1.5 Hz, 1H), 6.21 (dt, *J* = 1.5 Hz, 0.9 Hz, 1H), 7.07–7.11 (m, 4H). ¹³C NMR (100 MHz, CDCl₃): δ 13.9, 19.3, 21.2, 30.8, 37.8, 64.8, 126.0, 129.1, 129.2, 135.86, 135.94, 140.7, 167.2.

5-(*p*-Tolyl)-4,5-dihydro-[1,3]-dioxepine (11). ¹H NMR (400 MHz, CDCl₃): δ 2.33 (s, 3H), 3.43 (ddd, *J* = 11.5 Hz, 8.7 Hz, 0.4 Hz, 1H), 3.75–3.80 (m, 1H), 3.96 (dd, *J* = 11.6 Hz, 4.6 Hz, 1H), 4.84 (dd, *J* = 7.0 Hz, 0.4 Hz, 1H), 4.93 (dd, *J* = 7.4 Hz, 3.7 Hz, 1H), 5.19 (d, *J* = 7.0 Hz, 1H), 6.46 (dd, *J* = 7.4 Hz, 2.4 Hz, 1H), 7.12–7.17 (m, 4H). ¹³C NMR (100 MHz, CDCl₃): δ 21.2, 48.2, 77.1, 98.3, 112.5, 128.0, 129.5, 136.8, 138.0, 146.1.

Spectroscopic and analytical data for new compounds 4d, 4i, 6 and 8

***n*-Butyl (*E*)-3-(4-*n*-butylphenyl)acrylate (4d).** ¹H NMR (400 MHz, CDCl₃): δ 0.93 (t, *J* = 7.3 Hz, 3H), 0.97 (t, *J* = 7.4 Hz, 3H), 1.31–1.49 (m, 4H), 1.56–1.73 (m, 4H), 2.63 (t, *J* = 7.9 Hz, 2H), 4.21 (t, *J* = 6.7 Hz, 2H), 6.40 (d, *J* = 16.0 Hz, 1H), 7.18–7.20 (XX' part of an AA'XX' system, 2H), 7.43–7.45 (AA' part of an AA'XX' system, 2H), 7.67 (d, *J* = 16.0 Hz, 1H); ¹³C NMR (100 MHz, CDCl₃): δ 14.1, 14.3, 19.6, 22.7, 31.1, 33.7, 35.9, 64.7, 117.5, 128.4, 129.3, 132.3, 144.9, 146.0, 167.7; Anal. Calcd for C₁₇H₂₄O₂: C, 78.42; H, 9.29; O, 12.29; Found: C, 78.49; H, 9.39; O, 12.10.

***n*-Butyl (*E*)-3-(3-acetylphenyl)acrylate (4i).** ¹H NMR (400 MHz, CDCl₃): δ 0.97 (t, *J* = 7.4 Hz, 3H), 1.39–1.49 (m, 2H), 1.66–1.73 (m, 2H), 2.63 (s, 3H), 4.22 (t, *J* = 6.7 Hz, 2H), 6.52 (d, *J* = 16.0 Hz, 1H), 7.48 (br t, *J* = 7.7 Hz, 1H), 7.70–7.72 (m, 1H), 7.71 (d, *J* = 16.0 Hz, 1H), 7.94 (ddd, *J* = 7.7 Hz, 1.8 Hz, 1.1 Hz, 1H), 8.09–8.10 (m, 1H); ¹³C NMR (100 MHz, CDCl₃): δ 13.7, 19.2, 26.7, 30.7, 64.6, 119.7, 127.7, 129.2, 129.7, 132.2, 135.0, 137.7, 143.3, 166.7, 197.4; Anal. Calcd for C₁₅H₁₈O₃: C, 73.15; H, 7.37; O, 19.49; Found: C, 72.98; H, 7.26; O, 19.26.

2-((*E*)-2-*p*-tolylvinyl)-[1,3]-dioxolane (6). ¹H NMR (400 MHz, CDCl₃): δ 2.34 (s, 3H), 3.92–4.10 (m, 4H), 5.42 (dd, *J* = 6.1 Hz, 0.9 Hz, 1H), 6.12 (dd, *J* = 16.0, 6.1 Hz, 1H), 6.75 (d, *J* = 16.0 Hz, 1H), 7.12–7.14 (XX' part of an AA'XX'

system, 2H), 7.30–7.32 (AA' part of an AA'XX' system, 2H); ¹³C NMR (100 MHz, CDCl₃): δ 21.2, 65.0, 104.1, 124.0, 126.8, 129.3, 133.0, 134.9, 138.3. The identity of **6** was further confirmed by comparison of the NMR spectrum obtained from the hydrolyzed product, 3-(4-methylphenyl)-2-propenal, produced by 15 min stirring in 1 M HCl, with reference values.³⁰ Instability prevented elemental analysis from being carried out.

***N*-(1-[4-methylphenyl]ethenyl)-2-azapinone (8).** ¹H NMR (400 MHz, CDCl₃): δ 1.75–1.83 (m, 6H), 2.33 (s, 3H), 2.67–2.69 (m, 2H), 3.49–3.52 (m, 2H), 5.14 (s, 1H), 5.56 (s, 1H), 7.12–7.14 (XX' part of an AA'XX' system, 2H), 7.28–7.30 (AA' part of an AA'XX' system, 2H); ¹³C NMR (100 MHz, CDCl₃): δ 21.1, 23.5, 28.7, 30.0, 37.6, 51.8, 110.3, 125.8, 129.2, 133.4, 138.3, 149.0, 175.8. The identity of **8** was further confirmed by comparison of the GC spectra obtained from the hydrolyzed product, *p*-methylacetophenone, produced by stirring over night in 1 M HCl, with a genuine sample. Instability prevented elemental analysis from being carried out.¹⁴

Acknowledgements

We would like to express our sincere gratitude to the Knut and Alice Wallenberg Foundation and to the Swedish Research Council. We also thank Dr Kristofer Olofsson for linguistic advice and Prof. Anders Hallberg for fruitful discussions.

References

- I. P. Beletskaya and A. V. Cheprakov, *Chem. Rev.*, 2000, **100**, 3009.
- A. De Meijere and F. E. Meyer, *Angew. Chem., Int. Ed. Engl.*, 1994, **33**, 2379.
- M. Larhed and A. Hallberg, In *Handbook of Organopalladium Chemistry in Organic Synthesis*, ed. E. Negishi, John Wiley & Sons, Inc., New York, 2002; vol. 1, p. 1133.
- S. S. Stahl, *Angew. Chem., Int. Ed.*, 2004, **43**, 3400.
- R. C. Verboom, V. F. Slagt and J. E. Bäckvall, *Chem. Commun.*, 2005, 1282.
- C. X. Zhou and R. C. Larock, *Org. Lett.*, 2005, **7**, 259.
- J. P. Parrish, Y. C. Jung, S. I. Shin and K. W. Jung, *J. Org. Chem.*, 2002, **67**, 7127.
- K. Hirabayashi, J. Ando, J. Kawashima, Y. Nishihara, A. Mori and T. Hiyama, *Bull. Chem. Soc. Jpn.*, 2000, **73**, 1409.
- K. Matoba, S. Motofusa, C. S. Cho, K. Ohe and S. Uemura, *J. Organomet. Chem.*, 1999, **574**, 3.
- A. Inoue, H. Shinokubo and K. Oshima, *J. Am. Chem. Soc.*, 2003, **125**, 1484.
- (a) Y. C. Jung, R. K. Mishra, C. H. Yoon and K. W. Jung, *Org. Lett.*, 2003, **5**, 2231; (b) C. H. Yoon, K. S. Yoo, S. W. Yi, R. K. Mishra and K. W. Jung, *Org. Lett.*, 2004, **6**, 4037.
- F. Heck, *J. Am. Chem. Soc.*, 1969, **91**, 6707.
- (a) T. Ishiyama and N. Miyaoura, *J. Organomet. Chem.*, 2003, **680**, 3; (b) T. Ishiyama, J. Takagi, K. Ishida, N. Miyaoura, N. R. Anastasi and J. F. Hartwig, *J. Am. Chem. Soc.*, 2002, **124**, 390.
- M. M. S. Andappan, P. Nilsson, H. von Schenck and M. Larhed, *J. Org. Chem.*, 2004, **69**, 5212.
- A. F. Littke and G. C. Fu, *J. Am. Chem. Soc.*, 2001, **123**, 6989.
- J. P. Stambuli, S. R. Stauffer, K. H. Shaughnessy and J. F. Hartwig, *J. Am. Chem. Soc.*, 2001, **123**, 2677.
- W. Cabri, I. Candiani, A. Bedeschi and R. Santi, *J. Org. Chem.*, 1993, **58**, 7421.
- M. M. S. Andappan, P. Nilsson and M. Larhed, *Chem. Commun.*, 2004, 218.
- J. M. Keith, R. J. Nielsen, J. Oxgaard and W. A. Goddard, III, *J. Am. Chem. Soc.*, 2005, **127**, 13172.

- 20 G. J. ten Brink, I. Arends and R. A. Sheldon, *Science*, 2000, **287**, 1636.
 21 W. Cabri and I. Candiani, *Acc. Chem. Res.*, 1995, **28**, 2.
 22 M. M. S. Andappan, P. Nilsson and M. Larhed, *Mol. Div.*, 2003, **7**, 97.
 23 M.-Z. Cai, J. Zhou, H. Zhao and C.-S. Song, *J. Chem. Res., Synop.*, 2002, 76.
 24 E. J. Farrington, J. M. Brown, C. F. J. Barnard and E. Rowsell, *Angew. Chem., Int. Ed.*, 2002, **41**, 169.
 25 M. Feuerstein, H. Doucet and M. Santelli, *J. Org. Chem.*, 2001, **66**, 5923.
 26 Z. Xiong, N. Wang, M. Dai, A. Li, J. Chen and Z. Yang, *Org. Lett.*, 2004, **6**, 3337.
 27 R. K. Arvela, N. E. Leadbeater, M. S. Sangi, V. A. Williams, P. Granados and R. D. Singer, *J. Org. Chem.*, 2005, **70**, 161.
 28 V. Caló, A. Nacci, A. Monopoli, A. Detomaso and P. Iliade, *Organometallics*, 2003, **22**, 4193.
 29 Y. Koga, M. Sodeoka and M. Shibasaki, *Tetrahedron Lett.*, 1994, **35**, 8, 1227.
 30 G. Battistuzzi, S. Cacchi and G. Fabrizi, *Org. Lett.*, 2003, **5**, 777.

Chemical Technology

A well-received news supplement showcasing the latest developments in applied and technological aspects of the chemical sciences



Free online and in print issues of selected RSC journals!*

- **Application Highlights** – newsworthy articles and significant technological advances
- **Essential Elements** – latest developments from RSC publications
- **Free access** to the original research paper from every online article

*A separately issued print subscription is also available

RSC Publishing

www.rsc.org/chemicaltechnology

03000520

The green catalytic oxidation of alcohols in water by using highly efficient manganosilicate molecular sieves

Hareesh G. Manyar, Ganesh S. Chauré and Ashok Kumar*

Received 13th December 2005, Accepted 24th January 2006

First published as an Advance Article on the web 21st February 2006

DOI: 10.1039/b517662j

An efficient and green catalytic protocol for the oxidation of alcohols to the corresponding aldehydes is the need of industry and is continuously being sought for. This report describes the use of manganosilicate molecular sieves as an efficient heterogeneous catalyst in aqueous conditions using the peroxodisulfate ions as the oxidising agent. The advantageous feature of this oxidation methodology is the efficiency and selectivity with which it oxidizes the heterocyclic and aliphatic alcohols. The other interesting facet of this communication is the synthesis of manganosilicate molecular sieves by a facile complexing procedure leading to the uniform mesoporous cubic structure devoid of extra-framework bulk manganese oxide species.

Introduction

The oxidation of alcohols to the corresponding carbonyls is one of the most important synthetic transformations in organic chemistry.^{1–4} Today's stringent environmental and legislative concerns demand for the greener methods that minimise or eliminate the use of corrosive reagents and stop the stoichiometric formation of inorganic waste.^{5,6} As a consequence, numerous catalytic procedures for oxidation of alcohols have been developed including environment friendly protocols with special emphasis on benign solvents.^{7–19} In this regard, the use of water as a reaction solvent has attracted great attention in the recent past and has become an active area of research in green chemistry.^{20,21} In this direction, a wide variety of organic reactions including Diels–Alder reaction, Claisen-rearrangements, aldol reactions, allylation reactions, oxidations and hydrogenations of alkenes are reported,^{22,23} however, only a few reports of catalytic oxidation of alcohols in water have been reported to date.^{24–27} In continuation with the long lasting interest in this area,^{28–30} we herein report a new facile and efficient methodology for the oxidation of heterocyclic and alicyclic alcohols to the corresponding carbonyl compounds. This new methodology employs peroxodisulfate ions as the oxidising agent, in presence of the manganosilicate molecular sieves as the heterogeneous catalyst, in water as the medium. The readily available peroxodisulfate ions have been recognised as one of the strongest and versatile oxidant for a variety of organic and inorganic compounds.^{31–38} In this oxidation protocol, the manganosilicate catalyst was easily separated by filtration and could be regenerated and reused several times without loss of its activity and selectivity. The incorporation of manganese into the mesoporous silicates have been reported earlier, however, the reported methodologies suffer with the loss of the ordered mesoporous structure, low metal loadings or the

formation of bulk manganese species outside the mesoporous framework.^{39–42} The present work reports for the first time a new facile methodology to blend the manganese oxide gel into the synthesis mixture of silicate framework. The overall mesoporous cubic structure was maintained and no bulk manganese oxide was detected outside the mesoporous framework.

Experimental

Chemicals

All the chemicals were of AR grade and used without any further purification. KMnO_4 and maleic acid were procured from E-Merck India Ltd. Hexadecyl amine (HDA), tetraethylorthosilicate (TEOS) and all the alcohols were obtained from Merck-Schuchardt DHG, Germany. Ammonium peroxydisulfate was acquired from Qualigens Fine chemicals, a division of Glaxo India Ltd.

Synthesis of manganosilicate molecular sieves

The synthesis mixture of manganosilicate molecular sieves was composed of TEOS/HDA/maleic acid/ KMnO_4 /ethanol/ H_2O in the molar ratios 1 : 0.25 : 0.125 : 0.315 : 49 : 28. A solution of hexadecyl amine was made in ethanol and maleic acid was added in parts. To this mixture, aqueous KMnO_4 solution and TEOS were added simultaneously and dropwise with vigorous stirring. Brown coloured gel formed was stirred for two hours and then allowed to age for 24 hours at the ambient temperature. The upper water layer was decanted and material was air dried on a glass plate. This was then followed by calcination at 550 °C in air for 5 hours.

Catalyst characterisation

Manganosilicate molecular sieves were characterised by X-ray diffraction, electron spin resonance (ESR), tunneling electron microscope (TEM), and N_2 sorption analysis. Elemental analysis was performed by an inductively coupled plasma atomic emission spectrometer (ICP-AES). X-ray scattering measurements were made with $\text{CuK}\alpha$ radiation on a

Chemical Research & Development, IPCA Laboratories Ltd., 123 AB, Kandivali Industrial Estate, Kandivali (w), Mumbai - 400 067, India.
E-mail: ashokkumar@ipca.co.in; Fax: 91-22-5647 4757;
Tel: 91-22-5647 4755

SIEMENS D 5000 diffractometer equipped with reflection geometry, a NaI scintillation counter, a curved graphite crystal monochromator and a nickel filter. The scattered intensities were collected from 2° to 40° (2θ) by scanning at 0.030° (2θ) steps with a counting time of 0.5 s at each step. Transmission electron microscopy was carried out on a Philips CM 200 transmission electron microscope operating at 200 kV. Images were recorded on film. Surface area, pore volume and pore diameter measurements were carried out using nitrogen sorption technique on a Micromeritics ASAP 2010 instrument. Catalyst samples were pretreated under vacuum at 200°C , and then subjected to analysis at the temperature of liquid nitrogen.

General procedure for the oxidation of alcohols

The preliminary experiments were performed using 3-pyridyl methanol and ammonium peroxydisulfate in the absence of manganosilicate molecular sieves to find no oxidation of the substrate. This indicated the use of manganosilicate molecular sieves as essential. The initial studies were carried out with 3-pyridyl methanol and manganosilicate molecular sieve as the catalyst using ammonium peroxydisulfate as the oxidizing agent. The optimum reaction conditions were established. All the other substrates were oxidised under the same experimental conditions. The reactions were studied in a mechanically agitated contactor made of glass and a reflux condenser. The reaction mixture acidified with H_2SO_4 containing the required amount of alcohol and catalyst in water was stirred mechanically. Required amount of aqueous persulfate solution was added continuously with the help of a peristaltic pump. The reaction was performed in a water bath assembly where the desired temperatures were properly maintained.

Method of analysis

Samples were withdrawn periodically from the reaction mixture and were filtered before being analysed by HP 6890 N gas chromatograph equipped with autosampler 7683 series injector and HP chemstation. A ($30\text{ m} \times 0.32\text{ mm id} \times 0.25\ \mu\text{m}$) column packed with DB-5 (5% polyphenyl + 95% polymethyl siloxane) was used for analysis (injector/detector temperature 250°C , oven $60^\circ\text{C}-2\text{ min}-10^\circ\text{C min}^{-1}-250^\circ\text{C}-5\text{ min}$). 3-pyridyl methanol and 4-pyridyl methanol were analysed by Water's Alliance HPLC system equipped with 2695 sample handling unit and 2487 UV detector. Purosphere star ($250 \times 4.6\text{ mm} \times 5\ \mu\text{m}$) column was used with $0.02\text{ mol Na}_2\text{HPO}_4$ (pH 7) buffer : acetonitrile (90 : 10) mobile phase. For analysis of 2-n-butyl-5-chloro-imidazole-4-alcohol, Water's Atlantis (C-18) ($250 \times 4.6\text{ mm} \times 5\ \mu\text{m}$) column was used with buffer ($0.18\text{ g NaH}_2\text{PO}_4 + 1.18\text{ g Na}_2\text{HPO}_4$ in 1 litre deionised water, pH 7 with orthophosphoric acid): acetonitrile (65 : 35) mobile phase. Synthetic mixtures were prepared and used for calibration and quantification. GC-MS and LC-MS confirmed the products.

Results and discussion

Synthesis and characterisation of manganosilicate molecular sieves

We found manganese oxides with tunnel and layered materials to be fascinating for their multivalent character and high

efficiency in oxidation reactions.^{43,44} However, because of the small tunnel size, the number of the organic compounds that can be oxidized by manganese oxides is limited to molecules with smaller kinetic diameters. It was thought worthwhile to engineer a new type of material that has redox characteristics of octahedral manganese oxides with the advantages of high surface area and larger pore dimensions of mesoporous silicates. The synthesis methodology was designed to blend the manganese oxide gel in the synthetic mixture of mesoporous silica. The permanganate ions were chemically reduced in the solution at the time of hydrolysis of TEOS. The resulting manganosilicate molecular sieves had the Mn content of 11 weight% as determined by elemental analysis using ICP and the BET surface area of $552\text{ m}^2\text{ g}^{-1}$, pore volume $0.5\text{ cm}^3\text{ g}^{-1}$ and average pore diameter of $36\ \text{\AA}$. X-ray powder diffraction patterns of the manganosilicate molecular sieve are shown in Fig. 1. The XRD pattern of manganosilicate material showed 4 diffractions in the 2θ range of $2-8^\circ$, similar to XRD patterns previously reported for Mn-M41S materials.⁴⁵⁻⁴⁷ The material exhibits sharp and intense peaks, indicating that the cubic arrangement of mesopores is well ordered. The repeat distance (cubic, $a_o = d_{100}\sqrt{h^2 + k^2 + l^2}$) including the pore walls was calculated to be $36\ \text{\AA}$. The ESR spectra of manganosilicate molecular sieves are shown in Fig. 2. At room temperature a broad single line signal centered at $g = 2.0027$ was observed. CaCl_2 -exchanged manganosilicate samples depicted six well resolved hyperfine sextet lines at about 3300 gauss. Also forbidden transitions were observed between allowed sextet lines. The observation of forbidden transitions indicated presence of immobile Mn(II) species.⁴⁵⁻⁴⁷ Both Mn(II) and Mn(IV) can give similar ESR spectra. However, Mn(IV) shows g values less than 2.0 and the calcined manganosilicates appeared purple to violet in color, which is consistent with the color of Mn(II) ions but not Mn(IV) ions since Mn(IV) ions are usually yellow.⁴⁸ The g -factor and the hyperfine splitting obtained are characteristic of a Mn^{+2} complex in octahedral coordination. The hyperfine sextet lines signal obtained with CaCl_2 -exchanged manganosilicate samples concluded the presence of manganese ions in the framework sites in silicate molecular sieves.⁴⁹ The TEM micrograph for manganosilicate molecular sieves is shown in Fig. 3. It shows smaller particles with cubic morphology and average particle size of 100 nm. No bulk manganese or precipitates outside the silica particles were found.

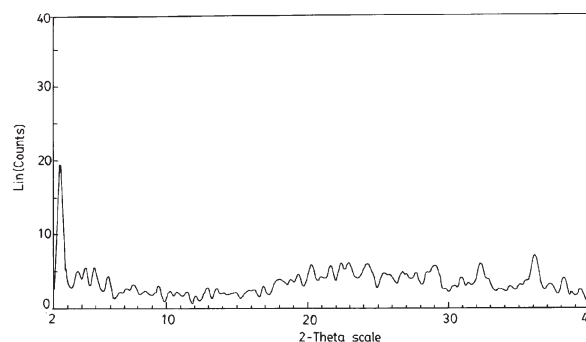


Fig. 1 X-ray diffraction pattern of manganosilicate.

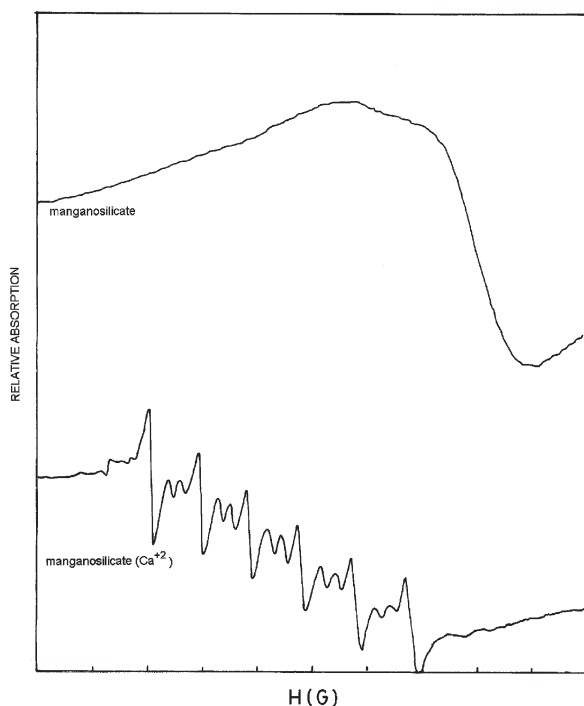


Fig. 2 ESR spectra of manganosilicate.

Oxidation of alcohols

The scope of manganosilicate to act as an oxidising catalyst was examined against various heterocyclic and alicyclic alcohols as depicted in Table 1. The oxidation protocol was successfully applied for the synthesis of the carbonyl compounds of high industrial importance, for their potential use as pharmaceutical intermediates. 2-n-Butyl-5-chloro-imidazole-4-carboxaldehyde (entry 1) is used for the synthesis of losartan, an antihypertensive, non-peptide angiotensin II receptor antagonist.⁵⁰ Substituted cyclohexanones (entries 2 and 3) are used for the synthesis of atovaquone, an antipneumocystic hydroxynaphthoquinone derivative that inhibits mitochondrial electron transport.⁵¹ 3-Pyridinecarboxaldehyde (entry 4), is a highly useful intermediate for preparing medicines, agricultural chemicals and dyestuff, for instance it is used in the synthesis of imidacloprid, a new type of insecticide that acts on the nicotinic acid

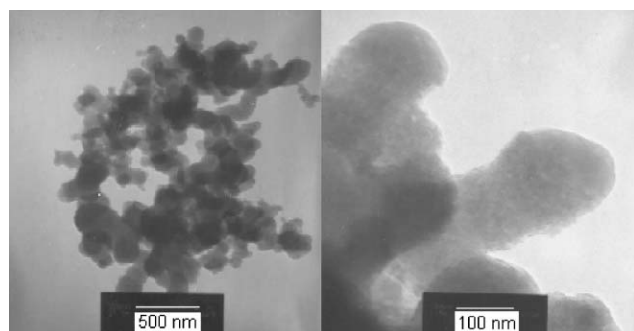


Fig. 3 TEM micrograph of manganosilicate molecular sieve.

receptors.⁵² 4-Pyridinecarboxaldehyde (entry 5) is used in the synthesis of porphyrin analogues that are potent antagonists to inhibit fibroblast growth factor (FGF 2) and vascular endothelial growth factor (VEGF) receptor binding for treatment of tumors and malignant tissues.⁵³ Furfuraldehyde (entry 7) is used in the synthesis of dantrolene and piperidolate that are antispasmodic and anticholinergic agents.^{54,55} Heterocyclic alcohols, which are usually regarded as difficult substrates in most oxidations involving transition metals, due to their strong coordination ability, were selectively converted to the corresponding aldehydes. This indicates that nitrogen-based moieties, at least for cases where the nitrogen atom is not susceptible to oxidation, do not interfere with the catalytic alcohol oxidation. This result is indicative of the better efficacy of our catalyst to perform oxidation of heterocyclic alcohols in comparison with previously reported monomeric transition metal complex catalysts. Proximity of the heteroatom in the aromatic ring to the site of oxidation appeared to have no effect on the course of the reaction (entries 4 and 5). It was contemplated that chloro group substitution in aromatic ring did not interfere with the oxidation of hydroxy group but accelerated the rate of reaction (entries 1 and 8). Secondary alcohols were all selectively oxidised to the corresponding ketone in good to high yields. The reaction appears to be truly heterogeneous. The oxidation of 3-pyridyl methanol stopped when the manganosilicate catalyst was filtered off the hot reaction mixture and the reaction was further continued at the same temperature.

Reusability of catalyst

The reusability of manganosilicate was established by carrying out repeated oxidation of 3-pyridyl methanol with recovered catalyst (Fig. 4). The catalyst was regenerated before being reused in subsequent batches. It was washed with water and air dried at 75 °C for 4 h, followed by subsequent heating at 300 °C for 2 h. With fresh catalyst, the conversion of 3-pyridyl methanol was 80%, however it went down to 77% during the third reuse. The interesting part was the selectivity towards the aldehyde that remained same during each run. The decrease in conversion could be attributed to the observed losses due to attrition, during filtration of the catalyst particles. No make up quantity of catalyst was added during subsequent experiments.

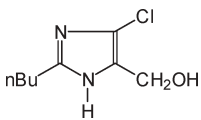
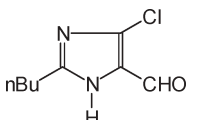
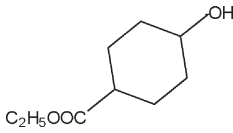
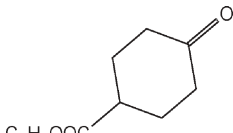
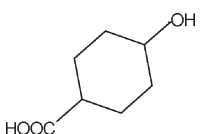
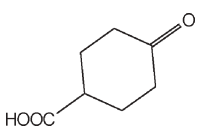
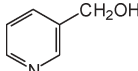
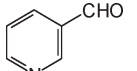
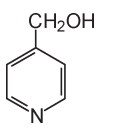
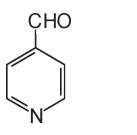
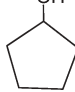

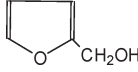
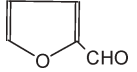
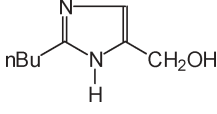
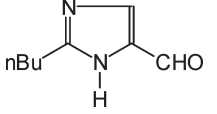
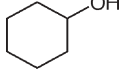
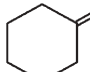
Conclusions

In summary, the paper describes a facile methodology to synthesise uniform cubic manganosilicate molecular sieves, devoid of any extra-framework manganese oxides; and the usefulness of the material as recyclable catalyst in the benign oxidation protocol for difficult to oxidize heterocyclic and aliphatic alcohols. This oxidation methodology conforms to 5 of the 12 guiding principles of green chemistry, as proposed by Anastas and Warner.⁵⁶

Acknowledgements

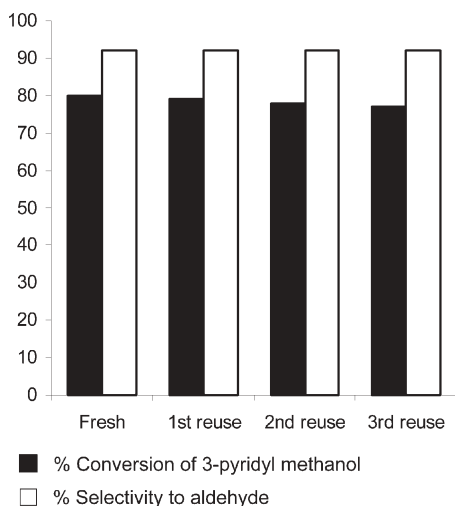
The authors are indebted to Dr Suneel Dike for helpful discussions.

Table 1 Oxidation of alcohols using disordered manganosilicate molecular sieves

No.	Substrate	Product	Time/h	% conversion ^a of alcohol	% selectivity ^b
1			6	97	93
2			2	92	92
3			3	87	95
4			4	80	92
5			4	79	92
6			2	80	92
7			0.5	90	81
8			6	71	81
9			2	25	80

^a % conversions based on GC analysis, ^b % selectivity towards corresponding aldehyde/ketone with remaining respective carboxylic acid.

^c Reaction conditions: alcohol: 0.01 mol; water 40 cm³; catalyst loading: 0.005 g cm⁻³; ammonium persulfate 0.013 mol; temperature: 70 °C.

**Fig. 4** Reusability of manganosilicate.

References

- 1 C. L. Hill, *Advances in Oxygenated Processes*, ed. A. L. Baumstark, JAI Press, London, 1988, vol. 1, p. 1.
- 2 *Comprehensive Organic Synthesis*, B. M. Trost and I. Fleming, Pergamon, Oxford, UK, 1991.
- 3 F. Trifiro and F. Cavani, *Catal. Stud.*, 1994, **419**, 350.
- 4 *Ullmann's Encyclopaedia of Industrial Chemistry*, VCH Publishers, Weinheim, 5th edn, 1985, vol. **A3**, p. 469.
- 5 R. A. Sheldon, *J. Chem. Technol. Biotechnol.*, 1997, **68**, 381.
- 6 J. Muzart, *Chem. Rev.*, 1992, **92**, 113.
- 7 K. Yamaguchi and N. Mizuno, *Angew. Chem., Int. Ed.*, 2002, **41**, 4538.
- 8 H. B. Ji, T. Mizugaki, K. Ebitani and K. Kaneda, *Tetrahedron Lett.*, 2002, **43**, 7179.
- 9 H. B. Ji, K. Ebitani, T. Mizugaki and K. Kaneda, *Catal. Commun.*, 2002, **3**, 511.
- 10 G. Brink, I. W. C. E. Arends and R. A. Sheldon, *Science*, 2000, **287**, 1636.
- 11 D. R. Jensen, J. S. Pugsley and M. S. Signam, *J. Am. Chem. Soc.*, 2001, **123**, 7475.
- 12 A. Cornelis and P. Laszlo, *Synthesis*, 1985, 909.

- 13 V. D. Makwana, Y.-C. Son, A. R. Howell and S. L. Suib, *J. Catal.*, 2002, **210**, 46.
- 14 H.-B. Ji, K. Ebitani, T. Mizugaki and K. Kaneda, *Catal. Commun.*, 2002, **3**, 511.
- 15 R. A. Sheldon and J. K. Kochi, *Metal-Catalyzed Oxidation of Organic Compounds*, Academic Press, New York, 1984.
- 16 E. Takezawa, S. Sakaguchi and Y. Ishii, *Org. Lett.*, 1999, **1**, 713.
- 17 B. Hinzen, R. Lenz and S. V. Ley, *Synthesis*, 1998, 977.
- 18 K. Kaneda, Y. Fujie and K. Ebitani, *Tetrahedron Lett.*, 1997, **38**, 9023.
- 19 K. Ebitani, Y. Fujie and K. Kaneda, *Langmuir*, 1999, **15**, 3557.
- 20 C.-J. Li and T.-H. Chan, *Organic Reactions in Aqueous Media*, John Wiley & Sons, New York, 1997.
- 21 *Organic Synthesis in Water*, P. A. Grieco, Blackie Academic and Professional, London, 1998.
- 22 C.-J. Li, *Chem. Rev.*, 1993, **93**, 2023.
- 23 U. M. Lindstrom, *Chem. Rev.*, 2002, **102**, 2751.
- 24 R. Liu, C. Dong, X. Liang, X. Wang and X. Hu, *J. Org. Chem.*, 2005, **70**, 729.
- 25 Y. Uozumi and R. Nakao, *Angew. Chem., Int. Ed.*, 2003, **42**, 194.
- 26 G.-J. ten Brink, I. W. C. E. Arends and R. A. Sheldon, *Science*, 2000, **287**, 1636.
- 27 G.-J. ten Brink, I. W. C. E. Arends and R. A. Sheldon, *Adv. Synth. Catal.*, 2002, **344**, 355.
- 28 H. G. Manyar, G. S. Chaure and A. Kumar, *J. Mol. Catal. A: Chem.*, 2006, **243**, 244.
- 29 H. G. Manyar, A. Kumar and G. S. Chaure, *Indian Patent 207/MUM/2005*, 2005.
- 30 G. D. Yadav, H. G. Manyar and C. K. Mistry, *Proceedings of Chemcon-2000, Indian Chemical Engineering Congress*, Indian Institute of Chemical Engineers, Kolkata, India, 2000, **1**, pp. REC 9–12.
- 31 Y. H. Kim, J. C. Jung, H. C. Choi and S. G. Yang, *Pure Appl. Chem.*, 1999, **71**, 3–377.
- 32 M. V. Bhatt and P. T. Perumal, *Tetrahedron Lett.*, 1981, **22**, 27–2605.
- 33 G. D. Menghani and G. V. Bakore, *Bull. Chem. Soc. Jpn.*, 1968, **41**, 2574.
- 34 M. Hirano, K. Kojima, S. Yakabe and T. Morimoto, *J. Chem. Res.*, 2001, **7**, 274.
- 35 H. Kochkar, L. Lassalle, M. Morawietz and W. F. Hoelderich, *J. Catal.*, 2000, **194**, 343.
- 36 H. Firouzabadi, P. Salehi and I. Mohammadpoor-Baltork, *Bull. Chem. Soc. Jpn.*, 1992, **65**, 2878.
- 37 J. M. Anderson and J. K. Kochi, *J. Am. Chem. Soc.*, 1970, **92**, 1651.
- 38 D. A. House, *Chem. Rev.*, 1962, **62**, 185.
- 39 M. Yonemitsu, Y. Tanaka and M. Iwamoto, *Chem. Mater.*, 1997, **9**, 2679.
- 40 L. Wang, J. Shi, J. Yu and D. Yan, *Nanostruct. Mater.*, 1998, **10**, 1289.
- 41 B. J. Aronson, C. F. Blanford and A. Stein, *J. Phys. Chem. B*, 2000, **104**, 449.
- 42 V. Caps and S. C. Tsang, *Catal. Today*, 2000, **61**, 19.
- 43 S. L. Suib, *Stud. Surf. Sci. Catal.*, 1996, **102**, 47.
- 44 Y.-C. Son, V. D. Makwana, A. R. Howell and S. L. Suib, *Angew. Chem., Int. Ed.*, 2001, **40**, 4280.
- 45 S. Gomez, O. Giraldo, L. J. Garces, J. Villegas and S. L. Suib, *Chem. Mater.*, 2004, **16**, 2411.
- 46 J. Xu, Z. Luan, M. Hartmann and L. Kevan, *Chem. Mater.*, 1999, **11**, 2928.
- 47 D. Zhao and D. Goldfarb, *J. Chem. Soc., Chem. Commun.*, 1995, 875.
- 48 D. Goldfarb, *Zeolites*, 1989, **9**, 509.
- 49 J. Xu, Z. Luan, T. Wasowicz and L. Kevan, *Microporous Mesoporous Mater.*, 1998, **22**, 179.
- 50 D. J. Carini, J. J. V. Duncia and P. C. B. Wong, *US Patent*, 1988, 5 138 069.
- 51 A. T. Hudson and A. W. Randall, *US Patent*, 1889, 5 053 432.
- 52 M. Yasuda, H. Ohkishi, K. Sato, Y. Morimoto and T. Nagasawa, *US Patent*, 1995, 5 436 145.
- 53 D. Aviezer, S. Cotton, M. David, A. Segev, N. Khaselev, N. Galili, Z. Gross and A. Yaron, *Cancer Res.*, 2000, **60**, 2973.
- 54 S. Davis, *US Patent*, 1968, 3 415 821.
- 55 J. H. Biel, *US Patent*, 1959, 2 918 407.
- 56 P. T. Anastas and J. C. Warner, *Green Chemistry: Theory and Practice*, Oxford University Press, Oxford, 1998.

Fluorine-free and hydrophobic room-temperature ionic liquids, tetraalkylammonium bis(2-ethylhexyl)sulfosuccinates, and their ionic liquid–water two-phase properties

Naoya Nishi, Takahiro Kawakami, Fumiko Shigematsu, Masahiro Yamamoto and Takashi Kakiuchi*

Received 12th August 2005, Accepted 11th January 2006

First published as an Advance Article on the web 30th January 2006

DOI: 10.1039/b511529a

Fluorine-free and hydrophobic room-temperature ionic liquids (RTILs) composed of the bis(2-ethylhexyl)sulfosuccinate (BEHSS) ion, which is known as the surface-active anion constituting Aerosol OT[®], and symmetric tetraalkylammonium ions ((C_nH_{2n+1})₄N⁺; n = 4–8), have been prepared. Physicochemical properties of the water-saturated RTILs such as density, conductivity, viscosity and mutual solubility with water (W) have been measured. The RTIL|W interface is polarizable for the RTILs with n = 5–8 in spite of the high water content, 3.6–8.9 wt% in the water-saturated RTILs. The width of the polarized potential window of the RTIL|W interfaces is quantitatively correlated with the solubility of the RTIL in W. The RTIL–W two-phase systems are not spontaneously emulsified and no reverse micelles are formed in the water-saturated RTILs, although BEHSS[−] is known to form stable water-in-oil emulsions and reverse micelles in oil–water two-phase systems.

Introduction

The properties of room-temperature ionic liquids (RTILs) can be tuned by choosing cations and anions constituting the RTILs. Various cations and anions have been combined to form RTILs having desired physicochemical characteristics.^{1–5} However, in the case of water-immiscible RTILs composed of hydrophobic cations and anions, the number of ions, especially anions, so far reported is limited because salts composed of hydrophobic and bulky ions tend to have high melting points (*T_m*). Two widely used anions for water-immiscible RTILs are the PF₆[−] and bis(trifluoromethylsulfonyl)imide (C₁C₁N) ion,⁷ both of which contain fluorine atoms. Fluorine-free and hydrophobic anions that are more environmentally friendly are highly desired.^{8–10}

Several ionic liquids composed of fluorine-free and hydrophobic anions have been reported. Tetraalkylammonium tetraalkylborates¹¹ and tetraphenylborates¹² having *T_m* below 100 °C were already found more than two decades ago. More recently, Larsen *et al.* prepared ionic liquids composed of bulky carborane anions, aiming at ionic liquids with little nucleophilicity, and found that some salts with carborane anion derivatives have a *T_m* below 50 °C.¹³ Wasserscheid *et al.* found that 1-butyl-3-methylimidazolium (C₄mim) octylsulfate has a *T_m* of 34–35 °C and explored their application to the solvent in the two-phase organic synthesis.¹⁴ Mukai *et al.* recently used dodecylsulfonate ions for ionic liquids, among which the 1,3,4-trimethylimidazolium salt has a *T_m* of 92.5 °C.¹⁵

To obtain salts having lower *T_m* values, the combination of a cation with higher symmetry and an anion with lower symmetry (or vice versa) may be promising. One candidate for the anions with lower symmetry is bis(2-ethylhexyl)sulfosuccinate (BEHSS) ion, which has a sulfo group and two branched alkyl chains. BEHSS[−] is a widely used surface-active anion constituting Aerosol OT[®] (Na[BEHSS]). A few research groups replaced the sodium ion of Na[BEHSS] with symmetric tetraalkylammonium ions ((C_nH_{2n+1})₄N⁺; n = 1–3) to study the cation-size effect on the structure of reverse micelles in oil.^{16–18} The salts obtained were waxy solids at room temperature.^{17,18} Recently, we found that BEHSS-based salts composed of the symmetrical tetraalkylammonium ions with longer alkyl chains (n = 4–8) and trioctylmethylammonium ion are liquid at room temperature.^{19,20}

In the present paper we will describe the physicochemical properties of BEHSS-based RTILs composed of symmetric tetraalkylammonium ions (n = 4–8). The electrochemical polarizability of the interfaces between water (W) and the BEHSS-based RTILs will also be reported. We will show that the solubility of these RTIL in water is correlated with the polarized potential window (ppw) of the RTIL|W interfaces, and that the RTIL–W two-phase systems are not spontaneously emulsified within the ppw and no reverse micelles are formed in the water-saturated RTILs although BEHSS[−] is known to form stable water-in-oil emulsions and reverse micelles in oil–water two-phase systems.

Experimental

Chemicals

Bromide salts of tetrabutylammonium (TBA), tetrahexylammonium (THxA) and tetraoctylammonium (TOA) ions, and iodide salts of tetrapentylammonium (TPnA) and

Department of Energy and Hydrocarbon Chemistry, Graduate School of Engineering, Kyoto University, Kyoto, 615-8510, Japan.
E-mail: kakiuchi@scl.kyoto-u.ac.jp; Fax: +81 75-383-2490;
Tel: +81 75-383-2489

tetraheptylammonium (THpA) ions, were purchased from Tokyo Kasei Kogyo. Na[BEHSS] was purchased from Sigma. All chemicals were used as received.

Preparation of RTIL

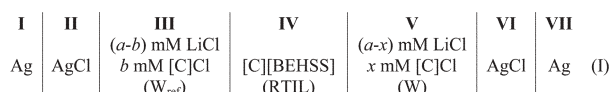
Equimolar amounts of tetraalkylammonium halide ((C_nH_{2n+1})₄NX; *n* = 4–8, X = Br, I) and Na[BEHSS] were dissolved in trichloromethane. The trichloromethane solution was then repeatedly washed with water until no halide ions were detected in the aqueous phase upon mixing with an AgNO₃ aqueous solution. After evaporation of trichloromethane, a yellow viscous liquid was obtained as a crude RTIL. In order to remove trace halide ions as precipitate, the crude RTIL was dissolved into methanol and Ag₂O was added. Ag₂O and precipitated AgX were filtered off. After repeated washing of RTIL with a methanol–water mixture and drying under vacuum, a clear and colorless RTIL was obtained.

Measurements of physicochemical properties

A 50 mL centrifugation glass vial containing RTIL and water was shaken by hand and then kept at 25 °C in a water bath for at least three days. After centrifugation at 3000 rpm for 20 min, a water-saturated RTIL was obtained as a transparent liquid. The glass transition points (*T_g*) of the water-saturated RTILs were measured using a differential scanning calorimeter (Pyris Diamond DSC, Perkin-Elmer) at a heating or cooling rate of 10 °C min⁻¹. Density (*d*), viscosity (*η*), conductivity (*κ*) and solubility of water in the water-saturated RTILs (*S_{W/R}*) were measured with a pycnometer, an oscillation type viscometer (VM-10A-M, CBC Materials), conductometer (CM-117, Kyoto Electronics), and a Karl Fischer moisturemeter (CA-21, Dia Chemical), at 25 °C, respectively.

Electrochemical measurements

Potentiometry. The solubility of RTILs in water (*S_{R/W}*) was measured using potentiometry at the RTIL|W interface. The shape of the cell for potentiometric measurements has been reported elsewhere.²¹ The electrochemical cell is represented as:



where mM stands for mmol dm⁻³, C denotes either the TBA, TPnA, THxA, THpA, or TOA ion, which is in common in the III, IV, and V phases. Before measurement, the aqueous solutions (the III and V phases) were equilibrated with RTIL, and RTIL (the IV phase) was equilibrated with water, at 25 °C. The potential of the Ag/AgCl electrode on the right-hand side with respect to the left is denoted as *E*. We measured *E* as a function of *x* keeping *a* and *b* constant for each RTIL at 25 °C.

Voltammetry. Cyclic voltammograms (CVs) were recorded for estimating the width of the ppw of the RTIL|W

interfaces.^{22,23} The RTIL|W interface was formed at the orifice of a micropipette tip having an inner diameter of several micrometers, typically 2 μm. A borosilicate glass capillary with the outer diameter of 1 mm was pulled by using a micropipette puller with a heat coil (PC-10, Narishige). The two-electrode electrochemical cell we employed is represented as:



The definition of *E* in cell (II) is the same as that for cell (I). The current, *I*, corresponding to the flow of a positive charge from W to RTIL is taken to be positive. The *IR* drop was not compensated for. The estimated solution resistance in this system was several tens of MΩ at most and the magnitude of the current in the ppw is in the sub-nA level. The effect of the *IR* drop on the shape of a CV would become discernible only at the edge of the ppw. All measurements were performed at 25 °C.

Results and discussion

Physicochemical properties of the water-saturated RTILs

Melting points and glass transition points. In the DSC traces of the BEHSS-based RTILs, only the glass transition was observed. The melting/freezing behavior was absent even when the samples were slowly heated and cooled at 1 °C min⁻¹ in the DSC measurements or after the RTILs were kept in a freezer (–20 °C) for a week. This behavior does not necessarily mean that BEHSS-based RTILs do not have *T_m*. They may be in the supercooled state below their *T_m*, not showing transition to the solid state. On the other hand, we found that [THxA][C₁C₁N] became solid when cooled in the DSC measurements at a moderate cooling rate (10 °C min⁻¹), though the viscosity is similar to those of the BEHSS-based RTILs (Table 1). Other RTILs composed of symmetric tetraalkylammonium ions and C₁C₁N⁻, [R₄N][C₁C₁N], have also been reported to show *T_m*.^{24,25}

The observed *T_g* values (Table 1) are in the range of *T_g* for most glass-forming RTILs, from –70 °C to –100 °C.^{26–29} *T_g* of these BEHSS-based RTILs gradually decreases with increasing *n*. Such a tendency has also been found in the cation-size effect on *T_g* of RTILs composed of aliphatic quaternary ammonium ions; *T_g* decreases with increasing size for the cations of relatively small size.^{24,30}

Table 1 Physicochemical properties (melting point (*T_m*), glass transition point (*T_g*), density (*d*), viscosity (*η*), and conductivity (*κ*)) for BEHSS-based RTILs and [THxA][C₁C₁N] saturated with water

RTIL	FW ^a	<i>T_m</i> /°C	<i>T_g</i> /°C	<i>d</i> ^b /g cm ⁻³	<i>η</i> ^b /Pa s	<i>κ</i> ^b /μS cm ⁻¹
[TBA][BEHSS]	664.1	— ^c	–71	0.993	0.373	86.8
[TPnA][BEHSS]	720.2	— ^c	–71	0.978	0.517	46.1
[THxA][BEHSS]	776.3	— ^c	–74	0.968	0.639	21.8
[THpA][BEHSS]	832.4	— ^c	–80	0.961	0.690	14.4
[TOA][BEHSS]	888.5	— ^c	–80	0.952	0.759	13.9
[THxA][C ₁ C ₁ N]	634.8	–8	–77	1.186	0.388	130

^a Formula weight. ^b At 25 °C. ^c Not observed.

Density. The density of these RTILs saturated with water are in the range of 0.95–0.99 g cm⁻³ (Table 1), *i.e.*, slightly lighter than that of water. These values are considerably smaller than those for imidazolium-based RTILs (1.1–1.6 g cm⁻³)³ or [R₄N][C₁C₁N] (1.0–1.2 g cm⁻³).²⁵ The decreasing tendency of *d* with increasing *n* has also been found for a series of [R₄N][C₁C₁N].²⁵

Conductivity and viscosity. With increasing *n*, η monotonically increased and κ monotonically decreased. Comparing η and κ for the BEHSS-based RTILs with those for [THxA][C₁C₁N], the BEHSS-based RTILs have higher η and lower κ than the corresponding C₁C₁N-based RTILs. This reflects the greater size of BEHSS⁻ than that of C₁C₁N⁻.

Solubility of the RTILs in water. We determined $S_{R/W}$ potentiometrically by measuring *E* of cell (I) as a function of $c_{C^+}^{W,0}$, where $c_{C^+}^{W,0}$ is the concentration of C⁺ in W before W is in contact with RTIL. The plots of *E* against $\log c_{C^+}^{W,0}$ for the BEHSS-based RTILs and [THxA][C₁C₁N] are shown in Fig. 1. For RTILs except for [TOA][BEHSS], *E* at high $c_{C^+}^{W,0}$ values was linearly dependent on $\log c_{C^+}^{W,0}$ with a common slope, 59.2 mV decade⁻¹ at 25 °C. This is because the equilibrium concentration of C⁺ in W in contact with RTIL, $c_{C^+}^W$, is almost equal to $c_{C^+}^{W,0}$ at higher $c_{C^+}^{W,0}$ than $S_{R/W}$ and thus *E* shows the Nernstian response to $c_{C^+}^{W,0}$ (See Appendix). At lower $c_{C^+}^{W,0}$ values *E* leveled off to that at $c_{C^+}^{W,0} = 0$, because, at $c_{C^+}^{W,0}$ values lower than $S_{R/W}$, $c_{C^+}^W$ is almost equal to $S_{R/W}$ and thus *E* is independent of $c_{C^+}^{W,0}$.

For each BEHSS-based RTIL, $S_{R/W}$ was estimated by fitting a theoretical curve to the experimental plot. The results, except for [TOA][BEHSS], are shown in Table 2. The increase in the length of four alkyl chains of the R₄N⁺ by one methylene unit resulted in the decrease in $S_{R/W}$ by one order of magnitude. The solubility of [TOA][BEHSS] cannot be determined

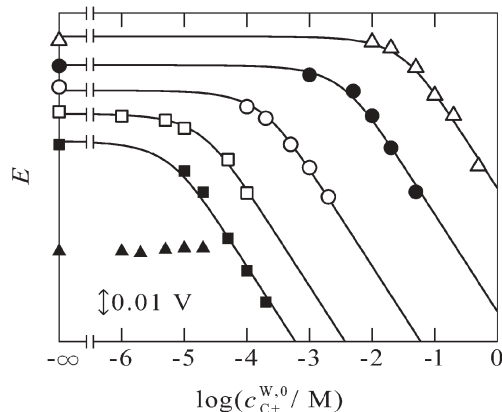


Fig. 1 Plots of the terminal voltage against the logarithm of the initial concentration of C⁺ in W with C = TBA (Δ), TPnA (\square), THxA (\circ), THpA (\square), and TOA (\blacktriangle) for [C][BEHSS], and with C = THxA for [C][C₁C₁N] (\blacksquare). The solid lines represent the fitting curves from eqn (11). The (*a*, *b*) values in cell (I) are (500, 100) for [TBA][BEHSS], (100, 10) for [TPnA][BEHSS], (10, 1) for [THxA][BEHSS], (1, 0.1) for [THpA][BEHSS], (0.2, 0.02) for [TOA][BEHSS], and (10, 1) for [THxA][C₁C₁N].

Table 2 Solubility of the RTILs in water ($S_{R/W}$) and solubility of water in the RTILs ($S_{W/R}$) for BEHSS-based RTILs and [THxA][C₁C₁N] saturated with water

RTIL	$S_{R/W}^a/M$	$S_{W/R}^a/wt\%$
[TBA][BEHSS]	3×10^{-2}	8.9 (3.6 ^c)
[TPnA][BEHSS]	3×10^{-3}	6.0 (2.6 ^c)
[THxA][BEHSS]	2×10^{-4}	4.5 (2.0 ^c)
[THpA][BEHSS]	2×10^{-5}	3.7 (1.8 ^c)
[TOA][BEHSS]	— ^b	3.6 (1.9 ^c)
[THxA][C ₁ C ₁ N]	7×10^{-6}	0.3 (0.1 ^c)

^a At 25 °C. ^b Not observed. ^c Molar ratio of water to RTIL in the RTIL phase.

because the *E* values did not vary with $c_{C^+}^{W,0}$. This is probably because the partition of Cl⁻ instead of TOA⁺ determines the phase-boundary potential across the RTIL|W interface, $\Delta_R^W \phi$; the hydrophobicity of TOA⁺ is stronger than the hydrophilicity of Cl⁻. The solubility of [THxA][BEHSS] (200 μ M) is greater than that of [THxA][C₁C₁N] (7 μ M), and this is ascribed to the more hydrophilic nature for BEHSS⁻ than C₁C₁N⁻.

Solubility of water in the RTILs. The water-saturated RTILs contain 3.6–8.9 wt% of water, as a function of *n* (Table 2). These values are significantly large compared with those of other hydrophobic RTILs. For example, the water content of water-saturated [THxA][C₁C₁N] was 0.3 wt%, less than a tenth of those of BEHSS-based RTILs (Table 2). Other hydrophobic RTILs have less water content than BEHSS-based RTILs: 0.9 wt% for [C₈mim][C₁C₁N]²¹ and 1.3 wt% for [C₈mim]PF₆.³¹ Such an exceptionally large water content in BEHSS-based RTILs probably results from the strong hydration of hydrophilic sulfo group in BEHSS⁻. The average number of water molecules per BEHSS⁻ is 2–4 (Table 2). These values are similar to the hydration number of the sulfo group of BEHSS⁻ reported in the reverse micelles, *i.e.*, 2.³²

It might be expected that reverse micelles of water are formed in the RTILs because BEHSS⁻ is a well-known surface-active ion to form reverse micelles in oil.^{33,34} However, for both dry and water-saturated RTILs, small angle X-ray scattering (SAXS) measurements showed one broad peak at the same periodicity.³⁵ The periodicity increased with increasing *n*. These results indicate that the observed structure is likely to originate from the disordered periodic structure of cations and anions in RTILs.³⁶ Water is thus likely to be uniformly distributed in the BEHSS-based RTILs, hydrating to the sulfo group of BEHSS⁻. This picture is in harmony with the IR spectroscopic studies of water structure in other RTILs such as [C₄mim]BF₄³⁷ and [C₁₀mim]Br.³⁸

The reason for the absence of reverse micelles in the BEHSS-based RTILs seems to be the hydrophobicity of the counter cations of BEHSS⁻. AOT[®] (Na[BEHSS]) forms reverse micelles in oil, where the water pool of the micelle is surrounded by the shell made from BEHSS⁻.^{33,34} A small and hydrophilic Na⁺ exists in the water pool.^{33,34} The hydrophobic cations constituting the BEHSS-based RTIL, R₄N⁺, are thermodynamically and geometrically difficult to exist as counter cations of BEHSS⁻ in the water pool.

Emulsification of the RTIL-W systems

Na[BEHSS] (Aerosol OT[®]) is well known to cause spontaneous emulsification in oil–water two-phase systems when added in water³⁹ or oil.^{40,41} However, we found in the present study that when the BEHSS-based RTILs were in contact with water, the spontaneous emulsification did not occur. This difference may be elucidated by using a criterion of the instability of oil(O)|W interfaces, *i.e.*, electrochemical instability.⁴²

According to the theory of the electrochemical instability, the interfaces become unstable only in a limited range of the phase-boundary potentials across the O|W interfaces ($\Delta_R^W\phi$) around the standard ion-transfer potential ($\Delta_O^W\phi_i^0$) of the surface-active ion.⁴² The width of the instability window, which is dependent on the surface activity of the surfactant ion and its concentration, is typically on the order of a few hundred millivolts.^{43–46} When only one kind of salt, C^+A^- , partitions between a RTIL–W two-phase system, $\Delta_R^W\phi$ at the partition equilibrium is given by:²³

$$\Delta_R^W\phi = \frac{\Delta_R^W\phi_{C^+}^0 + \Delta_R^W\phi_{A^-}^0}{2} \quad (1)$$

The values of $\Delta_R^W\phi_{C^+}^0$ and $\Delta_R^W\phi_{A^-}^0$ have not been determined. To estimate $\Delta_R^W\phi$ for the RTIL–W two-phase systems for the present case, we used the values of $\Delta_{DCE}^W\phi_{C^+}^0$ and $\Delta_{DCE}^W\phi_{A^-}^0$ for the 1,2-dichloroethane(DCE)–W two-phase systems. In the case of [THxA][BEHSS]|W interface, from the values $\Delta_{DCE}^W\phi_{THxA}^0 = -0.49$ V⁴⁷ and $\Delta_{DCE}^W\phi_{BEHSS}^0 = +0.03$ V⁴⁸ it is expected that $\Delta_R^W\phi = \Delta_R^W\phi_{BEHSS}^0 - 0.26$ V. Thus $\Delta_R^W\phi$ seems to be negative enough to be out of the window of the electrochemical instability around $\Delta_R^W\phi_{BEHSS}^0$ and no spontaneous emulsification takes place in these RTIL–water two-phase systems.

Polarized potential window

The CVs at the interface between water and the BEHSS-based RTILs are shown in Fig. 2(a). All the RTIL|W interfaces except for the [TBA][BEHSS]|W interface were found to be polarizable. If the ions in W are hydrophilic enough, the width of the ppw is determined by the hydrophobicity of the ions constituting the RTIL and a good measure of the ppw is $\Delta_R^W\phi_{A^-}^0 - \Delta_R^W\phi_{C^+}^0$.²² The [TBA][BEHSS]|W interface was nonpolarized because $\Delta_R^W\phi_{A^-}^0 - \Delta_R^W\phi_{C^+}^0$ is not large enough. For all the RTILs the positive end of the ppw was located at the same potential. The transfer of moderately hydrophobic BEHSS[−] from RTIL to water is likely to limit the positive end. On the other hand, the negative end of the ppw was dependent on the RTILs. With elongating the alkyl chain of the cations from TBA⁺ to THxA⁺ the negative end of the ppw shifted to the negative direction and the ppw widened. This shift indicates that the negative end of the ppw is limited by the transfer of hydrophobic cations, TBA⁺, TPnA⁺ and THxA⁺, from RTIL to water. The difference in the width of the ppw for [TBA][BEHSS] and [TPnA][BEHSS] or [TPnA][BEHSS] and [THxA][BEHSS] was about 0.1 V, which is similar to that observed for [R₄N][C₁C₁N]|W interfaces.²³ Further elongation of the alkyl chain from THxA⁺ to THpA⁺ or further to TOA⁺ did not widen the ppw. The negative ends of the ppw for

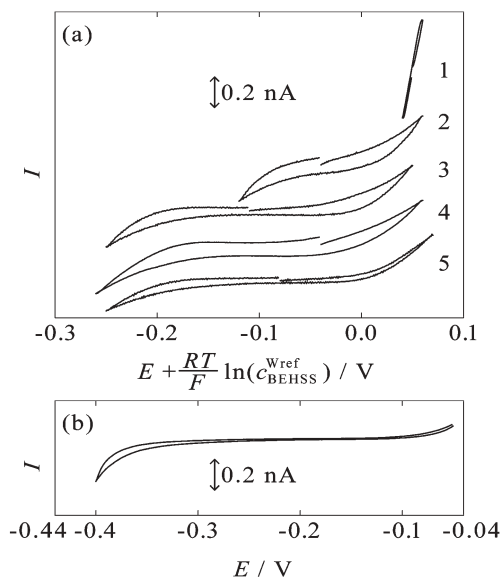


Fig. 2 (a) Cyclic voltammograms at the interface between water and [TBA][BEHSS] (1), [TPnA][BEHSS] (2), [THxA][BEHSS] (3), [THpA][BEHSS] (4), [TOA][BEHSS] (5). In the abscissa, the term $(RT/F)\ln c_{BEHSS}^{W,ref}$ was added to compensate for the n dependent change in the phase-boundary potential across the RTIL|W_{ref} interface. Here $c_{BEHSS}^{W,ref}$ is the equilibrium concentration of BEHSS[−] in W_{ref}. $c_{BEHSS}^{W,ref}$ was calculated using eqn (7) from $c_{BEHSS}^{W,0}$ (1 mM) and $S_{R/W}$ for the BEHSS-based RTILs. (b) Cyclic voltammograms at the interface between water and [THxA][C₁C₁N] at 25 °C. Scan rate: 10 mV s^{−1}. A solution of 100 mM LiCl and 20 mM Li[C₁C₁N] was used for W_{ref} in cell (II).

[THpA][BEHSS] and [TOA][BEHSS] are both likely to be limited by the transfer of Cl[−] from water to RTIL.

In Fig. 2(b), a CV at the [THxA][C₁C₁N]|W interface is shown for comparison with Fig. 2(a). The ppw of the [THxA][C₁C₁N]|W interface is wider than that of the [THxA][BEHSS]|W interface, indicating that C₁C₁N[−] is more hydrophobic than BEHSS[−], which is consistent with the results of the solubility measurement. In the CVs in Fig. 2, neither irregular current nor spike-like current was seen within the ppw, which is in contrast to that observed in CVs measured at the interface between water and DCE containing Na[BEHSS],^{41,49} and is consistent with the absence of spontaneous emulsification discussed above.

Relationship between the polarized potential window and the solubility product

The solubility product of the RTIL in W, K_s^W ($= S_{R/W}^2$), is related to the difference in the standard ion transfer potentials of the cation and the anion constituting RTIL, $\Delta(\Delta_R^W\phi_{CA}^0)$.²²

$$\Delta(\Delta_R^W\phi)_{CA} \equiv \Delta_R^W\phi_{A^-}^0 - \Delta_R^W\phi_{C^+}^0 = -\frac{RT}{F} \ln K_s^W \quad (2)$$

The positive end of the ppw where the current due to the transfer of A[−] from RTIL to W flows is determined by $\Delta_R^W\phi_{A^-}^0$ and, similarly, the negative end is determined by $\Delta_R^W\phi_{C^+}^0$. Therefore, the width of the ppw is related with $\Delta(\Delta_R^W\phi_{CA}^0)$.²¹

The width of the ppw and $\Delta(\Delta_R^W\phi)_{CA}$ for the BEHSS-based RTILs and [THxA][C₁C₁N] calculated from K_s^W are shown

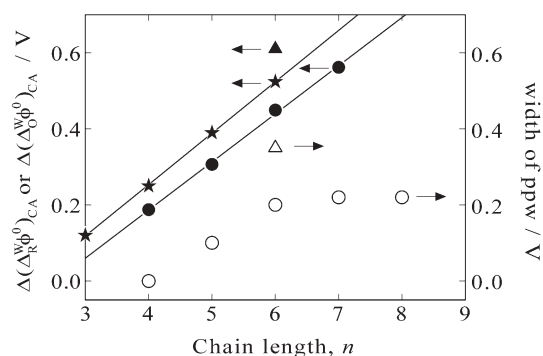


Fig. 3 Chain length dependence of $\Delta(\Delta_{\text{DCE}}^{\text{W}}\phi^0)_{\text{CA}}$ for R_4N^+ and BEHSS^- (\star), and $\Delta(\Delta_{\text{R}}^{\text{W}}\phi^0)_{\text{CA}}$ for the interfaces between water and $[\text{R}_4\text{N}][\text{BEHSS}]$ (\bullet) and $[\text{THxA}][\text{C}_1\text{C}_1\text{N}]$ (\blacktriangle), and the width of the ppw of the interfaces between water and $[\text{R}_4\text{N}][\text{BEHSS}]$ (\circ) and $[\text{THxA}][\text{C}_1\text{C}_1\text{N}]$ (\triangle). The straight lines are fitted to the plots of $\Delta(\Delta_{\text{R}}^{\text{W}}\phi^0)_{\text{CA}}$ for $[\text{R}_4\text{N}][\text{BEHSS}]$ and $\Delta(\Delta_{\text{DCE}}^{\text{W}}\phi^0)_{\text{CA}}$.

in Fig. 3 as a function of n . These parameters for the BEHSS-based RTILs show a similar chain-length dependence; the longer the alkyl chain, the greater the values. The plot of $\Delta(\Delta_{\text{R}}^{\text{W}}\phi^0)_{\text{CA}}$ vs. n was well fitted to the straight line. The slope was estimated to be 32 mV per methylene unit. For comparison, the plot of $\Delta(\Delta_{\text{DCE}}^{\text{W}}\phi^0)_{\text{CA}}$ ($\equiv \Delta_{\text{DCE}}^{\text{W}}\phi_{\text{A}^-}^0 - \Delta_{\text{DCE}}^{\text{W}}\phi_{\text{C}^+}^0$) is shown in Fig. 3. The $\Delta(\Delta_{\text{DCE}}^{\text{W}}\phi^0)_{\text{CA}}$ values are calculated using the values of $\Delta_{\text{DCE}}^{\text{W}}\phi_{\text{C}^+}^0$, -0.09 V, -0.23 V, -0.36 V, and -0.49 V for tetrapropylammonium ion, TBA^+ , TPnA^+ and THxA^+ ,⁴⁷ respectively, and $\Delta_{\text{DCE}}^{\text{W}}\phi_{\text{BEHSS}}^0$ (0.03 V).⁴⁸ The $\Delta(\Delta_{\text{DCE}}^{\text{W}}\phi^0)_{\text{CA}}$ values are greater than the corresponding $\Delta(\Delta_{\text{R}}^{\text{W}}\phi^0)_{\text{CA}}$ values. The slope of the straight line was 34 mV per methylene unit, and is slightly greater than that for the BEHSS-based RTILs, 32 mV. The absolute values of $\Delta_{\text{O}}^{\text{W}}\phi_i^0$ generally become smaller for a solvent with higher polarity.⁵⁰ Therefore $\Delta(\Delta_{\text{O}}^{\text{W}}\phi^0)_{\text{CA}}$ and the slope for the n dependence are also expected to show the same trend. It was found that the BEHSS-based RTILs apparently have higher polarity than DCE. A recent study on the mid-point potentials of ion transfer across the $[\text{THxA}][\text{C}_1\text{C}_1\text{N}]/\text{W}$ interface shows that $[\text{THxA}][\text{C}_1\text{C}_1\text{N}]$ has polarity in-between those of nitrobenzene and DCE.²²

The width of the ppw shows a similar chain-length dependence to $\Delta(\Delta_{\text{R}}^{\text{W}}\phi^0)_{\text{CA}}$ up to $n = 6$ (Fig. 3). The values of the width of the ppw are about 0.2 V smaller than those of $\Delta(\Delta_{\text{R}}^{\text{W}}\phi^0)_{\text{CA}}$ for the BEHSS-based RTILs for $n \leq 6$ and $[\text{THxA}][\text{C}_1\text{C}_1\text{N}]$. For $n = 7$, the limitation of the ppw by Cl^- transfer from W to RTIL makes the width of the ppw narrower than the expected value from $\Delta(\Delta_{\text{R}}^{\text{W}}\phi^0)_{\text{CA}}$. The apparent contradiction that $S_{\text{R}/\text{W}}$ (and $\Delta(\Delta_{\text{R}}^{\text{W}}\phi^0)_{\text{CA}}$) for $n = 7$ is measurable whereas the width of the ppw for $n = 7$ is narrower than expected is ascribed to the difference in the concentration of Cl^- in W for potentiometry and cyclic voltammetry: 1 mM for the former and 100 mM for the latter. It would be useful to make the criterion of the polarizability of the RTIL/W interfaces from the solubility or vice versa.²² The value 0.19 V of $\Delta(\Delta_{\text{R}}^{\text{W}}\phi^0)_{\text{CA}}$ for $[\text{TBA}][\text{BEHSS}]$ is not enough to make the $[\text{TBA}][\text{BEHSS}]/\text{W}$ interface polarizable whereas 0.31 V for $[\text{TPnA}][\text{BEHSS}]$ makes the $[\text{TPnA}][\text{BEHSS}]/\text{W}$

interface polarizable at the range of 0.1 V. The $\Delta(\Delta_{\text{R}}^{\text{W}}\phi^0)_{\text{CA}}$ value to differentiate nonpolarized interfaces and polarizable ones is likely to be between 0.2 and 0.3 V and the solubility is 10^{-3} – 10^{-2} M.⁵¹

Conclusions

Five RTILs composed of fluorine-free and hydrophobic BEHSS^- and symmetric tetraalkylammonium ions have been prepared. They are liquid at the temperature down to their glass transition points of ~ -80 °C. The potentiometric and voltammetric measurements have revealed that the width of the ppw of the RTIL/W interfaces is related to the solubility of RTILs in water. The fluorine-free and hydrophobic characteristics will make these RTILs suitable for the application of the RTIL–W two-phase systems such as liquid–liquid extraction.

No emulsification of the RTIL–W two-phase system occurs although the RTILs contain surface-active BEHSS^- with high content. The SAXS measurements revealed that no reverse micelle formation occurs in the BEHSS-based RTILs. These apparent surface-inactive properties originate from the hydrophobicity of R_4N^+ constituting the BEHSS-based RTILs and can, hence, be tuned by properly choosing the counter cations of BEHSS^- .

Appendix

First, we consider that a water-immiscible RTIL composed of a cation, C^+ , and an anion, A^- , is in contact with pure water. At equilibrium, W is saturated with C^+ and A^- . The amount of C^+ and A^- dissolved into W from RTIL is equal due to the electroneutrality in W. The equilibrium concentrations of C^+ and A^- , represented as $c_{\text{C}^+}^{\text{W}}$ and $c_{\text{A}^-}^{\text{W}}$ respectively, are equal if we neglect micelle formation and ion-pair formation in W. The concentration is defined as the solubility of RTIL in W, $S_{\text{R}/\text{W}}$. The concentrations, $c_{\text{C}^+}^{\text{W}}$, $c_{\text{A}^-}^{\text{W}}$, and $S_{\text{R}/\text{W}}$ are related to the solubility product of the RTIL in W, K_{s}^{W} , as,²¹

$$K_{\text{s}}^{\text{W}} = c_{\text{C}^+}^{\text{W}}c_{\text{A}^-}^{\text{W}} = S_{\text{R}/\text{W}}^2 \quad (3)$$

where we assumed that the activity coefficients of C^+ and A^- in W are unity.

Second, we consider that the water-immiscible RTIL is in contact with an aqueous solution where the C^+ salt of a hydrophilic anion, for example, $[\text{C}]\text{Cl}$, is dissolved at the concentration of $c_{\text{C}^+}^{\text{W},0}$ before the contact. The hydrophilic anion (such as Cl^-) dissolved in W will not affect the partition of other ions because the partition of Cl^- into RTIL is negligible. The amounts of C^+ and A^- dissolved into W from RTIL are then equal as is the case of the partition into pure water. In this case, the equilibrium concentrations, $c_{\text{C}^+}^{\text{W}}$ and $c_{\text{A}^-}^{\text{W}}$, are not equal because $c_{\text{C}^+}^{\text{W},0}$ is finite. They are represented by using the difference in the concentration of the ions in W at equilibrium and that before the contact with RTIL, Δc , as,

$$c_{\text{C}^+}^{\text{W}} = c_{\text{C}^+}^{\text{W},0} + \Delta c \quad (4)$$

$$c_{\text{A}^-}^{\text{W}} = \Delta c \quad (5)$$

From eqns (3), (4) and (5),

$$(c_{C^+}^{W,0} + \Delta c)\Delta c = S_{R/W}^2 \quad (6)$$

From eqns (4) and (6), $c_{C^+}^W$ is written as,

$$c_{C^+}^W = \frac{c_{C^+}^{W,0} + \sqrt{(c_{C^+}^{W,0})^2 + 4S_{R/W}^2}}{2} \quad (7)$$

At two limiting cases, $c_{C^+}^W$ is simply written as,

$$c_{C^+}^W \approx c_{C^+}^{W,0} \quad (\text{when } c_{C^+}^{W,0} \gg S_{R/W}) \quad (8)$$

$$c_{C^+}^W \approx S_{R/W} \quad (\text{when } c_{C^+}^{W,0} \ll S_{R/W}) \quad (9)$$

As shown in eqn (7), $c_{C^+}^W$ depends on $c_{C^+}^{W,0}$ and $S_{R/W}$. Therefore if we measure $c_{C^+}^W$ as a function of $c_{C^+}^{W,0}$, we can determine $S_{R/W}$. Instead of directly measuring $c_{C^+}^W$, we may utilize the Nernstian response of the phase-boundary potential across the RTIL|W interface, $\Delta_R^W \phi$, to $c_{C^+}^{W,0}$, as follows,²¹

$$\Delta_R^W \phi = \Delta_R^W \phi_{C^+}^0 + \frac{RT}{z_{C^+} F} \ln(c_{C^+}^W) \quad (10)$$

where $\Delta_R^W \phi_{C^+}^0$ stands for the standard ion-transfer potential of C^+ , R the gas constant, T temperature, z_{C^+} the charge on C^+ in signed units of electronic charge and F the Faraday constant. In cell (I) in the Experimental section, the measured voltage of the cell, E ($= \Delta_R^W \phi + E_{\text{ref}}$), is then represented as:

$E =$

$$\left(\Delta_R^W \phi_{C^+}^0 + E_{\text{ref}} \right) + \frac{RT}{z_{C^+} F} \ln \left(\frac{c_{C^+}^{W,0} + \sqrt{(c_{C^+}^{W,0})^2 + 4S_{R/W}^2}}{2} \right) \quad (11)$$

where E_{ref} denotes the contribution of the other nonpolarized interfaces to E . By fitting a curve from eqn (11) to the experimental E vs. $c_{C^+}^{W,0}$ plots, $S_{R/W}$ (and $c_{C^+}^W + E_{\text{ref}}$) can be evaluated.

Acknowledgements

The authors are grateful to Dr Hideki Matsuoka and Dr Tamotsu Harada (Department of Polymer Chemistry, Graduate School of Engineering, Kyoto University) for performing the SAXS measurements and analyzing the SAXS data. The authors are also grateful to Mr Satoshi Akasaka (Department of Polymer Chemistry, Graduate School of Engineering, Kyoto University) for the DSC measurements and Mr Hiroshi Murakami (Department of Energy and Hydrocarbon Chemistry, Graduate School of Engineering, Kyoto University) for recording CVs.

This work was partially supported by a Grant-in-Aid for Scientific Research (No. 14205120), a Grant-in-Aid for Exploratory Research (No. 15655008) and a Grant-in-Aid for Young Scientists (No. 16750060) from the Ministry of Education, Culture, Sports, Science and Technology, Japan. This work was conducted under the program, the Center of Excellence for United Approach to New Materials Science, Kyoto University.

References

- J. D. Holbrey and K. R. Seddon, *Clean Prod. Processes*, 1999, **1**, 223–236.
- R. Hagiwara and Y. Ito, *J. Fluorine Chem.*, 2000, **105**, 221–227.
- C. F. Poole, *J. Chromatogr., A*, 2004, **1037**, 49–82.
- J. H. Davis, Jr., *Chem. Lett.*, 2004, **33**, 1072–1077.
- M. C. Buzzeo, R. G. Evans and R. G. Compton, *ChemPhysChem*, 2004, **5**, 1106–1120.
- J. G. Huddleston, H. D. Willauer, R. P. Swatloski, A. E. Visser and R. D. Rogers, *Chem. Commun.*, 1998, 1765–1766.
- P. Bonhôte, A.-P. Dias, N. Papageorgiou, K. Kalyanasundaram and M. Grätzel, *Inorg. Chem.*, 1996, **35**, 1168–1178.
- N. Gathergood, M. T. Garcia and P. J. Scammells, *Green Chem.*, 2004, **6**, 166–175.
- M. T. Garcia, N. Gathergood and P. J. Scammells, *Green Chem.*, 2005, **7**, 9–14.
- R. A. Sheldon, *Green Chem.*, 2005, **7**, 267–278.
- W. T. Ford, R. J. Hauri and D. J. Hart, *J. Org. Chem.*, 1973, **38**, 3916–3918.
- J. E. Gordon and G. N. SubbaRao, *J. Am. Chem. Soc.*, 1978, **100**, 7445–7454.
- A. S. Larsen, J. D. Holbrey, F. S. Tham and C. A. Reed, *J. Am. Chem. Soc.*, 2000, **122**, 7264–7272.
- P. Wasserscheid, R. van Hal and A. Bösmann, *Green Chem.*, 2002, **4**, 400–404.
- T. Mukai, M. Yoshio, T. Kato and H. Ohno, *Chem. Lett.*, 2004, **33**, 1630–1631.
- H.-F. Eicke and H. Christen, *Helv. Chim. Acta*, 1978, **61**, 2258–2263.
- J. Eastoe, B. H. Robinson and R. K. Heenan, *Langmuir*, 1993, **9**, 2820–2824.
- J. Eastoe, S. Chatfield and R. Heenan, *Langmuir*, 1994, **10**, 1650–1653.
- F. Shigematsu, N. Nishi, M. Yamamoto and T. Kakiuchi, *Abstract of a paper presented at the 49th Meeting of the Polarographic Society of Japan*, Yamaguchi University, Japan, November 22–23, 2003, p. 209.
- T. Kawakami, F. Shigematsu, N. Nishi, M. Yamamoto and T. Kakiuchi, *Abstract of a paper presented at the Joint International Meeting of the Electrochemical Society and the Electrochemical Society of Japan*, Hawaii, October 3–8, 2004.
- T. Kakiuchi, N. Tsujioka, S. Kurita and Y. Iwami, *Electrochem. Commun.*, 2003, **5**, 159–164.
- T. Kakiuchi and N. Tsujioka, *Electrochem. Commun.*, 2003, **5**, 253–256.
- T. Kakiuchi, N. Tsujioka, K. Sueishi, N. Nishi and M. Yamamoto, *Electrochemistry*, 2004, **72**, 833–835.
- J. Sun, M. Forsyth and D. R. MacFarlane, *J. Phys. Chem. B*, 1998, **102**, 8858–8864.
- H. Matsumoto, H. Kageyama and Y. Miyazaki, *Chem. Lett.*, 2001, 182–183.
- J. D. Holbrey and K. R. Seddon, *J. Chem. Soc., Dalton Trans.*, 1999, **45**, 2133–2139.
- D. R. MacFarlane, J. Sun, J. Golding, P. Meakin and M. Forsyth, *Electrochim. Acta*, 2000, **45**, 1271–1278.
- J. G. Huddleston, A. E. Visser, W. M. Reichert, H. D. Willauer, G. A. Broker and R. D. Rogers, *Green Chem.*, 2001, **3**, 156–164.
- L. C. Branco, J. N. Rosa, J. J. M. Ramos and C. A. M. Afonso, *Chem.-Eur. J.*, 2002, **8**, 3671–3677.
- W. Xu, E. I. Cooper and C. A. Angell, *J. Phys. Chem. B*, 2003, **107**, 6170–6178.
- J. L. Anthony, E. J. Maginn and J. F. Brennecke, *J. Phys. Chem. B*, 2001, **105**, 10942–10949.
- H. Hauser, G. Haering, A. Pande and P. L. Luisi, *J. Phys. Chem.*, 1989, **93**, 7869–7876.
- R. W. Mattoon and M. B. Mathews, *J. Chem. Phys.*, 1949, **17**, 496–497.
- T. K. De and A. Maitra, *Adv. Colloid Interface Sci.*, 1995, **59**, 95–193.
- T. Kawakami, N. Nishi, T. Kakiuchi, H. Matsuoka and T. Harada, unpublished work.
- M. A. Firestone, J. A. Dzielawa, P. Zapol, L. A. Curtiss, S. Seifert and M. L. Dietz, *Langmuir*, 2002, **18**, 7258–7260.

- 37 L. Cammarata, S. G. Kazarian, P. A. Salter and T. Welton, *Phys. Chem. Chem. Phys.*, 2001, **3**, 5192–5200.
- 38 M. A. Firestone, P. G. Rickert, S. Seifert and M. L. Dietz, *Inorg. Chim. Acta*, 2004, **357**, 3991–3998.
- 39 N. Shahidzadeh, D. Bonn, O. Aguerre-Chariol and J. Meunier, *Colloids Surf., A*, 1999, **147**, 375–380.
- 40 T. Nishimi and C. A. Miller, *Langmuir*, 2000, **16**, 9233–9241.
- 41 M. Nakawaga, N. Sezaki and T. Kakiuchi, *J. Electroanal. Chem.*, 2001, **501**, 260–264.
- 42 T. Kakiuchi, *J. Electroanal. Chem.*, 2002, **536**, 63–69.
- 43 T. Kakiuchi, M. Chiba, N. Sezaki and M. Nakagawa, *Electrochem. Commun.*, 2002, **4**, 701–704.
- 44 T. Kakiuchi, N. Nishi, T. Kasahara and M. Chiba, *ChemPhysChem*, 2003, **4**, 179–185.
- 45 T. Kasahara, N. Nishi, M. Yamamoto and T. Kakiuchi, *Langmuir*, 2004, **20**, 875–881.
- 46 T. Kakiuchi, *J. Electroanal. Chem.*, 2004, **569**, 287–291.
- 47 J. Czapkiewicz and B. Czapkiewicz-Tutaj, *J. Chem. Soc., Faraday Trans. 1*, 1980, **76**, 1663–1668.
- 48 Y. Kitazumi, N. Nishi and T. Kakiuchi, to be published.
- 49 M. Y. Vagin, E. V. Malyh, N. I. Larionova and A. A. Karyakin, *Electrochem. Commun.*, 2003, **5**, 329–333.
- 50 H. Katano and M. Senda, *Anal. Sci.*, 2001, **17**, 1027–1029.
- 51 T. Kakiuchi and N. Tsujioka, *J. Electroanal. Chem.*, submitted.

Chemical Science

An exciting news supplement providing a snapshot of the latest developments across the chemical sciences



Free online and in print issues of selected RSC journals!*

Research Highlights – newsworthy articles and significant scientific advances

Essential Elements – latest developments from RSC publications

Free access to the originals research paper from every online article

*A separately issued print subscription is also available

RSC Publishing

www.rsc.org/chemicalscience

Polyethylene glycol as a non-ionic liquid solvent for Michael addition reaction of amines to conjugated alkenes†

Rupesh Kumar, Preeti Chaudhary, Surendra Nimesh and Ramesh Chandra*

Received 7th December 2005, Accepted 24th January 2006

First published as an Advance Article on the web 3rd February 2006

DOI: 10.1039/b517397c

Polyethylene glycol (PEG) is found to be an inexpensive, non-toxic, environmentally friendly reaction medium for the conjugate addition of amines to conjugated alkenes to afford the corresponding adducts in excellent yields under mild reaction condition. The use of PEG avoids the use of acid or base catalysts and moreover PEG can be recovered and reused.

Introduction

The search for alternative reaction media to replace volatile and often toxic solvents commonly used in organic synthetic procedures is an important objective of significant environmental consequence.¹ Media considered include: (a) the use of supercritical fluids² that have the advantage of facile solvent removal and easy recyclability but require high pressure; (b) fluorinated systems³ that have the advantage of being highly hydrophobic but expensive and for which the solvents are probably innocuous but have the disadvantage of being volatile; (c) more recently, environmentally benign solvents such as ionic liquids,⁴ water,⁵ and polyethylene glycol.⁶ Ionic liquids have a particularly useful set of properties, being non-volatile and virtually insoluble in water and alkanes but readily dissolving many transition metal catalysts. It is customary to measure the efficiency of a catalyst by the number of cycles for which it can be reused. Similarly, the value of a new solvent medium primarily depends on its environmental impact, the ease with which it can be recycled, low vapor pressure, nonflammability and high polarity for solubilization. In performing the majority of organic transformations, solvents play an important role in mixing the ingredients to make the system homogeneous and allow molecular interactions to be more efficient.

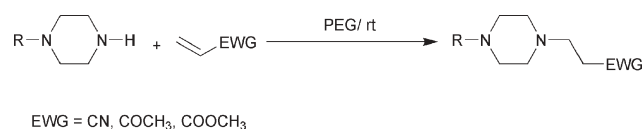
The Michael reaction, since its discovery in 1889,⁷ has been one of the most important reactions in organic chemistry. Recently, we have reported aza-Michael reaction of *N*-alkyl and *N*-aryl piperazine with acrylonitrile using copper nanoparticles as the catalyst under mild reaction conditions.⁸ In this article, we describe the use of a simple and widely available polymer, polyethylene glycol (PEG) as a non-toxic, inexpensive, non-ionic liquid solvent of low volatility. PEG and its monomethyl ethers are inexpensive, thermally stable, recoverable, and nontoxic media for phase transfer catalysts.⁹ PEG, a biologically acceptable polymer used extensively in drug delivery and in bioconjugates as tool for diagnostics, has

hitherto not been widely used as a solvent medium but has been used as a support for various transformations.^{6,10}

Herein, we report PEG 400 as a recyclable reaction medium for the conjugate addition of amines to conjugated alkenes at room temperature without any use of acid and base catalyst (Scheme 1). Such reactions do not generate any toxic waste by product.

Our efforts began with *N*-phenylpiperazine and acrylonitrile (Table 1, entry 1) in PEG (400 MW) at room temperature for 35 min, the corresponding adduct was obtained in 99% yields after a standardized workup protocol. Other piperazine and amines were treated with a variety of conjugated alkenes in PEG-400 as reaction media (Table 1). The reactions proceed efficiently at room temperature without the need for any further acid or base catalyst and goes to completion in a short time (30–50 min). This protocol is compatible with various α,β -unsaturated ketones, nitriles, and esters and different amines or various piperazine under mild reaction conditions. No by-product formation was observed. *N*-Methylpiperazine and acrylonitrile (entry 2, Table 1) produce cyanoethyl derivatives in 98% yield with ease. Verma *et al.*⁸ reported a similar drop-off in yield under catalysis of copper nanoparticles. PEG in these reactions eliminates the use of volatile organic solvents and as a recyclable reaction medium. In addition to the often referred advantages of using PEG 400 as solvent, this procedure has following remarkable features as compared to conventional method: (1) short reaction times, (2) clean reaction protocol, (3) high yielding.

In order to prove that the use of polyethylene glycol as solvent is also practical, it must be conveniently recycled with minimal loss and decomposition. Since polyethylene glycol is immiscible with aliphatic hydrocarbons, the desired product may be extracted with compounds such as cyclohexane, and the retained PEG phase may be reused.⁶ The solvent phase was recycled with no loss of reactivity for three cycles, although a weight loss ~5% of PEG was observed from cycle to cycle. A

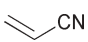
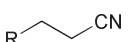
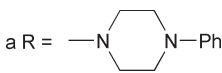
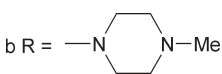
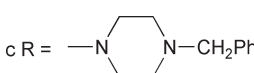
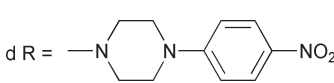
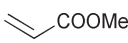
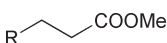
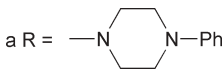
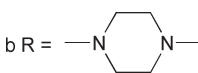
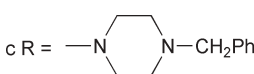
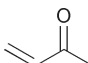
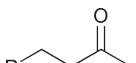
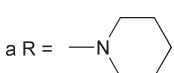
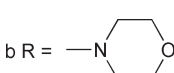
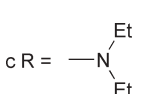


Scheme 1

Synthetic Organic Chemistry Research Laboratory, Department of Chemistry, University of Delhi, Delhi, 110007, India.
E-mail: chandra682000@yahoo.co.in; Fax: +91-11-23816312;
Tel: +91-11-9818901344

† Electronic supplementary information (ESI) available: Experimental. See DOI: 10.1039/b517397c

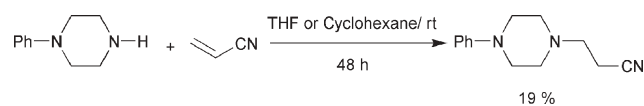
Table 1 The aza-Michael reaction of amines with electron deficient alkenes in PEG^a

Entry	Unsaturated alkenes	Product	Time/h	Yield (%) ^b
				
1		a R = 	35 min	99
2		b R = 	45 min	98
3		c R = 	45 min	99
4		d R = 	45 min	99
				
5		a R = 	30 min	99
6		b R = 	45 min	98
7		c R = 	35 min	99
				
8		a R = 	35 min	99
9		b R = 	35 min	99
10		c R = 	35 min	99

^a Reaction conditions: 1 mmol amine, 1.5 mmol alkenes, 2.5 g PEG-400, 25 °C. ^b Isolated yield.

control experiment was conducted in the absence of PEG 400 in ether or cyclohexane and it was observed that addition of *N*-phenyl piperazine to acrylonitrile produced the corresponding product (Scheme 2) in 18% yield in 48 h.⁸

There was no reaction in the absence of PEG. Thus, probable mechanism for the addition of amines to conjugated alkenes employing PEG as reaction medium may be due to the attraction between the PEG hydroxyl group oxygen and hydrogen attached to nitrogen of amine, which makes the N–H bond weaker, enhancing the nucleophilicity of nitrogen for addition to electron-deficient alkenes.

**Scheme 2**

Experimental

Different amines, electron deficient alkenes, acrylonitrile and PEG 400 were purchased from Aldrich. Typically reactions were carried out as follows: A mixture of amine (1 mmol), alkene (1.5 mmol) and PEG 400 (2.5 g) was placed in 20 mL round-bottomed flask. The reaction mixture was stirred at room temperature until the reaction was complete. The reaction mixture was extracted with dry ether, the extract dried and concentrated under reduced pressure and resulting crude product was purified by silica column chromatography using ethyl acetate and hexane as an eluent to obtain the adduct in excellent yield. The recovered PEG can be reused for a number of cycles without significant loss of activity. All organic compounds except 3-[4-(4-nitro-phenyl)-piperazin-1-yl]-propanitrile reported in literature,^{8,11} and are fully characterized by spectral analysis. Entry 4 in Table 1: ¹H NMR of 3-[4-(4-nitro-phenyl)-piperazin-1-yl]-propanitrile δ (ppm,

300 MHz) 8.12 (d, $J = 9$ Hz, 2 H), 6.83 (d, $J = 9$ Hz, 2 H), 3.44 (t, $J = 5$ Hz, 4 H), 2.75 (t, $J = 7$ Hz, 2 H), 2.66 (t, $J = 5$ Hz, 4 H), 2.56 (t, $J = 7$ Hz, 2 H). ^{13}C NMR δ (ppm, 75 MHz) 141.3, 132.4, 125.9, 114.2, 113.2, 51.3, 50.6, 46.6, 45.9. TOF MS (m/z) 261.6 ($M + 1$). IR (ν , cm^{-1}) 2245.41 (CN), 1328.72 (NO_2).

Conclusions

Polyethylene glycol offers a convenient, inexpensive, non-ionic liquid, non-toxic and recyclable reaction medium for Michael reaction of various amines with electron deficient alkenes, thus substituting for volatile organic solvents. This protocol offers a rapid and clean alternative and reduces reaction times. The recyclability of the catalyst makes reaction economically and potentially viable for commercial applications.

References

- 1 E. Wiebus and B. Cornils, *Chem.-Ing.-Tech.*, 1994, **66**, 916; B. Cornils and E. Wiebus, *Chem.-Tech. (Heidelberg)*, 1995, 33; R. V. Chaudhari and A. Bhattachayna, *Catal. Today*, 1995, **24**, 123; J. -B. ten Brink, I. W. C. E. Arends and R. A. Sheldon, *Science*, 2000, **287**, 1636.
- 2 R. S. Oakes, A. A. Clifford and C. M. Rayner, *J. Chem. Soc., Perkin Trans. 1*, 2001, 917.
- 3 I. T. Horvath and J. Rabai, *Science*, 1994, **266**, 72; L. P. Barthel-Rosa and J. A. Gladysz, *Coord. Chem. Rev.*, 1999, **190–192**, 587; J. A. Gladysz, D. P. Curran and I. T. Horvath, *Handbook of Fluorine Chemistry*, Wiley-VCH, Weinheim, 2004, pp. 1–595; M. A. Ubeda and R. J. Dembinski, *J. Chem. Educ.*, 2006, **83**, 84.
- 4 R. A. Sheldon, *Chem. Commun.*, 2001, 2399; C. L. Hussey, *Pure Appl. Chem.*, 1988, **60**, 1763; M. J. Earle and K. R. Seddon, *Pure Appl. Chem.*, 2000, **72**, 1391; T. Welton, *Chem. Rev.*, 1999, **99**, 2071; P. Wasserscheid and W. Keim, *Angew. Chem., Int. Ed.*, 2000, **39**, 3772.
- 5 *Organic Synthesis in Water*, P. A. Grieco, Blackie Academic and Professional, London, 1998; *Organic Reactions in Aqueous Media*, C.-J. Li, T.-H. Chan, John Wiley and Sons, New York, 1997; R. Breslow, *Acc. Chem. Res.*, 1991, **24**, 159.
- 6 V. N. Vasudevan and S. V. Rajendra, *Green Chem.*, 2001, **3**, 146; A. Haimov and R. Neumann, *Chem. Commun.*, 2002, 876; L. Heiss and H. J. Gais, *Tetrahedron Lett.*, 1995, **36**, 3833; S. Chandrasekar, C. Narsihmulu, S. S. Shameem and N. R. Reddy, *Chem. Commun.*, 2003, **1716**; K. Tanemura, T. Suzuki, Y. Nishida and T. Horaguchi, *Chem. Lett.*, 2005, **34**, 576.
- 7 S. D. Bull, S. G. Davies, S. Delgado-Ballester, G. Fenton, P. M. Kelly and A. D. Smith, *Synlett*, 2000, 1257; S. G. Davies and T. D. McCarthy, *Synlett*, 1995, 700; N. Srivastava and B. K. Banik, *J. Org. Chem.*, 2003, **68**, 2109.
- 8 A. K. Verma, R. Kumar, P. Chaudhary, A. Saxena, R. Shankar, S. Mozumdar and R. Chandra, *Tetrahedron Lett.*, 2005, **46**, 5229.
- 9 *Poly(ethylene Glycol) Chemistry, Biotechnological and Biomedical Applications*, ed. J. M. Harris, Plenum Press, New York, 1992, p. 3; *Polyethylene Glycol: Chemistry and Biological Application*, ACS Books, Washington, DC, 1997.
- 10 T. J. Dickerson, N. N. Reed and K. D. Janda, *Chem. Rev.*, 2002, **102**, 3325.
- 11 N. S. Shaikh, V. H. Despande and A. V. Bedekar, *Tetrahedron*, 2001, **57**, 9045; L.-W. Xu, J.-W. Li, S.-L. Zhou and C.-G. Xia, *New J. Chem.*, 2004, **28**, 183; T. Abe, H. Baba and I. Soloshonok, *J. Fluorine Chem.*, 2001, **108**, 21; H. Pieper, V. Austel, F. Himmelsbach, G. Linz, B. Guth and J. Weisenberger, De. Karl Thomae GmbH, Germany, *Ger. Offen.*, 1996, GWXXBX DE 4446301 A1 19960627, 34 pp. (patent written in German); T. Tsujikawa, S. Takei, S. Tsushima, T. Tsuda and K. Tsukamura, *Yakugaku Zasshi*, 1975, **95**, 499.

In situ generation of hydrogen for continuous hydrogenation reactions in high temperature water

Eduardo Garcia-Verdugo,^{†*} Zhimin Liu,[‡] Eliana Ramirez,[§] Juan Garcia-Serna,[¶] Joan Fraga-Dubreuil, Jason R. Hyde, Paul A. Hamley and Martyn Poliakoff*

Received 31st October 2005, Accepted 22nd December 2005

First published as an Advance Article on the web 31st January 2006

DOI: 10.1039/b515470g

The thermal decomposition of HCO₂H or preferably, HCO₂X (X = Na or NH₄) can be used to generate H₂ for the continuous hydrogenation of aromatic and cyclic aldehydes, ketones and nitroaromatics in high temperature pressurised water (HTPW). This means that hydrogenation reactions can be carried out in exactly the same equipment as has previously been used for selective oxidation in HTPW, thus facilitating relatively simple application of these reactions for non-specialists.

Introduction

The use of water as a greener reaction medium is highly attractive. High temperature pressurised water (HTPW) exhibits unique characteristics, *i.e.* high compressibility, tunability of density and solvent power, enhanced mass transfer due to low viscosity and high diffusion coefficients and high heat capacities which enable an ultra-efficient heat removal from the reaction. A key advantage of HTPW for performing chemistry is the possibility of varying the dielectric constant, ϵ , and the ionic product, pK_w of the reaction medium merely by changing the pressure and/or temperature.¹ This greatly facilitates reaction optimization and the rich potential of HTPW for reaction chemistry has been demonstrated by different research groups across the world.^{2–3}

Our group at Nottingham has investigated both near-critical water, ncH₂O, and supercritical water, scH₂O, as media for environmentally more acceptable reactions in both batch and continuous processes.⁴

Selective hydrogenation and oxidation are two of the most important industrial processes. HTPW provides several advantages, particularly for oxidation. It dissolves both gases and organic substrates resulting in a single phase reaction mixture thereby overcoming mass and heat transfer limitations and increasing reaction rates; and, of course, H₂O is totally non-flammable.

The exothermicity of oxidation means that HTPW reactions should be conducted on as small a scale as possible in the laboratory. Furthermore, the need for selectivity demands that the concentration of O₂ should be controlled precisely. However, we have found that the use of compressed O₂, although possible on a small scale, is expensive, and is difficult to control. Therefore, we have demonstrated the successful *in situ* generation of O₂ by the thermal decomposition of aqueous H₂O₂.⁵

We have already used this “gasless” approach for the selective oxidation of different methylaromatic compounds in scH₂O.^{5–7} The H₂O₂ decomposes rapidly during thermal treatment into O₂ and H₂O. The resulting mixture of O₂ dissolved in HTPW was then mixed with the appropriate catalyst and organic substrate, which was then oxidised to produce the desired carboxylic acid products.^{5–7}

Here, we present an extension of the “gasless” approach for carrying out the hydrogenation of different functional groups in HTPW by using the thermal decomposition of formic acid, HCO₂H, sodium formate, HCO₂Na, or ammonium formate, HCO₂NH₄ as the source of H₂. The key advantage is that one can use the same type of reactor for either oxidation or hydrogenation merely by choosing to use an aqueous solution of either H₂O₂ or HCO₂H (Fig. 1). In this paper, we first investigate the decomposition of HCO₂H and HCO₂Na in HTPW and then use these compounds as the precursors for a series of hydrogenations.

Experimental

All experiments were carried out at the University of Nottingham; the apparatus is shown in Fig. 1. Dilute aqueous HCO₂X (X = H, Na, NH₄) solution was pumped continuously into the system and decomposed in the pre-heater under the experimental conditions required to generate a mixture of H₂ and HTPW. The H₂ precursor solutions were prepared from HCO₂H 97% (Aldrich) and NaOH or NH₃ (35%) solution as required. After this, the organic and H₂-HTPW streams were mixed statically in a cross-piece before entering the reactor. The reaction mixture flowed through a tubular reactor with

School of Chemistry, University Park, Nottingham, UK NG7 2RD.
E-mail: martyn.poliakoff@nottingham.ac.uk; Fax: +44 (0)115 951 3058;
Tel: +44 (0)115 951 3520

[†] Present address: Organic and Inorganic Chemistry Department, Universidad Jaime I, Campus del Riu Sec E-12071, Castellón de la Plana, Spain. E-mail: eduardo.garcia-verdugo@mail.uji.es; Fax: +34 964 728214; Tel: +34 964 728215.

[‡] Present address: Institute of Chemistry, Chinese Academy of Sciences, Beijing, 100080, China. Fax: +86 10 6256 59373; Tel: +86 10 625 62821.

[§] Present address: Chemical Engineering Department, Universitat Politècnica de Catalunya, Diagonal Av. 647, 08028 Barcelona, Spain. Fax: +34 934 017150; Tel: +34 934 016676.

[¶] Present address: Chemical Engineering and Environmental Techniques Department, c/Prado de la Magdalena s/n 47001, Valladolid, Spain. Fax: +34 983 423013; Tel: +34 983 423174.

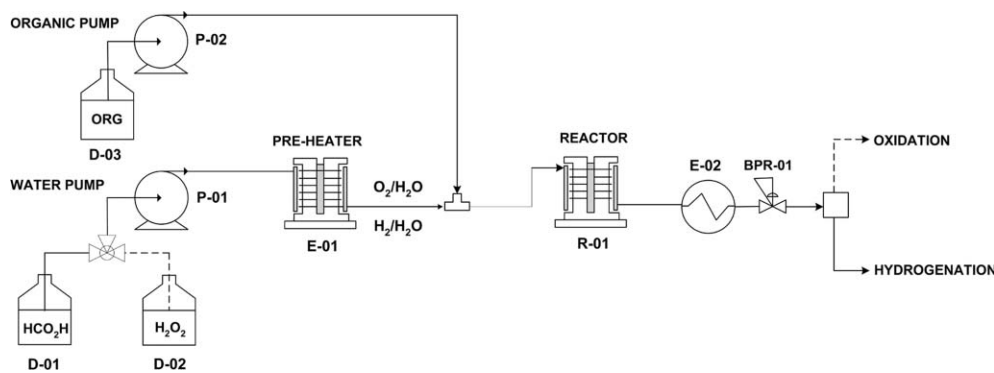


Fig. 1 Schematic diagram of the “gasless” bench-scale reactor for either hydrogenation or oxidation reactions in HTPW. Equipment description: D-01, HCO₂H solution feed vessel; D-02: H₂O₂ solution feed vessel; D-03, organic feed vessel; P-01, HCO₂H or H₂O₂ solution feed pump (HPLC pump, Gilson Model 304, flow rate = 2.5–10 mL min⁻¹, maximum allowed pressure (P_{\max}) = 40 MPa); P-02, organic feed pump (HPLC pump, Gilson model 304, flow rate = 0.25–1 mL min⁻¹, P_{\max} = 40 MPa); E-01, pre-heater (1/16 in AISI 316 tubing, 3 m, heat supplied by a cartridge heater (Watlow, 240 V, 200 W, FIREROD0247 NFRG2E164A) and a band heater (Watlow, 240 V, 200 W, NTB25X6UA3, 47 02 DM)); R-01, tubular reactor (1/16 in AISI 316 tubing, 0.115 m); E-02, concentric tube cooler (1/8 inside 3/8 in AISI 316 tubing, 0.3 m); BPR-01, back pressure regulator (Tescom 26-1722-24-043, P_{\max} = 42 MPa, C_v < 0.01).

short residence times (5 to 30 s). Reactor effluent was quenched down to 40 °C in a concentric-tube heat exchanger with counter-current cooling water. Finally, the cooled reaction mixture was filtered and depressurized using a back-pressure regulator. Samples were collected for consecutive periods of 10–15 min and were then analysed off-line.

Flow rates were controlled *via* the pump flowrates (HPLC volumetric pumps). The preheater and reactor temperatures were controlled by separate PID controller modules. Pressure was controlled manually using the back-pressure regulator.

The residence time (Rt) was estimated from the total reactor volume divided by the volumetric flow-rate at reactor temperature. The total volume was taken as the sum of the volume of the tubular reactor constructed from Hastelloy C276 pipework. The volumetric flow-rate, which changes with temperature (and density) along the tubing, was calculated using the physical properties of H₂O at the reaction conditions as published in the International Steam Tables and by the US National Institute of Science and Technology (NIST).

Cyclohexanone and its products were analyzed by GC with an Alltech ECONO-CATTM-ECTM-1 column (30 m × 0.32 mm id × 1 mm). Calibration standards were diluted in ethanol whereas reactor samples were injected undiluted. An initial column temperature of 150 °C was maintained for 10 min, followed by a 5 °C min⁻¹ gradient for a further 10 min. Detector initial temperature was 300 °C, injector temperature 250 °C and pressure 12 psi. An injection volume of 5 µL was used for all the samples. Retention times of 4.5 min for cyclohexanone and 4.41 for cyclohexanol were obtained.

Acetophenone, benzaldehyde and their respective products were analysed using a Waters Xterra reverse phase C18 column (3 × 150 mm), maintained at 40 °C; flow rate 0.7 mL min⁻¹, run time = 7 min, post-time = 2 min, injection volume = 5 µL; UV detection at 230, 254, 280 and 300 nm. A non-isocratic method with gradient elution of the solvents: Time = 0 min: 30% CH₃CN and 70% CH₃CO₂Na/CH₃CO₂H as a buffer, at 5 min 50% CH₃CN *vs.* 50% buffer and at 7 min 30% CH₃CN *vs.* 70% buffer were used. The stock buffer solution contained 15.0 g anhydrous CH₃CO₂Na in 250 mL

de-ionised H₂O, plus CH₃CO₂H (50% v/v, 100 mL). The pH was adjusted to 3.9 ± 0.1 with 5% CH₃CO₂H, before diluting to 500 mL. 30 mL of stock buffer was then diluted to a total volume of 500 mL with de-ionised H₂O. Standards were diluted in CH₃CN whereas reactor products were diluted in water (1 : 10).

Gases (CO, CO₂, CH₄ and H₂) were collected into a Varian 4900 micro-GC with an internal pump that drew gaseous samples into the injection port. Analysis was performed on two capillary columns: M5A 20 m with an 8 s back flush; 120 °C/20.0 psi isobaric; HSA 0.4 m; 80 °C/20.0 psi isobaric. Both channels used a 50 ms injection time).

CAUTION: This type of hydrogenation is potentially hazardous, and must be approached with care. A thorough safety assessment must be made for each particular apparatus. In our experiments, the possibility of a runaway exothermic reaction was reduced by using dilute solutions (<10% w/w) of the H₂ precursor. The equipment must be operated with adequate ventilation.

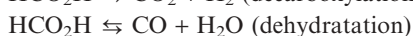
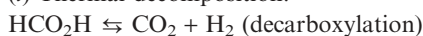
Results

Thermal decomposition of HCOOH or HCOONa in HTHP

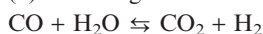
Table 1 summarises the composition (molar percentage) of the gases formed at different pressures and temperatures for an aqueous solution of HCO₂H and HCO₂Na. Under these conditions, both precursors produced H₂, CO₂ and CO, with traces of CH₄ also detected.

In the case of HCO₂H, the formation of gases can be explained by the following series of reaction equilibria:

(i) Thermal decomposition:⁸



(ii) “Water-gas shift”:⁹



(iii) Formation of methane:

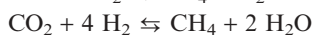
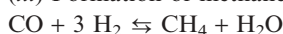


Table 1 Pressure and temperature effect on the HCO₂Na and HCO₂H decomposition

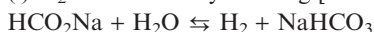
HCO ₂ H ⇌ H ₂ + CO + CO ₂					HCO ₂ Na ⇌ H ₂ + CO + CO ₂				
mol% H ₂ for HCO ₂ H decomposition ^a					mol% H ₂ for HCO ₂ Na decomposition ^b				
H ₂	Temperature/°C				H ₂	Temperature/°C			
P/MPa	250	300	350	400	P/MPa	250	300	350	400 ^c
15.0	30.3	48.8	51.8	51.4	15.0	90.8	90.5	97.2	—
20.0	39.6	49.6	49.2	52.7	20.0	88.2	93.7	98.0	—
26.0	37.5	43.8	47.4	52.1	26.0	79.1	95.8	98.4	—
30.0	35.7	42.6	49.0	47.0	30.0	71.8	96.6	98.5	—
33.0	35.3	41.4	43.7	51.8	33.0	64.5	97.2	98.5	—
mol% CO ₂ for HCO ₂ H decomposition ^a					mol% CO ₂ for HCO ₂ Na decomposition ^b				
CO ₂	Temperature/°C				CO ₂	Temperature/°C			
P/MPa	250	300	350	400	P/MPa	250	300	350	400 ^c
15.0	38.7	40.8	43.3	44.2	15.0	6.7	7.8	1.9	—
20.0	35.4	37.3	43.4	42.1	20.0	8.5	5.3	1.4	—
26.0	35.0	39.0	41.7	40.8	26.0	16.6	3.5	1.2	—
30.0	35.4	42.1	37.8	39.7	30.0	21.9	2.5	1.2	—
33.0	36.6	41.9	41.0	43.3	33.0	27.9	2.4	1.1	—
mol% CO for HCO ₂ H decomposition ^a					mol% CO for HCO ₂ Na decomposition ^b				
CO	Temperature/°C				CO	Temperature/°C			
P/MPa	250	300	350	400	P/MPa	250	300	350	400 ^c
15.0	31.0	15.2	4.8	4.3	15.0	2.5	1.8	0.9	—
20.0	25.0	13.1	7.4	5.2	20.0	3.3	1.0	0.4	—
26.0	27.4	16.9	11.0	7.1	26.0	4.3	0.7	0.2	—
30.0	28.7	14.7	13.2	13.3	30.0	6.3	0.8	0.1	—
33.0	27.7	16.2	15.2	4.8	33.0	7.5	0.4	0.1	—

^a Aqueous solutions with a concentration of 2.3 mol L⁻¹ of HCOOH at a flow rate of 10 mL min⁻¹ were used in all cases. ^b Aqueous solutions with a concentration of 2.3 mol L⁻¹ of HCOONa at a flow rate of 10 mL min⁻¹ were used in all cases. ^c At temperatures above 350 °C (near the critical point) a sudden precipitation of Na₂CO₃ was observed resulting in the blockage of the reactor.

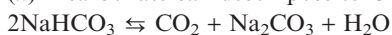
Pressure has very little effect on the composition of the gases with $\pm 5\%$ variation. By contrast, temperature showed a significant influence. Thus, the amount of H₂ increased from $35 \pm 5\%$ to $50 \pm 5\%$ on increasing the temperature from 250 to 400 °C. The corresponding variation in CO₂ was rather less, changing from $35 \pm 5\%$ to $40 \pm 5\%$ over the same temperatures interval. However, the CO concentration is reduced considerably at higher temperatures, e.g. from ca. 30% at 250 °C down to $<5\%$ at 400 °C. The amount of CO₂ was in general lower than the H₂ (according to the equation an equimolar amount of CO₂ and H₂ should be obtained), which suggests that some CO₂ is retained in the aqueous phase, since CO₂ has a relatively high solubility in water.

A totally different composition of gases was observed for the thermal decomposition of solutions of HCO₂Na because the Na⁺ can react with aqueous CO₂. The plausible reaction pathway is given below:¹⁰

(i) H₂ is obtained by reacting [HCO₂⁻] with water:



(ii) Bicarbonate can decompose to CO₂ and carbonate:



H₂ was the major component at all temperatures and pressures. CO and CO₂ were also present, although only very low molar percentages of CO were observed compared to those detected for the thermal degradation of HCO₂H.

The amount of CO₂ showed pressure dependence only when the decomposition was carried out at 150 °C, ranging from 6% to 27% when the pressure increased. However, at higher temperatures this variation was $<5\%$.

The higher percentages of H₂ suggest that HCO₂Na should be a better H₂ precursor for running hydrogenation reactions. However, there is another important aspect, namely the rate of decomposition of the precursor (e.g. the conversion of the H₂ source within the pre-heater). On the basis of conversion, the choice is not so clear because the rate of decomposition of HCO₂H is considerably higher than that of HCO₂Na. Up to 90% conversion was achieved for HCO₂H, while the maximum conversion for HCO₂Na was only ca. 35% for the 3 m length of preheater in our apparatus. Therefore, we carried out hydrogenation reactions with both precursors to establish which was better.

Reduction of nitrobenzene into aniline

Aromatic amines are of significant industrial importance being widely used as intermediates for the synthesis of dyes, pharmaceuticals and agrochemicals. The reduction of nitro compounds is one of the most common synthetic methods for their manufacture. The current industrial processes are based on the catalytic hydrogenation or stoichiometric reduction reactions.¹¹

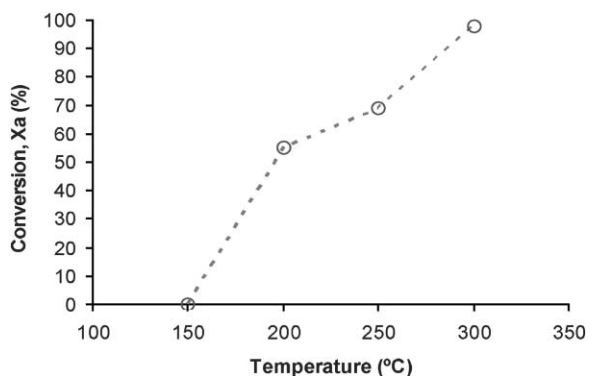


Fig. 2 Effect of the temperature on the hydrogenation of PhNO₂ using HCO₂Na as the source of H₂ at *P* = 20.0 MPa. Flow rates: HCO₂Na (2.3 mol L⁻¹), 5 mL min⁻¹; nitrobenzene, 0.5 mL min⁻¹.

We have already reported the selective reduction of nitroarenes to anilines using metallic zinc in nCH₂O.¹² However, this reduction was performed in batch reactors requiring greater than stoichiometric amounts of Zn. Thus, the development of a continuous zinc-free reduction in HTPW is highly attractive.

The reduction of nitrobenzene was carried out in H₂O from 150–300 °C and 15–30 MPa. All the reactions were performed by using relatively dilute solutions (<10% organic w/w). Initial experiments were performed using an aqueous solution of HCO₂Na as the H₂ precursor.

As expected, the reaction temperature has strong influence on the degree of the conversion of the nitrobenzene, Fig. 2. No reaction was observed at <150 °C. Increasing the temperature from 200 to 300 °C improved the yield from 55% to 98%. Aniline was the only detectable product at temperatures >200 °C.

The effect of residence time (Rt), at 25.0 MPa and 300 °C was also studied (see Fig. 3). The reaction was complete in only a few seconds in contrast to the reduction of the nitroarenes with Zn in HTPW where several hours were required to achieve equivalent yields of aniline.¹²

Similar trends for temperature and residence times were observed when HCO₂H was used as the H₂ precursor. Table 2

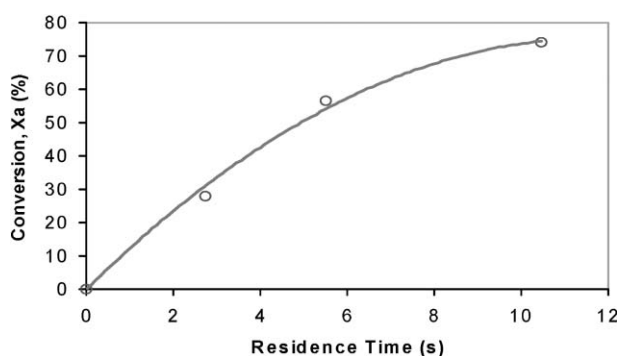


Fig. 3 The effect of residence time on the hydrogenation of PhNO₂ using HCO₂Na as the source of H₂ at 300 °C and 25.0 MPa. Flow rates: HCO₂Na (2.3 mol L⁻¹), 2.5–5.0–9.5 mL min⁻¹; nitrobenzene, 0.25–0.5–0.95 mL min⁻¹ (respectively).

Table 2 Continuous hydrogenation of nitrobenzene in HTPW

Entry ^a	<i>P</i> /MPa	<i>T</i> /°C	H ₂ source	Yield (%)
1	15.0	300	HCO ₂ H	75
2	20.0	300	HCO ₂ H	74
3	25.0	300	HCO ₂ H	62
4	30.0	300	HCO ₂ H	70

^a Flow rates: HCO₂H (10%), 5 mL min⁻¹; nitrobenzene, 0.5 mL min⁻¹.

summarises the results. As can be seen, there is no significant influence of pressure.

All of these reactions were undertaken without any catalyst. Numerous methods have been reported in the literature for the reduction of the nitroarenes to aniline, generally requiring the presence of a transition metal.¹¹ Therefore, it is quite likely that the stainless steel of the reactor could be playing an important catalytic role in the reaction. There are two possible mechanisms: a surface catalysed reaction by the reactor wall or the leaching of catalytically active components from the reactor wall, which is less likely since there are many examples of catalytic effect of reactor walls under similar conditions.

Reduction of benzaldehyde and cyclohexanone

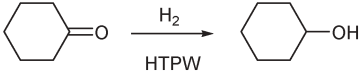
Bryson *et al.* have reported the selective batch reduction of benzaldehyde and cyclohexanone with HCO₂Na under conditions of temperature and pressure similar to ours.¹³ Tables 3 and 4 summarise our results for benzaldehyde and cyclohexanone, respectively, which are comparable in terms of yield with those obtained by Bryson *et al.* However, there were significant differences between our continuous and their batch processes. For similar yields, higher selectivity (fewer side products) is achieved at lower temperatures in the continuous process. This is probably the result of shorter residence times compared to the batch process (seconds *vs.* hours), thereby avoiding side reactions (Cannizzaro, dehydration and aldol reaction).

When we tried to repeat these reactions using HCO₂H as the H₂ precursor, neither cyclohexene nor benzaldehyde reacted at all. This was really quite surprising but could be due to catalyst poisoning by CO. Assuming that these hydrogenations involve

Table 3 Continuous hydrogenation of benzaldehyde in HTPW

Entry	<i>P</i> /MPa	<i>T</i> /°C	H ₂ source	Rt/s	Yield (%)
Bryson ^a	0.82	315	HCO ₂ Na	10 ^d	74
1 ^b	15.4	141	HCO ₂ Na	31	40
2 ^b	15.5	190	HCO ₂ Na	29	54
3 ^b	20.5	190	HCO ₂ Na	29	48
4 ^c	15.7	247	HCO ₂ Na	19	65
5 ^d	15.7	250	HCO ₂ H	19	0

^a Batch process, Org/HCO₂Na 1 : 3. ^b Org/HCO₂Na 1 : 13. ^c Org/HCO₂Na 1 : 19. ^d Org/HCO₂H 1 : 32.

Table 4 Continuous hydrogenation of cyclohexanone in HTPW


Entry	<i>P</i> /MPa	<i>T</i> /°C	H ₂ source	Rt/s	Yield (%)
Bryson ^a	0.82	315	HCO ₂ Na	10 ⁴	34
1 ^b	15.5	250	HCO ₂ Na	24	28
2 ^c	15.5	292	HCO ₂ Na	9	23
3 ^d	15.5	250	HCO ₂ H	10	2

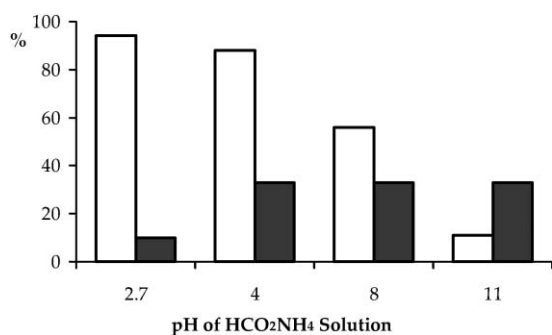
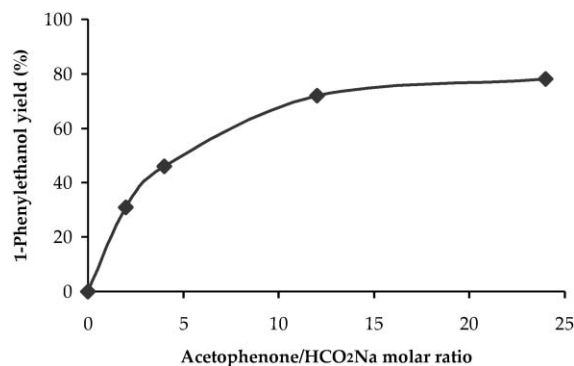
^a Batch process, Org/HCO₂Na 1 : 3. ^b Org/HCO₂Na 1 : 9. ^c Org/HCO₂Na 1 : 12. ^d Org/HCO₂H 1 : 12.

surface catalysed reactions, there are well established deactivation mechanisms involving CO and, it can be seen from Table 1 that the main difference between the decomposition of HCO₂H and HCO₂Na is the higher amount of CO produced by HCO₂H. Alternatively, reaction with [HCO₂⁻] could involve direct H-transfer rather than hydrogenation *via* H₂.

Fig. 4 shows an additional effect in the reduction of benzaldehyde, namely the result of increasing the pH of the H₂-precursor solution by deliberately adding ammonia to the formic acid. Consequently, in a similar way to HCO₂Na, the effect of HCO₂NH₄ was investigated at 250 °C and 15.0 MPa.

The results show that high yields (94%) of benzyl alcohol can be generated by adding sufficient NH₃ to give 10 equivalents of HCO₂NH₄ compared to benzaldehyde. As a result, the use of HCO₂NH₄ seems to be more efficient than HCO₂Na under similar conditions (see Table 3, entry 4) as less H₂-precursor is needed to obtain a higher benzyl alcohol yield. As the concentration of NH₃ is further increased to reach pH 4 (33-fold excess of HCO₂NH₄) the yield starts to decrease slightly to 88%. When higher concentrations of NH₃ are used (pH 8 and 11) the yields of benzyl alcohol drop dramatically. Thus, the large excess of NH₃ used is affecting the selectivity of the reaction because by-products are formed.

In summary, our method is comparable in terms of yields with those which were obtained in the batch experiment.¹³ However, in our case, the reaction is much faster (much lower residence time) and is more selective at a lower temperature. The lower yields obtained with cyclohexanone compared to benzaldehyde and nitro benzene are just due to the fact that

**Fig. 4** Effect of the HCO₂NH₄ solution pH on benzyl alcohol yield at 250 °C and 15.0 MPa. □ Benzyl alcohol yield. ■ Molar benzaldehyde/HCO₂NH₄ ratio.**Fig. 5** Effect of the HCO₂Na : acetophenone mol ratio (250 °C, 15.6 MPa and 20 s res. time) on the yield of 1-phenylethanol.

cyclohexanone is less reactive. Therefore, this method could be applicable for many substrates given an appropriate residence time.

Reduction of acetophenone to 1-phenyl ethanol

The hydrogenation of acetophenone in HTPW was successful without added catalyst using either HCO₂H or HCO₂Na as the H₂ precursor. Yields up to 78% were registered at 15.6 MPa and 250 °C with residence times as short as 20 s. Fig. 5 illustrates the influence of acetophenone/HCO₂Na ratio on the yield of 1-phenyl ethanol. It can be seen that at least a ten-fold excess of HCO₂Na is required to obtain reasonable yields. However this demonstrates the selectivity of this method because, even at this excess, no further reduction of the aromatic molecule was observed. The need for this large excess may also reflect the poor conversion of HCO₂Na to H₂, see above.

Conclusions

The “gasless” approach described here is not intended for a large-scale process. Indeed, the large excess of reagents contravenes several of the Principles of Green Chemistry. However, we believe that, on the laboratory scale, it has some definite advantages for the development of greener processes: (i) it is a simple, convenient and safe way to perform hydrogenation reactions on a laboratory scale; (ii) it avoids the use of a compressor, which is especially critical for hydrogen in terms of safety and equipment costs (a compressor is needed because the pressures of scH₂O experiments are higher than the pressures in standard gas cylinders and (iii) it gives a simpler control of the flow rates, at least in small scale apparatus, where very low flow rates are required. Finally, it can be used with exactly the same equipment as is used for selective oxidation, thereby extending the capabilities of a research group without the need for further equipment.

Acknowledgements

We thank Dr L. M. Dudd, Dr E. Lester and Professor M. J. Cocero for their help and advice. We are grateful for support from INVISTA[®] Performance Technologies, the EPSRC, EU Marie Curie Programme and the Royal Society. We also thank

M. Guyler, R. Wilson and P.A. Fields from the workshops at the School of Chemistry, University of Nottingham for assistance on technical and engineering issues.

References

- 1 M. Uematsu and E. U. Franck, *J. Phys. Chem. Ref. Data*, 1980, **9**, 1291.
- 2 (a) O. Kajimoto, *Chem. Rev.*, 1999, **99**, 355; (b) D. Broll, C. Kaul, A. Kramer, P. Krammer, T. Richter, M. Jung, H. Vogel and P. Zehner, *Angew. Chem., Int. Ed.*, 1999, **38**, 2998; (c) M. Siskin and A. R. Katrinzky, *Chem. Rev.*, 2001, **101**, 825; (d) N. Akiya and P. E. Savage, *Chem. Rev.*, 2002, **102**, 2725.
- 3 Selected examples. Diels–Alder reaction: (a) M. B. Korzenski and J. W. Kolis, *Tetrahedron Lett.*, 1997, **38**, 5611; (b) Y. Harano, H. Sato and F. Hirata, *J. Am. Chem. Soc.*, 2000, **122**, 2289; Friedel–Crafts alkylation; (c) K. Chandler, F. Deng, A. K. Dillow, C. L. Liotta and C. A. Eckert, *Ind. Eng. Chem. Res.*, 1997, **36**, 5175; Beckmann and pinacol rearrangements; (d) Y. Ikushima, O. Sato, M. Sato, K. Hatakeda and M. Arai, *Chem. Eng. Sci.*, 2003, **58**, 935; ester hydrolysis; (e) H. Oka, S. Yamago, J. Yoshida and O. Kajimoto, *Angew. Chem., Int. Ed.*, 2002, **41**, 623; Pd catalyzed Mizoroki–Heck reaction; (f) P. Reardon, S. Metts, C. Crittendon, P. Daugherty and E. J. Parsons, *Organometallics*, 1995, **14**, 3810; (g) R. Zhang, F. Fengyu Zhao, M. Masahiro Sato and Y. Ikushima, *Chem. Commun.*, 2003, 1548.
- 4 (a) P. A. Aleman, C. Boix and M. Poliakoff, *Green Chem.*, 1999, **1**, 65; (b) C. Boix, J. M. de la Fuente and M. Poliakoff, *New J. Chem.*, 1999, **23**, 641; (c) L. M. Dudd, E. Venardou, E. Garcia-Verdugo, P. Licence, A. J. Blake, C. Wilson and M. Poliakoff, *Green Chem.*, 2003, **5**, 187.
- 5 P. A. Hamley, T. Ilkenhans, J. M. Webster, E. Garcia-Verdugo, E. Vernardou, M. J. Clarke, R. Auerbach, W. B. Thomas, K. Whiston and M. Poliakoff, *Green Chem.*, 2002, **4**, 235.
- 6 E. Garcia-Verdugo, E. Vernardou, W. B. Thomas, K. Whiston, W. Partenheimer, P. A. Hamley and M. Poliakoff, *Adv. Synth. Catal.*, 2004, **2–3**, 307.
- 7 E. Garcia-Verdugo, J. Fraga-Dubreuil, P. A. Hamley, W. B. Thomas, K. Whiston and M. Poliakoff, *Green Chem.*, 2005, **7**, 294.
- 8 (a) N. Akiya and P. E. Savage, *AIChE J.*, 1998, **44**, 405; (b) J. Yu and P. E. Savage, *Ind. Eng. Chem. Res.*, 1998, **37**, 2.
- 9 (a) S. F. Rice, R. R. Steeper and J. D. Aiken, *J. Phys. Chem. A*, 1998, **102**, 2673; (b) T. Sato, S. Kurosawa, R. L. Smith, T. Adschiri and K. Arai, *J. Supercrit. Fluids*, 2004, **29**, 113.
- 10 (a) D. C. Elliot and L. J. Sealock Jr., *Ind. Eng. Chem. Prod. Res. Dev.*, 1983, **22**, 426; (b) D. C. Elliot, R. T. Hallen and L. J. Sealock Jr., *Ind. Eng. Chem. Prod. Res. Dev.*, 1983, **22**, 431; (c) J. Wang and T. Takarada, *Energy Fuels*, 2001, **15**, 356; (d) A. Kruse and E. Dinjus, *Angew. Chem., Int. Ed.*, 2003, **42**, 909.
- 11 R. S. Downing, P. J. Kunkeler and H. van Bekkum, *Catal. Today*, 1997, **37**, 121.
- 12 C. Boix and M. Poliakoff, *J. Chem. Soc., Perkin Trans. 1*, 1999, 1487.
- 13 (a) J. M. Jennings, T. A. Bryson and J. M. Gibson, *Green Chem.*, 2000, **2**, 88; (b) J. M. Jennings, T. A. Bryson and J. M. Gibson, *Tetrahedron Lett.*, 2000, **41**, 3523.

Expeditious approach to α -amino phosphonates *via* three-component solvent-free reactions catalyzed by NBS or CBr₄

Jie Wu,* Wei Sun, Xiaoyu Sun and Hong-Guang Xia

Received 9th December 2005, Accepted 2nd February 2006

First published as an Advance Article on the web 24th February 2006

DOI: 10.1039/b517488k

Three-component reactions of aldehydes, amines, and diethyl phosphite catalyzed by NBS or CBr₄ afforded the corresponding α -amino phosphonates in excellent yields under solvent-free conditions.

Introduction

Due to the growing concern for the influence of organic solvents on the environment as well as on the human body, organic reactions without use of conventional organic solvents have attracted the attention of synthetic organic chemists.¹ Although a number of modern solvents such as fluorinated media,² scCO₂,³ ionic liquids,⁴ and water⁵ have been extensively studied recently, not using a solvent at all is definitely the best option. Development of solvent-free organic reactions is thus gaining prominence.⁶

Furthermore, interest in the field of organocatalysis has increased spectacularly in the last few years as result of both the novelty of the concept and, more importantly, the fact that the efficiency and selectivity of many organocatalytic reactions meet the standards of established organic reactions.⁷ Catalysts of the same class may promote similar reactions or less closely related reactions. For instance, DABCO and its analogues show high efficiency in Morita–Baylis–Hillman reactions,^{8a} cyanation of ketones,^{8b} as well as ring-opening of aziridines^{8c} or epoxides.^{8d} NBS is another example of this catalyst class. It is able to mediate an astonishingly wide variety of transformations.⁹ Recently, we found that NBS, as well as CBr₄, was also efficient as a catalyst in the three-component reactions of aldehydes, amines and diethyl phosphite under solvent-free conditions, which is disclosed herein.

α -Amino phosphonic acids, their phosphonate esters, and short peptides incorporating this unit are excellent inhibitors of a wide range of proteolytic enzymes.¹⁰ In addition, α -amino phosphonate derivatives have broad application due to their antibacterial¹¹ and antifungal¹² activity, and as inhibitors of phosphatase activity.¹³ Lewis acid-catalyzed addition of diethyl phosphite to aldimines provides a useful method for the preparation of α -amino phosphonates.¹⁴ Recently, three-component synthesis starting from aldehydes, amines, and diethyl phosphite or triethyl phosphite have been reported by use of Lewis acids¹⁵ and Brønsted acids,¹⁶ or under microwave conditions.¹⁷ However, many of these procedures suffered from harsh reaction conditions, the heavy metal catalysts employed, and the use of stoichiometric and/or toxic, relatively expensive reagents. Since α -amino phosphonate derivatives are increasingly useful and important in pharmaceuticals and industry,

the development of simple, eco-benign, low cost protocols is still desirable. As α -amino phosphonate synthesis *via* three-component reactions is one of the most important acid-mediated reactions, development of a reaction that uses catalytic amounts of economic and readily available catalysts with low toxicity, while avoiding the use of metals, should greatly contribute to the creation of environmentally benign processes.

Results and discussion

As previously described, NBS has attracted much attention as a catalyst in various organic transformations recently.⁹ Inspired by these results, we conceived that NBS may also act as an efficient organocatalyst in α -amino phosphonate synthesis *via* three-component reactions of aldehydes, amines and diethyl phosphite. Initial studies were performed by using NBS (5 mol%) as catalyst in the reaction of benzaldehyde **1a** and aniline **2a** with diethyl phosphite in different solvents (THF, toluene, MeCN, CH₂Cl₂, DMF, EtOH) at room temperature. To our delight, we observed the formation of the corresponding product **3a**. Complete conversion and 95% isolated yield was obtained after 24 hours when the reaction was performed in EtOH. Further study showed that this reaction was carried out most efficiently under solvent-free conditions. Next, we surveyed the temperature for this reaction. We found that the result was dramatically improved when the reaction was performed at 50 °C. Only 2 hours was needed for completion and an almost quantitative yield of desired compound **3a** was isolated. Further examinations showed that 1 mol% of catalyst was also efficient in this reaction at the expense of reaction time (12 h, 96% yield, solvent-free). It is noteworthy that this reaction could be run under air without loss of efficiency (Scheme 1).

To demonstrate the generality of this method, we next investigated the scope of this reaction under the optimized conditions (solvent-free, 5 mol% of NBS, air, 50 °C) and the results are summarized in Table 1. As shown in Table 1, this method is equally effective for both aromatic aldehydes and amines. Various substituted aromatic aldehydes **1a–1d** reacted smoothly with amines **2** to produce a range of α -amino phosphonate derivatives. Complete conversion and good-to-excellent isolated yields were observed for all substrates employed. This reaction is very clean and free from side reactions. For example, almost quantitative yields of product **3a** and **3b** were obtained when aldehyde **1a** reacted with anilines **2a** and **2b** (entries 1 and 2). The reactions also

Department of Chemistry, Fudan University, 220 Handan Road, Shanghai, 200433, China. E-mail: jie_wu@fudan.edu.cn; Fax: +86 21 6510 2412; Tel: +86 21 5566 4619

(m, 1H), 3.92–3.95 (m, 1H), 4.08–4.14 (m, 2H), 4.71 (d, $J = 24.0$ Hz, 1H), 4.75 (b, 1H), 6.60 (d, $J = 7.5$ Hz, 2H), 6.66–6.69 (m, 1H), 7.07–7.13 (m, 4H), 7.33–7.35 (m, 2H).

Diethyl (4-methoxyphenylamino)(*p*-tolyl)methylphosphonate 3f

Colorless liquid. ^1H NMR (400 MHz, CDCl_3): δ (ppm) 1.14 (t, $J = 7.0$ Hz, 3H), 1.28 (t, $J = 7.0$ Hz, 3H), 2.30 (s, 3H), 3.67 (s, 3H), 3.69–3.71 (m, 1H), 3.92–3.93 (m, 1H), 4.09–4.14 (m, 2H), 4.66 (d, $J = 24.3$ Hz, 1H), 4.80 (br, 1H), 6.55 (d, $J = 9.2$ Hz, 2H), 6.68 (d, $J = 9.2$ Hz, 2H), 7.12 (d, $J = 7.8$ Hz, 2H), 7.31–7.34 (m, 2H).

Diethyl (4-fluorophenylamino)(*p*-tolyl)methylphosphonate 3g

Colorless liquid. ^1H NMR (400 MHz, CDCl_3): δ (ppm) 1.12 (t, $J = 7.0$ Hz, 3H), 1.28 (t, $J = 7.0$ Hz, 3H), 2.31 (s, 3H), 3.67–3.70 (m, 1H), 3.91–3.92 (m, 1H), 4.10–4.14 (m, 2H), 4.63–4.70 (m, 1H), 4.83–4.85 (m, 1H), 6.52–6.54 (m, 2H), 6.75–6.80 (m, 2H), 7.12 (d, $J = 7.8$ Hz, 2H), 7.33 (d, $J = 7.8$ Hz, 2H).

Diethyl (benzylamino)(*p*-tolyl)methylphosphonate 3h

Colorless liquid. ^1H NMR (400 MHz, CDCl_3): δ (ppm) 1.14 (t, $J = 7.0$ Hz, 3H), 1.27 (t, $J = 7.0$ Hz, 3H), 2.30 (s, 2H), 2.35 (s, 3H), 3.53 (d, $J = 13.2$ Hz, 1H), 3.78–3.82 (m, 2H), 3.96–4.06 (m, 3H), 7.26–7.31 (m, 9H).

Diethyl (4-chlorophenyl)(4-methoxyphenylamino)-methylphosphonate 3i

Colorless liquid. ^1H NMR (400 MHz, CDCl_3): δ (ppm) 1.16 (t, $J = 7.0$ Hz, 3H), 1.29 (t, $J = 7.0$ Hz, 3H), 3.69 (s, 3H), 3.80–3.81 (m, 1H), 3.94–4.03 (m, 1H), 4.09–4.14 (m, 2H), 4.51–4.53 (m, 1H), 4.62–4.70 (m, 1H), 6.50–6.70 (m, 4H), 7.29–7.39 (m, 4H).

Diethyl (benzylamino)(4-chlorophenyl)methylphosphonate 3j

Colorless liquid. ^1H NMR (400 MHz, CDCl_3): δ (ppm) 1.25 (t, $J = 7.0$ Hz, 3H), 1.27 (t, $J = 7.0$ Hz, 3H), 3.50 (d, $J = 13.2$ Hz, 1H), 3.77 (d, $J = 13.2$ Hz, 1H), 3.97–4.10 (m, 6H), 7.23–7.37 (m, 9H).

Diethyl furan-2-yl(4-methoxyphenylamino)methylphosphonate 3k

Colorless liquid. ^1H NMR (500 MHz, CDCl_3): δ (ppm) 1.20 (t, $J = 7.0$ Hz, 3H), 1.34 (t, $J = 7.0$ Hz, 3H), 3.70 (s, 3H), 3.87–3.89 (m, 1H), 4.03–4.07 (m, 1H), 4.16–4.20 (m, 2H), 4.23 (b, 1H), 4.78 (d, $J = 13.2$ Hz, 1H), 6.30 (s, 1H), 6.36–6.37 (m, 1H), 6.62–6.64 (m, 2H), 6.72–6.74 (m, 2H), 7.37 (s, 1H).

Diethyl (benzylamino)(furan-2-yl)methylphosphonate 3l

Colorless liquid. ^1H NMR (400 MHz, CDCl_3): δ (ppm) 1.22 (t, $J = 7.0$ Hz, 3H), 1.31 (t, $J = 7.0$ Hz, 3H), 3.59 (d, $J = 13.2$ Hz, 1H), 3.85–3.88 (m, 2H), 4.03–4.15 (m, 5H), 6.37–6.38 (m, 2H), 7.29–7.30 (m, 6H).

Acknowledgements

Financial support from the National Natural Science Foundation of China (20502004), the Ministry of Education

of China, the Science and Technology Commission of Shanghai Municipality, and Fudan University is gratefully acknowledged.

References

- 'Modern Solvents In Organic Synthesis', *Topics In Current Chemistry*, vol. 206, ed. P. Knochel, K. N. Houk and H. Kessler, Springer Verlag, Berlin, 1999.
- D. P. Curran, *Pure Appl. Chem.*, 2000, **72**, 1649.
- W. Leitner, *Top. Curr. Chem.*, 1999, **206**, 107.
- T. Welton, *Chem. Rev.*, 1999, **99**, 2071.
- (a) C.-J. Li and T.-H. Chan, *Organic Reactions in Aqueous Media*, John Wiley, New York, 1997; (b) *Organic Reactions in Water*, ed. P. Grieco, Blackie Academic & Professional, London, 1998.
- (a) F. Toda, *Acc. Chem. Res.*, 1995, **28**, 480; (b) J. O. Metzger, *Angew. Chem., Int. Ed.*, 1998, **37**, 2975; (c) K. Tanaka and F. Toda, *Chem. Rev.*, 2000, **100**, 1025.
- P. I. Dalko and L. Moisan, *Angew. Chem., Int. Ed.*, 2004, **43**, 5138.
- (a) D. Basavaiah, A. J. Rao and T. Satyanarayana, *Chem. Rev.*, 2003, **103**, 811; (b) S.-K. Tian, R. Hong and L. Deng, *J. Am. Chem. Soc.*, 2003, **125**, 9900; (c) J. Wu, X. Sun and Y. Li, *Eur. J. Org. Chem.*, 2005, 4271; (d) J. Wu and H.-G. Xia, *Green Chem.*, 2005, **7**, 708.
- Selected examples, see: (a) K. Surendra, N. S. Krishnaveni, V. P. Kumar, R. Sridhar and K. R. Rao, *Tetrahedron Lett.*, 2005, **46**, 4581; (b) B. Karimi, H. Hazarkhani and J. Maleki, *Synthesis*, 2005, 279; (c) S. K. Talluri and A. Sudalai, *Org. Lett.*, 2005, **7**, 855; (d) N. S. Krishnaveni, K. Surendra and K. R. Rao, *Adv. Synth. Catal.*, 2004, **346**, 346.
- For reviews of the biological activity of α -amino phosphonic acids, see: (a) J. Hiratake and J. Oda, *Biosci., Biotechnol., Biochem.*, 1997, **61**, 211; (b) P. Kafarski and B. Lejczak, *Phosphorus, Sulfur Silicon Relat. Elem.*, 1991, **63**, 193. For a fM inhibitor of carboxypeptidase A, see: (c) A. P. Kaplan and P. A. Bartlett, *Biochemistry*, 1991, **30**, 8165.
- (a) J. G. Allen, F. R. Atherton, M. J. Hall, C. H. Hassall, S. W. Holmes, R. W. Lambert, L. J. Nisbet and P. S. Ringrose, *Nature*, 1978, **272**, 56; (b) R. F. Pratt, *Science*, 1989, **246**, 917.
- L. Maier and P. J. Diel, *Phosphorus, Sulfur Silicon Relat. Elem.*, 1991, **57**, 57.
- S. A. Beers, C. F. Schwender, D. A. Loughney, E. Malloy, K. Demarest and J. Jordan, *Bioorg. Med. Chem.*, 1996, **4**, 1693.
- (a) S. Laschat and H. Kunz, *Synthesis*, 1992, 90; (b) J. S. Yadav, B. V. S. Reddy, K. S. Raj, K. B. Reddy and A. R. Prasad, *Synthesis*, 2001, 2277.
- (a) A. Heydari, A. Javidan and M. Shaffie, *Tetrahedron Lett.*, 2001, **42**, 8071; (b) M. R. Saidi and N. Azizi, *Synlett*, 2002, 1347; (c) B. C. Ranu, A. Hajra and U. Jana, *Org. Lett.*, 1999, **1**, 1141; (d) C. Qian and T. Huang, *J. Org. Chem.*, 1998, **63**, 4125; (e) K. Manabe and S. Kobayashi, *Chem. Commun.*, 2000, 669; (f) S. Lee, J. H. Park, J. Kang and J. K. Lee, *Chem. Commun.*, 2001, 1698; (g) S. Chandrasekhar, S. J. Prakash, V. Jagadeshwar and C. Narsihmulu, *Tetrahedron Lett.*, 2001, **42**, 5561; (h) J. S. Yadav, B. V. S. Reddy and C. Madan, *Synlett*, 2001, 1131; (i) B. Kaboudin and R. Nazari, *Tetrahedron Lett.*, 2001, **42**, 8211; (j) Z.-P. Zhan and J.-P. Li, *Synth. Commun.*, 2005, **35**, 2501; (k) Z.-P. Zhan, R.-F. Yang and J.-P. Li, *Chem. Lett.*, 2005, **34**, 1042; (l) K. R. Reddy, K. S. Reddy, C. V. Reddy, M. Mahesh, P. V. K. Raju and V. V. N. Reddy, *Chem. Lett.*, 2005, **34**, 444; (m) P. Sun, Z. Hu and Z. Huang, *Synth. Commun.*, 2004, **34**, 4293; (n) R. Ghosh, S. Maiti, A. Chakraborty and D. K. Maiti, *J. Mol. Catal. A: Chem.*, 2004, **210**, 53; (o) F. Xu, Y. Luo, M. Deng and Q. Shen, *Eur. J. Org. Chem.*, 2003, 4728; (p) N. Azizi, F. Rajabi and M. R. Saidi, *Tetrahedron Lett.*, 2004, **45**, 9233.
- (a) G. D. Joly and E. N. Jacobsen, *J. Am. Chem. Soc.*, 2004, **126**, 4102; (b) T. Akiyama, M. Sanada and K. Fuchibe, *Synlett*, 2003, 1463.
- (a) X.-J. Mu, M.-Y. Lei, J.-P. Zou and W. Zhang, *Tetrahedron Lett.*, 2006, **47**, 1125; (b) Z.-P. Zhan, R.-F. Yang and J.-P. Li, *Chem. Lett.*, 2005, **34**, 1042.

Zeolite catalyzed acylation of alcohols and amines with acetic acid under microwave irradiation†

K. V. V. Krishna Mohan, N. Narender and S. J. Kulkarni*

Received 3rd January 2006, Accepted 6th February 2006

First published as an Advance Article on the web 1st March 2006

DOI: 10.1039/b600031b

Zeolite H β is found to be an efficient catalyst for the acylation of alcohols and amines with acetic acid under microwave irradiation. The process is environmentally safe and heterogeneous with excellent yields.

1. Introduction

The acylation of alcohols and amines is one of the most frequently used transformations in organic synthesis as it provides an efficient and inexpensive means for protecting hydroxy and amino groups in a multistep synthetic process.¹ Despite a number of procedures, new efficient methods are still in strong demand. Acetyl chloride and acetic anhydride are routinely used as acylating agents in the presence of an acidic² and basic³ catalyst. However, both of these reagents, being corrosive and a lachrymator respectively, are not always ideal. Moreover, the acidic conditions in Lewis acid acylations lead to the cleavage of sensitive functional groups such as acetals and TBDMS ethers. Amine bases such as triethylamine, pyridine or 4-(*N,N*-dimethylamino) pyridine (DMAP), 4-pyrrolidinopyridine and triphenylphosphine were used as catalysts for acylation of alcohols with acetic anhydride. Sc(OTf)₃,⁴ TMSOTf^{5,6} and clays^{7,8} such as K-10, KSF were reported for the acylation of alcohols and amines respectively with acetic anhydride. Tetrabutylammonium salt,⁹ cyanide anion¹⁰ and Cp₂Sm(thf)₂¹¹ are also used in the acylation of amines with esters. Earlier, we reported the acylation of alcohols and amines with acetic acid using LaY and HY¹² as catalysts. Recently, Gd(OTf)₃¹³ and iodine,¹⁴ ZnO,¹⁵ bromodimethylsulfoniumbromide,¹⁶ lanthanide(III) tosylates,¹⁷ CoCl₂·6H₂O,¹⁸ ZrOCl₂·8H₂O¹⁹ have been reported to promote the acylation of alcohols and amines with acetic anhydride or acetylchloride. Acylation with acetic anhydride without catalyst has also been reported.²⁰ Though acylation of alcohols can also be brought about by the action of Lewis acid reagents in conjunction with carboxylic acids, the Lewis acid is destroyed in the work-up procedure resulting in substantial waste production.^{21–23} These catalysts suffer from some drawbacks. Scandium triflate is rather expensive and must be used under anhydrous conditions. Trimethylsilyl triflate is labile towards moisture, and its acidity is too strong for acid-sensitive alcohols as reagents.

However, most of these methods suffer from one or more of the following disadvantages: long reaction times, vigorous reaction conditions and the occurrence of side reactions.

Nevertheless, there is still a great demand for acid catalysts to generate esters under mild conditions.

The use of acetic acid rather than acetic anhydride or acetyl chloride is both economically and environmentally advantageous, because substances used in chemical synthesis may either be incorporated into the final product or into byproducts as waste. Increasingly, the chemical industry seeks products with high yield and low waste. The concept of “atom economy”^{24,25} has been introduced to monitor the fate of the reactants.

The use of heterogeneous catalysts in different areas of organic synthesis has now reached significant levels, not only because it enables environmentally benign synthesis, but also due to the good yields, accompanied by excellent selectivities, that can frequently be achieved. Zeolites are uniform microporous crystalline materials and have been investigated extensively and applied as solid catalysts in the field of petrochemistry.^{26,27} Zeolites are also known to catalyze various synthetic organic transformations much more effectively and selectively than the Lewis acid catalysts.

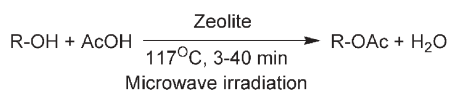
Microwave irradiation of organic reactions has rapidly gained in popularity as it accelerates a variety of synthetic transformations²⁸ *via* time- and energy-saving protocols. Herein, we report the microwave enhanced O,N-acylation of alcohols and amines respectively with acetic acid over zeolites as recyclable catalysts.

2. Experimental

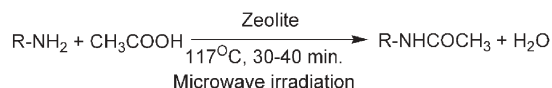
H β zeolite was obtained from Sud. Chemie, India. The Si/Al ratio was 15. In a typical reaction procedure, 2 mmol of substrate, 2 ml of acetic acid and 200 mg of zeolite catalyst were introduced into a two neck cylindrical flask (20 mm diameter and 10 cm height) equipped with a reflux condenser and temperature sensor. The microwave irradiation was carried out in a ETHOS MR microwave reactor (milestone, Italy) and the temperature was maintained at 117 °C at an operation power of 600 watts for 3–40 minutes. The reaction was carried out under stirring. At the end of the irradiation, the reaction mixture was cooled to room temperature and then the catalyst was filtered and the solid was washed with ether. The combined filtrates were washed with saturated sodium bicarbonate solution and then dried over anhydrous sodium sulfate and the solvent evaporated under reduced pressure.

Catalysis Group, Indian Institute of Chemical Technology, Hyderabad, India. E-mail: sjkulkarni@iictnet.org; Fax: +91-40-27160387/27160757; Tel: +91-40-27193161

† IICT Communication No: 020908.



Scheme 1



Scheme 2

3. Results and discussion

All the reactions (Scheme 1 and Scheme 2) were performed with 2 mmol of substrate in 2 ml of acetic acid using 200 mg of H β zeolite and modified beta zeolite at 117 °C with an irradiation power of 600 watts for the selected time in an ETHOS MR microwave reactor.

We have investigated the use of various zeolites, K10 montmorillonite, SiO₂ and SiO₂-Al₂O₃ as catalysts for the acylation of benzyl alcohol (Table 1) and acylation of aniline (Table 2) with acetic acid. The results showed that H β zeolite showed high catalytic activity compared to other catalysts. The acylation of benzyl alcohol failed to proceed in the absence of

Table 1 Acylation of benzyl alcohol with acetic acid: variation of catalyst^a

Entry	Catalyst	Time/min	Conversion (%)	Selectivity ^b (%)
1	H β	3	99	99
2	HY	3	13	99
3	HMordenite	3	—	—
4	HZSM-5(40)	3	18	99
5	HZSM-5(150)	3	21	99
6	MCM-41	3	25	99
7	Montmorillonite K10	3	—	—
8	SiO ₂ -Al ₂ O ₃	3	2	99
9	SiO ₂	3	1	99
10	No catalyst	3	—	—

^a Benzyl alcohol (2 mmol), acetic acid (2 ml), catalyst (200 mg).

^b The products were characterized by NMR, mass spectra and GC analysis. Selectivity = % formation of product (ester).

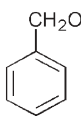
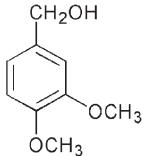
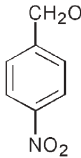
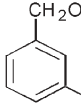
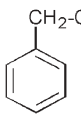
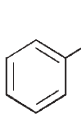
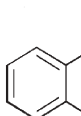
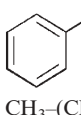
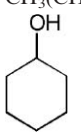
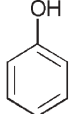
Table 2 Effect of variation of catalyst on acylation of aniline with acetic acid^a

Entry	Catalyst	Time/min	Conversion ^b (%)
1	H β	15	31
2	HY	15	26
3	H-Mordenite	15	27
4	HZSM-5(40)	15	14
5	HZSM-5(150)	15	24
6	HMCM-41	15	16
7	Montmorillonite K10	15	07
8	SiO ₂ -Al ₂ O ₃	15	<5
9	Silica	15	<5
10	HX	15	24
11	NaY	15	16
12	No catalyst	15	<5

^a Aniline (2 mmol), acetic acid (2 ml), catalyst: 200 mg, reaction temperature = 117 °C. ^b The products were characterized by NMR, mass and quantified by GC. Selectivity = % formation of product (amide) = 99%.

catalyst. To explore the generality and scope of this reaction a wide range of structurally varied alcohols were subjected to acylation by this procedure. The results are reported in Table 3.

Table 3 Acylation of alcohols with acetic acid over H β zeolite under microwave irradiation^a

Entry	Substrate	Time/min	Conversion (%)	Selectivity ^b (%)
1		3	98	99
2		4	99	99
3		10	97	99
4		30	89	99
5		5	99	99
6		3	95	82
7		3	98	64
8		4	99	99
9	CH ₃ -(CH ₂) ₈ -CH ₂ OH	6	95	99
10	CH ₂ -CH ₃ CH ₂ -CH-(CH ₂) ₃ -CH ₃ OH	30	93	99
11	CH ₃ (CH ₂) ₃ OCH ₂ -CH ₂ OH	4	77	92
12		40	89	99
13		30	30	99

^a Substrate (2 mmol), H β (200 mg), acetic acid (2 ml). ^b The products were characterized by NMR, mass spectra and GC analysis, selectivity = % formation of product (ester).

Table 4 Acylation of benzyl alcohol with acetic acid over H β : effect of amount of catalyst^a

Entry	Amount of catalyst/mg	Time/min	Conversion ^b (%)
1	200	3	99
2	100	3	51
3	50	3	30
4	25	3	18

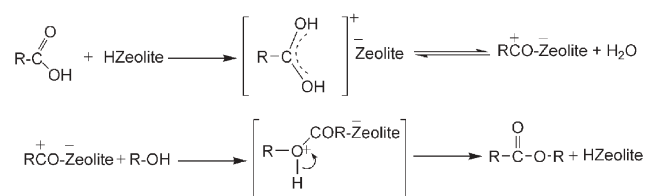
^a Benzyl alcohol (2 mmol), acetic acid (2 ml). ^b The products were characterized by NMR, mass spectra and GC analysis, reaction temperature = 117 °C, selectivity = % formation of product (ester) = 99%.

Good to high yields were obtained in all cases except phenol. Aromatic alcohols undergo reaction at a relatively faster rate compared to the aliphatic alcohols. Electron donating groups facilitate the reaction whereas electron withdrawing groups slow down the reaction (Table 3, entries 3 and 4).

It was found that primary alcohols undergo smooth acylation and give the desired ester, whereas with the secondary alcohols (Table 3, entries 6 and 7) a small amount of byproducts (olefin) was produced together with the desired acetate. In addition, allylic alcohols can be acylated in high yields (Table 3, entry 8). In the present catalytic system, the phenol reacts very slowly and yields 30% in 30 minutes. The effect of solvents (acetonitrile, acetone, dichloromethane, carbon tetrachloride and n-hexane) in the acylation of benzyl alcohol with acetic acid using H β zeolite as catalyst is studied. Under these conditions, the results were obtained only when acetic acid was used as a solvent. The present reaction was also conducted using different amounts of the catalyst (Table 4) and it was found that the reaction conducted with 200 mg of catalyst is optimum requirement for the better conversion.

To compare the efficiency of microwave irradiation with those of conventional heating, the reaction was carried out with benzyl alcohol as substrate in acetic acid at the same temperature (117 °C) without microwave irradiation. 30 minutes were required to complete the reaction. Zeolite H β shows good activity, which is independent of the different polarities of the reactants. Thus, it seems likely that almost all reagents utilized in the present study can reach the active sites of the catalyst surface. After the reaction, the catalyst (zeolite) is recovered with retention of its catalytic activity. It can be further reactivated for reuse by heating it at 500 °C in the presence of air. The catalyst shows good activity even after three cycles. The highly crystalline nature of H β before and after the reaction was confirmed by the X-ray diffraction pattern.

A tentative mechanism for the formation of ester (acylation of alcohols) is shown in Scheme 3. At the Brønsted acid sites of

**Scheme 3****Table 5** Effect of modified zeolites^a on the acylation of aniline with acetic acid^a

Entry	Catalyst	Time/min	Conversion ^b (%)
1	H β	15	31
2	5%Fe β	15	52
3	5%La β	15	36
4	5%Cu β	15	29
5	5%Cr β	15	36
6	5%Co β	15	31
7	5%Zn β	15	45
8	5%Ni β	15	47
9	5%Ce β	15	35
10	5%Pb β	15	21
11	5%W β	15	36

^a Aniline (2 mmol), acetic acid (2 ml), catalyst: 200 mg, reaction temperature = 117 °C. ^b The products were characterized by NMR, mass and quantified by GC. Selectivity = % formation of product (amide) = 99%.

H β zeolite the carbonyl group is protonated and the resulting acylium ion further reacts with alcohol to give the corresponding ester.

An efficient method for the acylation of amines to the corresponding amides using acetic acid over various metal ion modified zeolite beta under microwave irradiation (Scheme 2) has been reported. Table 2 shows the results of acylation of aniline over various zeolite catalysts with acetic acid under microwave irradiation. Results indicate that H β is the best catalyst, giving 31% conversion of aniline in 15 min of microwave irradiation.

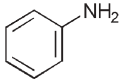
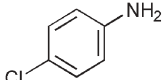
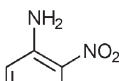
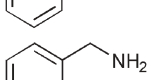
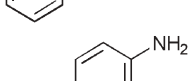
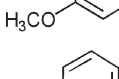
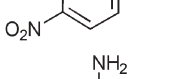
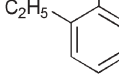
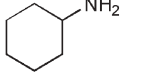
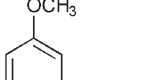
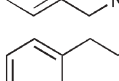
A comparison of the activity of various metal modified H β zeolites shows that Fe β is the most efficient compared to other catalysts (Table 5). 5 wt% Fe β showed 52% conversion of aniline within 15 min of microwave irradiation (Table 5, entry 2). Table 6 shows the results of acylation of various amines with acetic acid in the presence of 5 wt% Fe β catalyst under microwave irradiation. It is interesting, though perhaps not surprising, to note that electron donating groups facilitate the reaction whereas electron withdrawing groups slow down the reaction. The conversions of alkyl amines are found to be relatively higher than aryl amines and heterocyclic amines.

The conversion and selectivity percentages for different substrates can be noted from Table 6. The catalyst 5 wt% Fe β showed consistent results without any significant loss of activity even after three cycles. The reaction proceeds very smoothly at 117 °C under 30–40 min of microwave irradiation. In a control experiment without catalyst, only a small quantity (<5%) of the aniline was converted to acetanilide under similar reaction conditions (Table 2, entry 12). A plausible reaction mechanism of this acylation over zeolites is presented (Scheme 4). Here, the carbonyl group is protonated over the Brønsted acid sites of the zeolite. The resulting complex is the acylating agent or an acylium ion, formed in a cleavage reaction with H $_2$ O as byproduct. This further reacts with amine to give the corresponding amide.

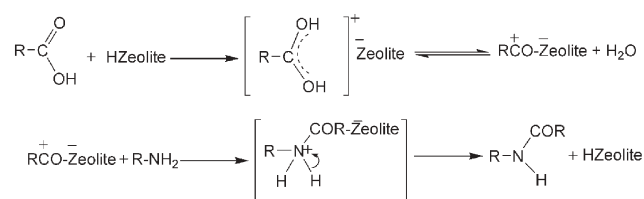
4. Conclusions

In conclusion, we have developed an efficient, rapid, safe, high yielding and eco-friendly method for acylation of alcohols and amines using acetic acid over zeolites and metal modified H β

Table 6 Acylation of amines using acetic acid over 5 wt% Fe β zeolite^a

Entry	Substrate	Time/ min	Conversion (%)	Selectivity ^b (%)
1		30	73	99
2		40	74	99
3		30	—	—
4		40	99	99
5		40	72	99
6		40	—	—
7		40	—	—
8		30	85	50
9		40	96	99
10		40	99	99
11		40	—	—

^a Amine (2 mmol), acetic acid (2 ml), 5 wt% Fe β (200 mg), reaction temperature: 117 °C. ^b The products were characterized by NMR, mass spectra and GC analysis, selectivity = % formation of product (amide).

**Scheme 4**

zeolites under microwave irradiation. The present method is applicable to primary and secondary alcohols, primary amines and anilines. Another advantage of the present method is that these zeolite catalysts can be reused. This is remarkable and makes the method economically valuable.

Acknowledgements

K. V. V. Krishna Mohan thanks CSIR, New Delhi for the award of a Research Fellowship.

References

- T. W. Green and P. G. M. Wuts, *Protective Groups in Organic Synthesis*, 3rd edn, Wiley, New York, 1999.
- J. Iqbal and R. R. Srivastava, *J. Org. Chem.*, 1992, **57**, 2001; K. Ishihara, M. Kubota, H. Kurihara and H. Yamamoto, *J. Am. Chem. Soc.*, 1995, **117**, 4413; J. Izumi, I. Shiina and T. Mukaiyama, *Chem. Lett.*, 1995, 141; A. G. M. Barret and D. C. Braddock, *Chem. Commun.*, 1997, 351; R. Ballini, G. Bosica, S. Carloni, L. Ciaralli, R. Maggi and G. Sartori, *Tetrahedron Lett.*, 1998, **39**, 6049.
- T. Nishiguchi, K. Kawamine and T. Ohtsuka, *J. Org. Chem.*, 1992, **57**, 312; Y. Kita, H. Maeda, K. Omori, T. Okuno and Y. Tamura, *J. Chem. Soc., Perkin Trans. 1*, 1993, 2999; J. Otera, *Chem. Rev.*, 1993, **93**, 1449; A. Loupy, A. Petit, M. Ramdani, C. Yuanaeft, M. Majdoub, B. Labiad and D. Villemin, *Can. J. Chem.*, 1993, **71**, 90; G. W. Breton, *J. Org. Chem.*, 1997, **62**, 8952; G. Hofle, V. Steglich and H. Vorbruggen, *Angew. Chem., Int. Ed. Engl.*, 1978, **17**, 569.
- K. Ishihara, M. Kubota, H. Kurihara and H. Yamamoto, *J. Am. Chem. Soc.*, 1995, **117**, 4413; K. Ishihara, M. Kubota and H. Yamamoto, *Synlett*, 1996, 265; A. G. M. Barrett and D. C. Braddock, *Chem. Commun.*, 1997, 351; K. Ishihara, M. Kubota, H. Kurihara and H. Yamamoto, *J. Org. Chem.*, 1998, **61**, 4560; H. Zhao, A. Pendri and R. B. Greenwald, *J. Org. Chem.*, 1998, **63**, 7559.
- P. A. Procopiou, S. P. D. Baugh, S. S. Flack and G. G. A. Inglis, *Chem. Commun.*, 1996, 2625.
- P. A. Procopiou, S. P. D. Baugh, S. S. Flack and G. G. A. Inglis, *J. Org. Chem.*, 1998, **63**, 2342.
- A. X. Li, T. S. Li and T. H. Ding, *Chem. Commun.*, 1997, 1389.
- P. M. Bhasker and D. Loganathan, *Tetrahedron Lett.*, 1998, **39**, 2215.
- T. Hogberg, P. Strom, M. Ebner and S. Ramsby, *J. Org. Chem.*, 1987, **52**, 2033; S. J. Chen, S. T. Chen, S. Y. Chen and K. T. Wang, *Tetrahedron Lett.*, 1994, **35**, 3583.
- P. M. Bhasker and D. Loganathan, *Tetrahedron Lett.*, 1998, **39**, 2215.
- B. Roberto, B. Giovanna, C. Cilia, C. Lara, M. Raimondo and S. Giovanni, *Tetrahedron Lett.*, 1998, **39**, 6049.
- N. Narender, P. Srinivasu, S. J. Kulkarni and K. V. Raghavan, *Synth. Commun.*, 2000, **30**, 1887; N. Narender, P. Srinivasu, S. J. Kulkarni and K. V. Raghavan, *Green Chem.*, 2000, **3**, 104.
- R. Alletti, M. Perambuduru, S. Samantha and V. Prakash Reddy, *J. Mol. Catal. A*, 2005, **226**, 57.
- P. Phukan, *Tetrahedron Lett.*, 2004, **45**, 24, 4785.
- M. H. Sarvari and H. Sharghi, *Tetrahedron*, 2005, **61**, 10903; F. Tamaddon, M. A. Amrollahi and L. Sharafat, *Tetrahedron Lett.*, 2005, **46**, 7841.
- A. T. Khan, S. Islam, A. Majee, T. Chattopadhyay and S. Ghosh, *J. Mol. Catal. A*, 2005, **239**, 158.
- T. N. Parac-Vogt, K. Deleersnyder and K. Binnemans, *Eur. J. Org. Chem.*, 2005, 1810.
- S. Velusamy, S. Borpuzari and T. Punniyamurthy, *Tetrahedron*, 2005, **61**, 2011.
- R. Ghosh, S. Maiti and A. Chakraborty, *Tetrahedron Lett.*, 2005, **46**, 147.
- N. Kammoun, Y. Le Bigot, M. Delmas and B. Boutevin, *Synth. Commun.*, 1997, **27**, 2777.
- J. Izumi, I. Shiina and T. Mukaiyama, *Chem. Lett.*, 1995, 141.
- I. Shiina and T. Mukaiyama, *Chem. Lett.*, 1994, 677.
- A. K. Kumar and T. K. Chattopadhyay, *Tetrahedron Lett.*, 1987, **28**, 3713.
- Chemistry of Waste Minimization*, ed. J. H. Clark, Blackie Academic, London, 1995.
- B. M. Trost, *Angew. Chem., Int. Ed. Engl.*, 1995, **34**, 259.
- D. W. Breck, *Zeolite Molecular Sieves*, Wiley, New York, 1974.
- A. Dyer, *An Introduction to Zeolite Molecular Sieves*, Chichester, 1988.

- 28 A. K. Bose, B. K. Banik, N. Lavlinskaia, M. Jayaraman and M. S. Manhas, *Chemtech*, 1997, **27**, 18; A. Loupy, *Microwaves in Organic Synthesis*, Wiley-VCH, Weinheim, 2002; P. Lidstrom and J. P. Tierney, *Microwave Assisted Organic Synthesis*, Blackwell, 2005; C. O. Kappe, *Angew. Chem., Int. Ed.*, 2004, **43**, 6250; D. Bogdal, M. Lukasiewicz and J. Pielichowski, *Green Chem.*, 2004, **6**, 110; K. T. J. Loones, B. U. W. Maes, G. Rombouts, S. Hostyn and G. Diels, *Tetrahedron*, 2005, **61**, 10338; A. Burczyk, A. Loupy, D. Bogdal and A. Petit, *Tetrahedron*, 2005, **61**, 179.



**Fast
Publishing?
Ahead of the field**

To find out more about RSC Journals, visit

RSCPublishing

www.rsc.org/journals

Recovery and reuse of ionic liquids and palladium catalyst for Suzuki reactions using organic solvent nanofiltration

Hau-to Wong, Christopher John Pink, Frederico Castelo Ferreira and Andrew Guy Livingston*

Received 25th November 2005, Accepted 18th January 2006

First published as an Advance Article on the web 8th February 2006

DOI: 10.1039/b516778g

The separation, post-reaction, of ionic liquids and catalysts from reaction products is an unresolved challenge in the application of ionic liquids to organometallic catalysis. This paper addresses this challenge using organic solvent nanofiltration technology. Suzuki reactions were carried out in a homogeneous solution, comprising 50 : 50 wt% ethyl acetate and ionic liquid. The post reaction mixture was diluted further with ethyl acetate and then separated by nanofiltration into a permeate fraction and a retained (retentate) fraction. The product was recovered in the nanofiltration permeate, while the ionic liquid and palladium catalyst were retained by the membrane and recycled into subsequent consecutive reactions. Thus, the organic solvent nanofiltration was able to separate the Suzuki reaction product from both catalyst and ionic liquid. Three ionic liquids were tested: cocosalkyl pentaethoxy methyl ammonium methosulfate (ECOENG[®]500), tetrabutylammonium bromide (TBAB) and trihexyl(tetradecyl)phosphonium chloride (CyPhos[®]101). All the ionic liquids screened showed positive effects on the catalytic stability, significantly reducing the formation of palladium black and providing high reaction yields over consecutive recycles. The best performance was observed for the CyPhos[®]101 system. Additional investigations employing this ionic liquid showed that the reaction–recycle process can be successfully performed at lower catalyst–substrate ratios, leading to higher catalyst turnover numbers.

Introduction

The properties of ionic liquids (ILs) can be engineered through ion selection, and this flexibility has earned them a reputation as “designer” solvents.^{1–8} ILs are used in a continually evolving range of applications, including cross-coupling reactions where the benefits of these highly polar yet non-coordinating solvents has been demonstrated.^{9–12} An example of such a reaction is the Suzuki coupling, a key step in the synthesis of active pharmaceutical ingredients,^{13,14} where ILs have provided enhanced catalytic activity and stability.^{15,16} However, an unresolved challenge is the efficient separation of IL from products in post-reaction mixtures. Separation of Suzuki reaction products from IL and homogeneous transition metal catalyst (TMC) *via* solvent extraction is the conventional choice^{9–11} for obtaining IL (and catalyst in some cases) in a recyclable form (see Fig. 1a). However, while solvent extraction is suitable for separation of apolar products, its use in separation of polar products is more problematic. For the latter case, a moderately polar extracting organic solvent (OS) is required, but since ILs tend to have significant partition coefficients into polar solvents, or are completely miscible with them, this can result in loss of IL to the product stream.

We propose that organic solvent nanofiltration (OSN) can provide a separation solution which reduces these problematic losses. In this context, we envisage two schemes for the use of OSN. In systems in which the IL and the moderately polar

extracting solvent form a biphasic mixture, a significant amount of IL can partition into the organic solvent phase. The first scheme involves (see Fig. 1b) separating the phases, and then applying OSN to the organic solvent phase to separate the product from the IL. The IL can be retained by the membrane, and then recycled to the reaction system. The second scheme, investigated in this paper, (see Fig. 1c) dispenses with the need for an intermediate solvent extraction. The reaction is carried out in a homogeneous solution of IL and organic solvent. The post reaction mixture is subjected to OSN, resulting in a permeate stream containing solvent and product, and a retentate stream containing solvent, TMC and IL.

This study extends our previous work using single-phase mixtures of IL with organic solvents for Suzuki couplings.¹⁷ We found that pure ILs can lower reaction rates due to unfavourable heat and mass transfer characteristics arising from their high viscosities (*e.g.* ECOENG[®]500 displays 3150 cP at 20 °C¹⁷). Using 50 : 50 wt% mixtures of organic solvent and miscible ILs avoided the problems associated with these high viscosities, while maintaining the beneficial effects of IL on the reaction. Crucially, this means that IL can be recycled for use in subsequent reactions as a single phase mixture with organic solvent, as opposed to in the form of pure IL. In these cases, the scheme shown in Fig. 1c is directly applicable.

The nanofiltration of organic solvents has been made possible by the development of solvent stable nanofiltration

Department of Chemical Engineering, Imperial College London, Exhibition Road, South Kensington, London, UK SW7 2AZ.
E-mail: a.livingston@imperial.ac.uk

† MWCO of the membranes used here was obtained from a plot of the rejections of a series of n-alkanes dissolved at 2 wt% in toluene, *versus* alkane molecular weight. MWCO is defined as the molecular weight (MW) for which rejection by the membrane is 90%.

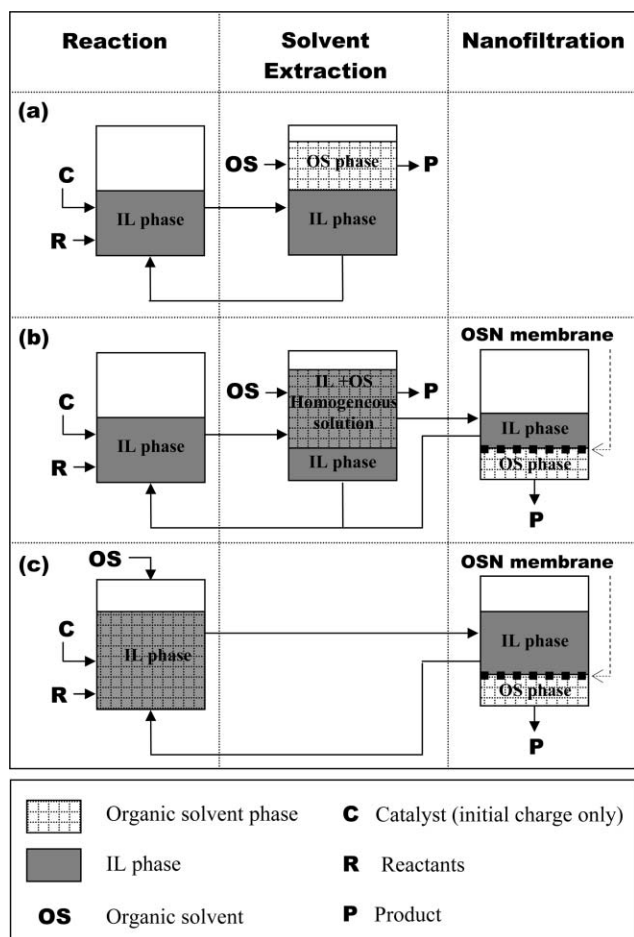


Fig. 1 IL/TMC recycle schemes for coupling reactions: (a) conventional product isolation *via* solvent extraction, (b) OSN used with a bi-phase IL/organic system, and (c) OSN used with a single phase IL–organic solvent system.

membranes.¹⁸ These membranes have molecular weight cut offs (MWCOs)[†] in the range 200–1000 g mol⁻¹. Separation of large molecules (*i.e.* large IL and TMC) from smaller sized molecules within this range (*i.e.* small reaction products) has been reported previously.^{19,20} Cross-flow nanofiltration of synthetic post reaction mixtures has demonstrated high IL rejections[‡], $R^i > 95\%$ for ECOENG[®]500 and CyPhos[®]101.²¹

In this study, for the first time, we combine a reaction in a single phase IL–organic solvent medium with OSN to

$$‡ R^i = \left(1 - \frac{C_{\text{permeate}}^i}{C_{\text{retentate}}^i}\right) \times 100\% \text{ where } C \text{ is concentration.}$$

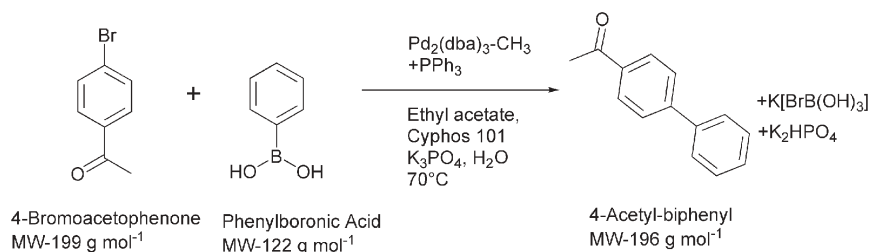


Fig. 2 Suzuki reaction forming 4-acetyl-biphenyl.

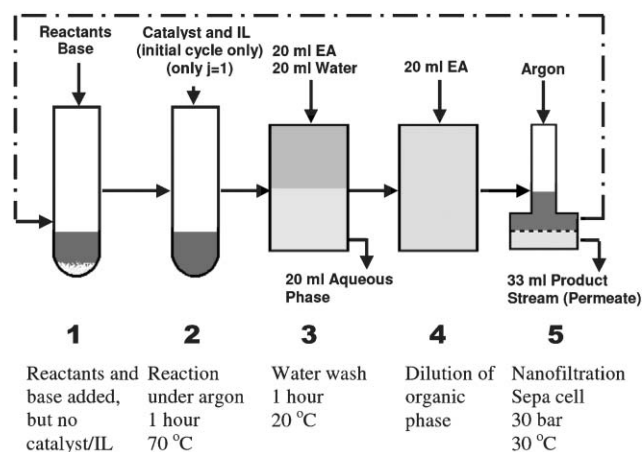


Fig. 3 Catalyst and IL recycle process, showing the different stages (1–5) involved between reaction and nanofiltration.

implement consecutive Suzuki reactions, using only a single initial charge of IL and TMC. We also investigate decreasing TMC loading, in order to minimise palladium contamination levels in the product stream.

Results and discussion

IL Screening

The following ILs were used in 50 : 50 wt% homogeneous mixtures with ethyl acetate: tetrabutylammonium bromide (TBAB), ECOENG[®]500 and CyPhos[®]101. The model reaction selected for this work (Fig. 2) was the formation of 4-acetyl-biphenyl (ABP) by the Suzuki coupling between 4-bromoacetophenone (BrAP) and phenylboronic acid. Tris(dibenzylideneacetone)dipalladium chloroform complex (Pd₂(dba)₃-CH₃) was used as the TMC, BrAP was added as the limiting reactant and reaction time was 1 hour in all the experiments. Reactions were also carried out in pure ethyl acetate to act as a control. ILs were selected based on achieving satisfactory yields for the Suzuki coupling as well as high R^{IL} (>95%) with STARMEM[®] 122§, the OSN membrane used throughout this work.^{17,21}

The product recovery and IL recycle process used in this work can be seen in Fig. 3. After the reaction (stage 2), an aqueous wash stage was used to remove solid water-soluble by-products. The post reaction mixture was then filtered,

§ STARMEM is a trademark of W.R. Grace and co.

where the OSN membrane retained the IL and TMC for recycling into following reactions, while the product and ethyl acetate permeated through.

This paper is focused on the recycle process as a whole, so the results are reported as process yields (Y), which are defined for each cycle (j) as:

$$Y_{j, \text{process}}(\%) = \left(\frac{\text{ABP}_{j, \text{stage 5 permeate}}(\text{mol})}{\text{BrAP}_{j, \text{fed to stage 1}}(\text{mol})} \right) \times 100\% \quad (1)$$

It is worth noting that the process yield (see eqn (1)) defined in this paper should be distinguished from the reaction yield (see eqn (2)), which does not take the process workup into account. In the process (see Fig. 3), the retentate from stage 5 is recycled to stage 1 of the following cycle. This retentate contains a small amount of the product (ABP) and unreacted BrAP, and so the reaction yield for each cycle (j) is calculated as:

$$Y_{j, \text{reaction}}(\%) = \left(\frac{\text{ABP}_{j, \text{fed to stage 5}} - \text{ABP}_{j-1, \text{stage 5 retentate}}(\text{mol})}{\text{BrAP}_{j, \text{fed to stage 1}} + \text{BrAP}_{j-1, \text{stage 5 retentate}}(\text{mol})} \right) \times 100\% \quad (2)$$

Fig. 4 shows the process yield (see eqn (1)) plotted against the number of process cycles for each solvent system. The first reaction for the pure ethyl acetate and the various ethyl acetate–IL mixtures shows a surprisingly constant yield of 75–85%. This is consistent with our previously reported work.¹⁷ In subsequent reactions the process yields for all but the ethyl acetate–CyPhos[®]101 system fall rapidly. The ethyl acetate–CyPhos[®]101 system maintains higher process yields (>70%) over a larger number of cycles than any of the other solvent systems screened. This indicates that CyPhos[®]101 provides an extraordinary level of catalyst protection compared to the other ILs, although ethyl acetate–EE500 and ethyl acetate–TBAB still maintain moderately higher yields than the pure ethyl acetate system. Fig. 4 also shows that process yields increase in all systems over cycles 2–4. This is explained by the initial accumulation of ABP within the process due to ABP in the retentate. For example, in the ethyl acetate–CyPhos[®]101 system, the yield increases over the first cycles and then reaches

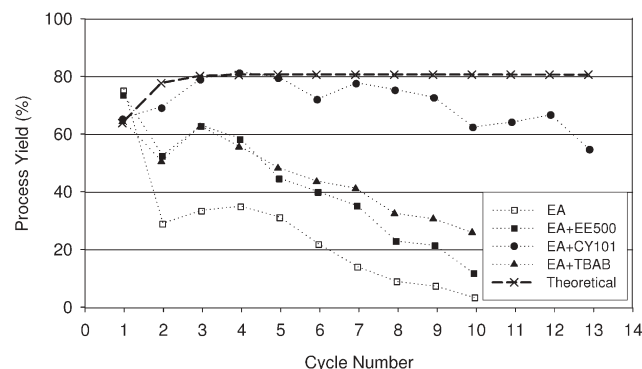


Fig. 4 Process yields from using recycled catalyst–IL, for pure ethyl acetate (EA), EA–ECOENG[®]500 (EE500), EA–CyPhos[®]101 (CY101) and EA–tetrabutylammonium bromide (TBAB) systems (all IL systems 1 : 1 wt% IL : EA). All experiments initially had 5.0 mol% catalyst loading.

a steady value, equal to the reaction yield, at the 3rd cycle. Finally, it starts to decline slowly after the 5th cycle. During this period it is evident that the OSN workup recovers all the ABP after the initial accumulation in the retentate fraction.

To understand this behaviour, the theoretical process yield was iteratively calculated assuming (a) consistent reaction yields of 80%; (b) no formation of side product, which means process yield and process conversion are equal; (c) $R^{\text{BrAP}} = 0$ and $R^{\text{ABP}} = 0$; and (d) that the ratio between the volume of feed solution and retentate in the filtration ($V_{j-1, \text{retentate}}/V_{j-1, \text{feed}}$) was 0.175 (see eqn (3)). Obviously, there is nothing recycled into stage 1 for the first cycle ($j = 1$) i.e. $\text{BrAP}_{j-1} = 0$, stage 5 retentate and $\text{ABP}_{j-1} = 0$, stage 5 retentate equal zero moles.

$$Y_{j, \text{calculated process}}(\%) = \left(1 - \frac{V_{j, \text{stage 5 retentate}}}{V_{j, \text{fed to stage 5}}} \right) \times \frac{\text{ABP}_{j, \text{fed to stage 5}}(\text{mol})}{\text{BrAP}_{j, \text{fed to stage 1}}(\text{mol})} \times 100\% \quad (3)$$

where,

$$\begin{aligned} \text{ABP}_{j, \text{fed to stage 5}}(\text{mol}) &= \frac{V_{j-1, \text{stage 5 retentate}}}{V_{j-1, \text{fed to stage 5}}} \times \\ &\text{ABP}_{j-1, \text{fed to stage 5}}(\text{mol}) + \frac{Y_{\text{reaction}}(\%)}{100} \times \\ &(\text{BrAP}_{j, \text{fed to stage 1}}(\text{mol}) + \text{BrAP}_{j-1, \text{stage 5 retentate}}(\text{mol})) \end{aligned} \quad (3a)$$

$$\begin{aligned} \text{BrAP}_{j-1, \text{stage 5 retentate}}(\text{mol}) &= \frac{V_{j-1, \text{stage 5 retentate}}}{V_{j-1, \text{fed to stage 5}}} \times \\ &\left[\left(1 - \frac{Y_{\text{reaction}}(\%)}{100} \right) \times (\text{BrAP}_{j-1, \text{fed to stage 2}}(\text{mol})) \right] \end{aligned} \quad (3b)$$

The theoretical process yield starts at less than 70%, reaches a value slightly above the reaction yield by the 4th cycle, and then gradually declines over subsequent reactions. This is because the ABP product recycled in the retentate from the first reactions gradually works its way out of the system, along with the ABP formed in each consecutive reaction. The theoretical and actual process yields deviate. There are two main explanations for this decline in process yields with increasing reaction–filtration cycles, and both are related to a decreasing reaction yield resulting from the loss of active palladium catalyst, which is only added to the first cycle. The first explanation is the physical loss of catalyst from the process *via* sampling of the nanofiltration feed (in this process, 2.5% of catalyst present in each cycle is lost). Some catalyst is also lost through the aqueous phase of the water wash.

The second explanation for the process yield decline arises from catalyst instability and the consequent decrease in its activity. One possible scenario is that the catalyst decomposes into smaller fragments, which can penetrate through the OSN membrane (stage 5, Fig. 3). An attempt was made to retain the palladium remaining in the permeate stream by using a second filtration stage. However, it was unsuccessful and this suggests that the palladium may pass through the membrane in a degraded form, which has a reduced size compared to its original catalytic structure.

This degraded form could be related to the formation of catalytically inactive palladium black precipitate. This

Table 1 Percentage of palladium initially added to system appearing as palladium black in different solvent systems, totalled over all the cycles

Solvent system	Catalyst loading (mol%)	Pd appearing as black precipitate (%)
EA	5	73.4
EA-CY101	5	24.8
EA-CY101	0.9	15.9

precipitate is a sign of palladium catalyst deactivation and this is thought to arise from agglomeration of palladium intermediates.²² In our system, significant palladium black was removed along with the aqueous phase leaving stage 3 (see Fig. 3) and was quantified by ICP analysis after dissolution with aqua regia. Palladium black was formed in all the solvent systems, indicating that the ILs screened could not completely prevent the deactivation of the catalyst. However, Table 1 shows 73% of palladium from the catalyst is lost as palladium black in the ethyl acetate system. This is almost three times the observed loss in the ethyl acetate-CyPhos[®]101 system, illustrating the significant degree of catalyst stabilisation provided by CyPhos[®]101. The enhancement of stability may arise from a mechanism which involves a monomolecular layer of IL²³ surrounding the palladium core and preventing the agglomeration of colloidal palladium.

It is also interesting to note that individual analysis of each cycle shows the majority of palladium black is formed during the first two cycles. For example, 66% of the initial amount of palladium was lost in the first cycle in the pure ethyl acetate system. An average of 0.08% was lost in each cycle from the 3rd cycle onwards. This palladium loss is clearly related to the sharp decline in the process yield (see Fig. 4) for the first two cycles of the ethyl acetate system.

The water wash (stage 3, Fig. 3) was introduced to remove the water soluble by-products. Water soluble potassium ions, introduced to the process by the addition of K₃PO₄, are removed in this stage. Quantitative analysis of the amount of potassium in the water phase showed that consistently 70–80% of the potassium added is removed in the water wash of the organic phase over all the cycles. The water wash also provides a relatively neutral pH environment for the nanofiltration membrane by extracting the base from the organic phase.

Quantitative analysis of boron has also been performed. The amount of boron in the water phase was compared with the amount of boron in the limiting reactant BrAP that forms the by-product. This mass balance closed within 90%, showing that the by-product, K[BrB(OH)₃], is removed from the process through the water wash. This avoids a build up of solid material within the process that might foul the membrane surface.

In the model reaction, BrAP is employed as the limiting reactant. From the number of moles of BrAP consumed in the reaction, an equivalent number of moles of product ABP should be generated, assuming no undesirable side reactions. This is expressed through the correlation between process yield and process conversion, see eqn (4). In Fig. 5, the correlation between them suggests that process conversion is consistently 10–20% higher than process yield for all the

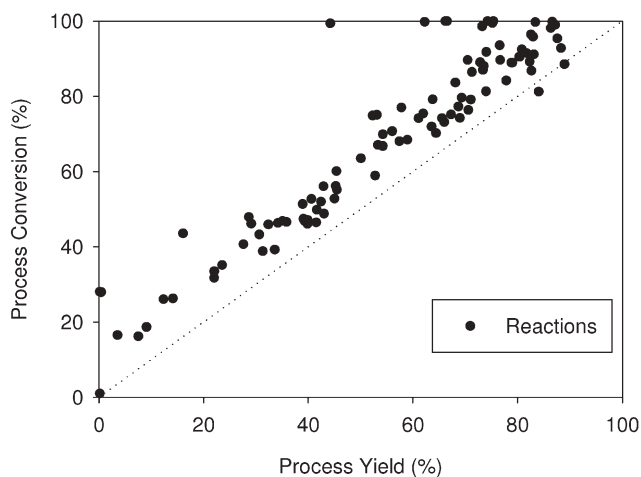


Fig. 5 Process yield vs process conversion (see eqns (2) and (5)).

solvent systems. This implies that around 80–90% of the reacted BrAP forms ABP, while the remaining 10–20% is consumed by the formation of unwanted side products. Process conversion (X) is defined as:

$$X_{j,\text{process}}(\%) = \left(1 - \frac{\text{BrAP}_{j,\text{stage 5 permeate}}(\text{mol})}{\text{BrAP}_{j,\text{fed to stage 1}}(\text{mol})} \right) \times 100\% \quad (4)$$

Palladium contamination

Fig. 6 shows the levels of palladium per unit mass product in the filtration permeate stream. This is a key variable in terms of pharmaceutical quality control and consumer safety, where a typical range of 2–10 mg palladium per kg of product²⁴ is required. Overall, although the palladium levels have been greatly reduced by the nanofiltration stage (e.g. by 79 times for the 1st CyPhos[®]101 cycle), the palladium levels in the permeate streams are still unacceptable for a pharmaceutical grade product and thus further reduction is desirable.

The results from the metal analysis show that the amount of metal in the permeate stream in all solvent systems follow a similar pattern shown in Fig. 6; initially decreasing and then appearing to spike after cycle 5. No plausible explanation can be offered for this unsystematic spiking. As suggested by the two stage filtration results described above, the palladium

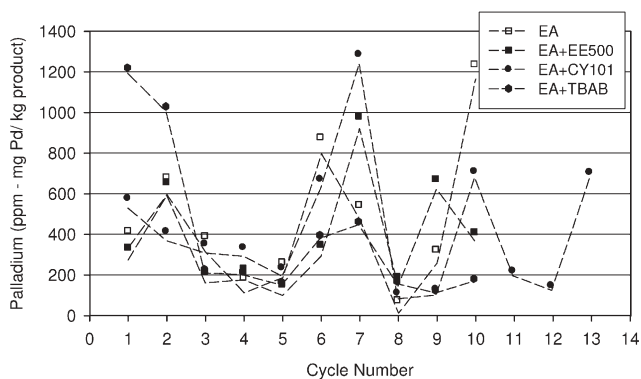


Fig. 6 Palladium loading in the nanofiltration permeate stream.

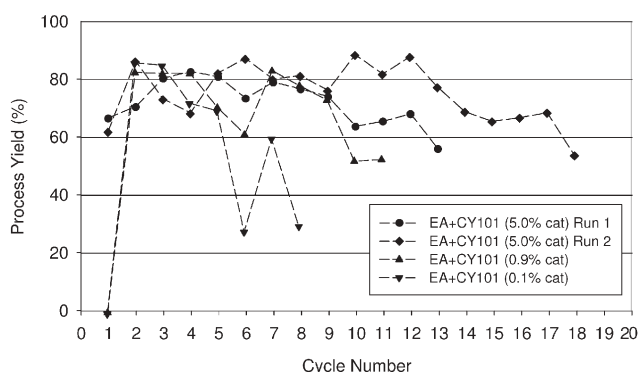
species may be in a degraded form. Nair *et al.*¹⁹ reported loss of the membrane selectivity for recycling palladium catalyst in Heck reactions over consecutive reactions, and speculated this was due to the degradation of catalyst into nanoparticles. A similar phenomenon could take place in the experiments reported here, with the spiking observed in the product stream of this system corresponding to the cycles in which, for some reason, more nanoparticles leave the system *via* the OSN permeation.

Catalyst loading reduction

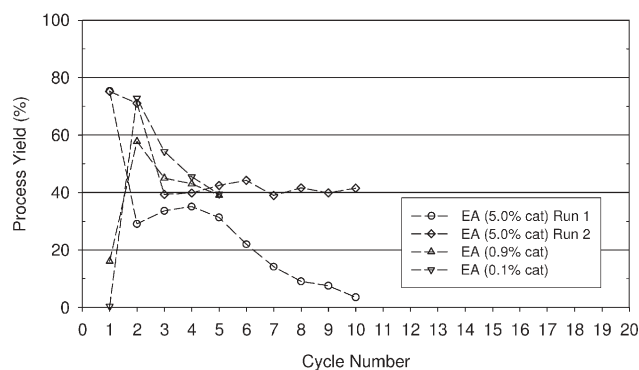
One obvious approach to reduce the palladium in the permeate is by using less initial catalyst for the reactions. In this study the catalyst loading was reduced from 5.0 mol% to 0.9 mol%, and then down to 0.1 mol% for reactions performed in ethyl acetate and ethyl acetate–CyPhos[®]101 systems. The process yields (see Fig. 7) also drop for the low catalyst loading, as one would expect. Palladium black was also observed for lower catalyst loadings (Table 1). Turn Over Number (TON) is calculated as:

$$\text{TON}_j = \frac{\sum_{k=1}^{k=j} \text{ABP}_{k, \text{ stage 5 permeate}} (\text{mol})}{\text{TMC}_{j=1, \text{ fed to stage 2}}^{\text{only initial charge}} (\text{mol})} \quad (5)$$

where k is a summatory index.



(a) EA-Cy101 systems



(b) EA systems

Fig. 7 Effects of reducing initial catalyst loading on process yield, analysed using GC of the permeate (a) EA–Cy101 systems (b) EA systems.

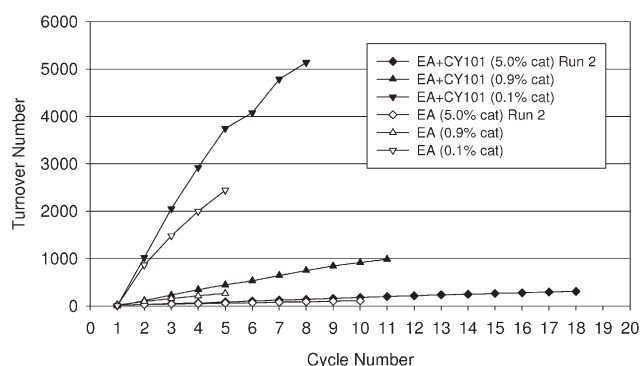


Fig. 8 Cumulative turnover numbers for each system showing the effect of reducing catalyst loading for different solvent systems.

The TON is significantly improved by using low catalyst loading in the same solvent system. For example, Fig. 8 shows the TON increases from 310 (5.0 mol% catalyst loading) up to 5100 (0.1 mol% experiment), taking all the cycles in the ethyl acetate–CyPhos[®]101 solvent system into account.

The benefits of the presence of CyPhos[®]101 are clearly shown in Fig. 7a, where over 70% yield is achieved in 4 cycles at 0.1 mol% catalyst loading. This result contrasts well with the ethyl acetate system where over 70% yield is achieved only in the initial two cycles even at 5.0 mol% catalyst loading (see Fig. 7b).

It is also interesting to note that negligible yields and conversions were observed in the first cycle for all low catalyst loadings (*i.e.* 0.9 mol% and 0.1 mol%) in both solvent systems. Subsequently, process yields increase to values over 60% in the second cycle. This may be due to lack of activation of the palladium catalyst in the initial cycle. This effect, observed by other research groups,^{10,12} seems to become more significant at low catalyst loading.

In order to further investigate this observation, four reaction cycles were performed after an initial catalyst pre-activation step, in which the catalyst (0.9 mol%) was activated in the presence of BrAP, triphenylphosphine, CyPhos[®]101 and ethyl acetate, under the reaction conditions, but without phenylboronic acid, water and base. Pre-activation provided a process yield of 66% for the first cycle. As alluded to above, this is consistent with a reaction yield of 80% because part of the ABP remains in the retentate. For the subsequent

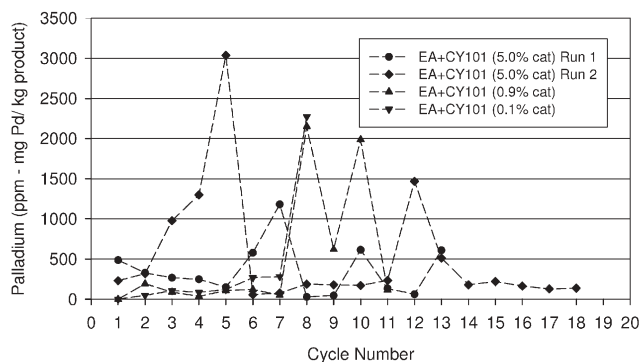


Fig. 9 Palladium loading in the nanofiltration permeate stream.

cycles, the values of the process yield increase and then decrease in a pattern similar to that obtained without catalyst pre-activation.

At low catalyst loading, the pattern of palladium levels (see Fig. 9) is similar to that observed previously (see Fig. 6), where the first five cycles were generally at consistent levels (100 ppm–1000 ppm), but spikes to higher values were seen towards the final cycles. Overall, only slight decreases in palladium content were observed with the resulting palladium level too high to be acceptable for pharmaceutical applications.

Conclusion

This study demonstrates that ionic liquids, particularly CyPhos[®]101, can stabilise palladium catalysts against deactivation. As a result, it enables the recycling and re-use of the catalyst with the assistance of OSN technology. Using low catalyst loading in the system enjoys the advantage of higher catalyst turnover numbers, but this is also accompanied by a more rapid rate of decline for the product yield.

OSN technology was successfully applied to the purification of the reaction products from a homogeneous post-reaction solution, initially containing ionic liquid and catalyst. The failure of two filtration stages to further reduce palladium levels suggests part of the catalyst degrades into small molecules, which the nanofiltration membrane is not able to retain. In terms of product purity, the palladium per unit mass of product in the permeate stream remains unacceptable for pharmaceutical applications without further treatment to reduce Pd levels.

Experimental

Suzuki reaction procedure

A typical procedure for Suzuki coupling using CyPhos[®]101 is as follows. Ethyl acetate was degassed in a 250 ml volume double necked round bottom flask using the Schlenk technique (15 min under argon). CyPhos[®]101 (1 ml), 4-bromoacetophenone (1 mmol, 1.0 equiv.) and phenylboronic acid (1.1 mmol, 1.1 equiv.) were added to a carousel tube. An atmosbag was inflated and evacuated three times using argon. Inside, the triphenylphosphine (0.5 mmol, 0.5 equiv.) was dissolved in degassed ethyl acetate (1 ml), tris(dibenzylidenacetone)dipalladium (0) (0.05 mmol, 0.05 equiv.) was weighed into the tube. Degassed ethyl acetate (1 ml) and 0.2 ml of the ligand solution was added along with the potassium phosphate (previously dried in an oven for an hour at 100 °C, 3.3 mmol 3.3 equiv.) and 0.4 ml of degassed, purified water. The tube was then connected to the carousel, stirring started, and left for 1 hour once the reaction mixture reached 70 °C. All reactants were purchased from Sigma Aldrich, UK apart from CyPhos[®]101, which was donated from Cytec Canada Inc., Canada.

OSN

All filtrations were carried out in a dead-end Sepa ST pressure cell (Osmonics, USA) at 30 bar pressure and 30 °C. The cell

was immersed in a temperature controlled water bath and temperature was allowed to stabilise before any filtrations were started. The solution was agitated using a magnetic plate and a Teflon stirrer bar. STARMEM[®] 122 membranes (polyimide, asymmetric type membrane, MWCO 220 g mol⁻¹), supplied by Membrane Extraction Technology Ltd, UK, were used throughout all experimental work. The membrane was preconditioned using the following process: 220 ml ethyl acetate was fed into the cell, the first 50 ml of permeate were discarded, then after collecting 100 ml more, the pressure was slowly released. The cell was then charged with the collected permeate and filtration was run again, collecting 150 ml permeate, which was returned to the cell for a third filtration. The same membrane was used throughout all the cycles and contamination between IL and purely organic systems was minimised by using two cells, one for each solvent strategy. 20–30 ml fresh ethyl acetate was permeated through the membrane in order to wash the cell and the membrane to reduce contamination.

Recycling process

After the reaction stage (see 2, Fig. 3) the recycling process began with the dilution of the post reaction mixture with 20 ml ethyl acetate. This was agitated for one hour with 20 ml of purified water (see 2, Fig. 3). After allowing phase separation, the lower aqueous phase was removed, and an aqueous sample was taken for metal analysis. The organic phase was made up to 40 ml with ethyl acetate and placed in a dead end SEPA ST pressure cell fitted with a preconditioned membrane. A 1 ml sample was taken from the nanofiltration feed for determination of feed Pd levels *via* ICP-OES. The filtration was terminated (stage 5) when 33 ml of permeate was collected. Analytical samples of the permeate were taken. The remaining retentate was then poured into a new reaction tube containing fresh base, bromoacetophenone and phenylboronic acid, but no additional IL, catalyst or ligand. Finally the reaction was restarted.

Analytical techniques

Gas chromatography was used to determine the concentration of 4-acetyl-biphenyl and bromoacetophenone using the 6850 Series II from Agilent Technologies, fitted with a flame ionisation detector and a HP-1 capillary column 30 m × 0.32 mm nominal diameter, 0.25 mm film thickness 100% dimethylpolysiloxane phase. A coefficient of variation for this assay was estimated to be below 2.5%, based on 44 measurements of a standard solution of ABP and BrAP at concentrations of 26 mM.

Inductively coupled plasma optical emission spectrometry (ICP-OES) was used to determine metal concentrations (Pd, K, B) in the nanofiltration feed, permeate and water wash. ICP analysis was carried out using a Perkin Elmer 2000DV ICP-OES. After initial sampling of the water washes the remaining water was evaporated, then digested with aqua regia to dissolve all the palladium black, to obtain data about levels of precipitation *via* ICP-OES. Each sample was analysed three times and the coefficient of variation for the values obtained was estimated to be lower than 4%.

Acknowledgements

The authors wish to acknowledge the support of The Crystal Faraday Partnership and Astra Zeneca for a PhD Studentship. H. Wong gratefully acknowledges the support of the Croucher Foundation, Hong Kong.

References

- 1 K. R. Seddon and J. D. Holbrey, *Clean Prod. Processes*, 1999, **1**, 223.
- 2 R. Sheldon, *Chem. Commun.*, 2001, 23, 2399.
- 3 T. Welton, *Chem. Rev.*, 1999, **99**, 2071.
- 4 T. Welton, *Coord. Chem. Rev.*, 2004, **248**, 21–24, 2459.
- 5 T. Welton and P. J. Smith, *Adv. Organomet. Chem.*, 2004, **51**, 251.
- 6 C. M. Gordon, *Appl. Catal., A*, 2001, **222**, 1–2, 101.
- 7 J. F. Brennecke and E. J. Maginn, *AIChE J.*, 2001, **47**, 11, 2384.
- 8 K. N. Marsh, J. A. Boxall and R. Lichtenthaler, *Fluid Phase Equilib.*, 2004, **219**, 1, 93.
- 9 J. McNulty, A. Capretta, J. Wilson, J. Dyck, G. Adjabeng and A. Robertson, *Chem. Commun.*, 2002, **17**, 1986.
- 10 C. J. Mathews, P. J. Smith and T. Welton, *Chem. Commun.*, 2000, **14**, 1249.
- 11 F. McLachlan, C. J. Mathews, P. J. Smith and T. Welton, *Organometallics*, 2003, **22**, 5350.
- 12 C. J. Mathews, P. J. Smith and T. Welton, *J. Mol. Catal. A: Chem.*, 2004, **214**, 1, 27.
- 13 N. Yasuda, *J. Org. Chem.*, 2002, **653**, 1–2, 279.
- 14 I. Andreu, N. Cabedo, F. Fabis, D. Cortes and S. Rault, *Tetrahedron*, 2005, **61**, 34, 8282.
- 15 W. A. Herrmann and V. P. W. Bohm, *J. Organomet. Chem.*, 1999, **572**, 141.
- 16 W. A. Herrmann and V. P. W. Bohm, *Chem.—Eur. J.*, 2000, **6**, 6, 1017.
- 17 H. Wong, S. Han and A. G. Livingston, *Chem. Eng. Sci.*, 2006, **61**, 1338.
- 18 L. S. White and A. R. Nitsch, *J. Membr. Sci.*, 2000, **179**, 1–2, 267.
- 19 D. Nair, S. S. Luthra, J. T. Scarpello, L. S. White, L. M. Freitas dos Santos and A. G. Livingston, *Desalination*, 2002, **147**, 1–3, 301.
- 20 J. T. Scarpello, D. Nair, L. M. Freitas dos Santos, L. S. White and A. G. Livingston, *J. Membr. Sci.*, 2002, **203**, 1–2, 71.
- 21 S. Han, H. Wong and A. G. Livingston, *Chem. Eng. Res. Des.*, 2005, **83**, A3, 309.
- 22 M. Tromp, J. Sietsma, J. Bokhoven, G. Strijdonck, J. Haaren, A. Eerden, P. Leeuwen and D. Koningsberger, *Chem. Commun.*, 2003, 1, 128.
- 23 M. T. Reetz and J. G. de Vries, *Chem. Commun.*, 2004, 1559.
- 24 C. Garrett and K. Parsad, *Adv. Synth. Catal.*, 2004, **346**, 8, 889.

Reductive cyclisation of propargyloxy and allyloxy α -bromoester derivatives using environmentally friendly electrochemical methodologies

E. Duñach,^{ab} A. P. Esteves,^c M. J. Medeiros*^c and S. Olivero^a

Received 21st September 2005, Accepted 13th December 2005

First published as an Advance Article on the web 18th January 2006

DOI: 10.1039/b513402a

The electrochemical intramolecular cyclisation of α -bromo propargyloxy (**1** and **2**) and allyloxy (**3**) esters was carried out in ethanol and in ethanol–water mixtures as environmentally friendly systems using Ni(II) complexes as the catalysts. The reduction of the substrates proceeds *via* one-electron cleavage of the carbon–bromine bond to form a radical-type intermediate that undergoes cyclisation to afford cyclic ethers in moderate to good yields.

1. Introduction

The formation of carbon–carbon bonds by radical cyclisations has become a highly valuable synthetic tool in organic chemistry, in particular for applications in the total synthesis of complex natural products.¹ While organotin reagents used in stoichiometric and over-stoichiometric amounts have dominated synthetic procedures involving radical chemistry over the last decade,^{1b} problems associated with the product purification, price and toxicity have stimulated the interest in the development of more user- and environmentally-friendly reagents. In addition to other synthetic methods, electrochemical radical-type cyclisations catalysed by transition-metal complexes have been developed.

Particular Ni(II) macrocyclic complexes have been reported to generate single electron reduced Ni(I) species, which can further catalyse the reductive radical cyclisation of organic halides,^{2–4} bromoacetals possessing electron-deficient olefinic moieties⁵ and 2-haloaryl ethers containing unsaturated side chains.⁶ The furofuran moiety is an important subunit in a wide range of biologically active natural products,^{7,8} therefore, the nickel-mediated radical cyclisation has also been applied to the synthesis of substituted tetrahydrofurans.^{9–11} In all these reported electrochemical cyclisations the solvent used is DMF. Preparative-scale reductive electrosynthesis needs a polar and generally aprotic solvent; however, DMF presents some toxicity as a solvent.¹² In a perspective aimed at cleaner and catalytic syntheses, we describe here the scope of these electrosyntheses in ethanol and ethanol–water mixtures as the solvents.

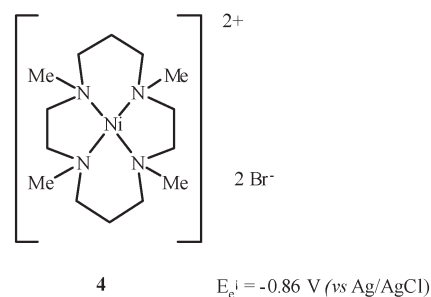
In the present work, we investigated the catalytic reductive behaviour of ethyl 2-bromo-3-(3',4'-dimethoxyphenyl)-3-propargyloxy-propanoate, **1**, ethyl 2-bromo-3-(3',4'-methylenedioxyphenyl)-3-propargyloxy-propanoate, **2**, and ethyl 2-bromo-3-(3',4'-dimethoxyphenyl)-3-allyloxy-propanoate, **3**, by Ni(II) complexes in these protic solvents. The use of EtOH

as an environmentally friendly solvent in reductive intramolecular reactions has not yet been reported.

2. Results and discussion

2.1. Cyclic voltammetric behavior of [Ni(tmc)]Br₂ (**4**) in EtOH solutions, in the absence and in the presence of bromo propargyloxy (**1** and **2**) and allyloxy (**3**) esters

Cyclic voltammetry experiments showed that the [Ni(tmc)]²⁺/[Ni(tmc)]⁺ redox couple (tmc = tetramethyl cyclam) gave a reversible Ni(II)L/Ni(I)L peak in EtOH and in EtOH/H₂O solutions containing 0.10 M TEABr. The formal electrode potential of [Ni(tmc)]Br₂, **4**, in EtOH occurred at -0.86 V vs. Ag/AgCl, 3 M KCl (Fig. 1, curve a).



After addition of bromoester **1** (Fig. 1, curve b) or of substrates **2** or **3** to the solution of [Ni(tmc)]Br₂, the cathodic peak current, due to the formation of [Ni(tmc)]⁺, increases significantly and the anodic wave due to oxidation of [Ni(tmc)]⁺ back to [Ni(tmc)]²⁺ vanishes because of the chemical consumption of [Ni(tmc)]⁺. These results suggest that, on the time scale of the cyclic voltammetry, the reaction between bromoesters **1–3** and electrogenerated [Ni(tmc)]⁺ is fast, as well as the regeneration of the original [Ni(tmc)]²⁺ species, since the increase in the cathodic peak current of the catalyst in the presence of bromoesters (I_{pc}), is a measure of the rate at which [Ni(tmc)]²⁺ is regenerated.

Hence, it can be established that the electron-transfer between the electrogenerated Ni(I) complex and the bromoesters **1–3** occurs, followed by substrate cyclisation, according to eqns (1)–(3). Similar conclusions were presented by Gosden *et al.*¹³ and by our previous work^{3,10} in the

^aLaboratoire Arômes, Synthèses, Interactions, Université de Nice-Sophia Antipolis, Parc Valrose, 06108 Nice Cedex 2, France

^bLaboratoire de Chimie Bioorganique, CNRS, UMR 6001, Université de Nice-Sophia Antipolis, Parc Valrose, 06108 Nice Cedex 2, France

^cCentro de Química, Universidade do Minho, Largo do Paço, 4704-553 Braga, Portugal

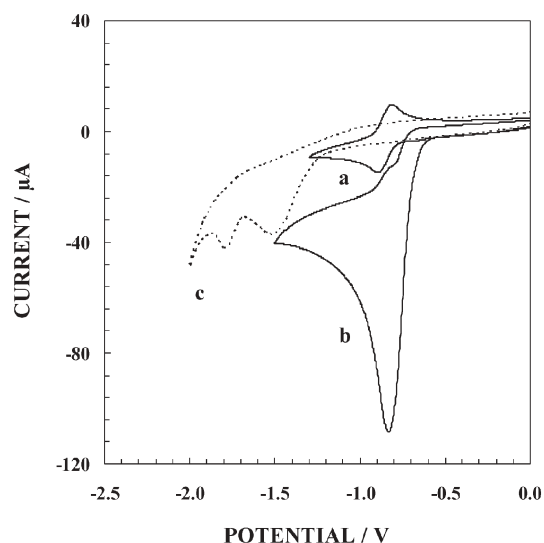


Fig. 1 Cyclic voltammograms recorded with a glassy carbon electrode (area = 0.077 cm²) at 100 mV s⁻¹ in EtOH containing 0.10 M TEABr: (a) 1 mM [Ni(tmc)]Br₂; (b) 1 mM [Ni(tmc)]Br₂ and 10 mM **1**; (c) 2 mM **1**.

investigations on the interaction of Ni(II) species with unsaturated halides in DMF containing tetraalkylammonium salts.

Cyclic voltammetric experiments were also carried out in EtOH–H₂O mixtures (9 : 1) and the results were similar. It is worth pointing out that it was not possible to use an amount of water higher than 10% in the EtOH–H₂O mixture because the bromoesters **1–3** were not soluble.

In the absence of [Ni(tmc)]²⁺, bromoesters **1–3** alone gave a reduction peak at potentials below –1.50 V under the same

experimental conditions. For example, Fig. 1 reports the voltammogram for the direct reduction of a 2 mM solution of **1** (curve **c**) at a glassy carbon electrode in EtOH containing 0.10 M TEABr and a first irreversible wave with a peak potential of –1.56 V can be observed.

2.2. Constant-current reduction of [Ni(tmc)]Br₂ (**4**) in the presence of bromo propargyloxy (**1** and **2**) and allyloxy (**3**) esters

The electroreduction of bromo propargyloxy (**1** and **2**) and allyloxy (**3**) esters by Ni(II) complexes was performed in a single-compartment cell fitted with a consumable sacrificial anode at constant current in EtOH at room temperature, under an inert gas. The cationic tetraamine nickel complex **4**, used in 10–20 mol% showed an efficient catalytic activity for the electrochemical cleavage of the carbon–bromine bond of substrates **1–3**.

The preparative-scale electrolysis of substrates **1–3** generally consumed 2–4 F mol⁻¹ of starting material and the reactions were followed by GC until conversions of 90–100%. Compounds **5–9** (see eqns (1)–(3)) were obtained in the different cyclisation reactions and by-products were formed in very low amounts (<5%) and were not isolated.

The results are summarised in Table 1. For the reactions in ethanol and ethanol–water mixtures, experimental parameters such as the ratio of bromoesters to catalyst and the influence of the nature of the electrodes were examined to evaluate their effect on the product distribution.

The study was initiated by carrying out the electrolysis of **1** in EtOH containing 0.1 M Et₄NBr with a Mg anode and a carbon fiber cathode in the presence of **4** (20 mol%). In this electrochemical system, the Mg anode is oxidised into Mg²⁺ ions and the Ni(II) complex is reduced at the cathode with further electron transfer to the substrate and is recycled. No

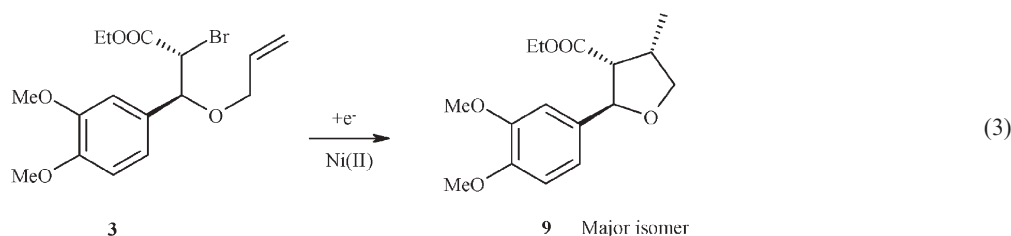
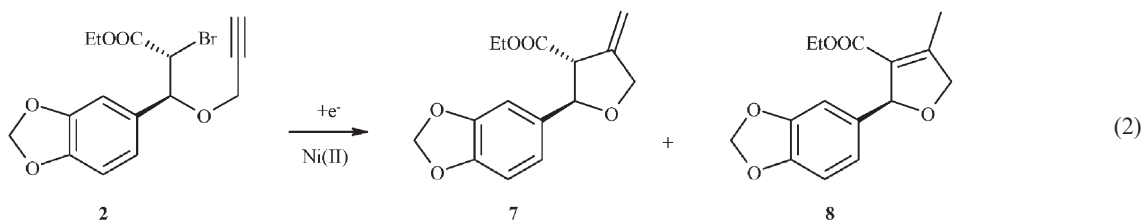
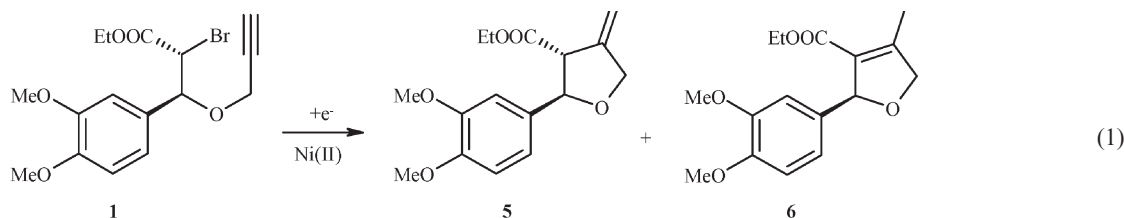


Table 1 Electrochemical intramolecular cyclisation of **1–3** (10 mM) catalysed by **4** (20 mol%) at a carbon fiber cathode containing Et₄NBr (6 mM)^a with $j = 0.15 \text{ A dm}^{-2}$

Entry	Substrate	Solvent	Anode	Products (ratio of isomers)	% yield of cyclised products
1	1	EtOH	Mg	5, 6 (21 : 79)	71
2 ^b	1	EtOH	Mg	5, 6 (40 : 60)	87
3	1	EtOH	Zn	5, 6 (82 : 18)	83
4	1	<i>n</i> -BuOH	Mg	5, 6 (63 : 37)	88
5	1	EtOH–H ₂ O (9 : 1)	Mg	5, 6 (88 : 12)	97
6 ^c	1	EtOH–H ₂ O (9 : 1)	Mg	5, 6 (79 : 21)	84
7	2	EtOH	Mg	7, 8 (61 : 39)	70
8	2	EtOH	Zn	7, 8 (61 : 39)	69
9	2	EtOH–H ₂ O (9 : 1)	Mg	7, 8 (75 : 25)	81
10 ^c	2	EtOH–H ₂ O (9 : 1)	Mg	7, 8 (73 : 27)	86
11	3	EtOH	Mg	9 (93 : 7)	61
12	3	EtOH	Zn	9 (93 : 7)	65
13	3	EtOH–H ₂ O (9 : 1)	Mg	9 (93 : 7)	75

^a Generally, 2–4 F mol⁻¹ of starting material were necessary to achieve a complete conversion in an undivided cell. ^b Carried out with *n*-Bu₄NBF₄ (6 mM) as supporting electrolyte. ^c [RBr]/[Ni(II)] = 10.

reaction occurred in the absence of electricity. The electroreduction of **1** led to 71% of cyclisation. Two cyclised furan derivatives were obtained: 2-(3',4'-dimethoxy)phenyl-3-ethoxycarbonyl-4-methylene-tetrahydrofuran, **5**, and its endocyclic isomer 2-(3',4'-dimethoxy)phenyl-3-ethoxycarbonyl-4-methyl-2,5-dihydrofuran, **6**, in a **5** : **6** ratio of 21 : 79 (Table 1, entry 1). Derivative **5** was obtained as a single *trans* stereoisomer, according to NMR and by comparison with an authentic sample. The efficient electrolysis carried out in EtOH indicated that the Ni-catalysed intramolecular cyclisation reactions were compatible with protic, catalytic and very mild reaction conditions, at room temperature. Moreover, it is to emphasise that the electrochemical set-up is extremely simple: the electrolysis is carried out with no separator, in a one-compartment cell and with a stabilised constant current supply as instrumentation.

The main reaction product, the cyclic ether **6**, was issued from a double bond isomerisation from **5**, **5** being the expected primary cyclisation compound. During the electrolysis in a protic solvent such as EtOH, some solvent reduction should generate ethoxide,¹⁴ able to effect the base-catalysed olefin isomerisation. It was independently tested that the formation of **6** could be induced by an efficient electrogenerated base.¹⁰

The results of the cyclisation of **1** in EtOH are in agreement with related results reported by Medeiros *et al.*^{9,10} in DMF, where the intramolecular cyclisation of analogous bromo propargyloxy esters led to the corresponding same cyclic ethers.

When the reaction of **1** was performed using *n*-Bu₄NBF₄ instead of Et₄NBr as the supporting electrolyte, it afforded cyclised ethers **5** and **6** in 87% overall yield, and a **5** : **6** ratio of 40 : 60 (entry 2). This result seems to indicate that the nature of the supporting electrolyte has an influence on the isomerisation process from **5** to **6**, possibly due to the influence of the nature of the organic salt on the acidity of the medium.

The influence of the nature of the anode on the electroreduction of **1** was examined with zinc instead of magnesium. The cyclisation occurred in 83% yield with a **5** : **6** ratio of 82 : 18 (entry 3) indicating that the nature of the anodic material

played an important role on the reaction selectivity. With Zn as the anode (entry 3), the **5** : **6** ratio was reversed as compared to that of entry 1. This may be indicative of a less efficient double bond isomerisation from the methylene derivative **5** to conjugated **6**, when changing from Mg²⁺ to Zn²⁺ ions in solution. Mg²⁺ being a stronger Lewis acid than Zn²⁺, a better complexation of Mg²⁺ to the ester group of **5** is to be expected, complexation that should facilitate the olefin isomerisation.

Other protic solvents were tested for the electrolysis of **1**. Thus, the use of *n*-BuOH instead of EtOH had also an important effect on the product distribution, leading to **5** as the major product, in 55% yield, together with 33% of **6**, in an overall cyclisation yield of 88% (entry 4).

The influence of the added water on the reaction selectivity was also examined in EtOH–H₂O (9 : 1) as the solvent. The electroreduction of **1** was very efficient affording 97% yield of cyclisation, with a **5** : **6** ratio 88 : 12 (entry 5). It is noteworthy that the presence of water afforded an almost quantitative yield of cyclisation, without any by-product, and it did not interfere with the overall cyclisation process. However, the presence of water influenced the selectivity of the reaction, inhibiting the base-catalysed isomerisation of **5** to **6**. It is also worth noting that in the friendly EtOH–water medium, the electrochemical cyclisation of **1** can be run quantitatively and catalytically, with a yield of **5** of 87%.

The catalyst to substrate ratio was changed from 20 to 10 mol% in the electroreduction using **1** with a Mg/C couple of electrodes in EtOH–H₂O (9 : 1). The reaction was more efficient with a higher catalyst ratio, but no significant change was observed (compare entries 5 and 6). This result indicates that the ratio [RBr]/[Ni(II)] does not interfere on the reaction mechanism.

The electroreduction in protic media was extended to substrates **2** and **3**. The reaction of **2** (eqn (2)) catalysed by **4** using a Mg/C couple of electrodes in EtOH afforded 70% overall cyclisation with a mixture of 2-(3',4'-methylenedioxophenyl)-3-ethoxycarbonyl-4-methylenetetrahydrofuran, **7**, and 2-(3',4'-methylenedioxophenyl)-3-ethoxycarbonyl-4-methyl-2,5-dihydrofuran, **8**, in a **7** : **8** ratio of 61 : 39 (entry 7).

The change of magnesium by zinc anode in the electrolysis of **2** led to similar results. The influence of the added water was studied using Mg/C electrodes in EtOH–H₂O (9 : 1). The electrolysis of **2** was here also more efficient leading to 81% cyclisation with the formation of **7** in 61% yield along with 20% yield of **8** (entry 9). In the presence of 10 mol% of catalyst the cyclisation occurred in 86% yield with a **7** : **8** ratio of 73 : 27 (entry 10). This result is in agreement with that presented above (entry 6) and supports that the ratio [RBr]/[Ni(II)] does not interfere on the reaction mechanism.

The electroreduction of olefin **3** was performed in EtOH under the standard conditions. The electrolysis led to two stereoisomers of 2-(3',4'-dimethoxyphenyl)-3-ethoxycarbonyl-4-methyltetrahydrofuran, **9**, in 61% yield and a 93 : 7 ratio (entry 11). According to NMR data, both stereoisomers present a *trans* ester to aryl configuration and differ by the *cis-trans* position of the methyl group. The main stereoisomer of **9** presents the methyl group of the tetrahydrofuran ring in a *cis* position with respect to the ester, according to 2D NMR experiments.¹¹

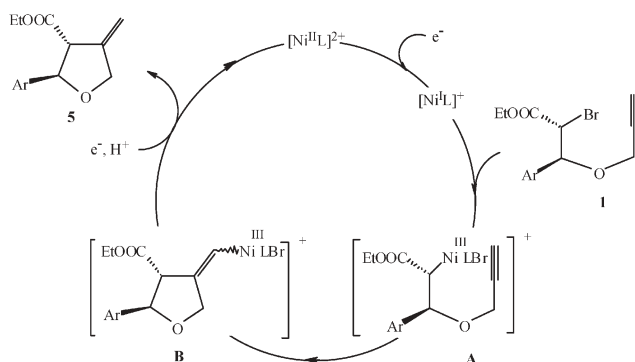


Fig. 2 Proposed catalytic cycle of the cyclisation of **1** catalysed by **4**. $4 = [\text{Ni}^{\text{II}}\text{L}]^{2+} = [\text{Ni}(\text{tmc})]\text{Br}_2$.

The use of a zinc anode led to the formation of **9** in 65% yield and the same stereoisomeric ratio (entry 12). When the electrolysis of **3** was carried out using EtOH–H₂O (9 : 1) as the solvent, the yield was increased to 75%, with identical *cis-trans* ratio of isomers (entry 13).

For the Ni(II)-catalysed cyclisation of compounds **1–3** we propose the catalytic cycle presented in Fig. 2. A first Ni(II) reduction to Ni(I) occurs at $-0.86\text{ V vs. Ag/AgCl}$ with its further oxidative addition into the carbon–halogen bond of the substrate to form an intermediate of type **A**. The organic moiety in intermediate **A** has a radical-type character, as shown by its ability to add to the double or triple bond and form a cyclised intermediate of type **B**. The further reduction of **B** with proton abstraction from the electrolytic medium affords the reaction product (ex. **5** from **1**) and enables the recycling of the Ni(II) complex.

Intermediate **A** can be considered as an organometallic intermediate (as in Fig. 2) or as a Ni(II)L with the free organic radical centered on the carbon α to the ester group. However, in both cases the reductive radical cyclisation leads to the same cyclic compounds.

It is interesting to briefly compare the reduction of **1–3** catalysed by **4** in protic media (EtOH, *n*-BuOH, EtOH–H₂O) with previously reported electrochemical studies in DMF. Unexpectedly, the yields and selectivities obtained in protic solvents are generally better than those obtained in DMF. For example, the cyclisation of **3** in DMF afforded **9** in 38% yield, whereas in EtOH–H₂O (9 : 1) the yield raises up to 75%.

The beneficial effect of using EtOH or EtOH–H₂O as the solvents as compared to DMF could be due to the fact that the key cyclisation step **A** \rightarrow **B** involves the presence of radical-type species. DMF being a good H-atom donor, it can react with radical species of type **A** (Fig. 2) to form the corresponding reduced species before cyclisation occurs. In contrast, EtOH and/or water are not H-atom donors, but good H-proton donors. As such, they can accelerate the last step of reductive protonation of **B** \rightarrow **5**, without interfering in the previous radical-type cyclisation step.

3. Conclusion

In conclusion, we report here the use of environmentally friendly solvents such as EtOH, *n*-BuOH or EtOH/H₂O as an alternative for the catalytic electrochemical radical-type

cyclisation of bromoesters **1–3** to the corresponding substituted tetrahydrofurans in high yields. The compatibility of these protic solvents with the catalytic system and the electroreductive conditions is remarkable.

This investigation provides an example of the feasibility of preparative-scale organic electrochemistry in “green” solvents such as ethanol or ethanol–water mixtures in catalytic and environmentally friendly procedures. Moreover, the simplicity and ease of application of the electrochemical method—working at constant current electrolysis, in a one-compartment cell, with no sophisticated instrumentation and no expensive separator needed—should also be emphasised and makes it an interesting and valuable synthetic tool.

4. Experimental

4.1. Reagents

Each of the following chemicals was used as received: nickel(II) bromide (Aldrich, 98%), 1,4,8,11-tetramethyl-1,4,8,11-tetraazacyclotetradecane (tetramethylcyclam, tmc, Fluka, 97%). Ethanol (EtOH), from Riedel-de-Häen, Analytical Reagent, was used as received. We purchased tetraethylammonium bromide (TEABr) with a purity of 98% from Fluka, and tetra-*n*-butylammonium tetrafluoroborate (TBABF₄) with a purity of 99% from Aldrich; these electrolytes were stored in a vacuum oven at 80 °C to remove traces of water. Deaeration procedures were carried out with zero-grade argon (Air Products). Published procedures were employed for the preparation of [Ni(tmc)]Br₂¹⁵ and of ethyl 2-bromo-3-(3',4'-dimethoxyphenyl)-3-propargyloxypropanoate (**1**), ethyl 2-bromo-3-(3',4'-methylene-dioxophenyl)-3-(propargyloxy)propanoate (**2**) and ethyl 2-bromo-3-(3',4'-dimethoxyphenyl)-3-(allyloxy)propanoate (**3**).¹⁶

Synthesis of 2-(3',4'-dimethoxyphenyl)-3-ethoxycarbonyl-4-methylene-tetrahydrofuran (**5**), 2-(3',4'-dimethoxyphenyl)-3-ethoxycarbonyl-4-methyl-2,5-dihydrofuran (**6**), 2-(3',4'-methylenedioxophenyl)-3-ethoxycarbonyl-4-methylenetetrahydrofuran (**7**), 2-(3',4'-methylenedioxophenyl)-3-ethoxycarbonyl-4-methyl-2,5-dihydrofuran (**8**) and 2-(3',4'-dimethoxyphenyl)-3-ethoxycarbonyl-4-methyltetrahydrofuran (**9**) was based on the method published by McCague *et al.*¹⁷

4.2. Electrodes

Electrodes for cyclic voltammetry were fabricated from 3 mm-diameter glassy carbon rods (Tokai Electrode Manufacturing Company, Tokyo, Japan, Grade GC-20) press-fitted into Teflon shrouds to provide planar, circular working electrodes with areas of 0.077 cm². Before use, the electrodes were cleaned with an aqueous suspension of 0.05 μm alumina (Buehler) on a Master-Tex (Buehler) polishing pad.

All potentials are quoted with respect to a Ag/AgCl/ 3 M KCl in water reference electrode.

4.3. Cells and instrumentation

Cells for cyclic voltammetry have been described in earlier publications.³ Cyclic voltammograms were obtained with the aid of an AUTOLAB model PGSTAT12 potentiostat-galvanostat. The data from the above experiments were acquired

and stored by locally written software, which controlled a data acquisition board installed in a personal computer.

The constant current electrolyses were carried out in a single-compartment cell (capacity 50 mL), such as described in ref. 18, with a Zn or Mg rod as the sacrificial anode (diameter 1 cm) and a carbon felt cathode (apparent surface, 20 cm²) was formed into a cylinder around the counter electrode. EtOH (50 mL), Et₄NBr (6 × 10⁻³ M), Ni^{II}L (2.0 × 10⁻³ M) and bromoester (1.0 × 10⁻² M) were introduced in the cell under an argon flow. The solution was stirred and electrolysed at room temperature, at a constant current of 30 mA (current density of 1.5 mA cm⁻² and 2–5 V between the rod anode and the carbon felt cathode) until disappearance of the bromoester (checked by GC analysis of aliquots). Generally, 2–4 F mol⁻¹ of starting material were necessary to achieve a complete conversion. The excess of electricity was mainly observed in the presence of a Zn anode, and can account for some partial reduction of the Zn²⁺ ions formed. It is not excluded that the freshly deposited cathodic Zn (as well as the metallic rod anodes) could have some parallel reactivity in terms of a direct chemical reduction of the C–Br bond of 1–3, as in the Reformatsky reaction. Controlled-current electrolyses were carried out with the aid of a stabilized constant current supply (Sodilec, EDL 36.07).

¹H NMR data were recorded on a Varian Unity Plus 300 Spectrometer in CDCl₃; δ ppm were measured *versus* residual peak of the solvent. Identities of the electrolysis products were confirmed by means of a Hewlett-Packard 5890 Series II gas chromatograph coupled to a Hewlett-Packard 5971 mass-selective detector.

4.4. Identification and quantification of products

The EtOH solvent was evaporated under vacuum, the reaction mixture was hydrolysed with 0.1 M HCl saturated with NaCl, up to pH 1–2, extracted with CH₂Cl₂ and washed with H₂O. The dried (MgSO₄) organic layer was evaporated and the residue analysed by GC, GC-MS and ¹H-NMR. The crude residue was submitted to flash chromatography over silica gel (230–400 mesh) using ethyl acetate–light petroleum mixtures as the eluents. Cyclised compounds 5–9 were identified by NMR and mass spectrometry and compared to authentic samples, prepared independently according to ref. 17.

The compounds were identified by means of ¹H NMR spectrometry (CDCl₃): (a) for 5, δ 1.28 (3H, t, *J* = 7.0 Hz, OCH₂CH₃), 3.49 (1H, apparent ddd, *J* = 8.7, 2.4 and 2.4 Hz, 3-H), 3.88 (3H, s, OCH₃), 3.90 (3H, s, OCH₃), 4.22 (2H, qABq, *J* = 7.0 and 18.0 Hz, OCH₂CH₃), 4.50 (1H, apparent dq, *J* = 13.2 and 2.4 Hz, 5-H), 4.65 (1H, broad apparent d, *J* = 13.2 Hz, 5-H), 5.11 (1H, apparent q, *J* = 2.4 Hz, C=CHH), 5.19 (1H, d, *J* = 8.7 Hz, 2-H), 5.20 (1H, apparent q, *J* = 2.4 Hz, C=CHH), 6.84 (1H, d, *J* = 8.7 Hz, 5'-H), 6.90 (1H, d, *J* = 1.8 Hz, 2'-H), 6.91 (1H, dd, *J* = 8.7 and 1.8 Hz, 6'-H); (b) for 6, δ 1.15 (3H, t, *J* = 7.0 Hz, OCH₂CH₃), 2.19 (3H, d, *J* = 1.2 Hz, 4-CH₃), 3.87 (3H, s, OCH₃), 3.88 (3H, s, OCH₃), 4.08 (2H, qABq, *J* = 7.0 and 11.0 Hz, OCH₂CH₃), 4.72 (1H, apparent ddd, *J* = 1.2, 3.6 and 15.0 Hz, 5-H), 4.89 (1H, apparent ddd, *J* = 0.9, 5.7, 15.0 Hz, 5-H), 5.88–5.92 (1H, m, 2-H), 6.83 (1H, d, *J* = 8.1 Hz, 5'-H), 6.84 (1H, broad s, 2'-H), 6.88 (1H, dd, *J* = 8.1, 1.8 Hz,

6'-H); (c) for 7, δ 1.28 (3H, t, *J* = 7.2 Hz, OCH₂CH₃), 3.42–3.47 (1H, m, 3-H), 4.21 (2H, qABq, *J* = 7.2 and 11.0 Hz, OCH₂CH₃), 4.49 (1H, apparent dq, *J* = 13.0, 2.4 Hz, 5-H), 4.63 (1H, br apparent d, *J* = 13.0 Hz, 5-H), 5.10 (1H, apparent q, *J* = 2.4 Hz, =CH), 5.15 (1H, d, *J* = 8.7 Hz, 2-H), 5.18 (1H, apparent q, *J* = 2.4 Hz, =CH), 5.96 (2H, s, OCH₂O), 6.77 (1H, d, *J* = 8.0 Hz, 5'-H), 6.88 (1H, dd, *J* = 8.0, 1.8 Hz, 6'-H), 6.90 (1H, d, *J* = 1.8 Hz, 2'-H); (d) for 8, δ 1.16 (3H, t, *J* = 7.2 Hz, OCH₂CH₃), 2.18 (3H, apparent d, *J* = 1.2 Hz, 4-CH₃), 4.09 (2H, qABq, *J* = 7.2 and 10.8 Hz, OCH₂CH₃), 4.71 (1H, apparent ddd, *J* = 15.0, 3.5, 1.0 Hz, 5-H), 4.87 (1H, apparent ddd, *J* = 15.0, 5.0, 1.0 Hz, 5-H), 5.83–5.87 (1H, m, 2-H), 5.94 (2H, s, OCH₂O), 6.76 (1H, d, *J* = 8.0 Hz, 5'-H), 6.77 (1H, d, *J* = 1.8 Hz, 2'-H), 6.82 (1H, dd, *J* = 8.0, 1.8 Hz, 6'-H); and (e) for 9, δ 1.07 (2.55H, d, *J* = 6.9 Hz, 4-CH₃), 1.18 (0.45H, d, *J* = 6.6 Hz, 4-CH₃), 1.25 (0.45H, t, *J* = 7.0 Hz, OCH₂CH₃), 1.28 (2.55H, t, *J* = 7.2 Hz, OCH₂CH₃), 2.55 (0.15H, apparent t, *J* = 9.0, 8.7 Hz, 3-H), 2.70–2.85 (1H, m, 4-H), 3.00 (0.85H, apparent dd, *J* = 9.0, 7.8 Hz, 3-H), 3.66 (1H, apparent dd, *J* = 8.7, 6.6 Hz, 5-H_a), 3.87 (3H, s, OCH₃), 3.89 (3 H, s, OCH₃), 4.12–4.24 (2H, m, OCH₂CH₃), 4.28 (1H, dd, *J* = 8.4 and 6.6 Hz, 5-H_b), 5.05 (0.15H, d, *J* = 9.0 Hz, 2-H), 5.19 (0.85H, d, *J* = 7.8 Hz, 2-H), 6.83 (1H, d, *J* = 9.0 Hz, 5'-H), 6.88–6.92 (2 H, m, 2'-H and 6'-H). These compounds were utilized as standards for the determination of gas chromatographic response factors.

Identities of the electrolysis products were confirmed by gas chromatograph/mass-selective detector: (a) for 5, *m/z* (70 eV) 292, M⁺ (23); 277, [M–CH₃]⁺ (0.6); 218, [M–CO₂C₂H₅–H]⁺ (6); 165, [(CH₃O)₂C₆H₃CO]⁺ (19); 126, [H₅C₂O₂CC₄H₅]⁺ (51); 98, [C₅H₆O₂]⁺ (100); (b) for 6, *m/z* (70 eV) 292, M⁺ (100); 277, [M–CH₃]⁺ (16); 263, [M–C₂H₅]⁺ (25); 215, [M–C₂H₅O–CH₃OH]⁺ (49); 165, [(CH₃O)₂C₆H₃CO]⁺ (66); 77, [C₆H₅]⁺ (20); 29, [COH]⁺ (44); (c) for 7, *m/z* (70 eV) 276, M⁺ (35); 247, [M–C₂H₅]⁺ (3); 202, [M–CO₂C₂H₅–H]⁺ (18); 149, [CH₂O₂C₆H₃CO]⁺ (45); 126, [H₅C₂O₂CC₄H₅]⁺ (59); 98, [C₅H₆O₂]⁺ (100); (d) for 8, *m/z* (70 eV) 276, M⁺ (100); 261, [M–CH₃]⁺ (17); 247, [M–C₂H₅]⁺ (34); 202, [M–CO₂C₂H₅–H]⁺ (82); 149, [CH₂O₂C₆H₃CO]⁺ (64); 77, [C₆H₅]⁺ (7); 29, [COH]⁺ (22); and (e) for 9, *m/z* (70 eV) 294, M⁺ (84); 279, [M–CH₃]⁺ (26); 265, [M–C₂H₅]⁺ (69); 220, [M–CO₂C₂H₅–H]⁺ (10); 205, [M–CO₂C₂H₅–CH₃–H]⁺ (35); 165, [(CH₃O)₂C₆H₃CO]⁺ (100); 29, [COH]⁺ (16).

Acknowledgements

Most of this research was conducted while M.J.M. was a Visiting Scholar at the University of Nice. In addition, we are grateful to the CRUP and Fundação para a Ciência e Tecnologia/FEDER (POCTI/QUI/37808/01) for financial support of this work.

References

- (a) B. Giese, B. Kopping, T. Gobel, J. Dickhaut, G. Thoma and F. Trach, *Org. React.*, 1996, **48**, 301 (and references therein); (b) B. Giese, *Radicals in Organic Synthesis, Formation of Carbon–Carbon Bonds*, Pergamon, Oxford, 1986; (c) J. Fossey, D. Lefort and J. Sorba, *Free Radicals in Organic Chemistry*, Wiley, New York, 1995.

- 2 S. Ozaki, E. Matsui, J. Waku and H. Ohmori, *Tetrahedron Lett.*, 1997, **38**, 2705 (and references cited therein).
- 3 A. P. Esteves, A. M. Freitas, M. J. Medeiros and D. Pletcher, *J. Electroanal. Chem.*, 2001, **499**, 95.
- 4 E. Duñach, A. P. Esteves, A. M. Freitas, M. J. Medeiros and S. Olivero, *Tetrahedron Lett.*, 1999, **40**, 8693.
- 5 M. Ihara, A. Katsumata, F. Setsu, Y. Tokunaga and K. Fukumoto, *J. Org. Chem.*, 1996, **61**, 677.
- 6 S. Olivero, J.-P. Rolland and E. Duñach, *Organometallics*, 1998, **17**, 3747 (and references cited therein).
- 7 S. C. Bobzin and J. D. Faulkner, *J. Nat. Prod.*, 1991, **54**, 225.
- 8 A. Merritt and S. V. Ley, *Nat. Prod. Rep.*, 1992, 243 (and references therein).
- 9 E. Duñach, A. P. Esteves, A. M. Freitas, M. A. Lemos, M. J. Medeiros and S. Olivero, *Pure Appl. Chem.*, 2001, **73**, 1941.
- 10 A. P. Esteves, D. M. Goken, J. L. Klein, M. A. Lemos, M. J. Medeiros and D. G. Peters, *J. Org. Chem.*, 2003, **68**, 1024.
- 11 E. Duñach, A. P. Esteves, M. J. Medeiros and S. Olivero, *Tetrahedron Lett.*, 2004, **45**, 7935.
- 12 (a) G. Long and M. E. Meek, *J. Environ. Sci. Heal.*, 2001, **C19**, 161; (b) J. H. Sohn, M. J. Han, M. Y. Lee, S.-K. Kang and J. S. Yang, *J. Pharmaceut. Biomed.*, 2005, **37**, 1654.
- 13 (a) J. Y. Becker, J. B. Kerr, D. Pletcher and R. Rosas, *J. Electroanal. Chem.*, 1981, **117**, 87; (b) C. Gosden, J. B. Kerr, D. Pletcher and R. Rosas, *J. Electroanal. Chem.*, 1981, **117**, 101; (c) C. Gosden and D. Pletcher, *J. Organometal. Chem.*, 1980, **186**, 401; (d) C. Gosden, K. P. Healy and D. Pletcher, *J. Chem. Soc., Dalton Trans.*, 1978, 972.
- 14 J. H. P. Utley and M. F. Nielsen, in *Organic Electrochemistry*, ed. H. Lund and O. Hammerich, Dekker, New York, 4th edn, 2001, pp. 1227–1257.
- 15 B. Bosnich, M. L. Tobe and G. A. Webb, *Inorg. Chem.*, 1965, **4**, 1109.
- 16 S. C. Roy and S. Adhikari, *Tetrahedron*, 1993, **49**, 8415.
- 17 R. McCague, R. G. Pritchard, R. J. Stoodley and D. S. Williamson, *Chem. Commun.*, 1998, 2691.
- 18 J. Chaussard, J. C. Folest, J. Y. Nédélec, J. Périchon, S. Sibille and M. Troupel, *Synthesis*, 1990, **5**, 369.

chemistryworld

A "must-read" guide to current chemical science!



Chemistry World provides an international perspective on the chemical and related sciences by publishing scientific articles of general interest. It keeps readers up-to-date on economic, political and social factors and their effect on the scientific community.

RSC Publishing

www.chemistryworld.org

Fabrication of porous polymer particles with high anion exchange capacity by amination reaction in aqueous medium

Jin Liu,^{ac} Jianfeng Yao,^b Huanting Wang^{*b} and Kwong-Yu Chan^{*a}

Received 7th October 2005, Accepted 13th January 2006

First published as an Advance Article on the web 30th January 2006

DOI: 10.1039/b514262h

Micrometre-sized porous polymer particles were fabricated by amination of chlorinated aliphatic polymer beads (chlorinated polypropylene (CPP), chlorinated polyethylene (CPE), and polyvinyl chloride co-vinyl acetate (PVCVAc)) in aqueous amine (polyethylenimine (PEI) and triethylamine (TEA)) solution. The polymer particles obtained were characterized by SEM, elemental analysis, titration, N₂ adsorption, FT-IR, solid-state NMR and thermogravimetry (TG). CPP-PEI, CPE-PEI, and PVCVAc-PEI had honeycomb-like pores whereas rugged textures with pores were developed in CPP-TEA, and skeleton-like pores were formed in PVCVAc-TEA. Aminated samples exhibit a BET surface area of 4–12 m² g⁻¹ and an anion exchange capacity of 1.10 to 4.27 mmol g⁻¹. The membranes fabricated with CPP-PEI and PVCVAc-PEI exhibited ionic conductivities as high as 4.5 × 10⁻² and 0.48 × 10⁻² S cm⁻¹, respectively. As a result, the hydrothermal amination could be an effective way to aminate chlorinated polymers without using organic solvents.

Introduction

Macroporous organic polymers have been of great interest in the past few years because of their uses in tissue engineering,¹ catalysis,² chemical sensing,³ biomineralization,⁴ and as templates for preparing other porous materials,⁵ etc. A number of approaches involving supercritical carbon dioxide as the porogenic solvent,⁶ colloidal particles, and well-defined star microgels as templates,^{7,8} controlled solvent evaporation,⁹ and lithography¹⁰ have been developed to create macroporous polymers. The functionalization of such porous structures could provide a great opportunity to broaden their applications.¹¹ Amination is considered as one of the most important ways to functionalize polymers, in which polymers are usually dissolved in organic solvents to enhance the effectiveness of the amination reaction. Generally, aminated polymers become more hydrophilic, biocompatible, adhesive and selective; and they are widely used as ion-exchangers,^{12,13} biomaterials,¹ coatings,¹⁴ and membranes in electrochemical devices.^{15–17}

Here we report a novel method for fabricating functional macroporous organic polymer particles by aminating chlorinated aliphatic polymers in aqueous amine solution. To aminate bulk polymers effectively, the amination reaction is carried out at elevated temperatures in a closed system, which is known as hydrothermal conditions in the field of inorganic synthesis.¹⁸ Chlorinated aliphatic polymers that are commercially mass-produced and of low cost possess a large quantity of chloride sites for amine substitution that can lead to high

anion exchange capacity. Aqueous amine solutions are used to avoid expensive and environmentally unfriendly organic solvents in the conventional amination reaction. The process used in this paper is referred to as *hydrothermal amination*. The detailed fabrication and characterization of aminated macroporous polymer particles will be described below.

Experimental

Hydrothermal amination

Three chlorinated aliphatic polymers, *i.e.*, chlorinated polypropylene (CPP, M_n ca. 150 000, beads with 6–8 mm in size, Shanghai Chemicals, China), chlorinated polyethylene (CPE, M_n ca. 25 000, beads with 2–3 mm in size, kindly provided by the Chemical Institute of Wuhu Sanjiang, China) and polyvinyl chloride co-vinyl acetate (PVCVAc, M_n ca. 27 000, 1–2 mm in size, Shanghai Chemicals, China) were hydrothermally aminated by polyethylenimine (PEI, M_n 423, Sigma-Aldrich) and triethylamine (TEA, 99.9%, Sigma-Aldrich). Typically, 4 g of polymer beads was suspended in an aqueous amine solution (4–6 g of amine in 20 g of deionized water). The amination reaction was carried out in a 45 mL Teflon-lined autoclave (Parr bomb) at 140 °C for 48 h, except that the CPP was aminated with PEI at 120, 140 and 180 °C to study the temperature effect. The as-aminated polymers were collected by filtering and thoroughly washing with deionized water, followed by drying at 60 °C for 2 days. Aminated polymers were denoted based on the names of the polymers and amines, *e.g.*, CPP aminated with PEI was referred to as CPP-PEI.

Characterization

SEM images were taken with a scanning electron microscope (SEM, Philips Cambridge S360). A low voltage (5 kV) was

^aDepartment of Chemistry, The University of Hong Kong, Hong Kong SAR, China. E-mail: hrsceky@hku.hk

^bDepartment of Chemical Engineering, Monash University, Clayton, VIC 3800, Australia. E-mail: huanting.wang@eng.monash.edu.au; Fax: +61 3 9905 5686; Tel: +61 3 9905 3449

^cDepartment of Materials Science and Engineering, Anhui Institute of Architecture and Industry, Anhui 230022, China

operated to lower the electron beam energy and avoid damaging the samples.

Sample preparation for elemental analysis: the aminated samples were ion exchanged with OH^- using 1 M NaOH solution, followed by washing with double deionized water and drying in a vacuum oven at 60 °C for 2 days. All analyses were carried out by the Lab for Elemental Analysis of the Institute of Chemistry, Chinese Academy of Sciences (Beijing, China).

Nitrogen content (ion exchange capacity, IEC) was also determined by a titration method.^{13,17} 0.5 g of the aminated polymer powders were treated in 1 M HCl at room temperature for 4 hours to ensure complete protonation and full conversion into the chloride salt. After filtering and washing, the samples were dispersed in 0.5 M NaOH solution, followed by titrating 10 mL of the supernate with 0.1 M HNO_3 and then with 0.05 M AgNO_3 .

FT-IR spectra were recorded by a BIO-RAD FTS165 FTIR spectrometer (32 scans at $2\text{ cm}^{-1}\text{ s}^{-1}$). The samples were prepared by a KBr wafer technique. Nitrogen adsorption measurements were carried out with a Micromeritics ASAP 2020MC. The samples were degassed at 60 °C for at least 24 h. ^{13}C solid-state NMR spectroscopy was carried out on a Bruker DRX-400 spectrometer.

Membrane fabrication and ionic conductivity measurement: CPP-PEI and PVCVAc-PEI were fabricated into membranes with a thickness of 60 μm and 10% PVA as binder. CPP-PEI (or PVCVAc-PEI) powders were mixed with 8% poly(vinyl alcohol) solution and a couple of drops of glutaraldehyde solution (GA, 25 wt% in water, Sigma-Aldrich) in a mortar with a pestle. The CPP-PEI-PVA (or PVCVAc-PEI-PVA) mixture obtained was cast on a silicon wafer at room temperature, followed by drying at 50 °C. The CPP-PEI (or PVCVAc-PEI) films were peeled off from the silicon wafer surface for the impedance measurement. 0.1 M NaCl was used as the electrolyte, and the impedance spectra were recorded with an AUTOLAB FRA2 impedance analyzer in the frequency range from 10 kHz to 100 Hz at ac signal amplitude of 10 mV and at room temperature. The ionic conductivity was calculated by the expression^{19,20}

$$\sigma = \frac{l}{(R_{\text{cell}} - R'_{\text{cell}})S}$$

where σ is the ionic conductivity of the membrane (S cm^{-1}), S is the area of the membrane (cm^2), l the thickness of the membrane (cm), and R_{cell} and R'_{cell} the cell alternating current impedance (Ω) at 1 kHz with and without membrane, respectively.

Results and discussion

SEM images shown in Fig. 1 reveal that CPP-PEI, CPE-PEI and PVCVAc-PEI are composed of fine particles with a size range of a few microns to a couple of tens of microns (Fig. 1 a, c, e), and these particles exhibit similar honeycomb structures whose pores are submicron-sized (Fig. 1 b, d, f). When the chlorinated polymers were aminated with a monoamine (triethylamine, TEA), different pore morphologies were observed. Rugged textures with pores developed in CPP-TEA, and skeleton-like pores formed in PVCVAc-TEA (Fig. 2). As a comparison, CPP was also hydrothermally

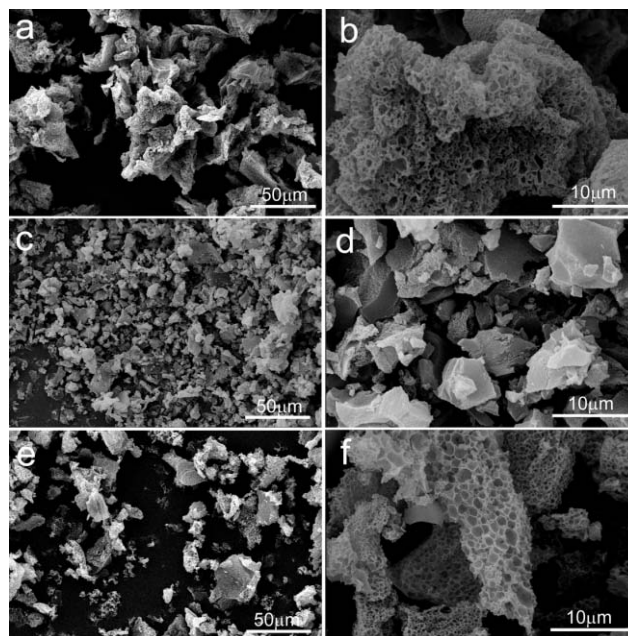


Fig. 1 SEM images of CPP, CPE and PVCVAc aminated with PEI aqueous solution at 140 °C for 48 h. (a, b) CPP-PEI, (c, d) CPE-PEI, and (e, f) PVCVAc-PEI. (a, c, e) at low magnification, (b, d, f) at high magnification.

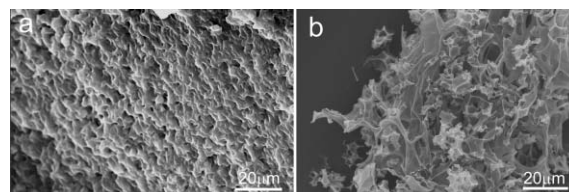


Fig. 2 SEM images of CPP and PVCVAc aminated with triethylamine solution at 140 °C for 48 h. (a) CPP-TEA, (b) PVCVAc-TEA.

treated in deionized water and 1 M KOH aqueous solution under the same hydrothermal conditions, only a few shallow surface pores were formed (Fig. 3). This clearly indicates that the amines play a vital role in the pore formation.

N_2 adsorption experiments were conducted on hydrothermally aminated samples and hydrothermally treated samples in the absence of amine, and the results showed that the samples treated in H_2O and KOH solution have a very low BET surface area ($0.1\text{--}0.5\text{ m}^2\text{ g}^{-1}$) similar to that of the starting polymers, and the samples aminated with PEI and TEA possess BET surface areas of $4\text{--}12\text{ m}^2\text{ g}^{-1}$. The

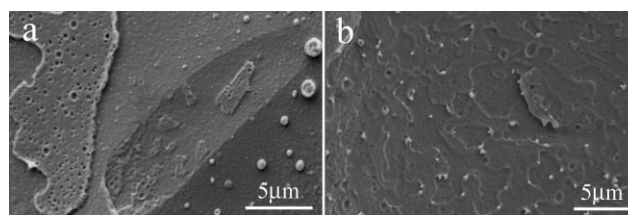


Fig. 3 SEM images of CPP treated in (a) water and (b) 1 M KOH solution at 140 °C for 48 h.

Table 1 Elemental analysis and titration results of chlorinated aliphatic polymers and corresponding aminated polymers by hydrothermal amination at 140 °C (unless indicated otherwise) for 48 h

Sample	C%	H%	O%	Cl%	mmol g ⁻¹	N%	mmol g ⁻¹	N _{titration} mmol/g
CPP	56.43	8.15	1.08	34.34	9.67	<0.30	—	—
CPP-PEI	68.23	10.17	6.12	9.42	2.65	6.05	4.32	4.27
CPP-PEI (120 °C)	54.44	8.46	0.91	31.50	9.01	2.69	1.92	1.80
CPP-PEI (180 °C)	78.30	10.84	5.14	2.49	0.70	3.23	2.31	2.06
CPP-TEA	67.35	10.05	3.66	17.44	4.91	1.50	1.11	1.10
CPE	27.30	2.575	0.51	69.62	19.60	<0.30	—	—
CPE-PEI	56.13	5.34	16.1	15.28	4.30	7.18	5.13	3.88
PVCVAc	40.86	5.17	5.10	48.87	13.77	<0.30	—	—
PVCVAc-PEI	67.22	7.80	16.80	3.84	1.08	4.34	3.10	2.62

significant increase in the BET surface area obviously arises from the porous structures of aminated samples, which is consistent with the SEM observations.

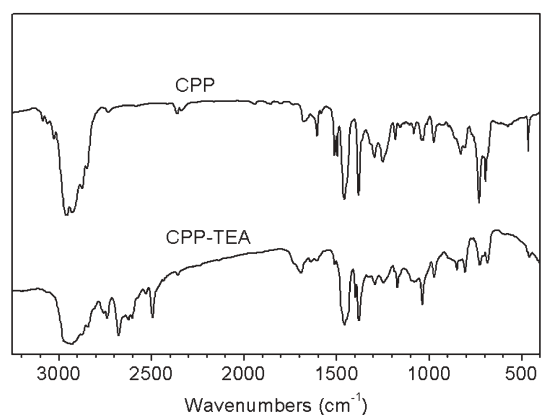
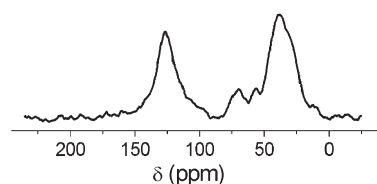
The elemental analysis (EA) and titration results are summarized in Table 1. Elemental analysis shows that the chlorine content is 9.67, 19.60 and 13.77 mmol g⁻¹ for CPP, CPE and PVCVAc, respectively. As can be seen, significant amounts of nitrogen were introduced into all CPP, CPE and PVCVAc through hydrothermal amination. CPP-PEI, CPP-TEA and PVCVAc-PEI have nitrogen contents ranging from 1.10 to 4.27 mmol g⁻¹, which are comparable to those for anion exchange membranes.^{16,17} In addition to the amination reaction (substitution reaction) that gives rise to the anion exchange capacity of porous polymer particles, the elimination reaction between Cl and its adjacent H^{13,15} causes additional Cl loss, which can be seen by comparing the change of Cl content before and after hydrothermal amination and N content of aminated samples. Owing to such elimination reactions, the polymer chains were cross-linked during the hydrothermal amination, as evidenced by the fact that porous polymer particles are insoluble in various solvents. Moreover, the reaction temperature has a significant influence on the degree of substitution and elimination. For instance, in the CPP-PEI system, the elimination reaction is very favorable at a higher temperature (180 °C) suppressing the amination reaction, whereas both amination and elimination reactions become slow at a lower temperature (120 °C). Consequently, the ion exchange capacity of the CPP-PEI prepared at 120 and 180 °C is much lower as compared to the CPP-PEI prepared at 140 °C. By comparing the nitrogen contents obtained with elemental analysis and titration, it can be seen that the majority of functional groups (amino- or quaternary ammonium) are accessible. It can be concluded that chlorinated aliphatic polymers were successfully functionalized, and hydrothermally aminated polymer particles exhibited remarkable anion exchange capacity.

The chemical structure of original polymer and porous polymer particles was analyzed by FT-IR spectroscopy. The spectra of CPP and CPP-TEA are shown in Fig. 4. The characteristic absorption bands at 694 cm⁻¹ and 733 cm⁻¹ arise from stretching vibrations of C-Cl bonds. The absorption bands at 2969–2845 cm⁻¹ are assigned to the C-H stretching vibrations. 1460 and 1380 cm⁻¹ are attributed to bending of C-H and stretching of C-C bonds. The band at 975 cm⁻¹ is ascribed to CH₂ vibration. After amination, the intensities of the bands at 694 and 733 cm⁻¹ significantly drop,

and the bands at 2800–2400 cm⁻¹ arising from the quaternary ammonium groups in CPP-TEA appear.²⁰ This clearly confirms the structural changes caused by hydrothermal amination. The CPP-TEA is further characterized by solid state NMR spectroscopy. The ¹³C NMR spectrum of CPP-TEA is shown in Fig. 5. The peaks at δ 39.1–40.6 and δ 13.0 ppm are assigned to CH₂, whereas those at δ 56.4–70.4 ppm and δ 127.9 ppm are assigned to CH₂-N and C=CH₂ carbons, respectively.^{21,22}

The thermogravimetry (TG) analysis shows that the aminated CPP-TEA experiences more mass loss at low temperatures (<300 °C) due to decomposition of the functional groups, and it exhibits better thermal stability at high temperatures due to crosslinked polymer structures as compared with its original polymer CPP (Fig. 6).

Under hydrothermal conditions, the amine molecules attack the active chloride sites, and then covalently bond to the polymer chains. As the amination proceeds, more amine molecules penetrate into the chlorinated polymers forming hydrophilic clusters inside the polymers. Then the hydrophilic clusters will form the pathways for further amine penetration;

**Fig. 4** FT-IR spectra of CPP and CPP-TEA.**Fig. 5** ¹³C solid-state NMR spectrum of CPP-TEA.

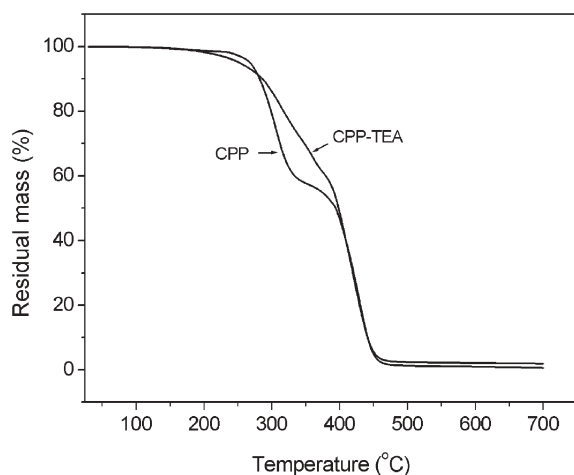


Fig. 6 TG curves of CPP and CPP-TEA.

meanwhile, the HCl gas evolved through the dehydrochlorination reaction may accelerate the process and expand the paths. The final pore walls are fixed in position by crosslinking of polymer chains.^{13,15} The chlorinated polymer beads that are thermoplastic partially melt, and thus they are broken down into micron-sized particles.

In order to explore the applicability of such aminated polymers in electrochemical devices, CPP-PEI and PVCVAc-PEI were fabricated into membranes with a thickness of 60 μm with 10% PVA binder. Impedance measurements showed that CPP-PEI and PVCVAc-PEI membranes had an ionic conductivity of as high as 4.5×10^{-2} and $0.48 \times 10^{-2} \text{ S cm}^{-1}$, respectively, corresponding to their high anion exchange capacity. Obviously, the porous structures of the aminated particles maximize the accessibility of functional groups, and facilitate ion transport through the membranes. These porous polymer particles with high anion exchange capacity should find a wide range of applications relating to ion exchange process and ion conduction.^{16,17,19}

Conclusion

In summary, we have shown that porous polymer particles with remarkable anion exchange capacity and ion conductivity can be fabricated by the amination of chlorinated aliphatic polymers in aqueous amine solution under hydrothermal conditions. These particles with different pore morphologies (e.g., honeycomb, skeleton) were formed by taking advantage

of heterogeneous amination, elimination and crosslinking reactions at elevated temperatures. The structures and physical properties such as anion exchange capacity and ion conductivity could be manipulated by using different amines. The approach demonstrated here would be unique, effective, and environmentally friendly for production of anion exchange materials from chlorinated polymers.

Acknowledgements

This work was supported by the University of Hong Kong, the Faculty of Engineering of Monash University and the Australian Research Council. H.W. gratefully acknowledges the Australian Research Council for the QEII Fellowship (DP0559724).

References

- 1 A. K. Salem, F. R. A. J. Rose, R. O. C. Oreffo, X. B. Yang, M. C. Davies, J. R. Mitchell, C. J. Roberts, S. Stolnik-Trenkic, S. J. B. Tendler, P. M. Williams and K. M. Shakesheff, *Adv. Mater.*, 2003, **15**, 210.
- 2 J. P. Badyal, A. M. Cameron, N. R. Cameron, D. M. Coe, R. Cox, B. J. Davis, L. J. Oates, G. Oye, C. Spanos and P. G. Steel, *Chem. Commun.*, 2004, 1402.
- 3 J. S. Yang and T. M. Swager, *J. Am. Chem. Soc.*, 1998, **120**, 11864.
- 4 K. Schwarz and M. Eppe, *Chem.—Eur. J.*, 1998, **4**, 1898.
- 5 D. K. Yi and D. Y. Kim, *Nano Lett.*, 2003, **3**, 207.
- 6 A. I. Cooper and A. B. Holmes, *Adv. Mater.*, 1999, **11**, 1270.
- 7 P. Jiang, J. F. Bertone and V. L. Colvin, *Science*, 2001, **291**, 453.
- 8 L. A. Connal, P. A. Gurr, G. G. Qiao and D. H. Solomon, *J. Mater. Chem.*, 2005, **15**, 1286.
- 9 G. Widawski, M. Rawiso and B. Francois, *Nature*, 1994, **369**, 387.
- 10 B. Xu, F. Arias and G. M. Whitesides, *Adv. Mater.*, 1999, **11**, 492.
- 11 Y. Ito, Y. Ochiai, Y. S. Park and Y. Imanishi, *J. Am. Chem. Soc.*, 1997, **119**, 1619.
- 12 E. S. Dragan, E. Avram, D. Axente and C. Marcu, *J. Polym. Sci., Part A: Polym. Chem.*, 2004, **42**, 2451.
- 13 L. J. Clemence and R. J. Eldridge, *React. Polym.*, 1988, **8**, 27.
- 14 X. Q. Jiang, H. Yu, R. Frayne, O. Unal and C. M. Strother, *Chem. Mater.*, 2002, **14**, 1914.
- 15 A. R. Roudman and R. P. Kusy, *Polymer*, 1998, **39**, 3641.
- 16 R. C. T. Slade and J. R. Varcoe, *Solid State Ionics*, 2005, **176**, 585.
- 17 T. W. Xu, Z. M. Liu and W. H. Yang, *J. Membr. Sci.*, 2005, **249**, 183.
- 18 H. T. Wang, B. A. Holmberg and Y. S. Yan, *J. Am. Chem. Soc.*, 2003, **125**, 9928.
- 19 J. Liu, H. T. Wang, S. A. Cheng and K. Y. Chan, *J. Membr. Sci.*, 2005, **246**, 95.
- 20 L. Vladescu, M. Costache and I. Badea, *Acta Chromatogr.*, 2004, **14**, 187.
- 21 D. Avci and L. J. Mathias, *J. Polym. Sci., Part A: Polym. Chem.*, 1999, **37**, 901.
- 22 K. Katsuraya, K. Hatanaka, K. Matsuzaki and K. Yamauri, *Macromol. Rapid Commun.*, 2000, **21**, 697.

Surface tension measurements of highly conducting ionic liquids

W. Martino,^a J. Fernandez de la Mora,^a Y. Yoshida,^b G. Saito^b and J. Wilkes^c

Received 31st October 2005, Accepted 19th December 2005

First published as an Advance Article on the web 25th January 2006

DOI: 10.1039/b515404a

The capillary rise method is used to measure the room temperature surface tension of several ionic liquids, selected mainly for their high electrical conductivity. They include salts based on the cations 1-ethyl-3-methylimidazolium (EMI⁺), 1-butyl-3-methylimidazolium (BMI⁺), and 1,3-dimethylimidazolium (DMI⁺), paired with anions such as GaCl₄⁻, FeCl₄⁻, C(CN)₃⁻, N(CN)₂⁻, SCN⁻, EtSO₄⁻, BF₄⁻, CF₃SO₃⁻, (CF₃SO₃)₂N⁻ (Tf₂N⁻) and Au(CN)₂⁻. The method consumes relatively little sample (<0.1 cm³) with measurement errors of 5%. Vacuum-dried samples are placed in the measurement cell under ambient (humid) air, but the meniscus is kept dry by a small flow of dry gas. Failure to dry the active interface leads to rapid contamination in the case of hydrophilic liquids, and to anomalously high surface tension. The highest surface tension measured (61 dyn cm⁻¹) corresponds to DMI–N(CN)₂.

1. Introduction

The surface tension of ionic liquids (ILs) has been the subject of a relatively small number of studies,^{1–10} with corresponding selected values condensed in Table 1 for imidazolium-based ILs. The table contains data on other physical quantities derived from additional sources.^{11–17} These studies have revealed modest surface tensions γ , comparable to those of organic liquids, and generally substantially smaller than typical values for molten inorganic salts (Table 2),¹⁰ or even water (72.7 dyn cm⁻¹ at 20 °C). On the basis of these data it appears that the surface tension γ of 1-alkyl-3-methylimidazolium salts increases with decreasing length of the alkyl chain in the imidazolium cation. It also increases by selection of small fluorinated anions such as PF₆ and BF₄ ($\gamma = 48.8$ dyn cm⁻¹ at 25 °C for 1-butyl-3-methylimidazolium-PF₆¹ (BMI–PF₆), and 54.4 dyn cm⁻¹ at 25 °C for EMI–BF₄⁸). EMI and BMI salts formed with metal (Fe and In) tetrachloride^{6,7} or trihalide anions⁹ exhibit room temperature γ values near or above 50 dyn cm⁻¹.

Our own interests on the surface tension of ionic liquids is related to the use of their Taylor cones¹⁸ *in vacuo* as sources of ions offering a remarkable range of molecular weights and chemical compositions. Taylor cones form when the interface between a conducting liquid and an insulating medium is charged electrically above a critical level, where electrostatic stresses overcome capillary forces. The liquid meniscus then turns from round to conical, with a micro-jet issuing from the apex and subsequently breaking up into charged drops. For increasingly conducting electrolytes, the apex region develops surface electric fields high enough (1 V nm⁻¹ at electrical conductivities $K \sim 1$ S m⁻¹) for solution ions to evaporate into the surrounding medium.¹⁹ When this medium is a vacuum, the ion beam formed can be used without the interference of gas discharges. In the extreme case of liquid metals,

conditions exist when drop emission ceases entirely, and the Taylor cone operates in the *purely ionic regime*, yielding μ A level currents of the metal ion.²⁰ Liquid metal ion sources (LMIS) are of high quality because they originate essentially from a point source and have a narrow energy range.²⁰

The purely ionic regime has not yet been reported for any electrolyte of neutral solvents, perhaps due to their substantial volatility, which either precludes exposing them to a vacuum, or limits the concentration of electrolyte tolerable without salt precipitation. However, this interesting regime arises in Taylor cones of certain ILs such as EMI–BF₄,²¹ whose very low volatility enables long time exposure to a vacuum, and whose high ion concentration often leads to the required high conductivities. High ion beam qualities have also been observed from Taylor cone sources of ILs.^{21b,22} Their interest over liquid metal ion sources resides in the possibility to also form negative ions, as well as their ability to operate at or near room temperature. Of particular interest are the facts that many more ILs exist than metals; that their range of possible chemical compositions and molecular masses is vastly larger than that of metals; that ILs are generally far better and less corrosive solvents than metals, *etc.* As a result, there is considerable current interest in the use of ionic liquids as *pure* ion sources, particularly for electrical propulsion applications. Because, only a few ILs have been found so far able to operate in the purely ionic regime, we are embarked in a systematic effort to identify more, and to establish what are the key liquid properties favoring this sought purely ionic regime.

The role of a high electrical conductivity in sharpening the cone tip, and hence intensifying the local electric field is well known.^{19a} One can also argue that a high surface tension γ also intensifies the electric field, which scales as $\gamma^{1/2}$ both in Taylor's static theory for the cone,^{18a} as well as in its dynamical extensions accounting for the structure of the tip region.^{19a} Consequently, because ion evaporation is activated primarily by the electric field on the meniscus surface, there are good reasons to expect that both high electrical conductivity and high surface tension will favor the production of ions rather than drops from Taylor cones. Accordingly, as part of our

^aMechanical Engineering Department, Yale University, New Haven, CT, USA

^bDivision of Chemistry, Graduate School of Science, Kyoto University, Kyoto 606-8502, Japan

^cUSAF Academy, Colorado Springs, CO, USA

Table 1 Representative published surface tensions of imidazolium-based ionic liquids with measurement temperature (in °C) in parenthesis

Liquid	$\gamma/\text{dyn cm}^{-1}$	$\rho/\text{g cm}^{-3}$ ^a	μ/cP	$K/S \text{ m}^{-1}$
BMI-I	54.7 (25) ¹	1.08(25) ¹	1110(25) ¹	$\sim 0.1(25)^{11}$
EMI-EtSO ₄	48.79(25) ²	1.2296(25) ²	126 ^{Merck} (20)	
EMI-Tf ₂ N	41(20), ³ 39(25), ⁴ 34.7(28) ¹⁰	1.52(25) ^{4,12,13}	25(25), ⁴ 32(25), ¹² 34(20) ¹³	0.90(25), ¹² 0.88(20) ¹³
C ₃ MI-Tf ₂ N	38(25) ⁴	1.475(25) ⁴	35(25) ⁴	
BMI-Tf ₂ N	37(25), ⁴ 31.5(30) ¹⁰	1.44(25), ^{4,12} 1.43(19) ¹³	44(25), ⁴ 50(25), ¹² 52(20) ¹³	0.39(25), ¹² 0.39(20) ¹³
C ₅ MI-Tf ₂ N	36(25) ⁴	1.403(25) ⁴	49(25) ⁴	
C ₆ MI-Tf ₂ N	35(25), ⁴ 30.6(31) ¹⁰	1.37(25) ^{4,12}	59(25), ⁴ 68(25) ¹²	0.22(25) ¹²
C ₆ MI-Tf ₂ N	29.1(33) ¹⁰			
BMI-PF ₆	48.8(25), ¹ 47(25), ⁴ 42.9(63), ⁵ 44.7(40) ¹⁰	1.368(25), ⁴ 1.37(30) ¹⁴	$\sim 270(25),4 312(30)14$	0.146(25) ¹⁴
C ₈ MI-PF ₆	32.8(63), ⁵ 34.3(40) ¹⁰	1.22(25) ¹	585(25) ¹	
C ₁₀ MI-PF ₆	30.7(28) ¹⁰			
C ₁₂ MI-PF ₆	23.6(63) ⁵			
EMI-BF ₄	54.4(25) ⁸	1.2853 (25) ⁸	38 (25) ⁸	1.36(25) ⁸
BMI-BF ₄	46.6(25), ¹ 38.4(63), ⁵ $\sim 41(20),5 39.7(40)10$	1.17(30), ¹⁴ 1.21(25) ¹⁵	152(20) ^{Merck} , 180(25) ¹⁵	0.173(25), ¹⁴ 0.35(25) ¹⁵
C ₈ MI-BF ₄	29.8(63), ⁵ 30.6(40) ¹⁰	1.11(20) ^{Merck}	468(20) ^{Merck}	
C ₁₂ MI-BF ₄	25.2(63) ⁵			
C ₈ MI-Br	32(63) ⁵			
C ₈ MI-Cl	30.5(63) ⁵	1(25) ¹	337(25) ¹	
EMI-InCl ₄	52.78(20) ⁶	1.6413(20) ⁶		
BMI-FeCl ₄	46.51(20) ⁷	1.369(20), ⁷ 1.38(20) ¹⁶	34(25), ¹⁶ $\sim 32(25)^{17}$	0.89(25), ¹⁶ $\sim 0.90(25)^{17}$
BMI-ICl ₂	54.6(RT) ⁹	1.708(RT) ⁹	50(RT) ⁹	0.57(RT) ⁹
BMI-Br ₃	51.5(RT) ⁹	1.702(RT) ⁹	93(RT) ⁹	0.89(RT) ⁹
BMI-IBr ₂	57.3(RT) ⁹	1.547(RT) ⁹	57(RT) ⁹	0.61(RT) ⁹

^a Densities are given with fewer decimals than in the original references. Tf₂N = bis(trifluoromethylsulfonyl)imide; EMI = 1-ethyl-3-methylimidazolium; C₃MI = 1-propyl-3-methylimidazolium, etc; BMI = C₄MI. RT = room temperature. Merck refers to the Merck home page on ionic liquid properties (<http://ildb.merck.de/ionicliquids/en/startpage.htm>). Superscripts denote bibliographic references. ^b

search for suitable ionic liquids for ion beam generation, we have measured the surface tension of a diversity of ionic liquids for which prior work had shown either high K ($\sim 1 \text{ S m}^{-1}$ at room temperature) or low viscosity μ . Due to its unusually high reported γ (48.78 dyn cm^{-1} at 25 °C, according to ref. 2), we have also reexamined EMI-EtSO₄, even though its considerable room temperature viscosity coefficient ($\mu\rho = \nu = 102 \text{ mm}^2 \text{ s}^{-1}$) makes a high electrical conductivity improbable.

2. Experimental

Surface tension measurement

The fact that only a few out of the hundreds of reported ionic liquids have known surface tensions is in part due to the circumstance that conventional measurement methods use relatively large samples (*i.e.*, 20 cm^3 in ref. 9). Yet, most of the materials to be examined in this work were available only in relatively small quantities. For this reason, we have selected the *capillary rise method* to measure surface tension, as it is compatible with the use of very little sample. The method is not new, and has even been used for IL characterization.³ However, our present use of the technique offers certain new features in terms of precision measurement and sample consumption, and will be described in some detail. It is based on measuring the rise h of a liquid held inside a cylindrical

Table 2 Typical surface tensions for inorganic molten salts, from ref. 10

Liquid	AgNO ₃	CdBr ₂	GaCl ₃	K ₂ SO ₄	LiBr	LiCl	LiF	ZnBr ₂
T/K	560	951	387	1383	923	979	1235	823
$\gamma/\text{dyn cm}^{-1}$	145	63.5	23	139.4	104	121.	224.5	48.6

capillary tube of inner radius R above the level of the liquid reservoir. If γ is the surface tension, ρ the density of the liquid, g the acceleration of gravity and θ the contact angle at the point where the liquid, the inner capillary surface and the surrounding gas meet (Fig. 1), then a simple force balance yields

$$2\pi R\gamma\cos\theta = \rho\pi R^2hg \quad (1a)$$

where one assumes that the meniscus height δ is much smaller than the capillary rise h . This assumption is generally accurate, and holds to a precision better than 1% in all our measurements. The main problem involved in the use of eqn (1a) to determine γ/ρ according to eqn (1b) is the need to establish accurately the wetting angle θ

$$\gamma/\rho = ghR/(2\cos\theta). \quad (1b)$$

θ is generally unknown for a particular glass-IL combination, as it is strongly dependent on the nature of the glass surface. θ is also difficult to infer directly by looking at the meniscus due to refraction from the curved glass. However, the height δ

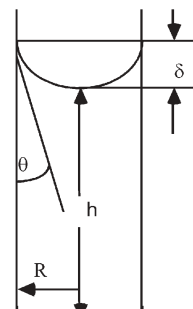
**Fig. 1** Sketch of the capillary.

Table 3 Room temperature (22–25 °C) surface tensions measured in the present study, together with other physical properties from the literature

Ionic liquid	$\cos\theta$	h/mm	$\gamma/\text{dyn cm}^{-1}$	$\rho/\text{g cm}^{-3}$	η/cP	$K/S \text{ m}^{-1}$
EMI-BF ₄	0.995	26.92	44.3 52(24) ^a	1.29(25) ⁸	38(25) ⁸	1.36(25) ⁸
EMI-TfO = EMI-CF ₃ SO ₃	0.995	26.92	39.2 36(22) ^a	1.39(22) ¹³	45(20) ¹³	0.86(20) ¹³
EMI-Tf ₂ N ^c	0.950	16.50	35.2, 34.9 ^a	1.52(22) ¹³	34(20) ¹³	0.88(20) ¹³
DMI-N(CN) ₂	0.996	29.23	61.6	1.14(20) ²⁶	15(25) ²⁶	3.6(25) ²⁶
EMI-N(CN) ₂	0.997	29.43	42.6	1.08(20) ²⁵	16(25) ²⁵	2.8(25) ²⁵
EMI-C(CN) ₃	0.999	32.11	47.9	1.11(20) ²⁵	18(22) ²⁵	2.2(25) ²⁵
EMI-SCN	0.963	31.96	49	1.11(20) ^{Merck}	23(20) ^{Merck} , 21(RT) ³⁰	~0.4(25) ³⁰
EMI-GaCl ₄	0.85–0.99		50	1.53(20) ²⁹	16(25) ²⁹	2.2(25) ²⁹
EMI-FeCl ₄	0.99		47.7	1.42(20) ²⁹	18(25) ²⁹	2.0(25) ²⁹
BMI-GaCl ₄	0.98		41.5	1.43(20) ^b	31(25) ^b	0.95(25) ^b
BMI-FeCl ₄	0.86–0.99		44.9	1.38(20) ¹⁶	34(25) ¹⁶ , ~32(25) ¹⁷	0.89(25) ¹⁶ , ~0.90(25) ¹⁷
BMI-Au(CN) ₂	0.98		46.6	1.87(20) ²⁷	279(25) ²⁷	0.12(25) ²⁷
EMI-EtSO ₄			42.5	1.23(25) ²	126(20) ^{Merck}	

^a Earlier measurements by I. Romero (Yale) without drying the meniscus. ^b Unpublished data from Yoshida and Saito. ^c Tf₂N = bis(trifluoromethylsulfonyl)imide.

of the meniscus from its rounded bottom to the contact point (Fig. 1) is not affected by refraction, and can be measured accurately with a cathetometer.

When the capillary radius R is much smaller than the capillary length l

$$l = (\gamma/\rho g)^{1/2}, \quad (2)$$

gravitational effects are negligible and the meniscus is almost spherical. The ratio δ/R is then simply related to the wetting angle *via*

$$\cos\theta = 2 \frac{(\delta/R)}{1 + (\delta/R)^2}. \quad (3)$$

Note that the error in $\cos\theta$ is much smaller than the measurement error in δ/R when δ is close to R and $\cos\theta$ approaches unity. This is the limit of perfect wetting, which is well met in all of our measurements (Table 3). Because eqn (1) may be rewritten $hR = 2l^2\cos\theta$, when $R \ll l$ and $\cos\theta$ is of order one, it also follows from eqn (1) that

$$R \ll l \ll h. \quad (4)$$

This limit applies to all our experiments, based on $R = 0.273$ mm (ACE glass microcapillary), where δ is typically 100 times smaller than h . This narrow section also leads to a negligible quantity of sample pulled up by the capillary. The weakest point about operating in the *spherical meniscus* limit eqn (4) is that δ takes small values, and its accurate determination is difficult. In our case, the availability of a cathetometer able (when used with high skill†) to resolve 2 μm , and the near perfect wetting of our capillaries by all our ILs

† High contrast can be obtained when the light source is perpendicular to the capillary and there is an angle of no more than 90° between the light source and the light aperture of the microscope. A mirror or reflective surface should also be placed in the back of the capillary to reflect the light from the source, thus illuminating it. Multiple vertical lines (reflected rays from the source) then become obvious, along with the meniscus itself contrasting against the reflective surface. The benefit of these lines is that some go for the length of the capillary while others begin where the meniscus ends. Therefore, by measuring the height at which these rays start, one can consistently and accurately measure the height of the top of the meniscus. Simply align the crosshairs with these lines to measure the top of the meniscus.

enabled use of eqn (3). Under less ideal circumstances it is preferable to use wider capillaries and to drop eqn (3) in favor of the method discussed in the Appendix. This method is based on the numerical solution of the equations governing the shape of the meniscus, combined with the experimental determination of R , δ and h . The interpretation of our own measurements includes gravitational corrections, which were negligible in all cases (the correction parameter λ defined in the Appendix was always smaller than 1%).

The experimental determination of the meniscus height h involves locating the meniscus bottom at the top of the capillary, and the reservoir level at a point of relatively small curvature. The first position can be determined with negligible relative error. Accurate determination of the second requires ideally a large liquid reservoir, but this was precluded by the small samples available. The reservoir was made of glass, and had the form of a cup with an inner diameter of 5.7 mm at its top and a rapidly tapering shape towards its bottom. It was made by cutting the wide end of a pipette, and closing its narrow end near the neck with a propane torch. To avoid contamination, a new reservoir was made for each liquid studied. The sample liquid inside the cup wets both the outer surface of the capillary and the inner surface of the cup, rising slightly at both points. The level of liquid in the reservoir was measured at the minimum level between these two contact points. However, the interface at this lowest position has nonzero curvature and fails to provide an exact reference for the origin of heights. The associated error is a fraction of l , certainly smaller than the capillary rise seen on the side of the cup or the outside of the capillary. This indeterminacy leads to the largest error in our measurement. It can be estimated first by ignoring the presence of the capillary inside the cup, and determining the capillary rise within the cup itself. We use for this estimation the known formulae for a two-dimensional problem.²³ For the typical case $\gamma/\rho = 40 \text{ cm}^3 \text{ cm}^{-2}$ ($l \sim 2$ mm) and $\theta = 0$, the height at the center of the cup (5.7 mm id) is about $0.3l$, or 0.6 mm. Compared with a typical value of $h \sim 2$ cm, this represents a 3% error. The presence of the capillary in the center of the system would worsen the situation, so an error in the range of 5% is more realistic. Note that the actual h is always larger than the measured value, so the reported surface tensions are lower bounds for the actual

surface tension. This reservoir error is not inherent to the capillary rise method, but is a consequence of our minimization of sample consumption by use of a cup of small diameter (5.7 mm).

An accurate determination of the meniscus height δ requires very careful optimization of the lighting to give high contrast and defining unambiguously the contact point. With good skill and practice one can determine δ within better than 2 μm , as established by repeated measurement. The associated error in δ/R is better than 1%. The corresponding error in $\cos \theta$ is considerably smaller when δ is close to R ($\cos \theta \rightarrow 1$), as is the case in all our measurements. This happy circumstance permits relatively small errors in δ/R , even with ordinary skill in the use of the cathetometer. We note that some of the glass capillaries showed a markedly different wetting angle than most. This was clearly seen in some experiments where up to four capillaries were immersed simultaneously in the same cup, showing substantial differences in both the capillary rise and the wetting angle. For instance, BMI-FeCl₄ gave values of 0.994, 0.9985, 0.919 and 0.856 for $\cos \theta$, though the ratio $h/\cos \theta$ remained relatively fixed ($\pm 1.5\%$ change). A similar variation was observed with EMI-GaCl₄. The observed occasional variation in wetting angle merely shows the strong sensitivity of this parameter to the peculiarities of the glass surface. The resulting variation in γ ($\sim h/\cos \theta$) is due to the greater inaccuracy in the measurement of $\cos \theta$ associated with poorer wetting conditions, a problem that can be overcome by using only the data associated with the better wetting capillaries.

Careful avoidance of hydration of the interface by contact with ambient air is extremely important. This is evident from the fact that the surface tension is a characteristic of the surface rather than the bulk, and the interface is highly accessible by diffusion of water vapor in the atmosphere. The effect is readily observed with hydrophilic ILs. Once the capillary is loaded with a dry liquid sample, the meniscus height is not steady but keeps increasing with a characteristic time of many minutes. This unsteadiness is not associated with the well-known slow advance of the contact point when moving against a dry surface. This problem was avoided by pulling initially the liquid up inside the capillary beyond its equilibrium height with a syringe, and releasing it, so that the meniscus moves on a wet capillary surface. The surface remains wet for a very long time due to the essentially null volatility of ILs. The observed unsteadiness is due to water uptake from the atmosphere at the interface, as evident from the fact that it disappears as soon as the interface is bathed in a slow flow of a dry gas. This was done by supplying the gas through a tube with an exit diameter of 2 cm, with the exit of the capillary being completely immersed inside the tube. The gas flow exiting this tube was made uniform by means of a laminarization screen. The flow rate of gas was monitored with a flowmeter ($\sim 0.5 \text{ l min}^{-1}$) in order to make it small enough to avoid modifying the pressure above the meniscus, though with the assurance that it was nonzero.

As an example, a dry meniscus of EMI-BF₄ reached its equilibrium height in a few minutes ($\gamma_{\text{dry}} = 44.3 \text{ dyn cm}^{-1}$). On turning off the flow of dry gas sheathing the meniscus from the atmosphere, a noticeable height increase is seen in as little as ten minutes (depending on the ambient humidity levels), and

eventually increases by as much as 20%. For EMI-EtSO₄ at ambient humidity we have found $\gamma_{\text{humid}} = 52.4 \text{ dyn cm}^{-1}$ ($\gamma_{\text{dry}} = 42.5 \text{ dyn cm}^{-1}$). No unsteadiness was seen in the case of the hydrophobic liquid EMI-Tf₂N when the meniscus was left in contact with the laboratory environment. In none of our experiments did we surround the cup with a dry medium. Hence, in the case of hydrophilic liquids, there is a slow uptake of water at the liquid-gas interface on the cup. However, this contamination from below takes a very long time to diffuse to the top of the capillary. Another potential source of error is the variability of the capillary radius R . All the measurements were made with capillaries from the same batch of 100, using a new capillary for each measurement in order to avoid contamination. The capillary diameters were measured for several of them by cutting them at several axial positions. The variation in tube diameter from one capillary to another or from different cuts on a given capillary never exceeded 2 μm . R is therefore known within better than 1%.

All new capillaries were cleaned first with acetonitrile and then acetone, followed by a few high pressure bursts from clean pressurized gas. The solvents were introduced into the capillary with a clean 27 gauge needle.

Ionic liquids

EMI-EtSO₄ and EMI-SCN were purchased from Sigma-Aldrich (both Basf quality, with reported purity >95%. Warning: these two materials are unstable and emit poisonous vapors). These as well as all other samples were used without further purification, other than drying under vacuum at room temperature. The water content remaining after this treatment was not measured. EMI-BF₄ was a special order from Solvent Innovations Inc., with the rather modest undefined purity required for its use as an ion source *in vacuo*. The presence of impurities was evident from its yellowish color. EMI-Tf₂N was from Covalent Associates (electronic grade). This liquid is hydrophobic and showed no increase in capillary height after relatively long exposure of the meniscus to the laboratory environment. EMI-TfO was from Fluka (purity >98%). All other liquids were prepared by Dr Yoshida at Professor Saito's laboratory, according to established protocols, and their purity was confirmed by elemental analysis (C, H, N, halogen) and ¹H NMR. EMI-N(CN)₂ was first prepared by MacFarlane *et al.* by metathesis of EMI-I and Ag-N(CN)₂ in water.²⁴ Judging from the elemental analysis data, however, the product is not pure, possibly due to the use of the starting material NaN(CN)₂ as received. EMI-N(CN)₂ and EMI-C(CN)₃ were prepared using the procedure of Yoshida *et al.*,²⁵ where the commercial NaN(CN)₂ (starting purity 96%) was recrystallized. The synthesis and properties of DMI-N(CN)₂ will be described elsewhere,²⁶ as will those of BMI-Au(CN)₂.²⁷ EMI-FeCl₄ was first prepared by Katayama *et al.*,²⁸ who also reported its density and electrochemical properties at 130 °C. Its viscosity and ionic conductivity have been given by Yoshida *et al.*,²⁹ who also report the synthesis and physical properties of EMI-GaCl₄. The viscosity and ionic conductivity of BMI-FeCl₄ were first measured by Angell's group,¹⁷ and have been confirmed by new data.¹⁶ The still unpublished data on BMI-GaCl₄ are from Yoshida and Saito. All these salts are

liquid at room temperature, except for DMI–N(CN)₂. The surface tension of this salt was also studied at room temperature, since, after melting, it remains as a supercooled liquid for long periods.

A much larger sample of EMI–N(CN)₂ (~5 cm³) was prepared at Prof. John Wilkes' laboratory by metathesis of EMI–Cl and Ag–N(CN)₂. The small precipitate of white AgCl crystals that formed after a few days was removed by decanting. The corresponding surface tension was indistinguishable from that of the Japanese sample.

3. Results and discussion

Table 3 shows our surface tension measurements, including the cosine of the wetting angle $\cos\theta$ on the glass capillary [computed from eqn (3)], and the capillary rise h (Fig. 1). As noted earlier, $\cos\theta$ is fairly close to unity in most measurements, a useful circumstance to reduce the error in γ/ρ resulting from errors in the measurement of δ . γ/ρ includes the gravitational correction of the Appendix, which was in all cases negligible. The tabulated γ is based on γ/ρ given by the capillary measurement, and the density ρ taken from the literature, and reported in the table.

Previous measurements are available for four of the materials studied here: EMI–Tf₂N, EMI–BF₄, BMI–FeCl₄ and EMI–EtSO₄.

EMI–Tf₂N. Our datum (35.2 dyn cm⁻¹) is in approximate agreement with ref. 10 {34.7(27)}, and is substantially lower than reported in ref. 3 and 4 {41(20);³ 39(25)⁴}. We believe these two high values are incorrect. We see almost no ambient humidity effect on the surface tension of EMI–Tf₂N.

EMI–BF₄. Our datum for EMI–BF₄ (44.3 dyn cm⁻¹) is substantially lower than reported in ref. 8 {54.4 (25)⁸}. The prior high value is consistent with our own measurements in a humid atmosphere (52 dyn cm⁻¹ in Table 3), and is also probably attributable to insufficient drying precautions.

EMI–EtSO₄. Our datum for EMI–EtSO₄ (42.5 dyn cm⁻¹) is substantially lower than reported in ref. 2 {48.79(25)²}. The prior high value is more consistent with our own measurements under ambient (humid) conditions (52.4 dyn cm⁻¹), and appears to be similarly attributable to insufficient drying precautions.

BMI–FeCl₄. Our datum for BMI–FeCl₄ (44.9 dyn cm⁻¹) agrees within experimental error with that in ref. 7 {46.51 (20)⁷}.
Several earlier studies on the effect of water addition on the physical properties of ionic liquids are worth discussing. Sung *et al.*³¹ have measured the surface tension of mixtures of water and the hydrophilic ionic liquid BMI–BF₄. They report an almost fixed $\gamma \sim 43$ dyn cm⁻¹ from the neat IL up to substantial water content, with a shallow peak ($\gamma \sim 44$ dyn cm⁻¹) between 90% and 95% molar fraction of water. At increasing water content there is a sharp drop to a minimum ($\gamma \sim 40$ dyn cm⁻¹) at 98.3% molar fraction of water, and then a rapid rise to the surface tension of pure water (~ 72 dyn cm⁻¹). The absence of an increase in the surface tension upon slight hydration of the pure salt is noteworthy. In contrast, Fitchett *et al.*³² have seen large variations on the electrical conductivity and viscosity in 1-alkyl-3-methylimidazolium

bis(perfluoroalkylsulfonyl) imide salts, following from the modest levels of hydration possible in these hydrophobic liquids. For instance, water-equilibrated C₆MI–Tf₂N contains 1.2% (w) water (22% molar fraction), but shows 70% of the viscosity and 112% of the electrical conductivity of the dry IL. These authors rationalize those effects on viscosity by the ideal mixing rule $\mu = \xi_1\mu_1 + \xi_2\mu_2$, where the ξ_i are component molar fractions. Noteworthy is the fact that, due to the large disparity in the molecular weight of water and the ionic liquids studied, the water-equilibrated ILs contain very little mass but a substantial molar concentration of water. Finally, Table 7 in ref. 1 includes γ data on water-equilibrated salts. Almost no effect of hydration is seen in BMI–PF₆ and BMI–Tf₂N, while C₆MI–PF₆ and C₈MI–PF₆ exhibit a retrograde effect, which is substantial in the case of C₆MI–PF₆ ($\gamma_{\text{humid}} = 36.8$ dyn cm⁻¹; $\gamma_{\text{dry}} = 43.4$ dyn cm⁻¹).

We have studied neither BMI–BF₄, nor PF₆ salts, but there is an evident conflict between our finding of a strong effect of slight hydration on γ for all hydrophilic liquids investigated, and the opposite conclusion for BMI–PF₆ in ref. 31. Possible explanations for this discrepancy are that (i) either BMI–BF₄ is far less hydrophilic than EMI–BF₄, or (ii) that the surface of the “dry” BMI–BF₄ was contaminated by atmospheric water vapor at a concentration almost independent of the water content of the bulk liquid. This surface concentration is probably fixed by slow diffusion of the surface water into the bulk. This would explain qualitatively the surprising slight effect of water concentration on surface tension, because diffusion of water through the gas into the surface is surely more effective than diffusion away from the surface into the (drier) bulk liquid. There is no mention in ref. 31 of any drying precautions taken during the surface tension measurement. The study was based on a DuNuoy Tensiometer (Surface Tensionmat, Fisher) with a platinum ring with a mean circumference of 6 cm, and this apparatus is not readily handled inside a glove box. Furthermore, the γ value reported of 43 dyn cm⁻¹ is almost as high as what we find for dry EMI–BF₄, while the larger cation in BMI would lead one to expect smaller γ values. Prior literature gives both high and low values for the surface tension of BMI–BF₄, as shown in Table 1. The lower value obtained by Law and Watson⁵ ($\gamma \sim 41$ dyn cm⁻¹ at 20 °C) was also based on a surface tensiometer, but they introduced it into a metal cell, and noted that “The cell ... insulated the sample from variations in the laboratory environment.” Their low measured value therefore supports the hypothesis (ii) that the *dry* sample of ref. 31 was not completely dried, but also indicates only a minor variation from a fully dried sample ($\gamma \sim 41$ dyn cm⁻¹ at 20 °C in ref. 5) to a less perfectly dried sample ($\gamma \sim 43$ dyn cm⁻¹ at 20 °C in ref. 31) for the case of BMI–BF₄.

Prior work of Bueno and Fernandez de la Mora³³ has shown that Taylor cones of ionic liquids with electrical conductivities K near or above 1 S m⁻¹ act as sources of pure ions in a vacuum provided their room temperature surface tension reaches a threshold value of about 40 dyn cm⁻¹ (the value for EMI–TfO). Liquids such as EMI–Tf₂N with comparable K but lower γ tend to emit a mixture of drops and ions, with a mass flux dominated by the drops and a comparable current for drops and ions. As shown in Fig. 2, all the liquids investigated

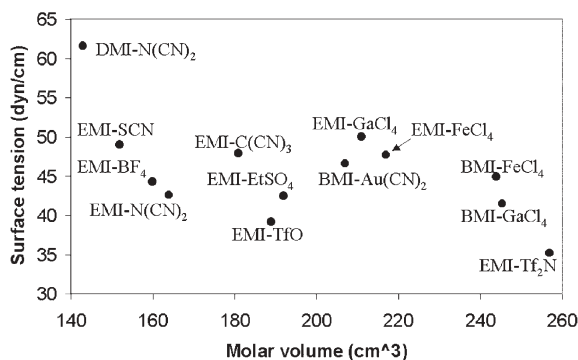


Fig. 2 Surface tension versus molar volume for the ILs investigated.

here except for EMI-Tf₂N fall above this critical surface tension, and are therefore expected to be pure ionic emitters. The number of potential candidates to exhibit this interesting behavior has therefore increased from just two (EMI-BF₄ and EMI-TfO) up to 11 (though the Taylor cones of EMI-EtSO₄ and BMI-Au(CN)₂ may need to be operated above room temperature in view of their limited ambient electrical conductivity³⁴).

Fig. 2 collects all of our surface tension data as a function of molar volume v . The selection of this horizontal variable is relatively arbitrary, but not entirely so. Corresponding state principle considerations³⁵ indicate that $\gamma v_c^{2/3}/kT = F(T/T_c)$, where v_c and T_c are the critical values for the molar volume and the temperature, respectively. F is a function of the single variable T/T_c for which several expressions have been proposed.^{10,35} Given empirical information on the temperature dependence of γ for the various substances examined together with information on their critical volumes, one could attempt a much better correlation than attained in Fig. 2. However, the effort of assembling such information is particularly challenging in the case of ionic liquids, whose negligible volatility makes it rather difficult to determine vapor liquid equilibria.¹⁰ As long as v/v_c and T/T_c take equal or similar values at room temperature for all the substances studied, it would make sense to expect a collapse of all our data into a single curve in Fig. 2. We cannot hope this equality to hold, so, it is not surprising to see several groups of points instead of a single curve. Most noticeable is the series of all salts containing the cyanide group and having molar volumes below 180 cm³. They all lie in a single curve, which includes also approximately the three substances studied having the lowest surface tensions: EMI-TfO, EMI-EtSO₄ and EMI-Tf₂N (far to the right). The two salts containing cyanide groups whose volumes exceed 180 cm³ [EMI-C(CN)₃ and BMI-Au(CN)₂] exhibit anomalously high surface tensions for their large molar volume. They fall approximately in line with the group of salts with metal tetrachloride cations, all of which also exhibit both large molar volumes and large surface tensions.

4. Conclusions

The room temperature surface tension of several highly conducting ILs has been characterized with relatively little sample consumption by the capillary rise method. It is important to keep the interface dry, as $\sim 20\%$ increases in γ may result from

atmospheric water uptake in the case of hydrophilic ILs. We have not quantified bulk water content following our vacuum drying procedure at room temperature. The bulk ILs may accordingly retain some traces of water, which are known to have significant electrochemical and other bulk effects. In spite of this uncertainty about the bulk, we have argued that the surface is dry because the gas surrounding it is completely dry, while diffusion rates of water from the surface into the gas are much faster than from the liquid (perhaps imperfectly dried) into the surface. Our surface tension measurements correspond therefore to a perfectly dry surface.

A number of materials have been identified enjoying surface tensions in excess of that of EMI-BF₄ ($\gamma = 44.3 \text{ dyn cm}^{-1}$), with a record high corresponding to DMI-N(CN)₂ ($\gamma = 61.6 \text{ dyn cm}^{-1}$).

Many of the materials studied enjoy both high electrical conductivity and high surface tension, and appear as first-rate candidates for ion generation from Taylor cones *in vacuo*.

Appendix: Gravitational corrections in the capillary rise method

We consider the case of wide enough capillaries where the meniscus is not necessarily spherical and eqn (3) does not hold. One can then compute the meniscus shape, and from it derive more general expressions relating σ/ρ to measurable quantities (σ is the surface tension in the notation of this Appendix).

Let p_o be the pressure at the gas, and p that in the liquid. $p = p_o - \rho g z$, where the level $z = 0$ is chosen at the liquid level in the large container. The reason for this choice is that, at this free surface, there is almost no curvature, and hence no pressure jump between liquid and gas. Using now the expression relating the pressure jump across the meniscus and the curvature:

$$\frac{1}{r} \frac{d}{dr} \frac{r z'}{(1+z'^2)^{1/2}} = \frac{\rho g z}{\sigma}, \quad (\text{g1})$$

where z is understood as a function of r , $z(r)$, giving the meniscus shape, and $z' = dz/dr$. Note that z and r are cylindrical coordinates (vertical coordinate and radial distance to the axis). For the purpose of minimizing the number of independent variables, we introduce dimensionless variables

$$\xi = \frac{r}{L} \quad (\text{g2})$$

$$y = \frac{z-h}{L} \quad (\text{g3})$$

$$L = \frac{\sigma}{\rho g h} \quad (\text{g4})$$

$$\lambda = \frac{\sigma}{\rho g h^2} \quad (\text{g5})$$

where the characteristic length L is chosen such as to make the value of the right hand side of eqn (g1) equal to unity in eqn (g6), eqn (g3) chooses the origin of the variable y to be right at the minimum of the meniscus ($z = h$), and $y' = dy/d\xi$:

$$\frac{1}{\xi} \frac{d}{d\xi} \frac{\xi y'}{(1+y'^2)^{1/2}} = 1 + \lambda y \quad (\text{g6a})$$

This equation needs to be solved numerically with initial conditions

$$y' = y = 0 \text{ at } \xi = 0. \quad (\text{g7})$$

Generally the meniscus height δ is of the order of the characteristic length $(\sigma/\rho g)^{1/2}$, while h is much larger. Hence, λ will typically be small (unless one uses wide capillaries). In the limit when $\lambda = 0$, eqn (g6) can be integrated once into:

$$\frac{\xi y'}{(1+y'^2)^{1/2}} = \xi^2/2, \quad (\text{g6b})$$

and once more (after expressing y' as a function of ξ) to yield the known spherical shape

$$y/2 = 1 - (1 - \xi^2/4)^{1/2} \quad (\lambda = 0). \quad (\text{g8})$$

In general, eqn (g6b) can be integrated numerically to yield a function

$$y = y(\xi, \lambda) \quad (\text{g9})$$

One could compare this function with experimental values, and the simplest approach is to use just the value of the function at the edge of the capillary $r = R$, where $y = \delta/L$ and $\xi = R/L$. Then, the experimental quantity δ/R is given theoretically as

$$\delta/R = y(\xi, \lambda)/\xi \quad (\text{g10})$$

It is hence convenient to make a graph of the function $y(\xi, \lambda)/\xi$ vs. ξ for several λ values $y(\xi, \lambda)/\xi = F(\xi, \lambda)$.

Similarly we know experimentally the quantity h , and one can easily see that

$$R/h = \lambda \xi \quad (\text{g11})$$

Now, from the experimentally known quantities δ/R and R/h we can determine the two parameters ξ , λ , and from them the surface tension as

$$\sigma = \frac{\rho g R h}{\xi} \quad (\text{g12})$$

This must be done iteratively. First one assumes $\lambda = 0$, and reads ξ from the graph $\delta/R = F(\xi, \lambda)$. With this value and eqn (g11) one finds λ and enters again into the graph $\delta/R = F(\xi, \lambda)$ to read a new value of ξ . Two such iterations will generally suffice, fixing ξ and therefore allowing the determination of the surface tension from eqn (g12). It is clear that the first iteration ($\lambda = 0$) gives exactly the same thing we would have obtained by ignoring gravitational effects, so that the ratio of the final ξ value to this initial value is the gravitational correction.

Acknowledgements

We thank Mr Sergio Castro and Mr Carlos Bueno for their many contributions to this study. Financial support from the US AFOSR through contract F-49620-01-1-1416 at Yale

University is gratefully acknowledged. This work was in part supported by a COE Research on Elements Science (No.12CE2005), and a Grant-in-Aid (21st Century COE program on Kyoto University Alliance for Chemistry) from the Ministry of Education, Culture, Sports, Science and Technology, Japan. YY and GS also acknowledge the financial support from the Grants-in-Aid for Scientific Research (No. 15205019) by JSPS.

References

- J. G. Huddleston, A. E. Visser, W. M. Reichert, H. D. Willauer, G. A. Broker and R. D. Rogers, Characterization and comparison of hydrophilic and hydrophobic room temperature ionic liquids incorporating the imidazolium cation, *Green Chem.*, 2001, **3**, 156–164.
- J.-Z. Yang, X.-M. Lu, J.-S. Guic and W.-G. Xua, A new theory for ionic liquids—the interstice model. Part 1. The density and surface tension of ionic liquid 1-ethyl-3-methylimidazolium ethylsulfate, *Green Chem.*, 2004, **6**, 541–543.
- V. Halka, R. Tsekov and W. Freyland, Peculiarity of the liquid/vapour interface of an ionic liquid: study of surface tension and viscoelasticity of liquid BMImPF₆ at various temperatures, *Phys. Chem. Chem. Phys.*, 2005, **7**, 2038–2043.
- S. V. Dzyuba and R. A. Bartsch, Influence of structural variations in 1-alkyl(aralkyl)-3-methylimidazolium hexafluorophosphates and bis(trifluoromethylsulfonyl) imides on physical properties of the ionic liquids, *ChemPhysChem*, 2002, **3**, 161–166.
- G. Law and P. R. Watson, Surface tension measurements of *N*-alkylimidazolium ionic liquids, *Langmuir*, 2001, **17**, 6138–6141.
- S.-L. Zanga, Q.-G. Zhang, M. Huang, B. Wang and J.-Z. Yang, Studies on the properties of ionic liquid EMI-InCl₄, *Fluid Phase Equilib.*, 2005, **230**, 192–196.
- Q. G. Zhang, J. Z. Yang, X. M. Lu, J. S. Gui and Z. Huang, Studies on an ionic liquid based on FeCl₃ and its properties, *Fluid Phase Equilib.*, 2004, **226**, 207–211.
- Z. B. Zhou, H. Matsumoto and K. Tatsumi, Structure and properties of new ionic liquids based on alkyl- and alkenyl-trifluoroborates, *ChemPhysChem*, 2005, **6**, 1324–1332.
- A. Bagno, C. Butts, C. Chiappe, F. D'Amico, J. C. D. Lord, D. Pieraccini and F. Rastrelli, The effect of the anion on the physical properties of trihalide-based *N,N*-dialkylimidazolium ionic liquids, *Org. Biomol. Chem.*, 2005, **3**, 1624–1630.
- L. P. N. Rebelo, J. N. C. Lopes, J. M. S. S. Esperanca and E. Filipe, On the critical temperature, normal boiling point, and vapor pressure of ionic liquids, *J. Phys. Chem. B*, 2005, **109**, 6040–6043.
- H. A. Every, A. G. Bishop, D. R. MacFarlane, G. Ora and M. Forsyth, Transport properties in a family of dialkylimidazolium ionic liquids, *Phys. Chem. Chem. Phys.*, 2004, **6**, 1758–1765.
- H. Tokuda, K. Hayamizu, K. Ishii, Md. Abu Bin, H. Susan and M. Watanabe, Physicochemical properties and structures of room temperature ionic liquids. 2. Variation of alkyl chain length in imidazolium cation, *J. Phys. Chem. B*, 2005, **109**, 6103–6110.
- P. Bonhôte, A. P. Dias, N. Papageorgiou, K. Kalyanasundaram and M. Graetzel, Hydrophobic, highly conductive ambient-temperature molten salts, *Inorg. Chem.*, 1996, **35**, 1168–1178.
- P. A. Z. Suarez, S. Einloft, J. E. L. Dullius, R. F. De Souza and J. Dupont, Synthesis and physical-chemical properties of ionic liquids based on 1-*n*-butyl-3-methylimidazolium cation, *J. Chim. Phys.-Chim. Biol.*, 1998, **95**, 1626–1639.
- T. Nishida, Y. Tashiro and M. Yamamoto, Physical and electrochemical properties of 1-alkyl-3-methylimidazolium tetrafluoroborate for electrolyte, *J. Fluorine Chem.*, 2003, **120**, 135–141.
- Y. Yoshida and G. Saito, Influence of structural variations in 1-alkyl-3-methylimidazolium cation and tetrahalogenoferrate(III) anion on physical properties of the paramagnetic ionic liquids, *J. Mater. Chem.*, 2006, **16**, DOI: 10.1039/b515391c.
- W. Xu, E. I. Cooper and C. A. Angell, Ionic liquids: ion mobilities, glass temperature, and fragilities, *J. Phys. Chem. B*, 2003, **107**, 6170–6178.
- G. I. Taylor, Disintegration of water drops in electric field, *Proc. R. Soc. London, Ser. A*, 1964, **280**, 283–397; J. Zeleny, Instability of

- electrified liquid surfaces, *Phys. Rev.*, 1917, **10**, 1–6; M. Cloupeau and B. Prunet-Foch, Electrostatic spraying of liquids in cone-jet mode, *J. Electrostat.*, 1989, **22**, 135–159.
- 19 M. Gamero-Castaño and J. Fernandez de la Mora, Direct measurement of ion evaporation kinetics from electrified liquid surfaces, *J. Chem. Phys.*, 2000, **113**, 815–832; M. Gamero-Castaño and V. Hruby, Electrospray as a source of nanoparticles for efficient colloid thrusters, *J. Propul. Power*, 2002, **17**, 977–987.
- 20 P. D. Prewett and G. L. R. Mair, *Focused Ion Beams from Liquid Metal Ion Sources*, Wiley, New York, 1991.
- 21 I. Romero-Sanz, R. Bocanegra, J. Fernández de la Mora and M. Gamero-Castaño, Source of heavy molecular ions based on Taylor cones of ionic liquids operating in the pure ion evaporation regime, *J. Appl. Phys.*, 2003, **94**, 3599–3605; I. Romero-Sanz and J. Fernandez de la Mora, Spatial structure and energy distribution of electrosprays of ionic liquids in vacuo, *J. Appl. Phys.*, 2004, **95**, 2123–2129.
- 22 P. Lozano and M. Martínez-Sánchez, Ionic liquid ion sources: characterization of externally wetted emitters, *J. Colloid Interface Sci.*, 2005, **282**, 415–421.
- 23 G. K. Batchelor, *An Introduction to Fluid Dynamics*, Cambridge University Press, New York, 1967; see eqn (1.8.5).
- 24 D. R. MacFarlane, J. Golding, S. Forsyth, M. Forsyth and G. B. Deacon, Low viscosity ionic liquids based on organic salts of the dicyanamide anion, *Chem. Commun.*, 2001, 1430–1431.
- 25 Y. Yoshida, K. Muroi, A. Otsuka, G. Saito, M. Takahashi and T. Yoko, 1-Ethyl-3-methylimidazolium based ionic liquids containing cyano groups: synthesis, characterization and crystal structure, *Inorg. Chem.*, 2004, **43**, 1458–1462.
- 26 G. Saito and Y. Yoshida, Development of conductive organic molecular assemblies: organic metals, superconductors, and exotic functional materials, *Bull. Chem. Soc. Jpn.*, submitted.
- 27 Y. Yoshida, J. Fujii, G. Saito, T. Hiramatsu and N. Sato, Dicyanoaurate(I) salts with 1-alkyl-3-methylimidazolium; luminescent properties and room-temperature liquid forming, *J. Mater. Chem.*, 2006, **16**, DOI: 10.1039/b515869a.
- 28 Y. Katayama, I. Konishiike, T. Miura and T. Kishi, Redox reaction in 1-ethyl-3-methylimidazolium-iron chlorides molten salt system for battery application, *J. Power Sources*, 2002, **109**, 327–332.
- 29 Y. Yoshida, A. Otsuka, G. Saito, S. Natsume, E. Nishibori, M. Takata, M. Sakata, M. Takahashi and T. Yoko, Conducting and magnetic properties of 1-ethyl-3-methylimidazolium (EMI) salts containing paramagnetic irons: liquids [EMI][M^{III}Cl₄] (M = Fe and Fe_{0.5}Ga_{0.5}) and solid [EMI]₂[Fe^{II}Cl₄], *Bull. Chem. Soc. Jpn.*, 2005, **78**, 1921–1928.
- 30 P. Wang, S. M. Zakeeruddin, R. Humphry-Baker and M. Gratzel, A binary ionic liquid electrolyte to achieve >7% power conversion efficiencies in dye-sensitized solar cells, *Chem. Mater.*, 2004, **16**, 2694–2696.
- 31 J. Sung, Y. Jeon, D. Kim, T. Iwahashi, T. Iimori, K. Seki and Y. Ouchi, Air–liquid interface of ionic liquid + H₂O binary system studied by surface tension measurement and sum-frequency generation spectroscopy, *Chem. Phys. Lett.*, 2005, **406**, 495–500.
- 32 B. D. Fitchett, T. N. Knepp and J. C. Conboy, 1-Alkyl-3-methylimidazolium bis(perfluoroalkylsulfonyl)imide water-immiscible ionic liquids. The effect of water on electrochemical and physical properties, *J. Electrochem. Soc.*, 2005, **151**, E219–E225.
- 33 C. Bueno and J. Fernandez de la Mora, Factors determining the appearance of the purely ionic regime in Taylor cones of ionic liquids: The effect of surface tension, *J. Appl. Phys.*, 2006, in preparation.
- 34 I. Romero-Sanz, I. Aguirre-de-Carcen and J. Fernandez de la Mora, Ionic propulsion based on heated Taylor cones of ionic liquids, *J. Propul. Power*, 2005, **21**, 239–242.
- 35 E. A. Guggenheim, The principle of corresponding states, *J. Chem. Phys.*, 1945, **13**, 253–261.

Surface tension measurements of highly conducting ionic liquids

W. Martino, J. Fernandez de la Mora, Y. Yoshida, G. Saito and J. Wilkes

Green Chem., 2006, **8**, 390–397 (DOI: 10.1039/b515404a)

The following transcription errors have been identified in Table 3 of the abovementioned article: γ for EMI-BF₄ is 46.7 dyn cm⁻¹. The first three numbers in the row for EMI-TfO are incorrect, the correct values being $\cos\theta = 0.973$; $h = 20.74$ mm; $\gamma = 39.6$ dyn cm⁻¹. Finally, in the row for EMI-N(CN)₂ the correct value for h is 40.2 mm. We are grateful to Mr Carlos Larriba for noticing slight inconsistencies between the table and eqn (1).

Mr Larriba has also reexamined some of the prior measurements and discovered that the surface tension of vacuum dried DMI-N(CN)₂ decreases through the measurement process over a time scale of 15 min, to reach a final value of 53.3 dyn cm⁻¹ at 23 °C. The apparent reason for this behavior is that the liquid is not properly dried under vacuum at room temperature (possibly due to the fact that it melts above room temperature, though it seems to remain liquid). However, because the meniscus region is surrounded by a dry gas during the experimental procedure, it slowly dries during the measurement. The new lower surface tension therefore is the correct one for a dried sample. The conclusion that DMI-N(CN)₂ has the highest surface tension of the group studied remains true, but the singularly high value reported of 61.6 dyn cm⁻¹ must be discarded.

The Royal Society of Chemistry apologises for these errors and any consequent inconvenience to authors and readers.

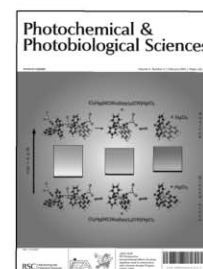
Additions and corrections can be viewed online by accessing the original article to which they apply.

Photochemical & Photobiological Sciences

The official journal of the European Society for Photobiology and the European Photochemistry Association

High-quality, peer-reviewed papers concerned with any aspect of the interaction of light with molecules, supramolecular systems or biological matter.

- Fast times to publication (typically 85 days)
- High visibility – indexed in MEDLINE
- A first impact factor of 1.798
- 12 issues a year



18030551

RSCPublishing

www.rsc.org/pps

Issues in Toxicology

New series from the RSC

Series Editors

Professor Diana Anderson, *University of Bradford, UK*

Dr Michael D Waters, *National Institute of Environmental Health Science, USA*

Dr Timothy C Marrs, *Food Standards Agency, UK*

This series is devoted to coverage of modern toxicology and assessment of risk and is responding to the resurgence in interest in these areas of scientific investigation.

Topics covered include: hair in toxicology; toxicogenomics; reproductive (particularly male mediated) toxicology; biomarkers in toxicology; and possible chemical warfare.

Ideal as a reference and guide to investigations in the biomedical, biochemical and pharmaceutical sciences.

Readership

Academic researchers, graduate students, government institutions

Market

Toxicology, biomedicine, biochemistry, forensics and environmental/pollution sciences

Format

Hardcover

First title in the series

Hair in Toxicology: An Important Bio-Monitor

Edited by Desmond John Tobin, *University of Bradford, UK*

The first book of its kind devoted exclusively to in-depth analysis of the hair shaft, as an important tool for a diverse range of scientific investigations.

It covers:

- Information on the exposure of hair to chemicals and pollutants
- Toxicological issues relevant to the use of 'hair care' products
- The ability of hair to capture information on personal identity, chemical exposure, and environmental interactions
- How hair can provide an understanding of human life from archaeological and historical perspectives
- Future direction in the use of hair in toxicology

2005 | 297 pages | £79.95 | RSC member price £51.75
ISBN-10: 0 85404 587 2 | ISBN-13: 978 0 85404 587 7



'I wish the others were as easy to use.'



'ReSource is the best online submission system of any publisher.'

'It leads the way for online submission and refereeing.'



ReSource



A selection of comments received from just a few of the thousands of satisfied RSC authors and referees who have used ReSource to submit and referee manuscripts. The online portal provides a host of services, to help you through every step of the publication process.

authors benefit from a user-friendly electronic submission process, manuscript tracking facilities, online proof collection, free pdf reprints, and can review all aspects of their publishing history

referees can download articles, submit reports, monitor the outcome of reviewed manuscripts, and check and update their personal profile

NEW!! We have added a number of enhancements to ReSource, to improve your publishing experience even further.

New features include:

- the facility for authors to save manuscript submissions at key stages in the process (handy for those juggling a hectic research schedule)
- checklists and support notes (with useful hints, tips and reminders)
- and a fresh new look (so that you can more easily see what you have done and need to do next)

A class-leading submission and refereeing service, top quality high impact journals, all from a not-for-profit society publisher ... is it any wonder that more and more researchers are supporting RSC Publishing? Go online today and find out more.

Registered Charity No. 207890

RSC Publishing

www.rsc.org/resource